THE ROLE OF CEREBRAL FUNCTIONAL NETWORK TOPOLOGY IN ALZHEIMER'S DISEASE

In a network state of mind

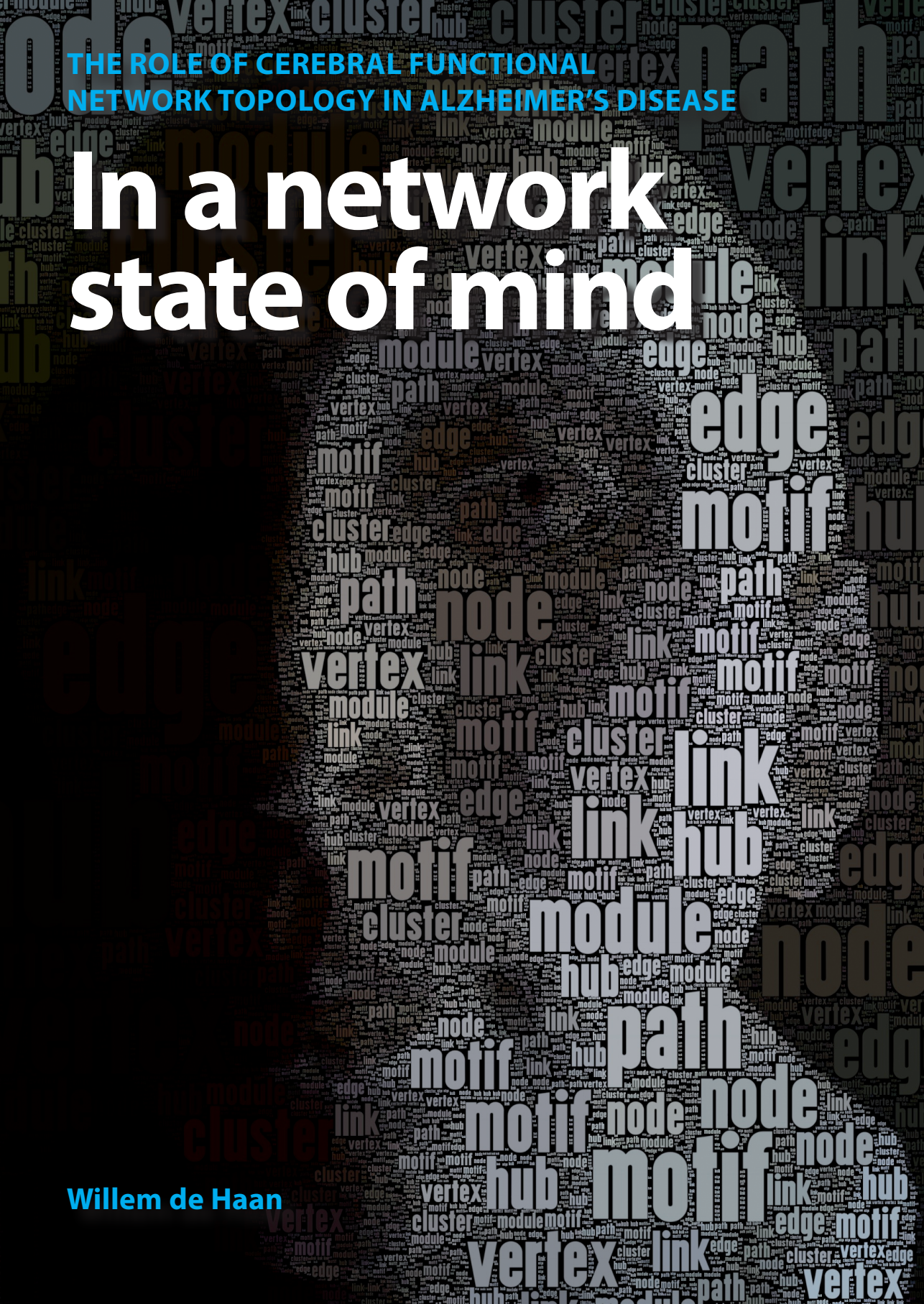

Willem de Haan

In a network state of mind

Willem de Haan

Cover Image: Sculpture by Ronald W. de Haan, word cloud transformation by Wordfoto

Layout and printing: Optima Grafische Communicatie, www.ogc.nl

Licenses to re-use articles, as published in journals, were granted by the publishers of these journals.

The studies described in this thesis were carried out at the Alzheimercenter of the VU University medical Center, Amsterdam, the Netherlands.

The Alzheimercenter Vumc is supported by Innovatiefonds Ziektekostenverzekeraars and by unrestricted grants to the Stichting Vumc Fonds from: AEGON Nederland NV, Ars Donandi Kas Bank Welzijnsfonds, Heer en Mw Capitain, Heineken Nederland NV, Nationale Nederlanden, Janssen Cilag NV, Gebroeders Boeschen, Genootschap Steun Alzheimercentrum, Kroonenberg Groep, KLM Royal Dutch Airlines, KPMG/Plexus, Marcel Boekhoorn, Nutricia Nederland, Onvergetelijke vrienden Alzheimercentrum, SNS Reaal, Soroptimisten Bussum e.o, Stichting ITON, Stichting De Merel, Stichting ZABAWAS, Stichting Alzheimer Nederland, Stichting Dioraphte, Stichting Mooiste Contact Fonds KPN, Stichting Buytentwist, Twentse Kabel Holding, Ton Aan de Stegge, van Leeuwen-Rietberg stichting, and many kind individual donors!

VUmc VU University Alzheimer Center Amsterdam

VRIJE UNIVERSITEIT

In a network state of mind

ACADEMISCH PROEFSCHRIFT

ter verkrijging van de graad Doctor aan
de Vrije Universiteit Amsterdam,
op gezag van de rector magnificus
prof.dr. L.M. Bouter,
in het openbaar te verdedigen
ten overstaan van de promotiecommissie
van de Faculteit der Geneeskunde
op vrijdag 2 november 2012 om 11.45 uur
in de aula van de universiteit,
De Boelelaan 1105

door
Willem de Haan
geboren te Nijmegen

promotoren:	prof.dr. Ph. Scheltens
	prof.dr. C.J. Stam
copromotor:	dr. W.M. van der Flier

CONTENTS

Node 1

Introduction, aims and outline

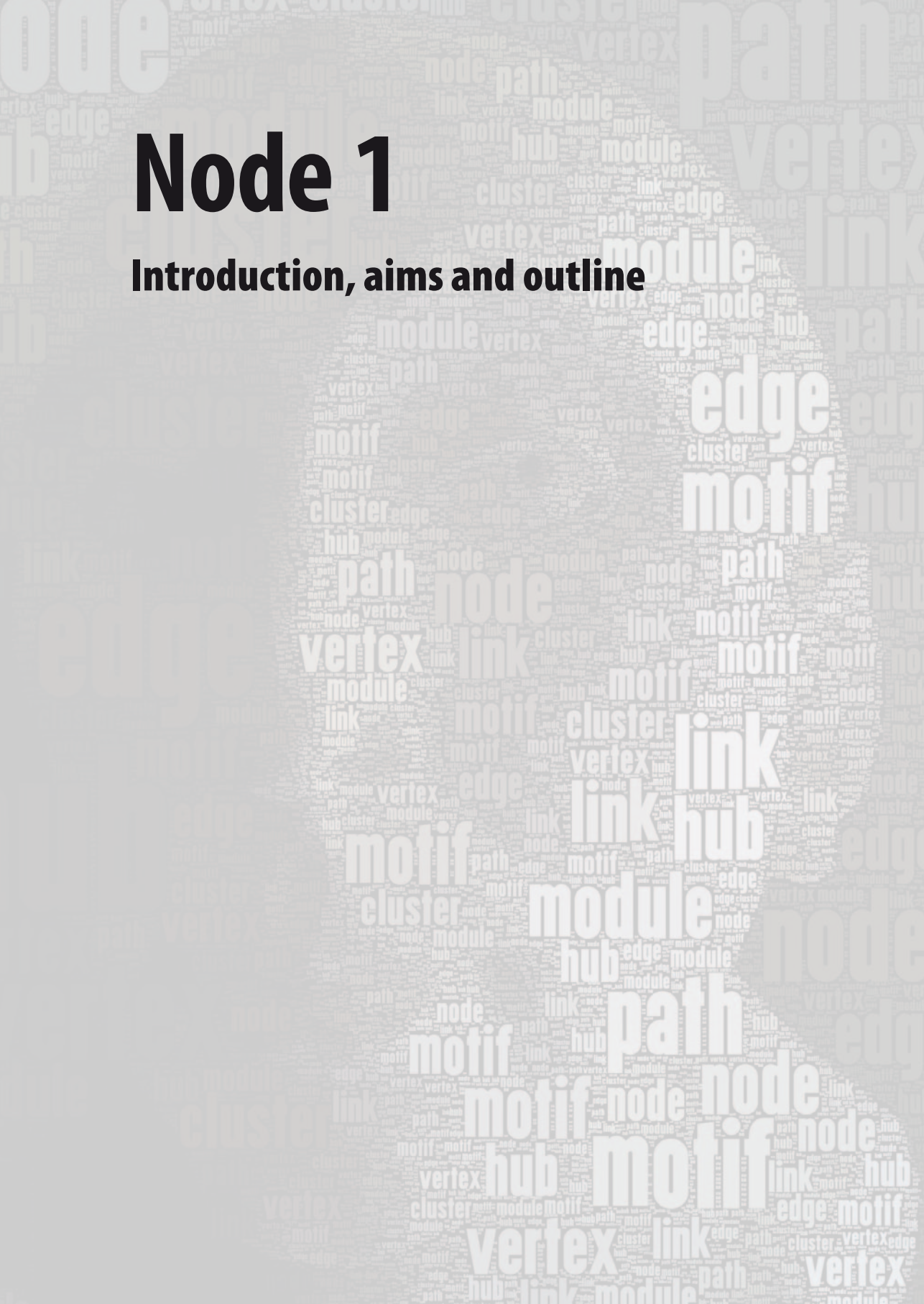

INTRODUCTION

A network perspective on dementia: why?

"So we have to come to the conclusion, that the plaques are not the cause of senile dementia but only an accompanying feature..."

Aloysius "Aloïs" Alzheimer, 1911

Über eigenartige Krankheitsfälle des späteren Alters.
Zeitschrift für die gesamte Neurologie und Psychiatrie
4:356-385

Alzheimer's disease

Having an intact brain is of vital importance to our quality of life; our cognitive abilities, emotions, personality and behavior all depend on it. Therefore, when brain disease manifests itself, it forms a direct threat to the very core of our existence. Brain disorders come in many different forms, are often incurable, and place a large burden on patient, caregivers and society. This dissertation focuses on Alzheimer's disease, the most prevalent type of neurodegenerative dementia. The gradual deterioration of the brain and cognitive functions occurring in Alzheimer's disease patients is a humiliating experience. Unfortunately, this condition is now a fact of life for more people than ever: 30 million people worldwide suffer from dementia, and this number is estimated to triple by 2050[1]. Life expectancy is increasing in most parts of the world, and above the age of 65 the chance of acquiring Alzheimer's disease doubles every five years. For Alzheimer's disease, as for most neurodegenerative diseases, there is no cure or effective treatment.

Although in recent decades much has been learnt about the pathophysiology of Alzheimer's disease, the exact relationship between brain damage and the gradual disruption of cognitive abilities is still poorly understood. For example, there is a large discrepancy between pathological burden and disease severity: persons with extensive damage are sometimes only mildly demented, while others with more subtle brain abnormalities can be clearly affected. In addition, there is a substantial pathological and clinical overlap between different forms of dementia, making an early and secure diagnosis more difficult to achieve. Therapeutic trials that have been aimed at amyloid-beta protein deposits, nowadays presumed to be one of the major pathological hallmarks, have produced disappointing results so far. It seems as if this pathological feature, which still forms the basis of most etiological hypotheses, is not the cause of Alzheimer's

disease, but rather an intermediate or even accompanying feature ('*Begleiterscheinung*' according to Aloïs Alzheimer). Thus, considering the impact of Alzheimer's disease on society, the incomplete understanding of the disease mechanism, and the lack of effective remedies, it is obvious that alternative perspectives and new approaches are desperately needed.

The main motivation for this dissertation is the hypothesis that a better understanding of brain *activity* and *connectivity* is essential to deal with cognitive dysfunction in general, and dementia in particular. These two aspects are crucial for cognitive processing, but have only played a marginal role in dementia research so far. Both technical limitations *and* advances may have contributed to this situation: while in recent decades structural brain imaging has greatly enhanced the spatial detail with which we can describe local brain abnormalities, no elegant method for accurately capturing and interpreting *in vivo* brain dynamics and connectivity has become generally available. This has favored a rather static and reductionist view of the brain as a collection of specialized regions as opposed to a highly dynamic, integrated system with distributed functions. However, a neglect of the brain's dynamic nature and complex architecture is a serious conceptual limitation, since it largely ignores the question of how cognitive processes are coordinated throughout the brain. For this purpose, approaches that combine accurate acquisition of large-scale brain dynamics and connectivity with appropriate analytical tools are required.

In this dissertation, the strategy of choice to explore the role of brain activity and connectivity in Alzheimer's disease is a combination of *neurophysiology* and *graph theory*. These two fundamental subjects will be briefly introduced in the next paragraphs, and will lead to the general aims and outline of this thesis.

Brain activity and neurophysiology

The human brain consumes 20% of the body's energy supply, while its weight is only about 2% of the total body weight. It is by far the most active organ we have in our body, and most energy is devoted to its core business: fast and flexible communication between cells. Brain structure and dynamics are very closely related: the plastic brain develops, reshapes and reorganizes itself constantly under the influence of internal and external forces. Hence, brain structure and activity should ideally be investigated collectively and within a single conceptual framework. Reaching this goal is easier said than done: investigating a detailed description of the brain structure *and* dynamics of living human beings in an accurate, patient-friendly manner is still a major technical challenge.

A crucial part of cognitive processing in the brain is accomplished by *neurons*; brain cells specialized in signal reception and transmission. When neurons receive signals from other neurons, it makes them more or less likely to *fire*, and pass on the signal to

other neurons. Instead of stimulating other neurons to fire, they can also *inhibit* the firing of others. So, the brain contains an enormous network of elements that are constantly stimulating and inhibiting each other. Since firing (groups of) neurons essentially show repetitive, rhythmic behavior, they are often described as *oscillators*. Coupled oscillators influence each other, causing their firing rates to fasten, slow down or even stop. A mechanism that is presumed to be vital to neuronal interaction is *synchronization*: when (groups of) neurons synchronize, they become more effective, and will exert a greater influence on their environment[2]. The selective routing of information needed to coordinate brain activity is realized by synchrony, and the level of synchronous firing between neuronal groups can be interpreted as the level of communication between them.

When many neurons fire, oscillate and synchronize, they generate an electromagnetic field that can be detected outside the human head. Whereas *electroencephalography* (EEG) records the electric component of this field, *magnetoencephalography* (MEG) records the magnetic part. Both EEG and MEG can measure variations in brain activity at the scale of milliseconds. However, there are a few obstacles: first of all, the muscles, eyes and heart and even surrounding equipment, cars, buildings, etc. all produce electromagnetic fields that can distort the recording. Their influence must be minimized, and the use of shielded rooms and artifact filters are therefore important. Second, since EEG and MEG measure brain activity from the outside, there is uncertainty about the exact location of the activity source. Although mathematical techniques can be used to locate sources, there is no unique solution to this so-called *inverse problem*. A third important aspect is that since different EEG and MEG sensors pick up activity from common sources, computations of the strength of synchronization and thus communication between them is overestimated. This issue is called *volume conduction*, and it will be discussed later on in this thesis.

Magnetoencephalography (MEG) system in upright position (source: Elekta ®)
Advantages of MEG over more traditional EEG are the cleaner signal, higher level of detail, and a shorter preparation time. Disadvantages are the necessity of a shielded room, immobility, and high cost.
Like EEG, MEG is completely non-invasive, silent, and it does not require radiation or strong magnetic fields.

To investigate how brain activity relates to cognitive abilities, it seems rational to measure brain activity during a mental task, such as reading, listening, counting or remembering. However, although task-based experiments have produced many important results, the view of the brain as a reactive or task-solving organ may be only part

of the truth, as widespread intrinsic processing is taking place continuously, even in the absence of external stimuli. Therefore, in recent years a lot of attention has been placed on so-called *resting-state* brain dynamics and networks. The term is misleading, because the brain maintains its high level of activity at all times. In fact, the energy consumption of the brain hardly increases (at most 5%) when cognitive tasks are performed[3]. In recent years, resting-state activity has been shown to display robust, characteristic patterns that are related to cognitive states and disease conditions. The studies in this thesis therefore focus on resting-state or 'spontaneous' brain activity, also because the performance of tasks requires instruction, which can be difficult or unreliable in test subjects, especially in dementia patients.

EEG literature shows that there is a gradual, diffuse slowing of brain activity and an overall loss of synchronization in Alzheimer's disease[4]. Although the oscillatory slowing is a common finding, it is not specific and constant enough to be used as a powerful diagnostic or prognostic marker. At present, the role of EEG in the clinical diagnostic work-up of dementia is mainly based on the exclusion of other, non-neurodegenerative causes of cognitive impairment such as intoxication, epilepsy or encephalopathy. The development of reliable neurophysiologic markers for different forms of dementia is highly desired, since EEG/MEG are relatively fast and patient-friendly techniques that might simplify the diagnostic workup of dementia. Moreover, in order to *understand* the observed changes in activity and synchronization we need to go beyond the descriptive level, and find out how brain activity is actually coordinated.

Brain networks and graph theory

An exploration of how brain dynamics are coordinated automatically leads to an observation that is the second center point of this thesis: the brain is a *network*. And as with other complex networks, it is much more than just the sum of its parts: interactions between regions are vital to major cognitive functions such as vision, language, memory and executive function[5]. In other words, *global* network connectivity is just as (or for some abilities maybe even *more*) important as local function. However, even if we would have a detailed description of complete structural and dynamical brain networks, there would still remain a need for a meaningful framework to make sense of the enormous complexity: a language of connectivity, that not only describes network features, but also explains their value. Fortunately, that language exists for smaller, more deterministic networks: *graph theory*. The application of graph theoretical principles to complex systems like the brain is giving rise to a new scientific field, often labeled as 'modern network theory'.

Graph theory is a branch of mathematics that studies the principles of network architecture. For example, it explores what organizational characteristics make a network robust, efficient, or flexible. It can explain the relation between network structure and function in a meaningful way. The human brain might be the most mysterious and

complex network or system known to man, but is certainly not the only one: social, economical, biological, and infrastructural (to name a few) networks are everywhere around and inside us. The impressive amount of graph theoretical network knowledge has been successfully translated to many of these fields[6]. Graph theory has illustrated that in completely different networks, common principles and patterns can be found: mechanisms that are found in engineering or telecommunication may apply to the brain and vice versa. Many major problems in other complex networks such as disease epidemics, traffic jams, economic crises or computer viruses can't be understood and solved by focusing on individual parts of the system, but require the system-level approach that graph theory offers. Likewise, using graph theory to investigate brain networks may be a powerful strategy to learn more about how the brain is wired, how it coordinates its activity, and how it copes with damage and illness.

Regardless of a network's context, graph theory purely focuses on the patterns of its connectivity. Graphs (abstract representations of networks) consist of elements (*nodes* or *vertices*) and the connections between them (*links* or *edges*); all other details are irrelevant. The strength and pattern of the connections is what determines many major network characteristics, and numerous graph measures have been developed to describe these characteristics quantitatively.

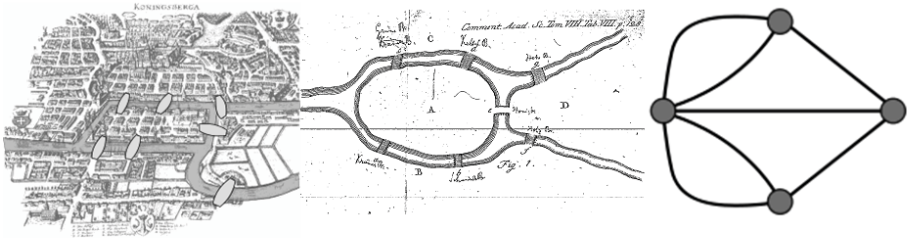

On the left, the Prussian city of Koningsbergen. The famous mathematician Leonhard Euler (1707-1783) solved the 'Seven bridges of Koningsbergen' problem by using what is generally considered as the first graph theoretical proof. The middle picture is a schematic top view of the city parts and their connecting bridges. On the right, an even more abstract representation is shown: a graph, consisting of nodes and links. By stripping away irrelevant details and purely focusing on the pattern of connectivity, Euler proved that there is no trail that crosses each bridge just once and ends at its starting point: to allow this, every city part would need to have an even amount of bridges.

The brain is actually a multi-level network: there is the physical wiring of brain cells, referred to as the *structural network* or *structural connectivity*, and superimposed on this is the *functional network*, the dynamics or 'traffic' of the brain. The connections in functional brain networks represent the strength of interaction (measured by synchronization in our case) between brain regions. The use of the term *functional* to refer to

dynamic connections or networks is slightly confusing, since structural characteristics of the brain contribute to its function just as well. It is also important to keep in mind that the distinction between the terms 'structural' and 'functional' is artificial to a certain extent: in reality, phenomena with overlapping time scales exist, such as spike-timing dependent plasticity and dendritic outgrowth. Nonetheless, in this thesis we focus on *functional* networks, based on neurophysiological (EEG/MEG) data.

Brain networks can be studied at different scales: from the cellular, single-neuron level to the large-scale cortical region level. However, meaningful patterns of coordinated brain activity may emerge at any level; the most detailed level is not necessarily the most informative one. Since neurophysiological techniques measure brain activity of large-scale regions containing millions of neurons, this limits the detail with which we can describe network dynamics. However, different scales and levels of detail can also be found in temporal dimensions; in other words, there is meaningful information in brain dynamics at different frequencies, similar to radio stations emitting at different wavelengths. Therefore, capturing brain dynamics over a wide range of frequencies is of vital importance, and at present no technique is better suited for this purpose than EEG or MEG.

Graph theoretical analysis of brain networks may feel like an abstract step away from the biomedical reality of brain disease. However, the transition from experimental data to a theoretical environment also has benefits: brain network models can be analyzed and manipulated in ways that are impossible in real human brains. This opens the door to a very different approach than the top-down process of measuring patient data and trying to interpret it: with computational network models we can simulate network damage or repair, in order to understand or even predict what will happen in brain disease. With this complementary 'in silico' strategy we can try to discover principles that govern brain structure and function. Consequently, it may lead to new hypotheses about disease mechanisms that can then be verified in empirical data.

Alzheimer's disease: a form of network failure?

The realization that the brain is a network and that cognition depends on network integrity has important consequences for understanding cognitive impairment as well. Traditionally, a cornerstone of any clinical neurological examination is the *localization* of functional deficits in specific parts of the nervous system, and this approach is usually very effective. However, many neurological functions (even reflexes) cannot be attributed to single regions, and are critically dependent on the communication between different regions. Cognition thus emerges from the network as a whole, and traditional localization principles might not always work. For instance, we know that there is no single region in the brain whose failure causes dementia; it is a widespread, gradual deterioration of many brain parts and their connections.

Traditionally, a *disconnection syndrome* is characterized by symptoms that arise when connections *between* brain areas disappear or malfunction[7,8]. Although this term points towards the importance of collaboration in the brain, it is still based on the notion of localized function. And while higher cognitive functions such as memory and executive function might be so highly distributed over the brain that functional localization is no longer meaningful, Alzheimer's disease has been labeled before as a disconnection syndrome, also based on the gradual, progressive loss of neurons and synapses[9]. This label might be considered a step forward compared to the idea that cognitive dysfunction is caused by dysfunction in a localized area, but it is also a rather generalist and vague term. Network theory can make more sense of connectivity and disconnectivity: it might thus be able to give us reasons *why* the effect of connectivity disruption between certain brain areas might be more catastrophic than between others. The observed changes in communication between different regions can then be used to better understand in which way this influences brain network characteristics like efficiency or robustness.

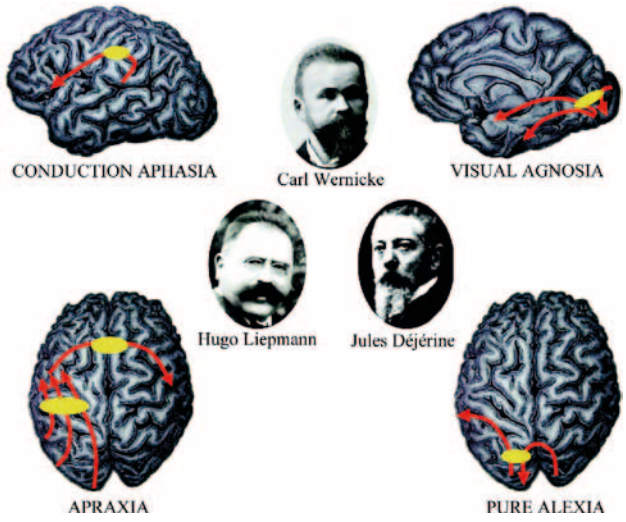

The classical disconnection syndromes. The pathways implicated in each syndrome are shown in red with the causal lesion in yellow. Wernicke is linked to both conduction aphasia and associative agnosia, the lesion in the former disconnecting Broca's and Wernicke's areas, the lesion in the latter disrupting the outflow of the visual cortex to other brain areas. Liepmann is linked to apraxia where the left-hand motor area is disconnected from other brain regions. Déjérine is linked to pure alexia in which the visual verbal centre is disconnected from visual areas in both hemispheres. Source: Catani and ffytche, The rises and falls of disconnection syndromes, Brain 2005 pp 2224–2239.

Cognitive impairment might not just be the consequence of localized damage, but of a malfunctioning brain network as well. This may seem a rather trivial statement, but the realization that network dysfunction is not necessarily due to local problems can have large implications for therapeutic strategies. For example, interventions aimed at seemingly unaffected brain parts or circuits may stabilize or improve global network function, and thus cognition[10].

What can modern network science teach us about Alzheimer's disease? Can we expect a better understanding, earlier detection, more accurate monitoring, or new hypotheses about the etiology of Alzheimer's disease? Maybe all of the above, maybe none: it is too early to tell. The main challenge is finding the most appropriate set of features to describe and understand connectivity loss in dementia. A few years ago, scientific literature about graph analysis applied to neuroscientific data was virtually non-existent, let alone with regard to dementia. This has changed, and now there are original research papers every week, appearing in high-impact journals. The promise of complex network theory is that it will enable us to go beyond labeling disorders as 'disconnection' syndromes by making the meaning of disconnection much more explicit, thereby possibly providing clues about new strategies to prevent and/or manage cognitive impairment. Whether the 'network perspective' will be a successful weapon in the battle against Alzheimer's disease is still uncertain; that it is a rational next step will hopefully become apparent from this work.

REFERENCE LIST

1 Hebert LE, Scherr PA, Bienias JL, Bennett DA, Evans DA (2003) Alzheimer disease in the US population: prevalence estimates using the 2000 census. Arch Neurol 60: 1119.

2 Buzsáki G (2006) Rhythms of the Brain. Oxford University Press, USA.

3 Raichle ME, Mintun MA (2006) Brain work and brain imaging. Annu Rev Neurosci 29: 449-476.

4 Jeong J (2004) EEG dynamics in patients with Alzheimer's disease. Clin Neurophysiol 115:7, 1490-505.

5 Kandel ER, Schwartz JH, Jessell TM (2000) Principles of neural science. New York: McGraw-Hill, Health Professions Division.

6 Newman M (2010) Networks : an introduction. Oxford ; New York: Oxford University Press.

7 Geschwind N (1965) Disconnexion syndromes in animals and man. I. Brain 88: 237-294.

8 Catani M, ffytche DH (2005) The rises and falls of disconnection syndromes. Brain 128: 2224-2239.

9 Delbeuck X, Van der Linden M, Collette F (2003) Alzheimer's disease as a disconnection syndrome? Neuropsychol Rev 13: 79-92.

10 Loscalzo J, Barabasi A-L (2011) Systems biology and the future of medicine. Wiley Interdisciplinary Reviews: Systems Biology and Medicine 3: 619-627.

AIMS AND OUTLINE

General aim

To gain more insight in the role of cerebral functional network topology in dementia, by describing the disruption of functional brain networks in Alzheimer's disease (AD) with the use of graph theoretical and neurophysiological techniques, and by exploring its relationship to cognitive symptoms and pathological features.

Specific aims and methods

To describe local and global abnormalities in oscillatory brain dynamics and functional connectivity in EEG and MEG data of Alzheimer patients.

- Spectral analysis.
- Functional connectivity analysis

To explore whether disruption of functional brain networks in AD can be meaningfully interpreted with the help of graph theoretical analysis.

- Graph theoretical analysis
    - Global network measures
    - Subnetwork (module) analysis
    - Nodal measures

To investigate whether abnormal patterns of functional network topology in Alzheimer patients are related to cognitive impairment.

- Statistical correlations between graph measures and cognitive performance

To find plausible mechanisms underlying the observed structural and functional brain network damage in AD using computational modeling.

- Computational modeling of disease-related changes and mechanisms

Outline

Since graph theoretical brain research is a relatively new and uncharted field, approaching it from different angles seems a sensible strategy. This is somewhat reflected by the various methodological approaches taken in this thesis. However, the individual studies are also part of a larger picture: key observations in the first empirical studies lead to an explicit hypothesis about the possible pathophysiological mechanism of AD: Activity dependent degeneration (ADD). This prediction is then investigated by means of computational modeling of neurodegeneration in the last study of this thesis.

In **Module 2**, we first investigate local differences of altered brain activity in AD by regional spectral power analysis of resting-state MEG data. **Module 3** starts with a study that describes global functional network changes in different types of dementia, taking into account not only the brain dynamics *within* but also *between* regions. Next, an MEG study in AD examines functional network disruption in larger detail, and tests the relation between network damage and cognitive test scores. In addition, network damage in Alzheimer patients is simulated with two different network damage models to find a plausible underlying 'disease' mechanism. A third study deals with the identification of sub-networks or "modules" and their relation with cognitive impairment in AD. **Module 4** takes a different approach to describe network properties by looking at the graph spectrum. This approach may have several methodological advantages over the more 'traditional' topological graph analysis. In **module 5** a computational neural mass model combines realistic neurophysiological dynamics with a human structural brain network topology. This model is used to test the hypothesis that the earlier observed selective vulnerability of functional network hubs in AD is due to high levels of neuronal activity. **Module 6** starts with a review on existing evidence for functional network disruption in neruodegenerative dementia, and then summarizes and integrates the findings of all studies, and discusses them with regard to the original aims of this thesis, and existing literature. In this module, methodological considerations and recommendations for future research will be discussed as well.

Node 2

Resting-state oscillatory brain dynamics in Alzheimer's disease

Journal of Clinical Neurophysiology 2008

W. de Haan[a,*], C.J. Stam[a], B.F. Jones[a,d], I. Zuiderwijk[a], B.W. van Dijk[a,c], and Ph. Scheltens[b]

[a.] Department of Clinical Neurophysiology and MEG, VU University Medical Center, Amsterdam, The Netherlands

[b.] Alzheimer Center, Department of Neurology, VU University Medical Center, Amsterdam, Netherlands

[c.] Department of Medical Physics and Technology, VU University Medical Center, Amsterdam, Netherlands

[d.] Dementia Research Centre, Institute of Neurology, UCL, London, UK

ABSTRACT

Altered oscillatory brain activity in Alzheimer's disease (AD) may reflect underlying neuropathological changes, and its characterization might lead to new diagnostic possibilities. The present study using quantitative magnetoencephalography (MEG) was set up to examine power spectrum changes in AD patients, and their diagnostic strength. Whole-head 151-channel MEG was recorded during an eyes-closed resting state. MEG channels were grouped in ten cortical regions, and both global and regional relative power was analyzed for the commonly used frequency bands.18 AD patients (mean age 72.1 years ± 5.6 (SD); 7 females; mean MMSE 19.2, range: 13-25) and 18 healthy controls (mean age 69.1 ± 6.8 (SD), 11 females; mean MMSE 29, range: 27-30) were recruited, controls being mainly spouses of patients. Relative power analysis showed significant differences in most frequency bands, particularly in the temporo-parietal regions, with some relation to MMSE scores. Greatest diagnostic accuracy was found in the beta band, especially in the right occipital area (sensitivity 94%, specificity 78%). Quantitative relative power analysis of MEG recordings is able to show widespread abnormalities in oscillatory brain dynamics in AD patients. By analyzing distinct cortical regions, this study provides a more detailed topographical view of abnormal brain activity in AD.

INTRODUCTION

Alzheimer's disease (AD) is the most prevalent form of dementia, and is imposing an increasing burden on our society [Andlin-Sobocki *et al.* 2005;Olesen and Leonardi 2003;Jonsson and Berr 2005]. Despite a massive boost in knowledge about the pathophysiological processes involved in AD over the past few decades, there is currently no antemortem test (or set of tests) that can provide a definitive diagnosis. Besides that, due to the neurodegenerative nature of the disease there exists a substantial delay between the moment of onset and the clinical diagnosis of AD [Cummings *et al.* 1998]. A more powerful diagnostic routine would be of great value for obvious reasons such as clarity for patients, greater interventional possibilities, and a better understanding of the disease in general.

In the most commonly used NINCDS-ADRDA criteria [McKhann *et al.* 1984], the diagnosis of AD is based upon a combination of clinical, laboratory and imaging tests. At this moment there is no prominent place for neurophysiologic tests in these guidelines, but since techniques extracting specific quantitative features from EEG and MEG (magnetoencephalography) recordings seem more and more capable of relating brain activity to cognitive function, they might become important contributors in the quest for an earlier and more decisive diagnosis of AD (for a review see [Jeong 2004])

Quantitative EEG studies have been conducted in AD patients for several decades, and have demonstrated a slowing of the dominant oscillatory brain activity, in particular over the posterior temporal, parietal and occipital brain areas [Boerman *et al.* 1994], [Jonkman 1997], [Jeong2004]. This slowing has been correlated with brain atrophy, APOE genotype and low central cholinergic activity [Lehtovirta *et al.* 1996], [Riekkinen *et al.* 1991]. The EEG, however, has not yet proven to be sufficiently discriminative to play a major role in the diagnostic workup of AD, and is primarily used for exclusion of other diagnoses [Waldemar *et al.* 2007].

Due to its superior temporal and spatial resolution, magnetoencephalography (MEG) is a promising neurophysiologic technique [Ioannides 2006]. Until now, MEG in AD has chiefly been used in more experimental research settings concerning task-related activity, source localization or functional connectivity (for a review see [Criado *et al.* 2006]). However, resting-state spectral analysis should be sufficient to produce noteworthy differences between AD patients and controls, and is perhaps more convenient for clinical settings. The few studies concerning spectral analysis of resting-state MEG recordings confirm the diffuse slowing of brain activity in AD, but they do not offer a straightfor-

ward relative power analysis for the commonly used frequency bands and for specific cortical regions [Berendse *et al.* 2000;Fernandez *et al.* 2006a;Fernandez *et al.* 2006b].

Therefore, in this study we grouped the MEG channels in ten distinct cortical regions, and analyzed the relative power both from a global and regional perspective. We also tested the correlation between relative power and cognitive status, and examined the diagnostic accuracy of relative power values.

METHODS

Subjects

The study involved 18 patients (mean age 72.1 years ± 5.6 (SD); 7 females; mean MMSE 19.2, range: 13-25) with a diagnosis of probable AD according to the NINCDS-ADRDA criteria [McKhann, Drachman, Folstein, Katzman, Price, and Stadlan1984] and 18 healthy control subjects (mean age 69.1 ± 6.8 (SD), 11 females; mean MMSE 29, range: 27-30), mostly spouses of the patients. Patients and control subjects were recruited from the Alzheimer Center of the VU University Medical Center. Subjects were assessed according to a clinical protocol, which involved history taking, physical and neurological examination, blood tests, a set of neuropsychological tests including a Dutch version of the MMSE [Folstein *et al.* 1975], MRI of the brain according to a standard protocol, and routine EEG. The final diagnosis was based upon a consensus meeting where all the available clinical data and the results of the ancillary investigations were considered. The MEG recordings were performed several weeks later. The study was approved by the Local Research Ethics Committee, and all patients or their caregivers had given written informed consent. The same MEG recordings were used for a study of functional connectivity in AD [Stam *et al.* 2006].

MEG recording

Magnetic fields were recorded while subjects were seated inside a magnetically shielded room (Vacuumschmelze GmbH, Hanau, Germany) using a 151-channel whole-head MEG system (CTF Systems Inc., Port Coquitlam, BC, Canada). Average distance between sensors in this system is 3.1 cm. A third-order software gradient (Vrba et al., 1999) was used with a recording pass band of 0.25 to 125 Hz. Sample frequency was 625 Hz. Fields were measured during a no-task eyes-closed condition.

At the beginning and at the end of each recording, the head position relative to the coordinate system of the helmet was recorded by leading small alternating currents through three head position coils attached to the left and right pre-auricular points and the nasion on the subject's head. Head position changes during the recording up to

approximately 1.5 cm were accepted. During the MEG recording, patients were sitting comfortably, and were instructed to close their eyes and move as little as possible.

Data processing

For further off-line processing, the recordings were converted to ASCII files and down-sampled to 312.5 Hz. Visual inspection and selection of the time segments was done with the DIGEEGXP software (CS) by two of the investigators (BFJ and IM). For each subject, three artifact-free time segments of 4096 samples (13,083 s) were selected. Typical artifacts were related to eye movements or muscle contractions.

For each selected time segment, relative power for all separate MEG channels was calculated in several frequency bands (delta 0.5-4 Hz, theta 4-8 Hz, alpha1 8-10 Hz, alpha2 10-13 Hz, beta 13-30 Hz and gamma 30-50 Hz) using the Fast Fourier Transformation. Results of the three segments were averaged for each subject. Subsequently, the MEG-channels were clustered into regions of interest corresponding to the major cortical areas (frontal, central, temporal, parietal and occipital) on the left and right side. The midline channels were left out of this clustering. A schematic distribution of these areas is shown in Fig. 1. The mean relative power for each of these groups was transformed with a logarithmic function (x=log[1/1-x]) to obtain a Gaussian distribution for further statistical analysis [Gasser *et al.* 1982].

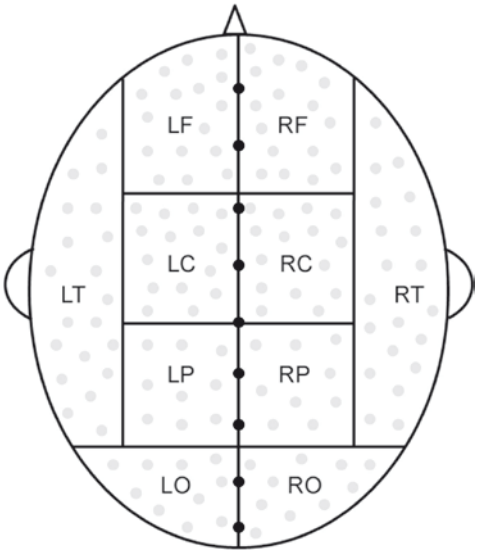

Figure 1: A schematic view of the head from above with MEG sensors grouped into 10 cortical regions. The number printed between parentheses indicates the number of MEG channels used. Midline sensors are shown in black (9 channels), and were left out of the analysis. LF = left frontal (16), RF = right frontal (16), LC = left central (15), RC = right central (15), LT = left temporal (20), RT = right temporal (20), LP = left parietal (9), RP = right parietal (n=9), LO = left occipital (n=10), RO = right occipital (n=10).

Statistical analysis

Subject characteristics of the AD patients and the controls were checked for possible significant differences in age or gender between the groups. MEG data was analyzed in several ways: first, an univariate ANOVA (general linear measurement with repeated measures) with group as intersubject factor, cortical area as intrasubject factor, and age as covariate was performed for all frequency bands, using Greenhouse–Geisser corrected p-values. A more descriptive comparison of means using independent-measure Student t-tests was made when appropriate.

Correlation analysis between MMSE score and relative power was performed for the AD patient group by means of Pearson's bivariate correlation test.

Receiver operating curves (ROC) were plotted of the global relative power in each frequency band, and of the separate regions. All analyses were performed at a significance level of .05 (two-tailed). Analysis was done using the SPSS 14.0 software package (SPSS inc., Chicago, USA).

RESULTS

Subject characteristics

Our project involved 18 AD patients and 18 healthy participants, whose characteristics are summarized in table 1. Differences in age and gender distribution between the groups were not significant. Six AD patients had been using cholinergic medication for a short period before the MEG registration was performed, either galantamine (Reminyl) 24 mg, or rivastigmine (Exelon) 12 mg. The delay between the primary diagnostic tests and the MEG registration was usually several weeks.

Table 1: Subject characteristics

	Alzheimer group (n=18)	Control Group (n=18)
Age (yrs)	72.1 ± 5.6 (SD)	69.1 ± 6.8 (SD)
Sex ratio (M/F)	11/7	7/11
MMSE score (points)	19.2 (range 13-25)	29 (range 27-30)
Cholinergic medication[1] (n)	6	0
Duration of complaints (yrs)	2.5	NA

Subject Characteristics. SD: standard deviation. NA: not applicable. [1] Reminyl 24mg or Exelon 12 mg.

Global relative power

The analysis of variance (ANOVA) results for each frequency band are shown in table 2. In the delta band a significant effect was found for Area x Group within subjects, and a significant effect of Group between subjects, with a consistently higher relative power in

the AD patient group. In the alpha1 band, a significant effect of Area x Group was found within subjects, and a significant effect of Group between subjects. Here, the relative power was significantly lower in AD patients. In the alpha2 band a significant effect was found of Area within subjects, and in Group between subjects. In the beta band a highly significant effect was found for Group between subjects. In these last two frequency bands relative power was significantly lower in AD.

Table 2: ANOVA of global relative power values for each frequency band

Within Subjects				**Between Subjects**	
	Area	**Area x Age**	**Area x Group**	**Age**	**Group**
Delta	F[9,297]=0.715 p<0.577	F[9,297]=0.440 P<0.771	**F[9,297]=4.793 p<0.001**	F[1,33]=0.100 p<0.754	**F[1,33]=7.530 p<0.010**
Theta	F[9,297]=0.811 p<0.500	F[9,297]=0.893 P<0.455	F[9,297]=1.556 p<0.200	F[1,33]=0.009 p<0.926	F[1,33]=0.823 p<0.371
Alpha 1	F[9,297]=0,176 p<0.935	F[9,297]=0.492 P<0.718	**F[9,297]=3.086 p<0.023**	F[1,33]=0.000 p<0.999	**F[1,33]=8.054 p<0.008**
Alpha 2	**F[9,297]=3.122 p<0.026**	F[9,297]=1.631 P<0.184	F[9,297]=2.109 p<0.099	F[1,33]=0.799 p<0.378	**F[1,33]=7.591 p<0.009**
Beta	F[9,297]=0.877 p<0.467	F[9,297]=0.172 P<0.934	F[9,297]=2.232 p<0.080	F[1,33]=0.134 p<0.717	**F[1,33]=14.005 p<0.001**
Gamma	F[9,297]=1.111 p<0.340	F[9,297]=1.282 P<0.285	F[9,297]=1.874 p<0.156	F[1,33]=0.137 p<0.713	F[1,33]=2.059 p<0.161

Mean relative power values for all cortical regions together were analyzed for each separate frequency band. In this figure, F values and their significance are shown, both for 'within subject' analysis (left of vertical line), and for 'between subject' analysis. Degrees of freedom are printed between square brackets. Bold text represents a significant effect on the variance in spectral power.

In addition, we performed t-tests to quantify differences in global relative power for the frequency bands that produced significant effects in the ANOVA. As expected, delta activity was increased in AD patients, whereas alpha1, alpha2 and beta activity was decreased. Particularly the beta band (13-30 Hz) showed a very significant decrease in relative power in the patient group ($p<0.001$).

Relative power per region

There were remarkable differences in relative power behavior between the various cortical regions, both in AD patients and controls. Figure 2 offers a visual comparison of means for the separate cortical regions in each frequency band. In general, temporal, parietal and occipital relative power changes were more outspoken. In the theta band the differences between AD patients and controls were not significant, but relative power was consistently higher in the AD group. The gamma band showed highly variable results, with only a significant decrease in relative power of the left temporal region.

In the beta band, all separate cortical regions demonstrated a significant decrease of relative power in AD.

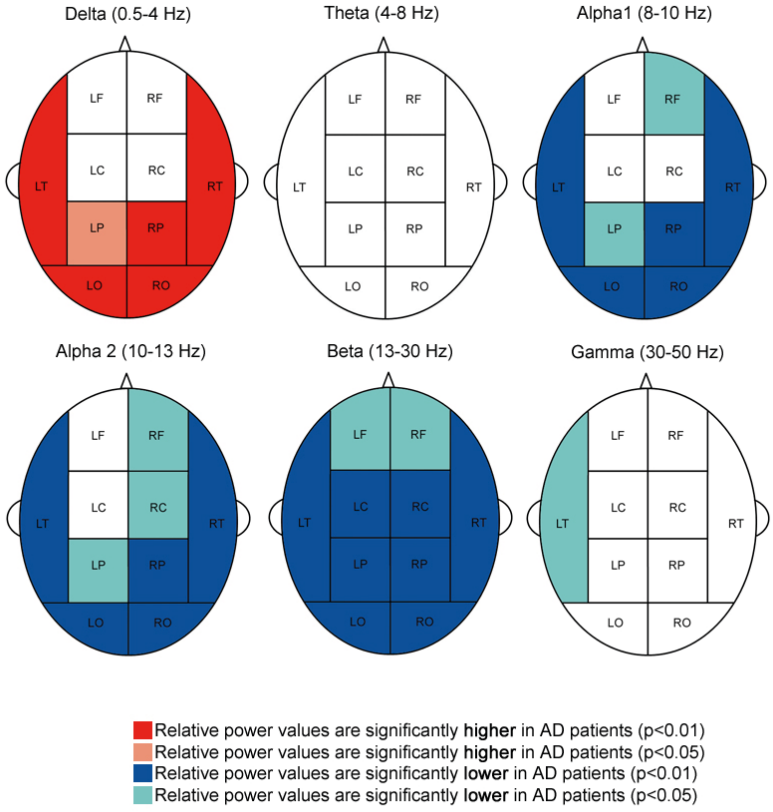

Figure 2: Relative power differences between AD patients and controls

Correlation relative power with MMSE score

Bivariate correlation (Pearson's) tests of relative power and MMSE scores were performed for global relative power and for the separate cortical regions. This was done only for the AD patient group. Global relative power values in the various frequency bands did not have a significant correlation with MMSE. In the alpha1 band, the left and right central regions showed a significant positive correlation (r=0.527; p=0.25 and r=0.531; p=0.23 respectively), as well as the right parietal cortical region (r=0.503; p=0.33). In the alpha2 band the left central region demonstrated a significant positive correlation (r=0.495; p=0.35).

Diagnostic accuracy

The discriminative capability of the global relative power was investigated by plotting receiver operating characteristic (ROC) curves. In figure 3 the ROC curves are shown for the various frequency bands. The greatest diagnostic accuracy, defined as the highest percentage of correctly classified subjects, was reached in the beta band (area-under-the-curve of 0.864). Using a relative power cut-off point of 0.105 produced a sensitivity of 94% and a specificity of 67%.

The same procedure was performed for single cortical regions, and the maximum diagnostic accuracy was obtained in the right occipital region in the beta band (area-under-the-curve 0.867, cut-off point 0.105: sensitivity 94%, specificity 78%). There were large differences between the discriminative capability of the various regions.

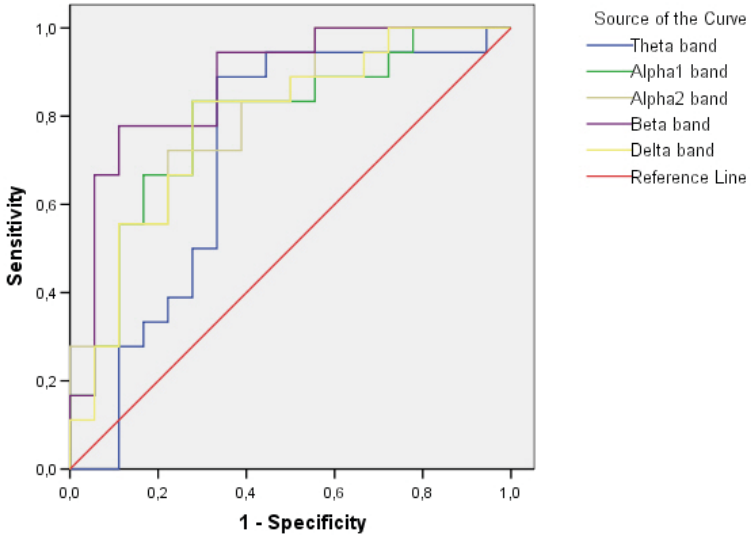

Figure 3: ROC curves of global relative power values in different frequency bands, showing the ability of relative power values to discriminate between AD patients and controls. Different colors indicate different frequency bands. The gamma band is not shown because of inconsistent classification performance.

DISCUSSION

The results of this MEG study confirm the slowing of resting-state oscillatory brain activity in AD, and add a more detailed topographic picture. In this section we will discuss the meaning of our main findings in the light of previous studies, and make a few remarks about relevant theoretical issues before concluding.

Methodological considerations

The multi-step process from a MEG registration to statistical analysis poses many interesting technical and interpretational difficulties, and knowledge about topics like for example measurement conditions, artifact selection, and mathematical techniques can probably be expanded and refined.

Medication that influences the cholinergic system can influence the EEG and the MEG results, most likely by reverting the slowing of activity due to AD pathology [Adler and Brassen 2001], [Osipova *et al.* 2003]. In our study, 6 of the 18 patients used a cholinesterase inhibitor (Reminyl or Exelon) for a short period prior to the MEG registration. To determine the possible influence of drug use on our results, we compared relative power results between AD patients who did and who did not use cholinesterase inhibitors. No significant differences were found, which suggests that our results are unlikely to be strongly influenced by medication effects. If a medication bias would exist, it would probably lead to underestimation of the differences between AD en controls. Of course, one question that remains is whether the persons that were selected for medication form a certain sub-group for some unknown reason.

Global relative power

The global increase in low frequency power (delta and theta band, <8 Hz) and decrease in high frequency power (alpha, beta and gamma bands, 8-50 Hz) that we found in AD patients is in agreement with previous EEG and MEG studies [Jeong2004], [Berendse, Verbunt, Scheltens, van Dijk, and Jonkman2000;Fernandez, Hornero, Mayo, Poza, Maestu, and Ortiz2006b;Osipova *et al.* 2005]. Fernandez et al. [2006] performed an elaborate 2 Hz-width sub-band analysis of relative power values, and produced similar results. A notable difference between this study and ours was the significant relative power decrease we found in the Alpha1 band (8-10 Hz) in AD patients. Perhaps this discrepancy is due to different data post-processing or statistical methods used. The highly significant changes in the beta band are an interesting similarity of both studies. Claus et al. also pointed to the prominent role of the beta band in several EEG studies [Claus *et al.* 1998b;Claus *et al.* 1998a;Claus *et al.* 2000]. We agree that the beta band results indicate a promising terrain for further research, and our characterization of regions provides a possible next step.

Cortical regions

Our rationale for grouping the MEG channels into local regions is twofold: first, EEG and MEG literature suggests remarkable topographic variety of oscillatory brain activity, both in spectral analysis and in source localization studies [Fernandez *et al.* 2006c;Fernandez *et al.* 2002;Maestu *et al.* 2003;Osipova *et al.* 2006;Osipova, Ahveninen, Jensen, Ylikoski, and Pekkonen2005;Jeong2004;Criado, Amo, Quint, Kurelowech, and Otis2006]. So for

comparison with previous literature, this local perspective gives a more accurate view. Second, from a more fundamental point of view, understanding the relationship between pathologic changes and abnormal functioning of the brain in AD requires a more detailed knowledge of local neurophysiologic dysfunction. It should be clear, however, that the grouping of MEG channels based on the major cortical areas is arbitrary, and that the regions formed do not necessarily reflect distinct functional units with clearly defined boundaries.

In our study, each cortical region showed abnormal oscillatory behavior across various frequency bands in AD patients. We sometimes found significant changes in a region when the global relative power for that frequency band did not produce any. Also, like previous EEG studies, our findings indicate that most marked changes seem to occur in the posterior temporal, parietal and occipital regions [Boerman, Scheltens, and Weinste in1994;Jonkman1997;Jeong2004], which corresponds with the area's with most marked pathological change in AD [Arnold *et al.* 1991]. Left temporal slow activity increase is often prominent in AD [Gianotti *et al.* 2007;Osipova, Ahveninen, Jensen, Ylikoski, and Pekkonen2005], and is related to left hippocampal volume loss [Fernandez *et al.* 2003]. In this study, the left temporal region produced most often a significant change in the various frequency bands. Central and frontal region changes were more modest, and perhaps the more anterior localization of alpha and beta rhythms in progressing AD [Huang *et al.* 2000] can partly account for this.

Examining both local brain activity and functional connectivity of different regions might contribute to understanding the pathophysiology of Alzheimer's disease. Using the same MEG recordings as studied here, Stam et al. found significant differences in Synchronization Likelihood (a non-linear measure of functional connectivity) between AD patients and controls; resting-state functional connectivity in Alzheimer's disease is characterized by specific changes of long and short distance interactions in the theta, alpha1, beta and gamma bands [Stam, Jones, Manshanden, van Cappellen van Walsum AM, Montez, Verbunt, de Munck, van Dijk, Berendse, and Scheltens2006]. The fact that regional relative power values behave differently is in our opinion a strong argument in favor of using regions.

Resting-state brain activity and cognitive performance

Our study was conducted during an eyes-closed no-task condition. One might raise the question whether resting-state activity should be correlated to performance on a task-related cognitive test. Nevertheless, in several resting-state EEG studies there [Gianotti, Kunig, Lehmann, Faber, Pascual-Marqui, Kochi, and Schreiter-Gasser2007;Jelic *et al.* 2000;Kwak 2006] were apparent correlations, and the Synchronization likelihood (see previous section) also demonstrated significant correlations with MMSE scores in the alpha1 and alpha2 band [Stam, Jones, Manshanden, van Cappellen van Walsum AM,

Montez, Verbunt, de Munck, van Dijk, Berendse, and Scheltens2006]. The correlation of relative power values with MMSE scores in our study was not very strong. This might partly be explained by the modest group size. Nevertheless, there were clear differences between regions; some showed a consistent trend in various frequency bands, whereas others did not.

A number of studies have shown that the 'resting state' is a far more stable and active condition than has often been assumed, and is characterized by the activation of a 'default' network, which consists of frontal, posterior cingulate, parietal and medial temporal areas [Laufs *et al.* 2003] [Raichle *et al.* 2001]. Abnormalities of this resting-state network have been demonstrated in AD [Lustig *et al.* 2003], as well as in Parkinson's Disease [Stoffers *et al.* 2007]. Although the use of specific tasks, aimed at activating brain areas assumed to be involved in pathology, might be expected to be more sensitive in demonstrating abnormalities [Morcom and Fletcher 2006], this is often not the case. One reason might be that pathology may be associated with abnormally high as well as abnormally low task-related activation, which seriously complicates interpretation of the results [Osipova, Ahveninen, Jensen, Ylikoski, and Pekkonen2005;Pijnenburg *et al.* 2004]. Since the definition and relation of such a 'default network' to cognition is not yet clear, questions are raised if it should be seen as a meaningful entity at all, and the validity of using a resting state to study cognitive performance remains a subject of discussion. Most important for the clinician, however, is the fact that the resting-state condition is sufficient to demonstrate remarkable changes in AD.

Diagnostic strength

A general problem in assessing the diagnostic strength of a test in AD is the inevitable circular reasoning that is involved, since there is no ultimate standard to compare results with; there is always a chance that a person does not have AD, but a different neurodegenerative problem, and thus a 100% accurate test would 'only' be as good as the present set of criteria. However, high sensitivity and specificity rates are still valuable. Can spectral analysis of MEG recordings contribute to achieving an earlier diagnosis of AD? In this study, the global relative power analysis reached a fair discriminative accurateness, notably in the beta range, and this is comparable with the results of Fernandez et al. [2006], and at least equivalent to EEG accuracy. The best classification score reached by a single region (right occipital region in the beta band) was comparable to the global beta band accuracy. However, there were striking differences between cortical regions, and this suggests that a regional approach might eventually produce greater diagnostic power.

Obviously, the AD patients in this study already had reached a clinical diagnosis of 'probable AD' based on the NINCDS-ADRDA criteria. The real challenge is to separate AD patients and others at an earlier stage. Fernandez et al. compared mean relative power

values of AD and MCI patients to controls, and found significant differences[Fernandez, Hornero, Mayo, Poza, Gil-Gregorio, and Ortiz2006a]. Other investigations suggest the ability of quantitative EEG and MEG methods to discriminate at an early stage between AD patients and healthy persons [Prichep 2007]. However, results are not yet strong enough to give EEG or MEG a prominent place in the diagnostic work-up of AD; more studies are needed to assess the potential clinical benefit.

Conclusion

Quantitative analysis of MEG registrations is able to show widespread abnormal patterns of resting-state oscillatory brain activity in AD patients. This is the first MEG study to provide a regional relative power analysis for the commonly used frequency bands in AD. In our opinion it gives a more detailed view of abnormal activity in AD, enables better comparison between MEG and EEG literature, and may contribute to more exact future studies and a more prominent role of MEG in the diagnostic work-up of AD.

Acknowledgement

The study was financially supported by a grant from Alzheimer Nederland.

REFERENCE LIST

Adler G, Brassen S. Short-term rivastigmine treatment reduces EEG slow-wave power in Alzheimer patients. 2001. p. 273-6.

Andlin-Sobocki P, Jonsson B, Wittchen HU, Olesen J. Cost of disorders of the brain in Europe. 2005. p. 1-27.

Arnold SE, Hyman BT, Flory J, Damasio AR, Van Hoesen GW. The topographical and neuroanatomical distribution of neurofibrillary tangles and neuritic plaques in the cerebral cortex of patients with Alzheimer's disease. Cereb Cortex 1991; 1: 103-116.

Berendse HW, Verbunt JP, Scheltens P, van Dijk BW, Jonkman EJ. Magnetoencephalographic analysis of cortical activity in Alzheimer's disease: a pilot study. 2000. p. 604-12.

Boerman RH, Scheltens P, Weinstein HC. Clinical neurophysiology in the diagnosis of Alzheimer's disease. 1994. p. 111-8.

Claus JJ, Kwa VI, Teunisse S *et al*. Slowing on quantitative spectral EEG is a marker for rate of subsequent cognitive and functional decline in early Alzheimer disease. Alzheimer Dis Assoc Disord 1998a; 12: 167-174.

Claus JJ, Ongerboer d, V, Bour LJ *et al*. Determinants of quantitative spectral electroencephalography in early Alzheimer's disease: cognitive function, regional cerebral blood flow, and computed tomography. Dement Geriatr Cogn Disord 2000; 11: 81-89.

Claus JJ, Ongerboer d, V, Walstra GJ, Hijdra A, Verbeeten B, Jr., van Gool WA. Quantitative spectral electroencephalography in predicting survival in patients with early Alzheimer disease. Arch Neurol 1998b; 55: 1105-1111.

Criado JR, Amo C, Quint P, Kurelowech L, Otis SM. Using magnetoencephalography to study patterns of brain magnetic activity in Alzheimer's disease. 2006. p. 416-23.

Cummings JL, Vinters HV, Cole GM, Khachaturian ZS. Alzheimer's disease: etiologies, pathophysiology, cognitive reserve, and treatment opportunities. Neurology 1998; 51: S2-17.

Fernandez A, Arrazola J, Maestu F *et al*. Correlations of hippocampal atrophy and focal low-frequency magnetic activity in Alzheimer disease: volumetric MR imaging-magnetoencephalographic study. 2003. p. 481-7.

Fernandez A, Hornero R, Mayo A, Poza J, Gil-Gregorio P, Ortiz T. MEG spectral profile in Alzheimer's disease and mild cognitive impairment. 2006a. p. 306-14.

Fernandez A, Hornero R, Mayo A, Poza J, Maestu F, Ortiz AT. Quantitative magnetoencephalography of spontaneous brain activity in Alzheimer disease: an exhaustive frequency analysis. 2006b. p. 153-9.

Fernandez A, Maestu F, Amo C *et al*. Focal temporoparietal slow activity in Alzheimer's disease revealed by magnetoencephalography. 2002. p. 764-70.

Fernandez A, Turrero A, Zuluaga P *et al*. Magnetoencephalographic parietal delta dipole density in mild cognitive impairment: preliminary results of a method to estimate the risk of developing Alzheimer disease. 2006c. p. 427-30.

Folstein MF, Folstein SE, McHugh PR. "Mini-mental state". A practical method for grading the cognitive state of patients for the clinician. 1975. p. 189-98.

Gasser T, Bacher P, Mocks J. Transformations towards the normal distribution of broad band spectral parameters of the EEG. Electroencephalogr Clin Neurophysiol 1982; 53: 119-124.

Gianotti LR, Kunig G, Lehmann D *et al*. Correlation between disease severity and brain electric LORETA tomography in Alzheimer's disease. 2007. p. 186-96.

Huang C, Wahlund L, Dierks T, Julin P, Winblad B, Jelic V. Discrimination of Alzheimer's disease and mild cognitive impairment by equivalent EEG sources: a cross-sectional and longitudinal study. Clin Neurophysiol 2000; 111: 1961-1967.

Jelic V, Johansson SE, Almkvist O *et al*. Quantitative electroencephalography in mild cognitive impairment: longitudinal changes and possible prediction of Alzheimer's disease. 2000. p. 533-40.

Jeong J. EEG dynamics in patients with Alzheimer's disease. 2004. p. 1490-505.

Jonkman EJ. The role of the electroencephalogram in the diagnosis of dementia of the Alzheimer type: an attempt at technology assessment. 1997. p. 211-9.

Jonsson L, Berr C. Cost of dementia in Europe. 2005. p. 50-3.

Kwak YT. Quantitative EEG findings in different stages of Alzheimer's disease. 2006. p. 456-61.

Laufs H, Krakow K, Sterzer P *et al*. Electroencephalographic signatures of attentional and cognitive default modes in spontaneous brain activity fluctuations at rest. 2003. p. 11053-8.

Lehtovirta M, Partanen J, Kononen M *et al*. Spectral analysis of EEG in Alzheimer's disease: relation to apolipoprotein E polymorphism. Neurobiol Aging 1996; 17: 523-526.

Lustig C, Snyder AZ, Bhakta M *et al*. Functional deactivations: change with age and dementia of the Alzheimer type. 2003. p. 14504-9.

Maestu F, Arrazola J, Fernandez A *et al*. Do cognitive patterns of brain magnetic activity correlate with hippocampal atrophy in Alzheimer's disease? 2003. p. 208-12.

McKhann G, Drachman D, Folstein M, Katzman R, Price D, Stadlan EM. Clinical diagnosis of Alzheimer's disease: report of the NINCDS-ADRDA Work Group under the auspices of Department of Health and Human Services Task Force on Alzheimer's Disease. 1984. p. 939-44.

Morcom AM, Fletcher PC. Does the brain have a baseline? Why we should be resisting a rest. 2006.

Olesen J, Leonardi M. The burden of brain diseases in Europe. 2003. p. 471-7.

Osipova D, Ahveninen J, Jensen O, Ylikoski A, Pekkonen E. Altered generation of spontaneous oscillations in Alzheimer's disease. 2005. p. 835-41.

Osipova D, Ahveninen J, Kaakkola S, Jaaskelainen IP, Huttunen J, Pekkonen E. Effects of scopolamine on MEG spectral power and coherence in elderly subjects. 2003. p. 1902-7.

Osipova D, Rantanen K, Ahveninen J *et al*. Source estimation of spontaneous MEG oscillations in mild cognitive impairment. 2006. p. 57-61.

Pijnenburg YA, Made Y, van Cappellen van Walsum AM, Knol DL, Scheltens P, Stam CJ. EEG synchronization likelihood in mild cognitive impairment and Alzheimer's disease during a working memory task. 2004. p. 1332-9.

Prichep LS. Quantitative EEG and electromagnetic brain imaging in aging and in the evolution of dementia. 2007. p. 156-67.

Raichle ME, MacLeod AM, Snyder AZ, Powers WJ, Gusnard DA, Shulman GL. A default mode of brain function. 2001. p. 676-82.

Riekkinen P, Buzsaki G, Riekkinen P, Jr., Soininen H, Partanen J. The cholinergic system and EEG slow waves. Electroencephalogr Clin Neurophysiol 1991; 78: 89-96.

Stam CJ, Jones BF, Manshanden I *et al*. Magnetoencephalographic evaluation of resting-state functional connectivity in Alzheimer's disease. 2006. p. 1335-44.

Stoffers D, Bosboom JL, Deijen JB, Wolters EC, Berendse HW, Stam CJ. Slowing of oscillatory brain activity is a stable characteristic of Parkinson's disease without dementia. Brain 2007; 130: 1847-1860.

Waldemar G, Dubois B, Emre M *et al*. Recommendations for the diagnosis and management of Alzheimer's disease and other disorders associated with dementia: EFNS guideline. Eur J Neurol 2007; 14: e1-26.

Node 3

Functional neural network analysis in frontotemporal dementia and Alzheimer's disease using EEG and graph theory

BMC Neuroscience 2009

Willem de Haan*[1], Yolande AL Pijnenburg[1], Rob LM Strijers[2], Yolande van der Made[2], Wiesje M van der Flier[1], Philip Scheltens[1] and Cornelis J Stam[2]

[1]Alzheimer center and Department of Neurology, VU University Medical Center, Amsterdam, the Netherlands

[2]Department of Clinical Neurophysiology, VU University Medical Center, Amsterdam, the Netherlands

ABSTRACT

Background: Although a large body of knowledge about both brain structure and function has been gathered over the last decades, we still have a poor understanding of their exact relationship. Graph theory provides a method to study the relation between network structure and function, and its application to neuroscientific data is an emerging research field. We investigated topological changes in large-scale functional brain networks in patients with Alzheimer's disease (AD) and frontotemporal lobar degeneration (FTLD) by means of graph theoretical analysis of resting-state EEG recordings. EEGs of 20 patients with mild to moderate AD, 15 FTLD patients, and 23 non-demented individuals were recorded in an eyes-closed resting-state. The synchronization likelihood (SL), a measure of functional connectivity, was calculated for each sensor pair in 0.5–4 Hz, 4–8 Hz, 8–10 Hz, 10–13 Hz, 13–30 Hz and 30–45 Hz frequency bands. The resulting connectivity matrices were converted to unweighted graphs, whose structure was characterized with several measures: mean clustering coefficient (local connectivity), characteristic path length (global connectivity) and degree correlation (network 'assortativity'). All results were normalized for network size and compared with random control networks.

Results: In AD, the clustering coefficient decreased in the lower alpha and beta bands ($p < 0.001$), and the characteristic path length decreased in the lower alpha and gamma bands ($p < 0.05$) compared to controls. In FTLD no significant differences with controls were found in these measures. The degree correlation decreased in both alpha bands in AD compared to controls ($p < 0.05$), but increased in the FTLD lower alpha band compared with controls ($p < 0.01$).

Conclusion: With decreasing local and global connectivity parameters, the large-scale functional brain network organization in AD deviates from the optimal 'small-world' network structure towards a more 'random' type. This is associated with less efficient information exchange between brain areas, supporting the disconnection hypothesis of AD. Surprisingly, FTLD patients show changes in the opposite direction, towards a (perhaps excessively) more 'ordered' network structure, possibly reflecting a different underlying pathophysiological process.

BACKGROUND

Understanding the relation between structure and function of the brain is one of the basic questions of neuroscience. Although a large body of knowledge about both healthy and pathological brain structure and function has been gathered over the last decades, we still have a poor understanding of their exact relationship. A clinical illustration of this state of affairs is dementia, a syndrome in which the link between pathophysiology and clinical symptoms is often ambiguous. There is a general consensus that cognition is a highly distributed and dynamic process, and thus depends on the coordinated interaction between many brain regions. It therefore seems reasonable to assert that approaches with an emphasis on structural damage will not be able fully explain cognitive (dys)function, since the complex interactions and interdependencies between different regions are neglected. A more complete perspective would have to take into account both the local and the global structural changes as well as the dynamics of the brain, and the way these different aspects are related. Therefore, several authors have argued that in addition to our present knowledge a more integrative network or system view on the brain is necessary [1-3]. Over the last decade, due to the development and interdisciplinary combination of techniques and methods, network analysis applied to biological research fields such as immunology, genetics and neuroscience has taken a great flight.

A novel approach, applying concepts from graph theory (a branch of the mathematical field of complex network theory) to neurophysiological data, is a promising new way to characterize brain activity [4-6]. It provides a method to evaluate whether the functional connectivity patterns between brain areas resemble the organization of theoretically efficient, flexible or robust networks (based on the strenght of synchronization in the oscillatory electromagnetic activity of different brain regions as measured by EEG or MEG). A fundamental hypothesis is that cognitive dysfunction can be illustrated and/or explained by a disturbed functional organization. Applied to patient data, this technique might provide more insight in the pathophysiological processes underlying the various forms of dementia, and potentially lead to the development of new diagnostic or monitoring tools.

Graph theory provides a method to study the relation between network structure and function, concerning for example qualities such as network efficiency, robustness, cost, or growth. Watts and Strogatz introduced so-called 'small-world' networks, that have an optimal balance between local specialization and global integration [7]. Small-world networks are optimal in the sense that they allow efficient information processing, are (wiring) cost-effective, and relatively resilient to network damage. Many real-life systems appear to have small-world properties [79]. Both anatomical and functional brain networks can be described by forming graphical network representations based on the measured (functional) connections. The presence of small-world network organization in brains of healthy humans was confirmed in numerous studies [5,6,10-14]. A few studies have recently shown that different types of brain pathology interfere with the normal

small-world architecture [15-17]. Furthermore, a loss of small-world network properties in several frequency bands of EEG and MEG recordings in AD has been reported, with a more 'random' overall network structure [12,18]. Loss of small-world structure in AD was also demonstrated in recent MRI studies applying graph theory [19,20].

In view of these findings, one might speculate that other types of dementia also demonstrate a disturbance of the 'normal' small-world configuration of brain networks, perhaps even in a disease-specific way. This hypothesis is explored in the present study.

Many network characteristics can be used to examine neuroscientific data [5,6]. Since our current interest was mainly with (loss of) general structure, we expanded our analysis with a third measure, the so-called 'degree correlation' (R) [8,21]. It describes the tendency of nodes to form connections with nodes with similar degree. With a positive degree correlation, the chance that a node with a certain amount of connections neighbors other nodes with approximately the same amount of connections is larger. When this is the case for many nodes, a graph is called 'assortative'. Interestingly, most social networks tend to be assortative, while most biological networks tend to be disassortative. Assortative networks are thought to be better connected as a whole, and more robust to damage, i.e. deletion of connections [22].

In FTLD, a neurodegenerative disorder that is associated with more focal pathology in the frontal and/or temporal areas, we expected to find changes in functional network organization, but not identical to the situation in AD. The observation that many patients with a clinical manifestation of FTLD lack typical structural abnormalities on neuro-imaging suggests that functional changes might play a more important role [23]. We therefore set out to study functional networks both in patients with AD and FTLD. Subjects and EEG data were identical to Pijnenburg et al. [24].

RESULTS

Subject characteristics

The main subject characteristics are summarized in Table 1. The FTLD group consisted of more males than the other two groups. Therefore, both SL and network measures were assessed for each gender group, not leading to any significant differences.

Table 1 – Subject Characteristics

	AD	FTLD	Controls	Significance
Age	65.5 (51-76)	63 (43-79)	59 (49-78)	p=0.48
M:F	7:13	12:3	14:9	p=0.02
MMSE	21.5 (14-27)	24.5 (13-30)	29 (27-30)	p=0.09[1] p<0.001[2] p=0.002[3]

[1]=AD compared to FLTD, [2]=AD compared to controls, [3]=FTLD compared to controls. AD=Alzheimer's disease, FTLD=frontotemporal lobar degeneration, M=male, F=female

Graph analysis

All subjects demonstrated small-world network properties in all frequency bands, expressed by the finding that the small-worldness (σ) values were larger than 1 in all frequency bands. In our study, the only significant change in σ was found in the AD group, where a decrease compared to controls was found in the beta band ($p < 0.05$).

Clustering coefficient, characteristic path length and degree correlation results have been summarized in figures 1, 2 and 3. The mean, normalized clustering coefficient (γ) was decreased in AD compared to controls in the lower alpha ($p < 0.05$) and beta ($p < 0.05$) frequency bands. FTLD showed a non-significant but constant trend in opposite direction in the higher frequency bands. In all frequency bands, AD and FTLD median values changed in opposite directions, reaching significance in both alpha bands ($p < 0.01$).

The normalized characteristic path length (λ) was decreased in AD compared to controls in the lower alpha ($p < 0.05$) and gamma ($p < 0.01$) frequency bands. In those same bands, the difference between AD and FTLD was highly significant ($p < 0.01$ and $p < 0.05$, respectively). In the FTLD group, no differences with the control group were found.

The degree correlation (R) was decreased in AD compared to controls and FTLD in both alpha frequency bands ($p < 0.05$ and $p < 0.01$, respectively). In FTLD compared to controls, the increase in R was highly significant in the lower alpha band ($p < 0.01$). All normalized network measures were within the same range as previously reported results (see also table 2).

Correlation between AD network characteristics and MMSE score

In the AD group, MMSE score was documented in 21 out of 23 subjects. In the lower alpha band in AD, normalized characteristic path length (λ) was positively correlated with MMSE score ($r = 0.50$, $p < 0.05$).

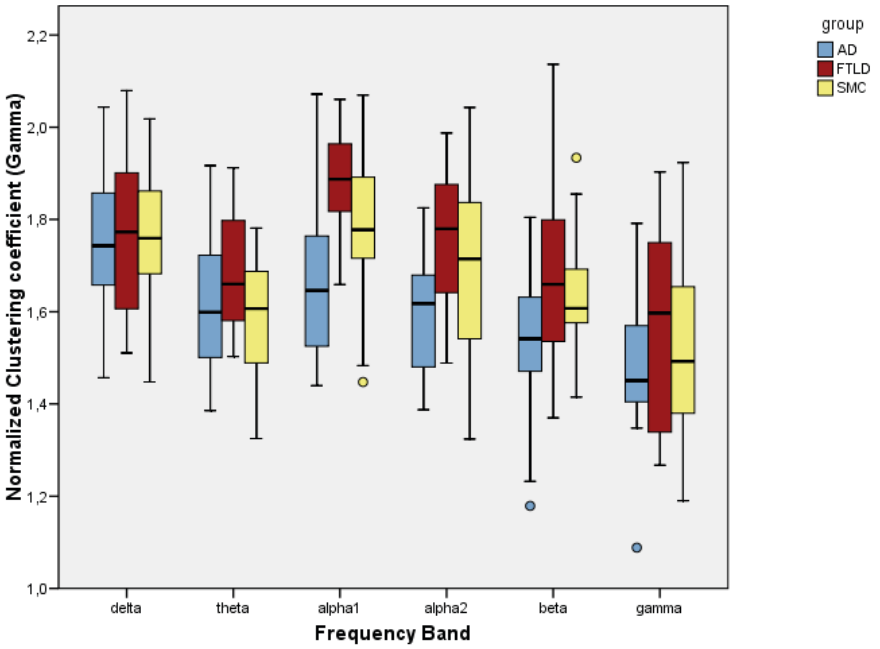

Figure 1 Clustering coefficient. Boxplots showing differences in normalized clustering coefficients (γ) for the separate frequency bands. Alpha1= lower alpha band (8-10 Hz), alpha2= upper alpha band (10-13 Hz).

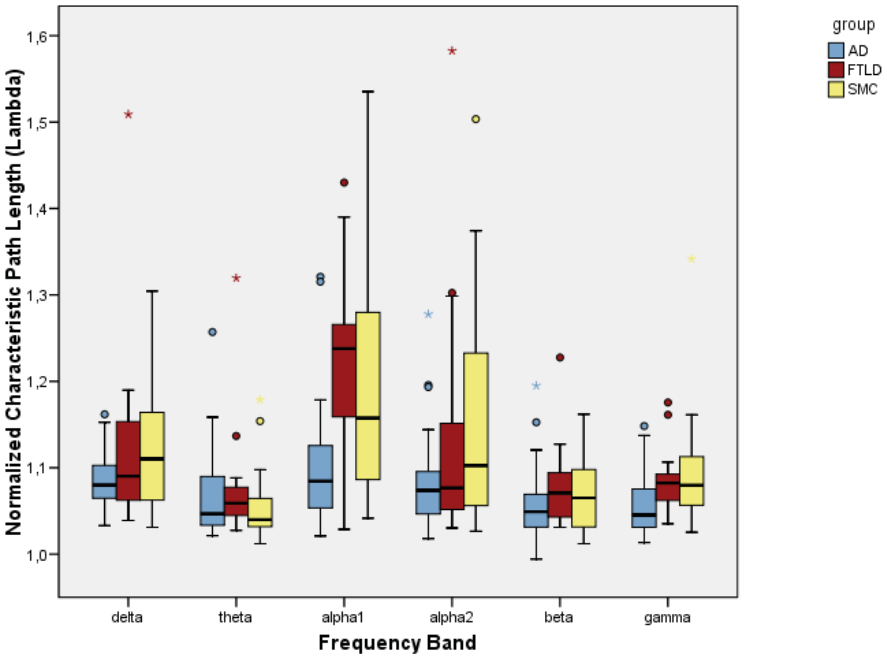

Figure 2 Path length. Boxplots showing differences in normalized path lengths (λ) for the separate frequency bands. Alpha1= lower alpha band (8-10 Hz), alpha2= upper alpha band (10-13 Hz).

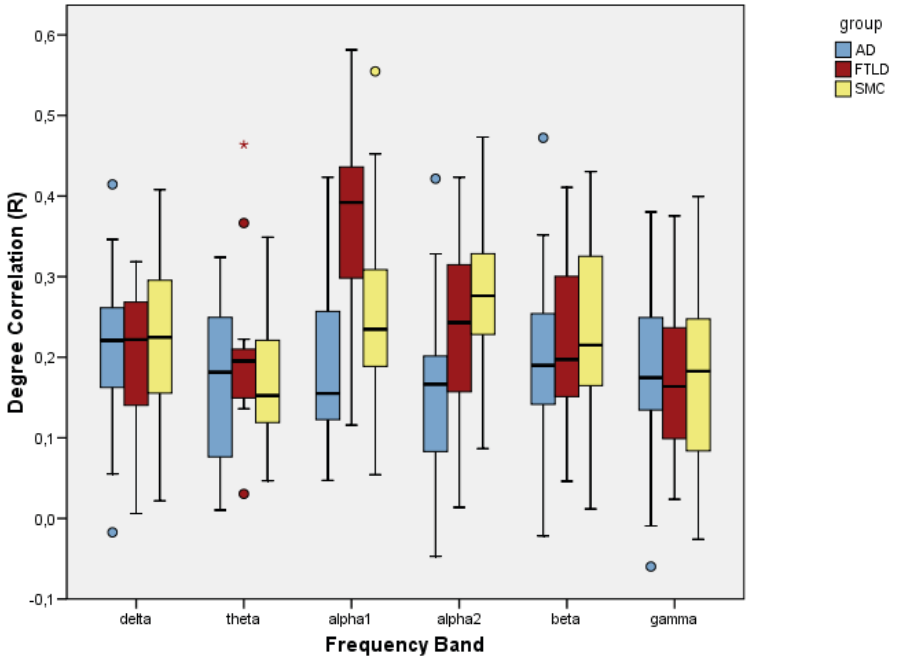

Figure 3 Degree Correlation. Boxplots showing differences in degree correlation (R) for the separate frequency bands. Alpha1= lower alpha band (8-10 Hz), alpha2= upper alpha band (10-13 Hz).

Table 2 – Comparison of small-world characteristics with AD network literature.

Study	group	N	γ	λ	σ
Present study	Control group	21	1.67	1.11	1.50
EEG (Stam 2007)	Healthy controls	21	1.58	1.07	1.48
MEG (Stam 2004)	Healthy controls	126	4.20	1.80	2.30
fMRI (Supekar 2008)	Healthy controls	90	1.74	1.05	1.66
Present study	AD	21	1.61	1.08	1.49
EEG (Stam 2007)	AD	21	1.60	1.12	1.43
fMRI (Supekar 2008)	AD	90	1.56	1.04	1.50
Present study	FTLD	21	1.73	1.12	1.55

Comparison for unweighted network characteristics of the present study with earlier reported work. Although there are considerable methodological differences between these studies, all results indicate that network structure in both healthy persons and AD patients fall can be described as having Small-world network characteristics (σ>1). N= number of nodes in the graph, γ=normalized clustering coefficient, λ=normalized characteristic path length, σ= small-worldness (γ/ λ). In the EEG and MEG studies, values have been averaged over all frequency bands.

DISCUSSION

In this study we applied graph analysis to resting-state EEG data of AD, FTLD and control subjects to characterize the large-scale organization of brain networks based on functional connectivity strength. The main finding is that this approach is able to demonstrate notable differences in functional brain network organization in AD and FTLD patient groups. FTLD network changes were often significantly different and in opposite direction compared to AD, possibly reflecting a different underlying disease mechanism.

Frontotemporal lobar degeneration

To the best of our knowledge, this is the first documentation of graph analysis applied to FTLD patient data. First, it is important to recognize that network characteristics can show change regardless of the fact that no significant changes in underlying functional connectivity were found [24]. This is because they should primarily reflect global (changes in) network organization, and not in connectivity strength. Although we found no significant changes in the clustering coefficient and characteristic path length in FTLD compared to controls, a consistent trend (especially in the higher frequency bands) was that these network variables increased, and thus changed in the opposite direction compared to the AD group (see figures 1 and 2), leading to highly significant differences between FTLD and AD in the lower alpha frequency band. In a spectral analysis study, a similar divergence between AD and FTLD qEEG data was reported [25].

Clustering coefficient and path length are not the only graph measures sensitive to detect network structure. The degree correlation R increased significantly in the lower alpha band, which is also a sign of more structure in the network. The fact that only the degree correlation reached significance suggests that, in this case, it is a more sensitive measure for capturing network structure differences between FTD and AD. The tendency towards a more regular network structure can be interpreted as a deviation from the presumably optimally balanced small-world network architecture. Why this strong increase in degree correlation is mainly found in the lower alpha band is not easy to explain in physiological terms, but involvement of the alpha band in FTD has been reported before [26].

Since there are not many discriminating EEG measures between FTLD and healthy persons, the increased assortativity as measured by the degree correlation (R) in the FTLD lower alpha frequency band is intriguing. An assortative network is generally associated with a more efficient information processing and a lower vulnerability to network damage [8,21,22]. Thus, the higher degree correlation we found in FTD compared to healthy controls seems paradoxical. In this regard, it is interesting to note that hierarchy in a network has been described as the tendency of hubs to connect to nodes that are not otherwise connected to each other [27]. Assortativity and hierarchy might thus be

reflected upon as complementary network phenomena. Basset et al. showed in their resting-state fMRI study that in the multimodal sub-network of persons with schizophrenia, assortativity increased and hierarchy decreased [28]. Our increase in assortativity in the FTLD lower alpha band could perhaps also be interpreted as a loss of network hierarchy in this regard.

Since the application of graph analysis to neuroscientific data is still a very new approach, it is too soon to relate FTD network analysis outcomes to FTD pathophysiology, and draw firm conclusions. However, based on recent literature, one could argue as follows: FTLD is usually characterized by frontotemporal dysfunction and/or atrophy and related neuropsychological impairments, like loss of executive functions. Seeley et al. recently demonstrated in an fMRI study that specific patterns of atrophy and functional network activity converge in several neurodegenerative diseases, including FTD [29]. Meunier et al. showed that human functional brain networks appear to be modular, and that a large frontal module has extensive connections with other brain areas [30]. In FTLD, particularly the fronto-subcortical and temporo-subcortical circuits are affected, whereas the parietal and occipital cortices are relatively spared. The frontal and temporal lobes are responsible for highly complex cognitive functions such as social cognition. Clinically, the disorder presents with personality and behavioral changes resulting for example in mental rigidity, loss of cognitive flexibility and perseveration. It is conceivable that FTLD leads to a pathologically ordered and rigid network by altering long-distance network traffic to and from the coordinating frontal areas, but this hypothesis has to be explored in future studies. Interestingly, in an fMRI study of ADHD patients a similar shift towards a more ordered network type was reported [31], and the same seems to be happening in patients with Parkinson's disease dementia (Olde Dubbelink KTE, unpublished results).

Alzheimer's Disease

With decreasing local and global network parameters in AD in the present study, the large-scale functional brain network structure deviates towards a more random type. The loss of structure as expressed by the lower clustering and path length in the higher frequency bands in AD seems to support the notion of AD as a disconnection syndrome, together with the well known slowing of brain activity and loss of functional connectivity in AD [32]. The lower alpha band in particular has been related to global arousal/attention, and deterioration of this cognitive domain is a common feature of AD. The finding that the lower alpha band produces the most striking differences between AD and controls could suggest that network changes mainly affect the level of attention/arousal, which has an effect on other cognitive abilities, and thus contributes to the multi-domain, non-specific cognitive impairment as seen in AD. However, as work by Klimesch et al. has pointed out, attributing global arousal level as physiological meaning

to the alpha band is more reliable when the individual alpha frequency peak (IAF) is taken into account [33]. For easier comparison with previous research, fixed bands were used in this study.

A recent magnetoencephalographic AD study showed very similar results: a decreased clustering coefficient and characteristic path length in the lower alpha band [18]. At first, a shorter path length related to a worse cognitive status seems counter-intuitive. However, theoretically, a shorter path length is not necessarily an advantage in a complex network, since it is the overall structure that must be an effective balance between local specialization and global integration. Decreases in both clustering coefficient and path length mean a more rapid shift towards network randomness. Earlier EEG work [12] did find an increase of the characteristic path length in the beta frequency band in AD, not in line with the present findings. The explanation for this might be found in two methodological developments. First, for the present study (and the MEG study) a different algorithm was adopted for determining the characteristic path length, which deals better with disconnected nodes in a graph [22]. Another major difference is that here, the network measures are normalized by comparing them to random networks (see methods section for a more detailed explanation of both issues). For comparison with results from other studies, table 2 provides an overview of all AD-related graph analysis findings so far.

Our finding that in AD the R decreases in both alpha bands is in agreement with the notion of the AD network losing structure and becoming more random and disorganized, as shown by the decrease of γ and λ in AD. All these findings taken together seem to support the 'disconnection syndrome' hypothesis of AD; deterioration of cognition due to loss of functional connectivity and organization. The positive correlation of the characteristic path length with MMSE score in the lower alpha band in AD also supports this idea.

Methodological issues

In this study a few issues regarding methodological limits or possible confounders should be addressed. Subjects and EEG data were identical to Pijnenburg et al., and several study limits have been discussed there [24].

Using SMC as a control group is a debatable choice, since people in this group have been reported to show differences compared to persons without SMC [34], and have a higher chance of having an underlying neurodegenerative disease such as AD or FTLD than healthy controls [35], and this might have led to a slight underestimation of group differences in our study. However, the chance that SMC subjects have an underlying FTLD is very small, and since FTLD and AD subjects showed opposite network changes, an underestimation of the differences between SMC and FTLD is not very likely. We have the following reasons for choosing SMC as a control group: First, SMC subjects are more

representative of the population visiting memory clinics than completely healthy persons. Therefore, when searching for clinically relevant features, a comparison involving SMC might be more useful. Second, SMC subjects in our clinic have had a comprehensive screening with proven test methods, after which no objective impairments are found. The absence of cognitive impairment in this group might be more reliable then in a so-called 'healthy' control group who have not participated in extensive testing.

Another concern is medication use, since it can affect recorded brain activity [36,37]. However, since the EEG, MMSE and other diagnostic tests had been performed as part of the diagnostic process, no pharmacological therapy (like e.g. cholinesterase-inhibitors in AD) had yet been initiated. There was an incidental report on the use of pre-diagnostic psycho-active medication (benzodiazepine use in two FTD patients and two controls, Exelon use in two AD patients), but since these persons did not show outlying SL values, network analysis results or clinical characteristics, we are convinced this can not have had any notable influence on the results in this study.

While interpreting our results, readers should be aware of several statistical limitations: first, we did not apply corrections for multiple testing. However, since network measure data did not show a Gaussian distribution, we used nonparametric statistical testing, which makes less a priori assumptions. Also, the most important significant findings we report are not near the $p = 0.05$ level, and almost all the non-significant results in other bands showed constant trends in the same direction (see figures 1, 2 and 3), rendering it unlikely that significant effects are based on coincidence. Finally, in the non-parametric Kruskal-Wallis it is not possible to adjust for covariates such as age, but since our groups were age-matched this should not have a large effect.

A graph theoretical concern deals with the decision to form unweighted graphs based on binary connectivity matrices obtained by filtering the original SL values with an arbitrarily chosen threshold. A justified question is how to determine the height of this threshold, since network results are dependent on this. This question has been addressed in [12], where network variables were analyzed as a function of different K (mean degree of the network) thresholds. This was also to ensure that the resulting networks would be of similar size, and therefore more easily comparable in terms of structure. In a similar way we have analyzed network results across a range of K-values [see additional files 1, 2, 3 and 4]. To avoid disconnected and fully connected, random graphs, K values outside this range were not examined. For clarity reasons, we chose one threshold value ($K = 5$) as representative for the whole range. An alternative approach is to convert the original SL-based connectivity matrix directly into a 'weighted' graph, in which the connections between nodes in a graph have variable strengths. This approach is explored in a recent MEG-study in Alzheimer patients [18].

Future directions

Whether functional network changes in neurophysiologic data can be linked to specific pathophysiological mechanisms or clinical symptoms, is still unclear at this stage, and further systematic study is needed. Graph theory offers a growing amount of techniques to describe topological network features like modularity, node centrality (e.g. 'betweenness'), or synchronizability [5,6,8,22]. Furthermore, comparison of network findings with other neurodegenerative diseases (e.g. Huntington's disease, PSP) and clinical/pathophysiological measures (e.g. (f)MRI, CSF, APOE status [38,39] or neuropsychological test-scores) would be of interest; it is conceivable that different cognitive symptoms arise from different types of network disturbance, or that neuronal or synaptic loss in discrete regions leads to specific network disturbance. Another relevant question is whether loss of neurotransmitter function (e.g. acetylcholine in AD) has notable implications for network function, because this could lead to a non-invasive method to monitor or even predict cholinergic status and potential medication effectiveness. Cholinergic effects have been associated with enhanced functional connectivity [36]. Finally, it would be of interest to compare graph analysis results of EEG and MEG recordings in the same individuals, and to look at longitudinal measurements, taking into account effects of aging and disease course.

Conclusion

AD and FTLD patients show dissimilar resting-state functional brain network disturbance. Whereas in AD there is a general loss of connectivity and network structure, FTLD shows a tendency towards a more ordered network structure. This suggests that the approach used in our study, applying graph analysis to EEG data, can be used for identifying differences and possibly for gaining more insight in the pathophysiological processes underlying these forms of dementia. With this new, integrative perspective on large-scale brain function emerging, we may contribute to bridging the gap in our understanding between brain structure and function.

METHODS

Patient diagnosis and recruitment

Subjects and EEG data were identical to Pijnenburg et al. [24]. Fifteen consecutive patients with FTLD according to the criteria of Neary and Snowden [40] were recruited from the Alzheimer Centre of the VU University Medical Centre. Twenty patients with probable AD according to the NINCDS-ADRDA criteria [41] matched for age and disease severity were drawn from the Alzheimer Center clinical database. All patients underwent a standard battery of examinations including medical history, inform-ant-based history,

physical and neurological examination, screening laboratory tests, psychometric tests, MRI, and EEG. All diagnoses were made by consensus in a multidisciplinary team. The diagnoses were kept under review and only considered correct if the clinical course over a period of at least one year of follow up was consistent with the diagnosis. Twenty-three subjects with subjective cognitive complaints served as a control group. They presented with cognitive (mostly memory related) complaints at our clinic, but were found to have no objective cognitive disorder after thorough testing (the same diagnostic procedure as described above). The study was conducted in accordance with regional research regulations and conformed to the Declaration of Helsinki.

EEG Acquisition

EEGs were recorded using an OSG digital EEG equipment (Brainlab (R)) at the following positions of the international 10–20 system: Fp2, Fp1, F8, F7, F4, F3, A2, A1, T4, T3, C4, C3, T6, T5, P4, P3, O2, O1, Fz, Cz, Pz with an average reference (including all electrodes except Fp2/1 and A2/1). ECG was recorded in a separate channel. Electrode impedance was below 5 kOhm. Initial filter settings were: High pass filter = 0.16 Hz, low pass filter = 70 Hz. Sample frequency was 500 Hz and A-D precision 16 bit. Subjects were seated in a slightly reclined chair in a sound attenuated, dimly lit room, and instructed to stay alert as much as possible during the whole recording. Further offline post-processing and epoch selection was performed by an experienced investigator (CS), who was blinded to the diagnosis, and who took care to exclude data with artifacts due to for example (eye) movements, drowsiness, or technical issues. For this study, 4 epochs (sample frequency 500 Hz; 8.19 s) of a no-task eyes-closed condition were selected and band-pass filtered for the commonly used frequency bands: delta (0,5–4 Hz), theta (4–8 Hz), lower alpha (8–10 Hz), upper alpha (10–13 Hz), beta (13–30 Hz) and gamma (30–45 Hz). All further analyses were performed for these bands separately.

Graph theory

A short illustration of the basic principles of graph theory used in this study is provided in figure 4.

Graphical representations of the functional brain network are formed using the functional connectivity measure 'synchronization likelihood' (SL) as a basis; this multi-step procedure is outlined in figure 5. The SL is a general measure of the synchronization between two time series, sensitive for linear and nonlinear interdependencies. SL procedure and results for this group have been published in [24]. A more detailed technical description is provided in [42,43].

For each frequency band, the SL calculation produces a value of connectivity strength for every sensor pair, which results in a matrix showing the connectivity between all possible sensor pairs (step 2 in figure 5). For this study we used unweighted, binary graphs,

which means that only connections with a SL value higher than a (chosen) threshold will be realized in the representing network graph. Here, an important methodological problem has to be tackled; when forming graphs (step 3 in figure 5), the results might be influenced by differences in the mean level of synchronization between groups. Because the SL is expected to be significantly lower for Alzheimer patients than controls, for a given threshold, AD graphs will have fewer connections than the controls graphs. Therefore, thresholds are chosen in such a way that the resulting graphs of the different groups have an equal mean degree K (see figure 6). Persisting dissimilarities between group networks will more likely be due to true differences in network organization.

Since network-derived measures are not just dependent on network structure, but also on network size, between-group comparison should be done on networks of equal size. To achieve this, the SL-threshold is chosen in such a way that graphs in both groups are guaranteed to have the same average number of edges, so that any remaining network differences between the groups reflect differences in graph structure. Because the choice of the threshold is arbitrary, a range of different thresholds is examined (see Additional files 1, 2, 3 and 4).

Graphs can be formed by a set of nodes and connections, and can then be characterized by various measures (step 4 and 5 in figure 5). The number of connections a node possesses is called the degree (k) of that node. The degree (K) of a network is the average degree of all nodes. In the following analyses the results of networks with an average degree of K = 5 are shown, since they were representative for the findings at other threshold levels. Two other core network measures are the clustering coefficient C and the characteristic path length L (see also figure 4). The clustering coefficient C of a node is the ratio of all existing connections between the 'neighbors' of a node (nodes that are one step away) and the maximum possible number of edges between the neighbors. The mean clustering coefficient is computed for all nodes of the graph and then averaged. It is a measure for the tendency of network elements to form local clusters. The characteristic path length is the average shortest path connecting any 2 nodes of the graph: the length of a path is indicated by the number of connections it contains. The characteristic path length L (averaged shortest path length between all node pairs) is an emergent property of the graph, which indicates how well its elements are integrated/interconnected. In the conventional method to calculate path length L, disconnected nodes in a network pose a problem. Newman proposed to define L to be the 'harmonic mean' distance between pairs, or the reciprocal of the average of the reciprocals [22]. In this way, calculation of L resembles the 'global efficiency' introduced by Latora and Marchiori [44].

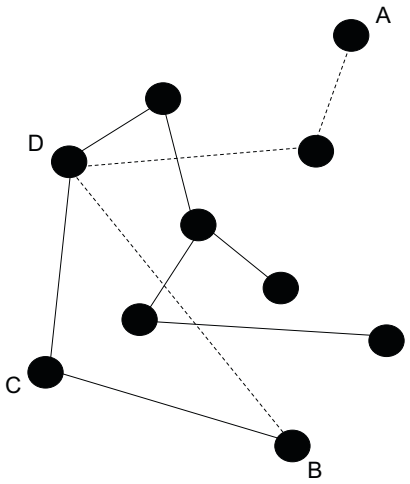

Figure 4 Graph theory principles. Graphs can represent any kind of network. Dots represent *nodes*, and lines connecting the dots are the *connections*. The degree (K) of a node is it's number of connections. The clustering coefficient (C), measuring local connectivity of a node, is the likelihood that its neighbors are connected. For node C, with neighbours B and D, the clustering coefficient is 1. The path length (L), a measure of global connectivity, is the minimum number of connections between two nodes. The path length between vertices A and B consists of three edges, indicted by the striped lines. The degree correlation (R), a measure of network clustering according to degree, is the ratio of the degrees of two neighboring nodes. Figure taken with permission from *Stam and Reijneveld. Graph theoretical analysis of complex networks in the brain. Nonlinear Biomedical Physics. 2007c; 1: 3.*

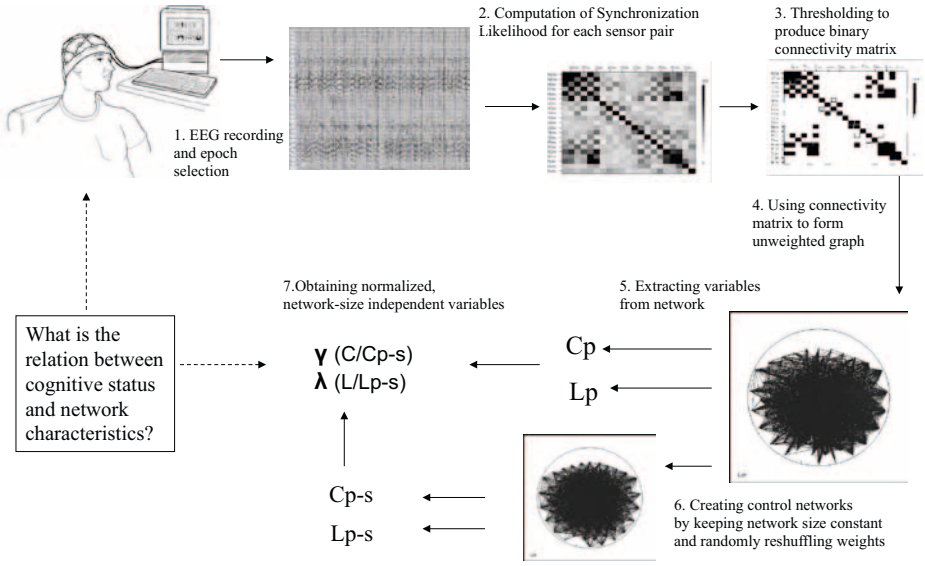

Figure 5 From EEG recording to unweighted graph. Multi-step procedure to obtain normalized network-derived variables. C= clustering coefficient, L= Path length, γ=normalized clustering coefficient, λ=normalized path length

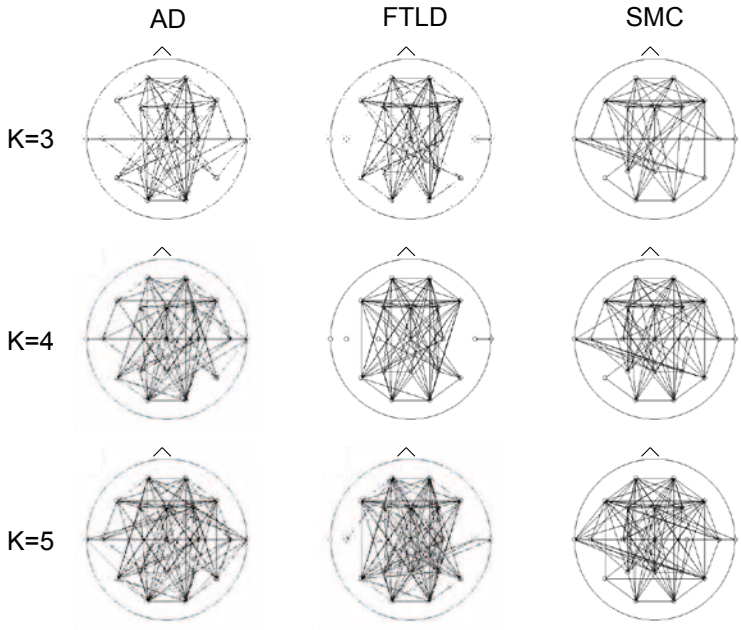

Figure 6 Unweighted graphs of the lower alpha band (8-10 Hz) for different patient groups and different fixed average degrees (K). For the AD, FTLD and SMC groups, the functional connectivity (SL) based graphs are shown as headplots for different values of K. Lower K values (higher threshold) result in a sparser network. On visual inspection, it is obvious that there are inter-group differences.

To obtain normalized measures, network-derived variables are compared with 50 control networks of the same size (step 6 and 7 in figure 5). In the resulting connectivity matrices (after SL computation), all sensor values were consecutively swapped with a different sensor value in the same diagonal halve of the matrix. Since the networks are undirected, both diagonals should be symmetrical, and therefore the new, 'swapped' halve was copied to the other halve of the matrix. This results in an equally-sized network with an identical degree distribution, but a different structure. This same procedure was repeated to obtain 50 random surrogate networks. Gamma (γ) is used for the normalized C (C/C-random), and Lambda (λ) is used for the normalized L (L/L-random).

'Small-worldness' (σ) is the ratio of γ and λ, and is used to describe the balance between the local connectedness and the global integration of a network. When this ratio is larger than 1, a network is said to have Small-world properties [9].

Another investigated graph property concerning network structure is the degree correlation [8,21,22]. The degree correlation (R) indicates whether the degree of a node is influenced by the degree of another node to which it connects. The degree correlation is calculated by obtaining the Pearson's correlation of the degrees of two connected nodes, repeating this for every connected node pair, and then averaging these correlations.

Correlations between network measures and MMSE score were tested for the AD group only, since documentation for the FTD group was incomplete (10 of 15 MMSE scores known).

Statistical evaluation

For statistical analysis, the SPSS 15.0 package for Windows was used. Since not all network-derived variables showed a Gaussian distribution (Kolmogorov-Smirnov test), network variable comparison between the three diagnostic groups was performed using nonparametric statistics (Kruskal-Wallis test followed by Mann Whitney-U tests when appropriate). Correlations between network measures and MMSE score were calculated with Spear-man's correlations. Separate analyses were performed for each of the six frequency bands. A significance level of $\alpha = 0.05$ was used.

Authors' contributions

WH performed all analyses, and wrote most of the manuscript. CS designed the study, gave advise on neurophysiological and graph theoretical issues, and helped to draft the manuscript. YP recruited and examined patients, gave advise on clinical issues, and helped to draft the manuscript. WF gave advise on statistical and methodological issues, and helped to draft the manuscript. PS, RS and YM helped to draft the manuscript. All authors read and approved the final manuscript.

Acknowledgements

The authors thank mrs. Els van Deventer for continuing support in retrieving relevant literature.

ADDITIONAL MATERIAL

Additional file 1

Threshold analysis in the lower alpha frequency band (8–10 Hz). Graph analysis results of unweighted networks as presented in this paper are dependent on an arbitrarily chosen threshold (in our study K, mean degree of the network). This supplement, including 3 figures, shows that the reported results (K = 5) are representative for a broad range of K thresholds.

[http://www.biomedcentral.com/content/supplementary/14712202-10-101-S1.doc]

Additional file 2

Clustering coefficient. Group comparison of the normalized clustering coefficient (Cp/Cp-s or γ) between conditions for different mean network degrees K (* $p < 0.05$ ** $p < 0.01$ compared to SMC).

[http://www.biomedcentral.com/content/supplementary/14712202-10-101-S2.tiff]

Additional file 3

Path Length. Group comparison of the normalized characteristic path length (Lp/Lp-s or λ) between conditions for different mean network degrees K (* $p < 0.05$ ** $p < 0.01$ compared to SMC).

[http://www.biomedcentral.com/content/supplementary/14712202-10-101-S3.tiff]

Additional file 4

Degree correlation. Group comparison of the degree correlation (R) for different mean network degrees K (* $p < 0.05$ ** $p < 0.01$ compared to SMC).

[http://www.biomedcentral.com/content/supplementary/14712202-10-101-S4.tiff]

REFERENCES

1. Varela F, Lachaux J-P, Rodriguez E, Martinerie J: The brainweb: phase synchronization and large-scale integration. Nature Reviews Neuroscience 2001, 2:229-239.
2. Le van Quyen M: Disentangling the dynamic core: a research program for a neurodynamics at the large scale. Biol Res 2003, 36:67-88.
3. Börner K, Sanyal S, Vespignani A: Network Science. Annu Rev Inform Sci Technol 2007, 41:537-607.
4. Bassett DS, Bullmore E: Small-world brain networks. The neuroscientist 2006, 12:512-523.
5. Stam CJ, Reijneveld JC: Graph theoretical analysis of complex networks in the brain. Nonlinear Biomedical Physics 2007, 1:3.
6. Bullmore E, Sporns O: Complex brain networks: graph theoretical analysis of structural and functional systems. Nat Rev Neurosci 2009, 10(3):186-98.
7. Watts DJ, Strogatz SH: Collective dynamics of "small-world" networks. Nature 1998, 393:440-442.
8. Boccaletti S, Latora V, Moreno Y, Chavez M, Hwang D-U: Complex networks: structure and dynamics. Physics Reports 2006, 424:175-308.
9. Humphries MD, Gurney K: Network 'Small-World-Ness': A Quantitative Method for Determining Canonical Network Equivalence. PLoS ONE 2008, 3(4):e0002051.
10. Bassett DS, Meyer-Linderberg A, Achard S, Duke Th, Bullmore E: Adaptive reconfiguration of fractal small-world human brain functional networks. PNAS 2006, 103:19518-19523.
11. Smit DJ, Stam CJ, Posthuma D, Boomsma DI, de Geus EJ: Heritability of "small-world" networks in the brain: A graph theoretical analysis of resting-state EEG functional connectivity. Hum Brain Mapp 2008, 29(12):1368-78.
12. Stam CJ, Jones BF, Nolte G, Breakspear M, Scheltens Ph: Small-world networks and functional connectivity in Alzheimer's disease. Cereb Cortex 2007, 17:92-99.
13. Gong G, He Y, Concha L, Lebel C, Gross DW, Evans AC, Beaulieu C: Mapping Anatomical Connectivity Patterns of Human Cerebral Cortex Using In Vivo Diffusion Tensor Imaging Tractography. Cereb Cortex 2008, 19(3):524-36.
14. Sporns O, Zwi JD: The small world of the cerebral cortex. Neuroinformatics 2004, 2(2):145-62.
15. Bartolomei F, Bosma I, Klein M, Baayen JC, Reijneveld JC, Postma TJ, Heimans JJ, van Dijk BW, de Munck JC, de Jongh A, Cover KS, Stam CJ: Disturbed functional connectivity in brain tumour patients: evaluation by graph analysis of synchronization matrices. Clin Neurophysiol 2006, 117:2039-2049.
16. Micheloyannis S, Pachou E, Stam CJ, Breakspear M, Bitsios P, Vourkas M, Erimaki S, Zervakis M: Small-world networks and disturbed functional connectivity in schizophrenia. Schizophr Res 2006, 87:60-66.
17. Ponten SC, Bartolomei F, Stam CJ: Small-world networks and epilepsy: graph theoretical analysis of intracerebrally recorded mesial lobe seizures. Clin Neurophysiol 2007, 118(4):918-27.
18. Stam CJ, de Haan W, Daffertshofer A, Jones BF, Manshanden I, van Cappellen van Walsum AM, Montez T, Verbunt JPA, de Munck JC, van Dijk BW, Berendse HW, Scheltens P: Graph theoretical analysis of magnetoencephalographic functional connectivity in Alzheimer's disease. Brain 2009, 132:213-224.
19. He Y, Chen Z, Evans A: Structural insights into aberrant topological patterns of large-scale cortical networks in Alzheimer's disease. J Neurosci 2008, 28(18):4756-66.
20. Supekar K, Menon V, Rubin D, Musen M, Greicius MD: Network analysis of intrinsic functional brain connectivity in Alzheimer's disease. PLoS Comput Biol 2008, 27;4(6):e1000100.
21. Newman MEJ: Assortative mixing in networks. Phys Rev Lett 2002, 89:208701.

22. Newman MEJ: The structure and function of complex networks. Siam Rev 2003, 45(2):167-256.
23. Davies RR, Kipps CM, Mitchell J, Kril JJ, Halliday GM, Hodges JR: Progression in frontotemporal dementia: identifying a benign behavioral variant by magnetic resonance imaging. Arch Neurol 2006, 63(11):1627-31.
24. Pijnenburg YAL, Strijers RL, Made YV, Flier WM van der, Scheltens P, Stam CJ: Investigation of resting-state EEG functional connectivity in frontotemporal lobar degeneration. Clin Neurophysiol 2008, 119(8):1732-8.
25. Lindau M, Jelic V, Johansson SE, Andersen C, Wahlund LO, Almkvist O: Quantitative EEG abnormalities and cognitive dysfunctions in frontotemporal dementia and Alzheimer's disease. Dement Geriatr Cogn Disord 2003, 15(2):106-14.
26. Yener GG, Leuchter AF, Jenden D, Read SL, Cummings JL, Miller BL: Quantitative EEG in frontotemporal dementia. Clin Electroencephalogr 1996, 27(2):61-8.
27. Ravasz E, Barabasí AL: Hierarchical organization in complex networks. Phys Rev E 2003, 67:026112.
28. Bassett DS, Bullmore E, Verchinski BA, Mattay VS, Weinberger DR, Meyer-Lindenberg A: Hierarchical organization of human cortical networks in health and schizophrenia. J Neurosci 2008, 28(37):9239-4827.
29. Seeley WW, Crawford RK, Zhou J, Miller BL, Greicius MD: Neurodegenerative diseases target large-scale human brain networks. Neuron 2009, 62(1):42-52.
30. Meunier D, Achard S, Morcom A, Bullmore E: Age-related changes in modular organization of human brain functional networks. Neuroimage 2009, 44(3):715-23.
31. Wang L, Zhu C, He Y, Zang Y, Cao Q, Zhang H, Zhong Q, Wang Y: Altered small-world brain functional networks in children http://www.biomedcentral.com/1471-2202/10/101 with attention-deficit/hyperactivity disorder. Hum Brain Mapp 2009, 30(2):638-49.
32. Delbeuck X, Linden M Van der, Collette F: Alzheimer's disease as a disconnection syndrome? Neuropsychol Rev 2003, 13(2):79-92. Review
33. Klimesch W: EEG alpha and theta oscillations reflect cognitive and memory performance: a review and analysis. Brain Res Brain Res Rev 1999, 29(2–3):169-95.
34. Rodda JE, Dannhauser TM, Cutinha DJ, Shergill SS, Walker Z: Subjective cognitive impairment: increased prefrontal cortex activation compared to controls during an encoding task. Int J Geriatr Psychiatry 2009, 24(8):865-74.
35. Mitchell AJ: The clinical significance of subjective memory complaints in the diagnosis of mild cognitive impairment and dementia: a meta-analysis. Int J Geriatr Psychiatry 2008, 23(11):1191-202.
36. Wink AM, Bernard F, Salvador R, Bullmore E, Suckling J: Age and cholinergic effects on hemodynamics and functional coherence of human hippocampus. Neurobiol Aging 2006, 27(10):1395-404.
37. Adler G, Brassen S: Short-term rivastigmine treatment reduces EEG slow-wave power in Alzheimer patients. Neuropsychobiology 2001, 43:273-276.
38. Kramer G, Flier WM van der, de Langen C, Blankenstein MA, Scheltens P, Stam CJ: EEG functional connectivity and ApoE genotype in Alzheimer's disease and controls. Clin Neurophysiol 2008, 119(12):2727-32.
39. Jelic V, Julin P, Shigeta M, Nordberg A, Lannfelt L, Winblad B: Apolipoprotein E epsilon4 allele decreases functional connectivity in Alzheimer's disease as measured by EEG coherence. J Neurol Neurosurg Psychiatry 1997, 63:59-65.

40. Neary D, Snowden JS, Gustafson L, Passant U, Stuss D, Black S, Freedman M, Kertesz A, Robert PH, Albert M, Boone K, Miller BL, Cummings J, Benson DF: Frontotemporal lobar degeneration: a consensus on clinical diagnostic criteria. Neurology 1998, 51:1546-54.
41. McKhann G, Drachman D, Folstein M, Katzman R, Price D, Stadlan EM: Clinical diagnosis of Alzheimer's disease: report of the NINCDS-ADRDA Work Group under the auspices of Department of Health and Human Services Task Force on Alzheimer's Disease. Neurology 1984, 34:939-44.
42. Stam CJ, van Dijk BW: Synchronization likelihood: an unbiased measure of generalized synchronization in multivariate data sets. Physica D 2002, 163:236-251.
43. Montez T, Linkenkaer-Hansen K, van Dijk BW, Stam CJ: Synchronization likelihood with explicit time-frequency priors. Neuroimage 2006, 33:1117-25.
44. Latora V, Marchiori M: Efficient behavior of small-world networks. Phys Rev Lett 2001, 87(19):198701.

Node 4

Graph theoretical analysis of magnetoencephalographic functional connectivity in Alzheimer's disease

Brain 2009

C.J. Stam[1], W. de Haan[2], A. Daffertshofer[5], B.F. Jones[7], I. Manshanden[1], A.M. van Cappellen van Walsum[3,8], T. Montez[4], J.P.A. Verbunt[1,6], J.C. de Munck[6], B.W. van Dijk[1,6], H.W. Berendse[2], P. Scheltens[2]

[1] Department of Clinical Neurophysiology and MEG, VU University Medical Center, Amsterdam

[2] Alzheimer Center, Department of Neurology, VU University Medical Center, Amsterdam

[3] Radboud University Nijmegen Medical Centre, Department of anatomy, Nijmegen

[4] Institute of Biophysics and Biomedical Engineering, Faculty of Sciences, University of Lisbon, Portugal

[5] Research Institute MOVE, VU University, Van der Boechorststraat 9, 1081 BT Amsterdam, The Netherlands

[6] Department of Physics and Medical Technology, VU University Medical Center, Amsterdam

[7] Dementia Research Centre, Institute of Neurology, UCL, London, UK

[8] Institute of Technical Medicine, University of Twente, Enschede, The Netherlands.

ABSTRACT

In this study we examined changes in the large-scale structure of resting-state brain networks in patients with Alzheimer's disease (AD) compared to non-demented controls, using concepts from graph theory. MEG was recorded in 18 AD patients and 18 non-demented control subjects in a no-task, eyes-closed condition. For the main frequency bands, synchronization between all pairs of MEG channels was assessed using a phase lag index (PLI, a synchronization measure insensitive to volume conduction). PLI-weighted connectivity networks were calculated, and characterized by a mean clustering coefficient and path length. AD patients showed a decrease of mean PLI in the lower alpha and beta band. In the lower alpha band, the clustering coefficient and path length were both decreased in AD patients. Network changes in the lower alpha band were better explained by a 'Targeted attack' model than by a 'Random failure' model. Thus, AD patients display a loss of resting-state functional connectivity in lower alpha and beta bands even when a measure insensitive to volume conduction effects is used. Moreover, the large-scale structure of lower alpha band functional networks in AD is more random. The modelling results suggest that highly connected neural network 'hubs' may be especially at risk in AD.

INTRODUCTION

A central question in cognitive neuroscience is how cognitive functions depend upon coordinated and integrated activity of specialized, widely distributed brain regions. There is strong support that a network perspective on the brain is required in order to understand higher brain functioning (Le van Quyen, 2003; Varela *et al.*, 2001). How do functional interactions between brain regions take place, and how can this be measured and assessed? For answering these questions an important idea is the so-called functional connectivity that refers to linear or nonlinear statistical interdependencies between time series of physiological signals recorded from different brain regions (Aertsen *et al.*, 1989; Fingelkurts *et al.*, 2005; Friston, 2001; Lee *et al.*, 2003). Functional connectivity is assumed to reflect functional interactions between the underlying brain regions.

The concept of functional connectivity has become very important in the study of brain mechanisms underlying disturbed cognition in Alzheimer's disease (AD), the most frequent cause of dementia in the western population (van der Flier and Scheltens, 2005). AD is characterized by degeneration of neurons starting in the hippocampus, later spreading to the temporal and parietal cortex, and finally involving most cortical areas. Loss of neurons, involvement of white matter as well as disturbed synaptic transmission, e.g. due to decreased levels of acetylcholine (Osipova *et al*., 2003), account for abnormal functional interactions between cortical regions. It has even been suggested that AD can be viewed as a disconnection syndrome (Delbeuck *et al.*, 2003). Support for this concept comes from a number of electro- and magnetoencephalographic (EEG and MEG) studies using conventional coherence as a measure of functional connectivity (Adler *et al.*, 2003; Berendse *et al.*, 2000; Besthorn *et al.*, 1994; Dunkin *et al.*, 1994; Hogan *et al.*, 2003; Jelic *et al.*, 1996; Jiang 2005; Knott *et al.*, 2000; Koenig *et al.*, 2005; Leuchter *et al.*, 1992; Locatelli *et al.*, 1998; Pogarell *et al.*, 2005; Stevens *et al.*, 2001). In most of these studies a consistent decrease of coherence in the alpha and beta band was reported, whereas results for other bands were more variable. Abnormalities of functional connectivity have also been demonstrated with nonlinear synchronization methods (Babiloni *et al.*, 2004; Jeong *et al.*, 2001; Pijnenburg *et al.*, 2004; Stam *et al.*, 2002, 2006). While these studies in general support the hypothesis of a disconnection syndrome in AD, two problems need further attention: (i) assessment of functional connectivity with EEG and MEG can be biased by volume conduction, which may yield spurious correlations between nearby sensors and hence render interpretation unreliable; (ii) connectivity studies in AD are generally very descriptive and lack a more robust framework to discriminate between normal and abnormal networks in the brain.

Nearby EEG electrodes or MEG sensors are likely to pick up activity of identical sources, resulting in strong correlations between recorded signals that reflect simple volume conduction rather than true functional connectivity (Nunez *et al.*, 1997, Srinivasan et al., 2007). Two approaches have been submitted to overcome this problem. First, one may study interdependencies between time series of reconstructed sources rather than signals of recording electrodes or sensors (Amor *et al.*, 2005; David *et al.*, 2002; Gross *et al.*, 2001; Hadjipapas *et al.*, 2005; Lehmann *et al.*, 2006; Tass *et al.*, 2003). While this approach has certainly the added benefit of dealing with interactions between anatomically well-defined brain regions, a major pitfall is the absence of a unique definition of the corresponding source space. Different assumptions may lead to different source models and, hence, different results. However, to date there is no reliable way to decide which model is the proper choice. Second, one may look for time series analysis techniques that extract interdependencies between signals which are not or at least unlikely due to volume conduction. This measure therefore reflects true interactions. An early attempt in this direction was summarized in a study by Nunez and colleagues (1997) who proposed to subtract a baseline random coherence from the measured coherence in order to obtain a reduced, task-related coherence, which is less influenced by volume conduction effects. More recently Nolte and colleagues (2004) proposed to use the imaginary part of the (complex-valued) coherency between two signals. Indeed volume conduction cannot give rise to imaginary coherency, but the magnitude of the imaginary part does not appear to be a proper value to quantify synchronization, since it mixes information on coupling strength and coupling delay. As an alternative, a so-called phase lag index (PLI) was introduced, which reflects the consistency with which one signal is phase leading or lagging with respect to another signal (Stam *et al.*, 2007b). The PLI was shown to be less affected by volume conduction than more traditional measures like coherence, and at the same token, it was rather sensitive to true changes in synchronization. We will exploit this capacity to address possible changes in functional connectivity due to AD. We see an advantage of PLI compared to 'reduced coherency', since although this last method might represent an improvement over traditional coherence, it does rely on several a priori assumptions such as stationarity and linearity, and is still sensitive to signal amplitude. PLI is sensitive to non-linear data and can handle non-stationary data, at least to some degree.

The theoretical framework for understanding large-scale networks is given by 'modern network theory' (for a review see: Boccaletti *et al.*, 2006), a new branch in graph theory, in which networks are represented by a set of nodes (vertices) and connections (edges). See figure 1 for an explanation of the basic principles of graph theory used in this study.

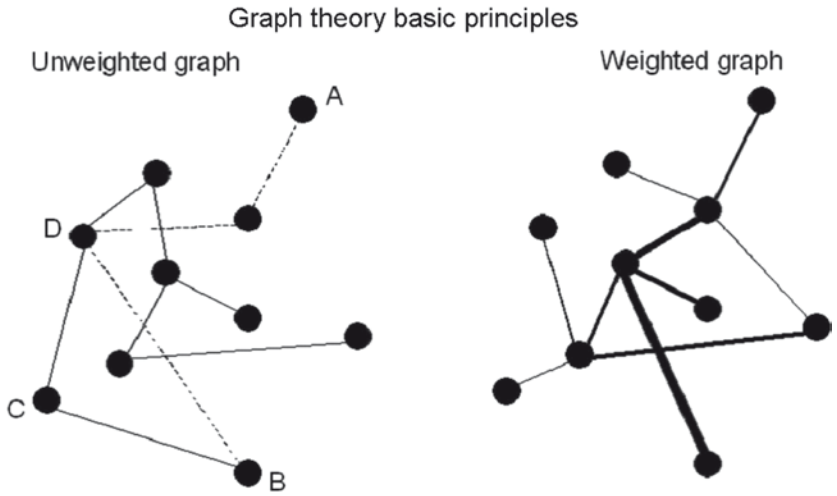

Figure 1. Representation of a network as a graph. Black dots represent the nodes or vertices, and the lines connecting the dots the connections or edges. The left panel shows an unweighted graph. The shortest path length (L) between vertices A and B consists of three edges, indicted by the striped lines. The clustering coefficient (C) of a vertex is the likelihood that its neighbours are connected. For vertex C, with neighbours B and D, the clustering coefficient is 1. When weights are assigned to the edges, the graph is weighted (right panel). Here the weights of the edges are indicated by the thickness of the lines. Figure taken with permission from *Stam and Reijneveld. Graph theoretical analysis of complex networks in the brain. Nonlinear Biomedical Physics. 2007c; 1: 3.*

In recent years, graph theory has been introduced to the study of anatomical and functional networks in the central nervous system (Bassett and Bullmore, 2006; Stam and Reijneveld, 2007c). Graph theory provides models of complex networks in the brain, and allows one to better understand the relations between network structure and the processes taking place on those networks. It can also provide a concept of an 'optimal' network (for example in terms of balancing segregation and integration, performance and cost), and offers scenarios of how complex networks might develop, and how they might respond to different types of damage. Watts and Strogatz (1998) introduced so-called 'small-world'networks, which have a balance between local specialization and global integration that is optimal for information processing, and they showed that several real-life networks possess small-world features. Small-world networks have a relatively high amount of so-called 'local clustering', meaning that nodes are often connected to their neighbours, combined with relatively short 'path lengths', which means that from any node it takes just a few steps to reach any other node in the network. There is now accumulating evidence that different types of structural brain networks display a 'small-world' type network organization characterized by a combination of high local clustering as well as short path lengths (He *et al.*, 2006; Hilgetag *et al.*, 2000; Iturria-Medina *et al.* 2008; Watts and Strogatz, 1998). A similar approach has also been used to study networks of functional connectivity. In several fMRI studies of healthy

subjects, small-world patterns were found (Achard *et al.*, 2006; Salvador *et al.*, 2005; Supekar *et al.,* 2008). The presence of small-world type functional networks in healthy subjects was also confirmed in numerous EEG and MEG studies (Bassett *et al.*, 2006; Smit *et al.*, 2007; Stam, 2004; Stam *et al.*, 2007a). However, only a few studies have yet shown that brain pathology may interfere with the normal small-world architecture. According to Bartolomei *et al.* (2006) brain networks in patients with low-grade glioma's are more random compared to healthy controls. A similar change in network structure was reported in patients with schizophrenia and in patients with epilepsy during the interictal state (Micheloyannis *et al.*, 2006; Ponten *et al.*, 2007; Rubinov *et al.*, 2007). In a recent pilot study on AD a loss of the normal small-world architecture was reported (Stam *et al.*, 2006). In view of these findings one might speculate that brain disease in general gives rise to a deviation from the normal, optimal small-world configuration of brain networks. It is not clear however how such network changes come about.

As mentioned above two questions were addressed in the present study: (i) is it possible to confirm previous EEG and MEG reports of decreased resting state functional connectivity in AD using a method that is less affected by volume conduction? (ii) can graph analysis reveal abnormalities in the large-scale topology of functional connectivity networks in AD, and can such network changes be explained by modelling?

MATERIALS AND METHODS

Patients and controls

Subjects and recordings were identical to Stam *et al.* (2006). The study involved 18 patients (mean age 72.1 years, S.D. 5.6; 11 males; mean MMSE 19.2, range: 13-25) with a diagnosis of probable AD according to the NINCDS-ADRDA criteria (McKhann *et al.*, 1984) and 18 healthy control subjects (mean age 69.1 years, S.D. 6.8; 7 males; mean MMSE 29, range: 27-30), mostly spouses of the patients. Patients and controls were recruited from the Alzheimer Centre of the VU University Medical Centre. Subjects were assessed according to a clinical protocol, which involved history taking, physical and neurological examination, blood tests, MMSE (Folstein *et al.*, 1975) neuropsychological work up (administration of a battery of neuropsychological tests), MRI of the brain according to a standard protocol and routine EEG. The final diagnosis was based upon a consensus meeting in which all the available clinical data and results of the ancillary investigations were considered. As reported in Stam *et al.* (2006), 6 patients used cholinesterase inhibitors, which was found to have no influence on functional connectivity. In the control and patient group both benzodiazepine and anti-depressive drug use was reported by one person. The study was approved by the Local Research Ethics Committee and all

patients or their caregivers had given written informed consent. Since subjects were included years ago, medical files were checked again recently to verify initial diagnosis; no notable changes (besides disease progression) were discovered.

MEG recording

Magnetic fields were recorded while subjects were seated inside a magnetically shielded room (Vacuumschmelze GmbH, Hanau, Germany) using a 151-channel whole-head MEG system (CTF Systems Inc., Port Coquitlam, BC, Canada). Average distance between neighbouring sensors in this system was 3.1 cm. A third-order software gradient (Vrba *et al.*, 1999) was used after online band-pass filtering between 0.25 and 125 Hz. Sample frequency was 625 Hz. For technical reasons two channels had to be omitted yielding 149 channels or sensors for analyses. Fields were measured during a no-task, eyes-closed condition. At the beginning and at the ending of the recording the head position relative to the coordinate system of the helmet was recorded by leading small alternating currents through three head position coils attached to the left and right pre-auricular points and the nasion on the subject's head. Head position changes during the recording up to approximately 1.5 cm were accepted. During the MEG recording, persons were instructed to sit comfortably, close their eyes and reduce eye movements, but remain awake as much as possible. During the recordings, the investigator and MEG technician checked the signal on-line for visual signs of drowsiness (e.g. slow eye movement activity) and observed the patient using a video monitor.

As a filtering process, offline frequency analysis is performed on the raw data, using a Fourier transformation. In the obtained frequency spectrum all frequencies outside the studied bands are set to zero, and using an inverse Fourier transformation the filtered signal is then obtained, with preservation of all phase information of the original data. For the subsequent off-line processing the recordings were converted to ASCII files and down-sampled to 312.5 Hz. For each subject care was taken to find and select exactly three artifact-free epochs of 4096 samples (13,083 s) by two of the investigators (BFJ and IM). MEG registrations were converted to datafiles with a coded filename before epoch selection, so the investigators were blind to the subjects' diagnosis during this process. Typical artifacts were due to (eye) movements, drowsiness or technical issues. Visual inspection and selection of epochs was realized with the DIGEEGXP software (CS). Epochs were band-pass filtered for the commonly used frequency bands: delta (0,5-4 Hz), theta (4-8 Hz), lower alpha (8-10 Hz), upper alpha (10-13 Hz), beta (13-30 Hz) and gamma (30-45 Hz), and all further analyses were performed for these bands separately.

Phase Lag Index

The phase lag index (PLI) is a measure of the asymmetry of the distribution of phase differences between two signals. It reflects the consistency with which one signal is phase leading or lagging with respect to another signal (Stam *et al.*, 2007b). The PLI performs at least as well as the Synchronization Likelihood (SL) (Montez *et al.* 2006) in detecting true changes in synchronization but it is much less affected by the influence of common sources. A more detailed explanation is offered in the supplementary material to this article.

Beside a global, mean PLI calculation a more regional approach was used. For this analysis MEG sensors were grouped into five regions (frontal, temporal, central, parietal, and occipital) for each hemisphere, and average PLI for all sensors within a region (local) or between two regions (long distance) were computed following the procedure described in Stam *et al.* (2006).

Graph analysis

In principle, networks can be represented by graphs, which are sets of vertices and corresponding sets of edges (Boccaletti *et al.*, 2006; Stam and Reijneveld, 2007c). One may say that an edge or connection either exists or not but one may also assign a certain weight to an edge that reflects the importance or strength of the relation between two vertices. While the first one yields unweighted graphs in that edges are either 0 or 1, the latter produces so-called weighted graphs. To define the corresponding weights a matrix of correlations between signals recorded at different electrodes is generally suitable. We denote the matrix' coefficients as w_{ij}, i.e. they connect vertex *i* with vertex *j* and specified their values using the afore-explained PLI. That is we defined a network of 149 vertices (matching the 149 available MEG channels) and used the matrix of PLI values between all pairs of MEG channels as edge weights.

Graphs can be characterized by various measures. Two fundamental ones are the clustering coefficient, which denotes the likelihood that neighbours of a vertex will also be connected to each other, and the average path length, i.e. the average number of edges of the shortest path between pairs of vertices (see figure 1).

Well ordered networks are strongly clustered and show large path lengths. In contrast, random networks are weakly clustered with small path lengths. Neither ordered nor random networks are good candidates for real networks like the human brain. Hence, Watts and Strogatz (1998) suggested a new type of networks, so-called small-world networks, which have both large clustering coefficients as well as small path lengths. Interestingly, these networks can be designed to be scale-free by having very short path lengths and a power law degree distribution (Barabási and Albert, 1999). Both small-world and scale-

free networks are optimal in the sense that they allow efficient information processing with a minimal number of connections. By now it has been shown that many types of network ranging from metabolic and genetic to social are either small-world or scale-free (Amaral and Ottino., 2004; Boccaletti *et al.*, 2006).

The clustering index C_i of a vertex *i* generally represents the likelihood that other vertices *j* that are connected to the vertex *i* will also be connected to each other. This notion can be adopted for use with weighted graphs in various ways (Boccaletti *et al.*, 2006). Here we propose a simple definition, closely related to the proposal of Onnela *et al.* (2005), which only requires symmetry ($w_{ij} = w_{ji}$) and that $0 \leq w_{ij} \leq 1$ holds. Indeed, both conditions are readily fulfilled when using PLI as weight definition. The (weighted) clustering index of vertex *i* is then defined as

$$C_i = \frac{\sum_{k \neq i} \sum_{\substack{l \neq i \\ l \neq k}} w_{ik} w_{il} w_{kl}}{\sum_{k \neq i} \sum_{\substack{l \neq i \\ l \neq k}} w_{ik} w_{il}} \tag{1}$$

Notice that in all sums in (1) terms with $k = i$, $l = i$, or $k = l$ are skipped. In the special case in which w_{ij} equals either 0 or 1, this definition is equivalent to the classical definition for unweighted graphs (Watts and Strogatz, 1998). For isolated vertices, i.e. vertices that do not have any connections, all weights w_{ij} vanish, and the clustering index is defined as $C_i=0$ (Newman, 2003). The mean clustering coefficient of the entire network can be determined via (1) as

$$C_w = \frac{1}{N} \sum_{i=1}^{N} C_i \tag{2}$$

Watts and Strogatz (1998) also defined the path length of unweighted graph. We extend this definition to weighted graphs building on the approach of Latora and Marchiori (2001). In detail we define the length of an edge as the inverse of the aforementioned edge weight, i.e. $L_{ij} = 1/w_{ij}$ if $w_{ij} \neq 0$, and $L_{ij} = +\infty$ if $w_{ij} = 0$; recall that w_{ij} is positive because we use the PLI as edge weight. The length of a weighted path between two vertices is then defined as the sum of the lengths of the edges of this path. The shortest path l_{ij} between two vertices *i* and *j* is the path between *i* and *j* with the shortest length. Analogously to definition (2) the average weighted path length of the entire graph is computed as

$$L_w = \frac{1}{(1/N(N-1)) \sum_{i=1}^{N} \sum_{j \neq i}^{N} \left(1/L_{ij}\right)} \tag{3}$$

Notice that instead of the arithmetic mean we here employed the harmonic mean (see Newman, 2003), so that we can handle infinite path lengths between disconnected edges, i.e. $1/\infty \geq 0$.

By definition, both values of C_w and L_w depend on edge weights and network structure but also on network size. In order to obtain measures that are independent of network size, the mean edge weight $\hat{C}_w = C_w \Big/ \left\langle C_w^{(\text{surrogate})} \right\rangle$ and the mean path length $\hat{L}_w = L_w \Big/ \left\langle L_w^{(\text{surrogate})} \right\rangle$ were computed, in which $\left\langle C_w^{(\text{surrogate})} \right\rangle$ and $\left\langle L_w^{(\text{surrogate})} \right\rangle$ denote weighted clustering coefficient and path length averaged over an ensemble of 50 surrogate random networks that were derived from the original networks by randomly reshuffling the edge weights. The steps involved in weighted graph analysis of the MEG data are illustrated schematically in Fig. 2.

Modelling network damage

To understand the general mechanisms underlying network changes in Alzheimer patients two models were compared, adopted from Albert and Barabási (2002). The first model (Random failure) assumes that network changes are due to a random decrease in strength of edges. The second model (Targeted attack) assumes that edges connecting high degree vertices ('hubs') will be more vulnerable to attack than edges connecting low degree vertices. The models were implemented by taking the PLI data of a control subject, selecting an edge at random, and then decrease its weight by a factor 2 with probability 1 (random failure model), or a probability that depended on the degree of both vertices connected by the edge (Targeted attack model). This procedure was repeated until the average PLI of the network was decreased to the average PLI of the Alzheimer group. Data of all control subjects were treated in a similar way. This resulted in two new data sets, one for each model, which were subjected to the same graph analysis as the original control and Alzheimer data sets.

Statistical analysis

Statistical analysis was done with SPSS for MS-Windows (version 15). Group differences in respectively gender distribution and PLI and were tested with ANOVA and two-tailed t-tests for independent samples (not assuming equal variance). Since graph measures showed a non-Gaussian distribution, group differences were tested with Mann-Whitney U-tests for independent samples. The effect of and medication use on PLI and network measures was assessed using Kruskal-Wallis tests. Associations between cognitive status (MMSE) and PLI or network-derived measures were assessed with Spearman's bivariate correlation test. A significance level of $\alpha < 0.05$ was used.

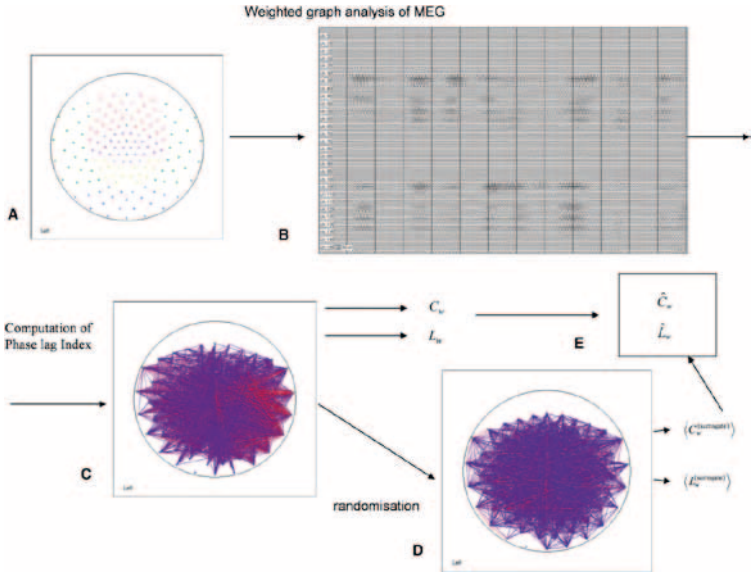

Figure 2. Schematic illustration of the steps involved in weighted graph analysis of MEG recordings. At each of the MEG sensors, illustrated in panel A, MEG signals are recorded. Epochs of MEG data are filtered, as shown in panel B, and correlations between all pairs of channels are determined with the phase lag index. This results in a weighted graph, with the strength of the synchronization between pairs of sensors indicated in color (blue low, red high PLI), as shown in panel C. From each graph the weighted clustering coefficient C_w and the weighted path length L_w are computed. Also, from each graph, and ensemble of random graphs is generated by randomly shuffling the connection weights (panel D). The C_w and L_w of each of the random graphs is determined and the mean values for the ensemble, $\left\langle C_w^{(\text{surrogate})} \right\rangle$ and $\left\langle L_w^{(\text{surrogate})} \right\rangle$, are determined. Finally, the ratios $\hat{C}_w$ and $\hat{L}_w$ are computed (panel E).

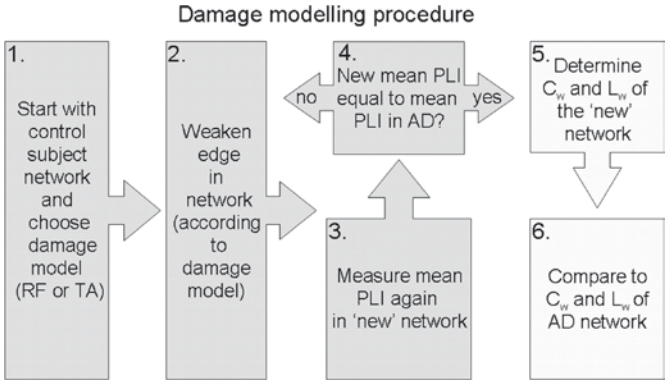

Figure 3. Damage modelling procedure. The mean PLI of a control subject network is lowered by randomly weakening edges in the network, until it reaches the same value as in a AD patient network. The effect of this damage is then examined by comparing the network characteristics of the damaged network to the AD patient network characteristics. AD=Alzheimer's disease, PLI=phase lag index, RF=random failure, TA=Targeted attack, C_w=mean weighted clustering coefficient, L_w=mean weighted path length.

RESULTS

Subject characteristics

No effect of gender distribution in the groups on PLI values and network measures was found. In the AD patient group, 6 persons used cholinesterase inhibitors (rivastigmine or galantamine). However, use of this medication did not produce a significant effect on PLI or network measure outcomes. This was also the case for the use of other psychoactive drugs in both the patient and control group (see methods-subjects subsection above).

Phase lag index

The average networks for AD patients and controls computed with PLI in six different frequency bands are shown in Fig. 4.

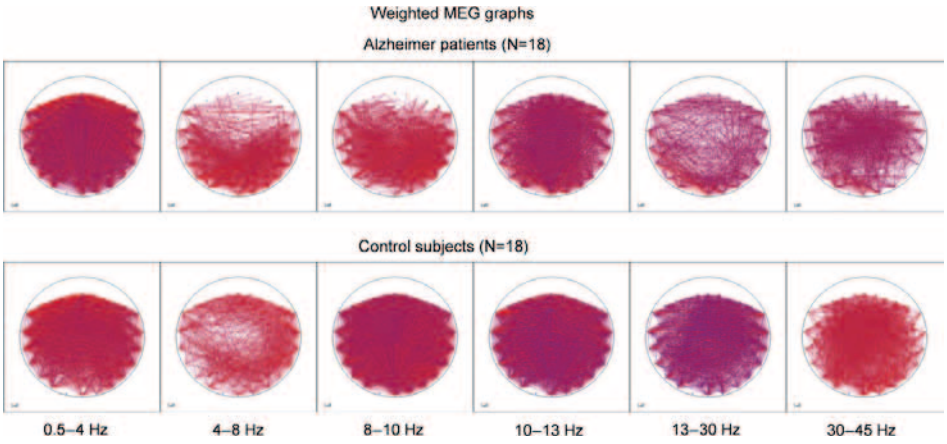

Figure 4. Average weighted graphs of AD patients and controls in six frequency bands. The value of the PLI for all individual pairs of MEG sensors is indicated in color (blue: low PLI; red: high PLI).

Visual inspection already suggested differences between the two groups, especially in the 8-10 Hz and 13-30 Hz bands. Group differences in mean PLI for each frequency band were tested with two-tailed t-tests for independent samples. The results are shown in Fig. 5.

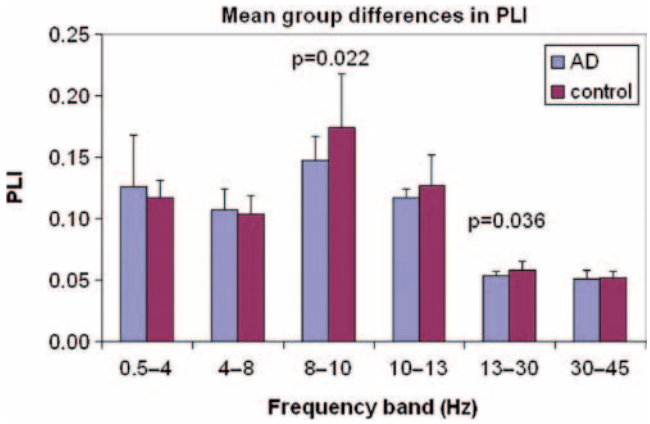

Figure 5. Mean PLI averaged over all pairs of MEG sensors for AD patients and controls in six frequency bands. Error bars are standard deviations. The mean PLI was significantly lower in AD patients compared to controls in the lower alpha band (two-tailed t-text, $p < 0.022$) and the beta band (two-tailed t-test, $p = 0.036$).

The mean PLI was significantly lower in the AD group in the 8-10 Hz band ($p = 0.022$) and in the 13-30 Hz band ($p = 0.036$). A non-significant trend in the same direction was found in the 10-13 Hz band ($p = 0.112$). No clear differences could be observed in other bands. By way of illustration, for the two frequency bands with a significant mean difference in PLI more detailed, regional results are shown in Fig. 6.

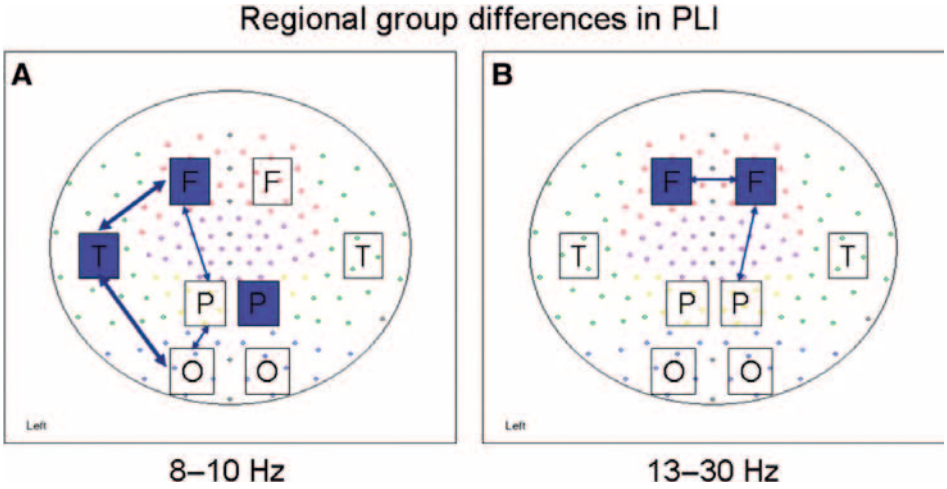

Figure 6. Schematic illustration of significant differences in long distance (indicated by arrows) and short distance (indicated by filled squares) PLI in the 8-10 Hz and 13-30 Hz band. AD patients had lower left sided fronto-temporal, fronto-parietal, temporo-occipital and parieto-occipital PLI in the 8-10 Hz band. Local left frontal and temporal, and right parietal PLI were also decreased in AD patients (panel A). For the 13-30 Hz band, AD patients had lower inter hemispheric frontal, right fronto-parietal and bilateral frontal PLI (panel B).

For the 8-10 Hz band, AD patients had significantly lower left fronto-parietal (p = 0.026), fronto-temporal (p = 0.007), parieto-occipital (p = 0.025) and temporo-occipital (p = 0.009) PLI. Local left frontal (p = 0.034), temporal (p = 0.011) and right parietal (p = 0.021) PLI were also decreased in the AD group. For the 13-30 Hz band, AD patients showed a decrease in interhemispheric frontal (p = 0.032), right fronto-parietal (p = 0.041) and local right (p = 0.020) and left (p = 0.046) frontal PLI.

Network analysis

Results of the weighted graph analysis are shown in Table 1.

Table 1. Results of weighted graph analysis for AD patients and controls in six frequency bands. Values are medians, with range printed between parentheses. C_w : mean weighted clustering coefficient. L_w : mean weighted path length. $\hat{C}_w$: mean normalized average weighted clustering coefficient (see method section). $\hat{L}_w$: mean normalized average weighted path length. Significant differences between AD and controls with non parametric testing (Mann-Whitney U-test, p<0.05) are given in bold.

	C_w		L_w		$\hat{C}_w$		$\hat{L}_w$	
	AD	control	AD	control	AD	control	AD	Control
0.5-4 Hz	0.12 (0.10-0.32)	0.12 (0.10-0.17)	4.05 (1.69-4.40)	3.92 (2.89-4.59)	1.04 (1.03-1.12)	1.04 (1.02-1.11)	1.09 (1.06-1.33)	1.08 (1.05-1.34)
4-8 Hz	0.11 (0.09-0.20)	0.10 (0.09-0.15)	4.23 (2.48-4.99)	4.44 (3.22-5.01)	1.05 (1.03-1.17)	1.04 (1.03-1.13)	1.14 (1.04-1.41)	1.15 (1.05-1.43)
8-10 Hz	**0.15 (0.12-0.21)**	**0.17 (0.13-0.29)**	**3.27 (2.25-3.76)**	**2.69 (1.80-3.73)**	**1.04 (1.02-1.12)**	**1.07 (1.04-1.13)**	**1.08 (1.05-1.32)**	**1.19 (1.07-1.30)**
10-13 Hz	0.12 (0.11-0.14)	0.13 (0.11-0.22)	3.83 (3.28-4.36)	3.72 (2.36-4.30)	1.04 (1.03-1.10)	1.04 (1.03-1.21)	1.10 (1.05-1.35)	1.12 (1.04-1.45)
13-30 Hz	0.06 (0.05-0.06)	0.06 (0.05-0.08)	7.97 (6.44-9.24)	7.61 (5.18-9.35)	1.04 (1.02-1.07)	1.04 (1.03-1.16)	1.11 (1.05-1.50)	1.12 (1.04-1.50)
30-45 Hz	0.05 (0.05-0.09)	0.05 (0.05-0.08)	8.70 (5.17-9.07)	8.54 (6.06-9.14)	1.02 (1.02-1.07)	1.02 (1.02-1.07)	1.09 (1.06-1.33)	1.04 (1.02-1.30)

The non-parametric Mann-Whitney U-test for independent samples revealed that C_w was lower in AD subjects in the 8-10 Hz band (U = 89.5; p = 0.022), but not in the 13-30 Hz band (U = 107.0; p = 0.081). L_w was higher in AD subjects in the 8-10 Hz band (U = 82.0; p = 0.011). In the 8-10 Hz band AD patients had a lower $\hat{C}_w$ (U = 76.0; p = 0.006) and a lower $\hat{L}_w$ (U = 86.0; p = 0.016).

Modelling of network changes

Modelling with the Random failure and the Targeted attack model was applied to the data of the 8-10 Hz band since this band showed the most consistent differences in graph

measures between the two groups. The average PLI graphs for AD patients, controls and both models are shown in Fig. 7. On visual inspection, both models look quite similar to the average network in the AD group. Please note that, by definition, the average PLI of both models is the same as the average PLI of the AD data.

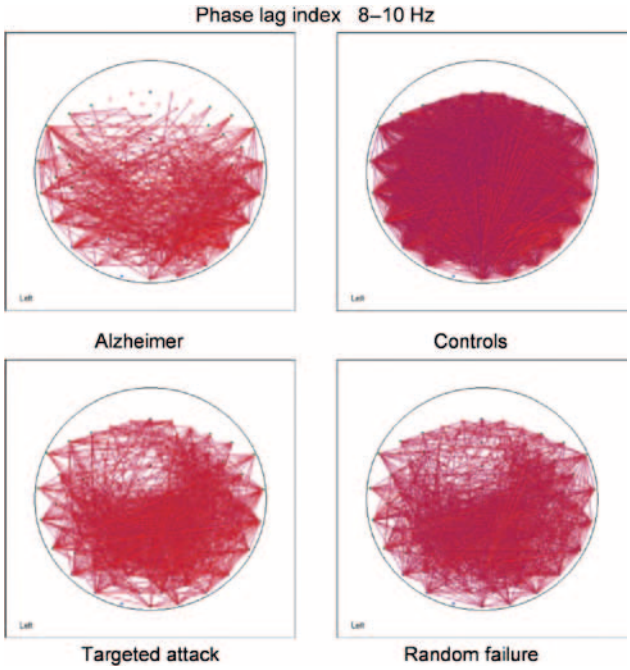

Figure 7. Comparison of real and modelled networks in the 8-10 Hz band. Top left: average PLI for the Alzheimer patients. Top right: average PLI for the control subjects. Bottom left: average PLI after application of the 'targeted attack' model to control data. Bottom right: average PLI after application of the 'random failure' model to control data.

Further analysis of the model data compared to the real data is shown in Fig. 8. For the Random failure model the $\hat{C}_w$ was not different from the control data, and significantly higher than $\hat{C}_w$ of the AD group (Mann-Whitney U test, U=76.5; p = 0.007). In contrast, $\hat{C}_w$ of the Targeted attack model was not significantly different from the AD group, but significantly lower than $\hat{C}_w$ of the control group (U= 87.0; p = 0.018). The weighted path length $\hat{L}_w$ showed a decreasing trend going from controls to Random failure, Targeted failure and controls (Fig. 8, right panel). $\hat{L}_w$ of both models did not differ significantly from control data.

Correlation with MMSE

No significant correlations between MMSE and PLI or network measures were found in the AD patient group. When correlation with MMSE was analyzed for all subjects (AD and control) put together in one group, we found significant effects between MMSE and mean PLI in the beta band (Spearman's r = 0.570, p = 0.001) and between MMSE and $\hat{C}_w$ in the lower alpha band (Spearman's r = 0.475, p = 0.008).

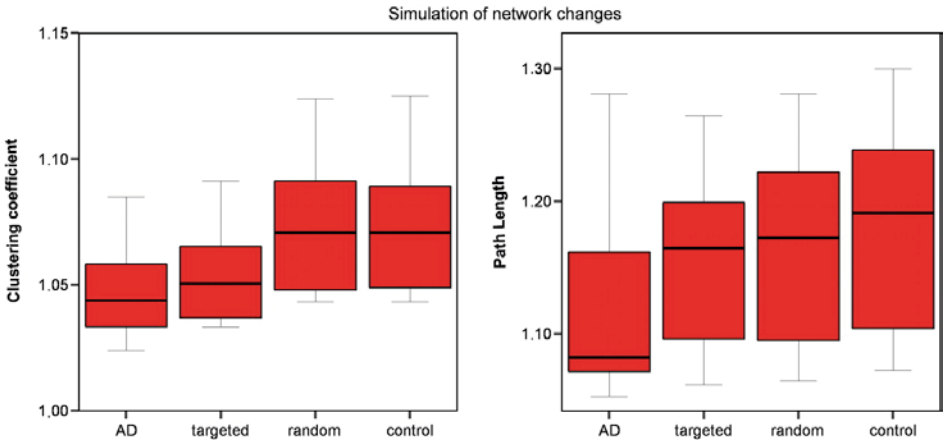

Figure 8. Comparison of normalized weighted clustering coefficient (left panel) and path length (right panel) for Alzheimer patients, targeted attack model, random failure model and controls in the 8-10 Hz band. Boxplots show median, interquartile range and extremes. AD = Alzheimer's Disease

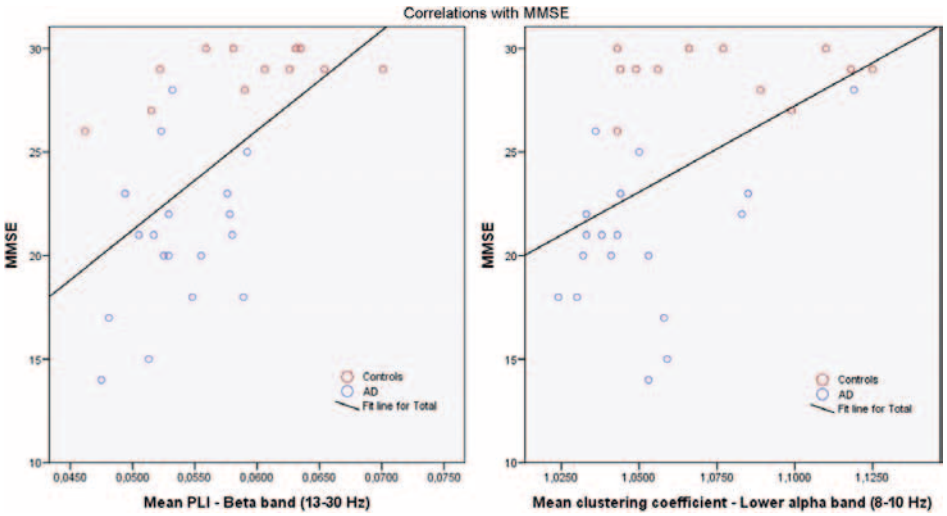

Figure 9. In the left panel the correlation of mean PLI in the lower alpha band and MMSE is shown (Spearman's r = 0.570, p = 0.001), in the right panel the correlation of the mean clustering coefficient with MMSE in the beta band (Spearman's r = 0.475, p = 0.008). AD and controls group were combined for this analysis. AD = Alzheimer's disease.

DISCUSSION

The present study showed that resting-state functional connectivity of MEG is decreased in AD patients in the lower alpha and beta bands using a recently developed measure, the PLI, that appears invariant against volume conduction. This finding supports the concept of AD as a disconnection syndrome. Moreover, changes in functional connectivity in AD patients did not involve all brain regions to the same extent, suggesting a heterogeneous disruption of overall network structure. This idea was confirmed by graph analysis of the functional connectivity data, which revealed lower normalized clustering coefficients and path lengths in the AD group in the lower alpha band. This type of change suggests that brain networks in AD patients are closer to random networks than those of non demented control subjects. The modelling results suggest that this change was brought about by a preferential decrease of connections between high degree nodes ('hubs'), rather than a non-specific decrease of connection strength.

Volume conduction

A decrease of resting state functional connectivity in AD patients in the alpha and often also in the beta band has been reported in many EEG and MEG studies (Adler *et al.*, 2003; Besthorn *et al.*, 1994; Dunkin *et al.*, 1994; Hogan *et al.*, 2003; Jelic *et al.*, 1996; Jiang 2005; Koenig *et al.*, 2005; Knott *et al.*, 2000; Leuchter *et al.*, 1992; Locatelli *et al.*, 1998; Pogarell *et al.*, 2005; Stevens *et al.*, 2001). However, a major point of criticism is that such studies were done on the raw EEG and MEG time series. It is well known that estimates of statistical interdependencies in EEG and MEG may be biased by the effects of volume conduction and, in the case of EEG, by the influence of the reference electrode (Guevara *et al.*, 2005; Nunez *et al.*, 1997). More specifically, nearby EEG electrodes or MEG sensors are likely to pick up activity of the same source, and thereby to display spuriously high correlations between their time series. This problem can be solved to a large degree by acknowledging that spurious couplings due to volume conduction or active reference electrodes cannot give rise to phase delays between channels. The PLI is only sensitive to phase synchronization between two channels when one is consistently leading or lagging in phase with respect to the other. That is, with PLI any coupling with a phase difference which centres around 0 mod are discounted. Put differently, our finding of a significant decrease of PLI in the lower alpha and the beta band cannot be explained by volume conduction but strongly supports the idea that resting-state functional connectivity is decreased in AD. Since the PLI results are largely in line with the previous studies we can conclude that the influence of volume conduction and reference electrode in these studies may have been smaller than has sometimes been suggested. However, a detailed comparison of our study with a previous study, in which the same data were analyzed with several linear and nonlinear measures, does display a few differences

(Stam *et al.*, 2006). For example, if we compare Fig. 6 of the present study with Figs. 3, 4, and 7 of Stam *et al.* (2006), one finds that the PLI in the beta band only showed decreases in the AD group, whereas coherence and Synchronization Likelihood (SL) also showed centro-parietal increases. A possible explanation could be that the increases in connectivity reported for SL and coherence might be influenced by volume conduction, while the decreases seems to be confirmed by the PLI and may reflect true loss of connectivity, but this should be subject to further study.

Resting state

Functional connectivity can be determined in relation to tasks as well as during a resting state. More recently there has been a growing interest in resting state functional connectivity because it appears that in particular memory-related brain networks are consistently activated during this state (Damoiseaux *et al.*, 2006; Gusnard and Raichle, 2001; Laufs *et al.*, 2003). Moreover, resting state functional connectivity has a strong genetic component, and shows characteristic changes in various psychiatric and neurological disorders (Posthuma *et al.*, 2005; Stam, 2005, 2006).

Network analysis

In the present study C_w was decreased in the lower alpha and beta band and L_w was increased in the lower alpha band in the AD group. It should be stressed that these changes in C_w and L_w are likely to be influenced by changes in the PLI. A lower mean level of PLI will decrease the estimate of C_w, irrespective of changes in network structure. Similarly, a lower PLI will give rise to longer weighted path lengths. These results should be compared to Fig. 4 in Stam et al, (2007a). Here C_w and L_w were compared between controls and AD patients for the same threshold, showing a non significant trend to a lower C_w and a significant increase of L_w in the AD group. By using the same threshold for both groups, differences in mean PLI could have influenced the results. Thus changes in C_w and L_w in both studies are consistent, but cannot be taken as 'pure' measures of changes in network structure as they are likely to be influenced by the lower mean level of connectivity in the AD group.

In contrast, the normalized coefficients $\hat{C}_w$ and $\hat{L}_w$ are corrected for differences in mean PLI between subjects, since each network is compared to its own random counterpart. The most important result is thus the decrease of $\hat{C}_w$ and $\hat{L}_w$ in the AD group in the lower alpha band. Within the framework of the Watts and Strogatz model this suggests that network architecture in AD patients is significantly closer to that of random networks.

However, $\hat{C}_w$ was very close to one in both groups, and much lower than reported in other studies, where $\hat{C}_w$ was usually around 2 (Achard *et al.*, 2006; Bassett *et al.*, 2006; Salvador *et al.*, 2005; Stam, 2004; Stam *et al.*, 2007a). It is possible that correlations between nearby sensors due to volume conduction could have produced spuriously high estimates of C_w in previous EEG and MEG studies.

Damage modelling

Modelling was used to investigate whether the observed network changes in AD in the 8-10 Hz band could be explained by a general mechanism. In the literature on complex networks generally two types of network damage are considered: random failure, where edges and / or vertices are lost randomly, and targeted attack, where damage mainly affects high degree, critical vertices and / or edges (section 3 in Boccaletti et al, 2006, for a more practical application see Kaiser et al., 2007). In our study the Targeted attack model performed better than the random error model in explaining the network changes in AD, in particular with respect to the clustering coefficient. While both models lowered the mean PLI to the level observed in the AD group, only the Targeted attack model produced a clustering coefficient as low as in the patients, whereas the Random failure model did not change the clustering coefficient at all. These results suggest that the disease process in AD may specifically affect association fibres connecting brain areas that are highly connected to the rest of the brain, that is: higher order association areas. The distribution of amyloid plaques in AD is in agreement with this suggestion (Nordberg, 2007).

Several studies have investigated the nature of network changes in different types of brain pathology. In the case of brain tumours, schizophrenia and interictal recordings of patients with epilepsy pathological networks were characterized by a smaller C_w and a smaller L_w (Bartolomei *et al.*, 2006; Micheloyannis *et al.*, 2006; Ponten *et al.*, 2007; Rubinov *et al.*, 2007). Considering the model of Watts and Strogatz, where the edges of a fully ordered network with degree K (number of edges per vertex) are rewired randomly with a certain probability P, a lower C_w and L_w would correspond with a higher value of the rewiring probability, and a more random network. The findings in the AD group in the present study seem to fit in the same scheme: decrease of both C_w and L_w, and a more random network in the patient group. Moreover, the values were close to (although significantly different from) 1, which indicates that the difference between real and random networks was very small. The one finding that does not fit in this pattern is the increase in beta band path length for AD patients reported in the previous pilot study (Stam *et al.*, 2007a). This result was obtained only for some values of degree K, with K identical for both groups (Fig. 5 in Stam *et al.*, 2007a). One explanation could be that in the EEG pilot study disconnected points (which occur already for values of $K = 3$) were

excluded from the computation of the path length, whereas in the present study they were included (see formula in methods section). This is an essential difference, excluding or including disconnected points may decrease or increase the estimated path length considerably. The lower alpha band, which was the only band to show clear changes in normalized clustering coefficient and path length in the current MEG study, was not investigated in the EEG study. Therefore, the evidence in favour of more random network topology in AD seems to be stronger, and in line with changes in other disorders. To be able to find a disease-specific 'network change profile' probably requires further exploration of this network approach and its relation to clinical features of AD. Possibly 'network randomization' may be a final common pathway for different types of brain damage, resulting from loss of neurons and connections as well a random outgrowth of new connections. A related concept of increased entropy relating to ageing and Alzheimer's disease has recently been formulated by Drachmann: "Increasing entropy, manifest through a complex network of interacting age related changes, is seen as the fundamental driving cause of neural and cognitive decline in the elderly, as well as the overriding etiologic principle in further transition to sporadic AD" (Drachmann, 2006). It would be of considerable interest to study how different types of treatment will interfere with this process of network randomization, and how the network parameters relate to disease severity and cognitive performance.

Acknowledgements

The authors thank mrs. Els van Deventer for continuing support in retrieving relevant literature.

REFERENCES

Achard S, Salvador R, Whitcher B, Suckling J, Bullmore E. A resilient, low-frequency, small-world human brain functional network with highly connected association cortical hubs. The Journal of Neuroscience 2006; 26: 63-72.

Adler G, Brassen S, Jajcevic A. EEG coherence in Alzheimer's dementia. J Neural Transm 2003; 110, 1051-1058.

Aertsen AMHJ, Gerstein GL, Habib MK, Palm G. Dynamics of neuronal firing correlation: modulation of 'effective connectivity'. Journal of Neurophysiology 1989; 61: 900-917.

Albert R, Barabási AL. Statistical mechanics of complex networks. Rev Mod Physics 2002:74:47–97.

Amaral LAN, Ottino JM. Complex networks. Augmenting the framework for the study of complex systems. Eur. Phys. J. B 2004 : 38 : 147-162.

Amor F, Rudrauf D, Navarro V, N'diaye K, Garnero L, Martinerie J, Le van Quyen M. Imaging brain synchrony at high spatio-temporal resolution : application to MEG signals during absence seizures. Signal Processing 2005; 85: 2101-2111.

Babiloni C, Ferri F, Moretti DV, Strambi A, Binetti G, Dal Forno G, Ferreri F, Lanuzza B, Bonato C, Nobili F, Rodriguez G, Salinari S, Passero S, Rocchi R, Stam CJ, Rossini PM. Abnormal fronto-parieto coupling of brain rhythms in mild Alzheimer's disease: a multicentric EEG study. European Journal of Neuroscience 2004; 19: 1-9.

Barabasi AL, Albert R. Emergence of scaling in random networks. Science 1999; 286: 509-512.

Bartolomei F, Bosma I, Klein M, Baayen JC, Reijneveld JC, Postma TJ, Heimans JJ, van Dijk BW, de Munck JC, de Jongh A, Cover KS, Stam CJ. Disturbed functional connectivity in brain tumour patients: evaluation by graph analysis of synchronization matrices. Clin Neurophysiol 2006; 117: 2039-2049.

Bassett DS, Bullmore E. Small-world brain networks. The neuroscientist 2006; 12: 512-523.

Basset DS, Meyer-Linderberg A, Achard S, Duke Th, Bullmore E. Adaptive reconfiguration of fractal small-world human brain functional networks. PNAS 2006; 103: 19518-19523.

Berendse HW, Verbunt JPA, Scheltens P, van Dijk BW, Jonkman EJ. Magnetoencephalographic analysis of cortical activity in Alzheimer's disease. A pilot study. Clin Neurophysiol 2000; 111, 604-612.

Besthorn C, Forstl H, Geiger-Kabisch C, Sattel H, Gasser T, Schreiter-Gasser U. EEG coherence in Alzheimer disease. Electroenceph clin Neurophysiol 1994; 90, 242-245.

Boccaletti S, Latora V, Moreno Y, Chavez M, Hwang D-U. Complex networks: structure and dynamics. Physics Reports 2006; 424: 175-308.

Damoiseaux JS, Rombouts SARB, Barkhof F, Scheltens P, Stam C, Smith SM, Beckmann CF. Consistent resting-state networks across healthy subjects. PNAS 2006; 103: 13848-13853.

David O, Garnero L, Cosmelli D, Varela FJ. Estimation of neural dynamics from MEG / EEG cortical current density maps: application to the reconstruction of large-scale cortical synchrony. IEEE Transactions on Biomedical Engineering 2002; 49: 975-987.

Delbeuck X, Van der Linder M, Colette F. Alzheimer's disease as a disconnection syndrome? Neuropyschology Review 2003; 13: 79-92.

Drachman DA. Aging of the brain, entropy, and Alzheimer disease. Neurology. 2006: 24; 67: 1340-1352.

Dunkin JJ, Leuchter AF, Newton TF, Cook IA. Reduced EEG coherence in dementia: state or trait marker? Biol Psychiatry 1994; 35, 870-879.

Fingelkurts AA, Fingelkurts AA, Kahkonen S. Functional connectivity in the brain – is it a elusive concept? Neurosci Biobehav Rev 2005; 28: 827-836.

Folstein MF, Folstein SE, McHugh PR. "Mini-mental state". A practical method for grading the cognitive state of patients for the clinician. J Psychiatr Res. 1975 Nov;12(3):189-98.

Friston KJ. Brain function, nonlinear coupling, and neuronal transients. The Neuroscientist 2001; 7: 406-418.

Friston KJ. Functional integration and inference in the brain. Progress in Neurobiology 2002; 68: 113-143.

Gross J, Kujala J, Hamalainen M, Timmermann L, Schnitzler A, Salmelin R. Dynamic imaging of coherent sources: studying neural interactions in the human brain. PNAS 2001; 98: 694-699

Guevara R, Velazguez JLP, Nenadovic V, Wennberg R, Senjanovic G, Dominguez LG. Phase synchronization measurements using electroencephalographic recordings. What can we really say about neuronal synchrony? Neuroinformatics 2005; DOI: 10.1385/NI:03:04:301.

Gusnard DA, Raichle ME. Searching for a baseline: functional imaging and the resting brain. Nature Reviews Neuroscience 2001; 685-694.

Hadjipapas A, Hillebrand A, Holliday IE, Singh K, Barnes G. Assessing interactions of linear and nonlinear neuronal sources using MEG beamformers: a proof of concept. Clin Neurophysiol 2005; 116: 1300-1313.

He Y, Chen ZJ, Evans AC. Small-world anatomical networks in the human brain revealed by cortical thickness form MRI. Cerebral Cortex 2006 doi: 10.1093/cercor/bh149

Hilgetag CC, Burns GAPC, O'Neill MAO, Scannell JW, Young MP. Anatomical connectivity defines the organization of clusters of cortical areas in the macaque monkey and the cat. Philospiphical Transactions: Biological Sciences 2000; 355: 91-110.

Hogan MJ, Swanwick GRJ, Kaiser J, Rowan M, Lawlor B. Memory-related EEG power and coherence reductions in mild Alzheimer's disease. Int J Psychophysiol 2003; 49, 147-163.

Iturria-Medina Y, Sotero RC, Canales-Rodriguez EJ, eman-Gomez Y, Melie-Garcia L. Studying the human brain anatomical network via diffusion-weighted MRI and Graph Theory. Neuroimage 2008; 40: 1064-1076.

Jelic V, Shigeta M, Julin P, Almkvist O, Winblad B, Wahlung WO. Quantitative electroencephalography power and coherence in Alzheimer's disease and mild cognitive impairment. Dementia 1996; 7, 314-323.

Jeong J, Gore JC, Peterson BS. Mutual information analysis of the EEG in patients with Alzheimer's disease. Clin Neurophysiol 2001; 112: 827-835.

Jiang ZY. Abnormal cortical functional connections in Alzheimer's disease: analysis of inter- and intrahemispheric EEG coherence. J Zheniang Univ Sci B. 2005 ; 6: 259-264.

Kaiser M, Martin R, Andras P, Young MP. Simulation of robustness against lesions of cortical networks. Eur J Neurosci. 2007 May;25(10):3185-92.

Koenig T, Prichep L, Dierks T, Hubl D, Wahlund LO, John ER, Jelic V. Decreased EEG synchronization in Alzheimer's disease and mild cognitive impairment. Neurobiol Aging 2005; 26, 165-171.

Knott V, Mohr E, Mahoney C, Ilivitsky V. Electroencephalographic coherence in Alzheimer's disease: comparisons with a control group and population norms. J Geriatr Psychiatry Neurol 2000; 13: 1-8.

Latora V, Marchiori M. Efficient behavior of small-world networks. Physical Review Letters 2001; 87: 198701

Laufs H, Krakow K, Sterzer P, Eger E, Beyerle A, Salek-Haddadi A, Kleinschmidt A. Electroencephalographic signatures of attentional and cognitive default modes in spontaneous brain acitivity fluctuations at rest. PNAS 2003; 100: 11053-11058.

Lee L, Harrison LM, Mechelli A. A report of the functional connectivity workshop, Dusseldorf 2002. NeuroImage 2003; 19: 457-465.

Lehmann D, Faber PL, Gianotti LRR, Kochi K, Pascual-Marqui RD. Coherence and phase locking in the scalp EEG and between LORETA model sources, and microstates as putative mechanisms of brain temporo-spatial functional organization. J Physiology 2006; 99: 29-36.

Leuchter AF, Newton TF, Cook AA, Walter DO. Changes in brain functional connectivity in Alzheimer-type and multi-infarct dementia. Brain 1992; 115: 1543-1561.

Le van Quyen M. Disentangling the dynamic core: a research program for a neurodynamics at the large scale. Biol Res 2003; 36: 67-88.

Locatelli T, Cursi M, Liberati D, Francheschi M, Comi G. EEG coherence in Alzheimer's disease. Electroenceph clin Neurophysiol 1998; 106: 229-237.

McKhann G, Drachman D, Folstein M, Katzman R, Price D, Stadlan EM. Clinical diagnosis of Alzheimer's disease: report of the NINCDS-ADRDA Work Group under the auspices of Department of Health and Human Services Task Force on Alzheimer's Disease. Neurology 1984;34:939-44.

Micheloyannis S, Pachou E, Stam CJ, Breakspear M, Bitsios P, Vourkas M, Erimaki S, Zervakis M. Small-world networks and disturbed functional connectivity in schizophrenia. Schizophr Res. 2006; 87: 60-66. Epub 2006 Jul 27.

Montez T, Linkenkaer-Hansen K, van Dijk BW, Stam CJ. Synchronization likelihood with explicit time-frequency priors. Neuroimage 2006; 33: 1117-1125.

Newman ME. Properties of highly clustered networks.

Phys Rev E Stat Nonlin Soft Matter Phys. 2003 Aug;68(2 Pt 2):026121.

Nordberg A. Amyloid imaging in Alzheimer's disease. Curr Opin Neurol. 2007 Aug;20(4):398-402.

Nolte G, Wheaton OBL, Mari Z, Vorbach S, Hallett M. Identifying true brain interaction from Eeg data using the imaginary part of coherency. Clin Neurophysiol 2004;115: 2292-2307.

Nunez PL, Srinivasan R, Westdorp AF, Wijesinghe RS, Tucker DM, Silberstein RB, Cadusch PJ. EEG coherency I: statistics, reference electrode, volume conduction, Laplacians, cortical imaging, and interpretation at multiple scales. Electroenceph clin Neurophysiol 1997; 103: 499-515.

Onnela J-P, Saramaki J, Kertesz J, Kaski K. Intensity and coherence of motifs in weighted complex networks. Physical Review E 2005; 71: 065103(R)

Osipova J Ahveninen S Kaakkola IP Jääskeläinen J Huttunen, Pekkonen E. Effects of scopolamine on MEG spectral power and coherence in elderly subjects. Clin. Neurophysiol. 2003; 114; 1902–1907.

Pijnenburg YAL, van de Made Y, van Cappellen van Walsum, AM, Knol DL, Scheltens Ph, Stam CJ. EEG synchronization likelihood in mild cognitive impairment and Alzheimer's disease during a working memory task. Clin Neurophysiol 2004; 115: 1332-1339.

Pikovsky A, Rosenblum M, Kurths J. Synchronization. A universal concept in nonlinear sciences. Cambridge Nonlinear Science Series 12, Cambridge University Press, Cambridge, 2001.

Pogarell O, Teipel SJ, Juckel G, Gootjes L, Moller T, Burger K, Leinsinger G,

Moller HJ, Hegerl U, Hampel H. EEG coherence reflects regional corpus callosum area in Alzheimer's disease. J Neurol Neurosurg Psychiatry 2005; 76: 109-111.

Ponten SC, Bartolomei F, Stam CJ. Small-world networks and epilepsy: graph theoretical analysis of intracerebrally recorded mesial lobe seizures. Clin Neurophysiol 2007, doi: 10.1016/jclinph.2006.12.002

Posthuma D, de Geus EJC, Mulder EJCM, Smit DJA, Boomsma DI, Stam CJ. Genetic components of functional connectivity in the brain: the heritability of synchronization likelihood. Human Brain Mapping 2005; 26: 191-198.

Rubinov M, Knock SA, Stam CJ, Micheloyannis S, Harris AW, Williams LM, Breakspear

M. Small-world properties of nonlinear brain activity in schizophrenia. Hum Brain Mapp. 2007 Dec 10 [Epub ahead of print]

Salvador R, Suckling J, Coleman MR, Pickard JD, Menon D, Bullmore E. Neurophysiological architecture of functional magnetic resonance images of human brain. Cereb Cortex. 2005; 15: 1332-1342.

Srinivasan R, Winter WR, Ding J, Nunez PL. EEG and MEG coherence: measures of functional connectivity at distinct spatial scales of neocortical dynamics.

J Neurosci Methods 2007 Oct 15;166(1):41-52.

Smit DJ, Stam CJ, Posthuma D, Boomsma DI, de Geus EJ. Heritability of "small-world" networks in the brain: A graph theoretical analysis of resting-state EEG functional connectivity. Hum Brain Mapp. 2007 Dec 6 [Epub ahead of print]

Stam CJ. Functional connectivity patterns of human magnetoencephalographic recordings: a "small-world" network? Neuroscience Letters 2004; 355: 25-28.

Stam CJ. Nonlinear dynamical analysis of EEG and MEG: review of an emerging field. Clin Neurophysiol 2005; 116: 2266-2301.

Stam CJ. Nonlinear brain Dynamics. Nova Science Publishers, New York, 2006

Stam CJ, van Cappellen van Walsum AM, Pijnenburg YAL, Berendse HW, de Munck JC, Scheltens Ph, van Dijk BW. Generalized synchronization of MEG recordings in Alzheimer's disease: evidence for involvement of the gamma band. J Clin Neurophysiol 2002; 19: 562-574.

Stam CJ, Jones BF, Manshanden I, van Cappellen van Walsum AM, Montez T, Verbunt JPA, de Munck JC, van Dijk BW, Berendse HW, Scheltens P. Magnetoencephalographic evaluation of resting-state functional connectivity in Alzheimer's disease. Neuroimage 2006 ; 32: 1335-1344.

Stam CJ, Jones BF, Nolte G, Breakspear M, Scheltens Ph. Small-world networks and functional connectivity in Alzheimer's disease. Cerebral Cortex 2007a; 17: 92-99.

Stam CJ, Nolte G, Daffertshofer A. Phase lag index: Assessment of functional connectivity from multi channel EEG and MEG with diminished bias from common sources. Hum Brain Mapp. 2007b Jan 31

Stam CJ, Reijneveld JC. Graph theoretical analysis of complex networks in the brain. Nonlinear Biomedical Physics. 2007c; 1: 3.

Stevens A, Kircher T, Nickola M, Bartels M, Rosellen N, Wormstall H. Dynamic regulation of EEG power and coherence is lost early and globally in probable DAT. Eur Arch Psychiatry Clin Neurosci 2001; 251, 199-204.

Supekar K, Menon V, Rubin D, Musen M, Greicius MD. Network Analysis of Intrinsic Functional Brain Connectivity in Alzheimer's Disease. PLoS Comput Biol 2008:4(6): e1000100. doi:10.1371/journal.pcbi.1000100

Tass PA, Fieseler T, Dammers J, Dolan K, Morosan P, Majtanik M, Boers F, Muren A, Zilles K, Fink GR. Synchronization tomography: a method for three-dimensional localization of phase synchronized neuronal populations in the human brain using magnetoencephalography.

Phys Rev Lett. 2003 Feb 28;90(8):088101.

van der Flier WM, Scheltens P. Epidemiology and risk factors of dementia. J Neurol Neurosurg Psychiatry. 2005; 76 Suppl 5:v2-7.

Varela F, Lachaux J-P, Rodriguez E, Martinerie J. The brainweb: phase synchronization and large-scale integration. Nature Reviews Neuroscience 2001; 2: 229-239.

Vrba, J., Anderson, G., Betts, K., et al., 1999. 151-Channel whole-cortex MEG system for seated or supine positions. In: Yoshimoto, T., Kotani, M., Kuriki, S., et al., (Eds.), Recent Advances in Biomagnetism. Tohoku Univ. Press, Sendai, Japan, pp. 93–96.

Watts DJ, Strogatz SH. Collective dynamics of "small-world" networks. Nature 1998; 393: 440-442.

Node 5

Disrupted modular brain dynamics reflect cognitive dysfunction in Alzheimer's disease

Neuroimage 2012

W. de Haan[a, b*], W.M. van der Flier[b,c], T. Koene[d], L.L. Smits[b], P. Scheltens[b] and C.J. Stam[a]

[a.] Department of Clinical Neurophysiology and MEG, VU University Medical Center, Amsterdam, The Netherlands

[b.] Alzheimer Center and Department of Neurology, VU University Medical Center, Amsterdam, The Netherlands

[c.] Department of Epidemiology and Biostatistics, VU University Medical Centre, Amsterdam, The Netherlands

[d.] Department of Medical Psychology, VU University medical Centre, Amsterdam, The Netherlands

ABSTRACT

The relation between pathology and cognitive dysfunction in dementia is still poorly understood, although disturbed communication between different brain regions is almost certainly involved. In this study we combine magneto-encephalography (MEG) and network analysis to investigate the role of functional sub-networks (modules) in the brain with regard to cognitive failure in Alzheimer's disease. Whole-head resting-state (MEG) was performed in 18 Alzheimer patients (age 67±9, 6 females, MMSE 23±5) and 18 healthy controls (age 66±9, 11 females, MMSE 29±1). We constructed functional brain networks based on interregional synchronization measurements, and performed graph theoretical analysis with a focus on modular organization. The overall modular strength and the number of modules changed significantly in Alzheimer patients. The parietal cortex was the most highly connected network area, but showed the strongest *intra*-modular losses. Nonetheless, weakening of *inter*modular connectivity was even more outspoken, and more strongly related to cognitive impairment. The results of this study demonstrate that particularly the loss of communication *between* different functional brain regions reflects cognitive decline in Alzheimer's disease. These findings imply the relevance of regarding dementia as a functional network disorder.

INTRODUCTION

A theoretical framework to interpret the rapidly increasing amount of experimental data describing the complex organization of the human brain is highly desired. In recent years, graph theory has emerged as a promising candidate for this purpose (Rubinov and Sporns, 2010; Stam, 2010; Bullmore *et al.*, 2009). Graph theory investigates the principles of network architecture, and the relation between network structure and function (Watts and Strogatz, 1998; Barabasi and Albert, 1999; Newman, 2010; Sporns, 2010). The application of graph theoretical analysis to neuroscientific data has revealed important organizational brain features such as an efficient 'small-world' architecture (combining good global and local connectivity) and the existence of highly connected network regions, called *hubs* (Eguiluz *et al.*, 2005; Achard *et al.*, 2006; Salvador *et al.*, 2005; Stam *et al.*, 2009; van den Heuvel and Hulshoff Pol, 2010; He *et al.*, 2008). Changes in brain network topology have been related to normal cognitive development and aging as well as to a wide range of brain diseases, implying a close relation between connectivity and cognitive status (Achard and Bullmore, 2007; Stam and Reijneveld, 2007; Bullmore and Sporns, 2009).

In the most prevalent type of dementia, Alzheimer's disease (AD), cognitive functions that depend strongly on communication between different brain areas are particularly disturbed, and it has therefore been characterized as a 'disconnection syndrome' (Geschwind, 1965; Delbeuck *et al.*, 2003). Graph theoretical studies of AD patient data have consistently revealed perturbations of brain network organization (He *et al.*, 2008; He *et al.*, 2009; Supekar *et al.*, 2008; de Haan *et al.*, 2009; Stam and Reijneveld, 2007; Stam *et al.*, 2009). Interestingly, highly connected *hub* regions (e.g. the posterior cingulate gyrus and precuneus) seem most susceptible to AD pathology, which consists of amyloid deposition, hypometabolism and atrophy (Buckner *et al.*, 2005; Celone *et al.*, 2006; Greicius *et al.*, 2004; Sperling *et al.*, 2009). What causes this hub vulnerability in AD is unclear, but a more detailed description and understanding of hubs, or network clustering in general, could provide further clues.

A related network characteristic dealing with clustering is *modularity*, which expresses the extent to which networks can be decomposed into smaller functional sub-groups or *modules* (Guimerà and Amaral, 2005; Boccaletti *et al.*, 2006; Newman and Girvan, 2004; Newman, 2006). Network nodes belonging to the same module have a higher level of inter-connectivity than with the rest of the network. In the brain, a high level of structural or functional connectivity among a group of regions implies a collective function or goal (Hilgetag *et al.,* 2000; Varela *et al.,* 2001; Salvador *et al.*, 2005). Therefore, large-scale modular organization might be an appropriate level to examine cognitive

processing and its impairment in brain disease. In this MEG study, we focus on *functional* modularity: the description of distinct sub-networks with intensive dynamical interaction, as expressed by levels of neuronal synchronization.

Theoretically, there are several advantages of a modular brain network structure. It offers an elegant solution for balancing the opposing demands that are placed on many dynamical systems: a high level of local specialization, while maintaining tight global integration (Sporns *et al.*, 2004). In a modular network, hubs can have different roles; *connector* hubs form bridges between different modules, while *provincial* hubs are central nodes within modules. Graph theoretical measures that quantify inter- and intra-modular connectivity and are able to classify (hub) nodes accordingly have been developed (Guimerá and Amaral, 2005) and incorporated in the present study.

Using graph theoretical methods, several previous studies have demonstrated the presence of modular organization in the brain (Leise, 1990; Hilgetag *et al.*, 2000; Kaiser *et al.*, 2007; Chen *et al.*, 2008; Hagmann *et al.*, 2008). Moreover, modularity seems to develop during infancy and to degrade with age, suggesting a relation with cognitive abilities (Meunier *et al.*, 2009; Fair *et al.*, 2009; Fan *et al.*, 2010; van den Heuvel and Hulshoff Pol, 2010; Schwarz *et al.*, 2008; Ferrarini *et al.*, 2009). Consequently, the progressive impairment of specific cognitive domains in AD might well be reflected by changes in functional modularity.

In this study we explore functional modularity in resting-state MEG data of AD patients and healthy controls using a well-known graph theoretical modularity algorithm (Newman and Girvan, 2004). Our main aim is to examine whether and to what extent modular organization of spontaneous brain activity changes in AD, and if these changes are related to cognitive performance. Our hypothesis is that cognitive impairment in AD will be primarily reflected by impaired communication *between* functional modules, based on the notions that cognition requires intensive distributed processing and that vulnerable hub regions in AD are mainly located in association cortex areas (that integrate information from multiple modalities). In network terms, we expect AD to be a 'connector hub disease'.

MATERIALS AND METHODS

Patients and controls

The study involved 18 patients with a diagnosis of probable AD according to the NINCDS-ADRDA criteria (McKhann *et al.*, 1984) and 18 healthy controls who were all recruited from the Alzheimer Center of the VU University Medical Center. Controls were often spouses of the patients. AD patients were assessed according to a standard clinical

protocol, which involved history taking, physical and neurological examination, an interview with a spouse or close family member, blood tests, MRI of the brain according to a standard protocol, routine EEG, and a neuropsychological assessment. The diagnosis was made in a consensus meeting in which all the available clinical data were considered by a multidisciplinary team. Cognitive tests of special interest for this study with AD patients were the delayed recall of the Dutch version of the Rey auditory verbal learning task (RAVLT) (memory), Visual Association Test (VAT, effortless learning) and category fluency (executive functions and language) (Rey, 1970), (Lindeboom *et al.*, 2002), (Luteijn and Ploeg,). The VAT is an adequate test to examine learning ability in dementia. Level of education was classified according to the system of Verhage ranging from 1 to 7 (low to highly educated) (Verhage and F., 1965). Controls were screened by a neurologist and underwent the same neuropsychological tests as the patients. Exclusion criteria for this study were active psychiatric or neurologic disease, or a Mini Mental State Examination (MMSE) score below 16. The Local Research Ethics Committee approved the study and all participants gave written informed consent. Main subject characteristics are summarized in table 1. AD patients were mild to moderately demented (MMSE 23±1). In both groups a few individuals were on psychoactive drugs like benzodiazepines or cholinesterase inhibitors (in the AD group).

Table 1. Subject characteristics

	Control	Alzheimer	
Group	18	18	
Age	66 (±9)	67 (±9)	p = 0.82
Gender (M/F)	7/11	12/6	p = 0.16
MMSE	29 (±1)	23 (±1)	**p < 0.001**
Education (Verhage score)	5 (±1)	5 (±1)	p = 0.89

M=males, F=females, MMSE=mini mental state examination score.

From MEG to module

The description of modular structure in oscillatory brain dynamics requires a combination of mathematical techniques. The multi-step procedure is outlined in figure 1; first (1), the recording of eyes-closed resting-state MEG data, then (2) the calculation of the strength of synchronization between different brain areas (functional connectivity), (3) the construction of undirected, weighted network graphs from these results, and finally (4) the graph analysis, focussing on modularity measures, both on a global and a local scale. The subsequent steps are discussed in more detail in the following paragraphs.

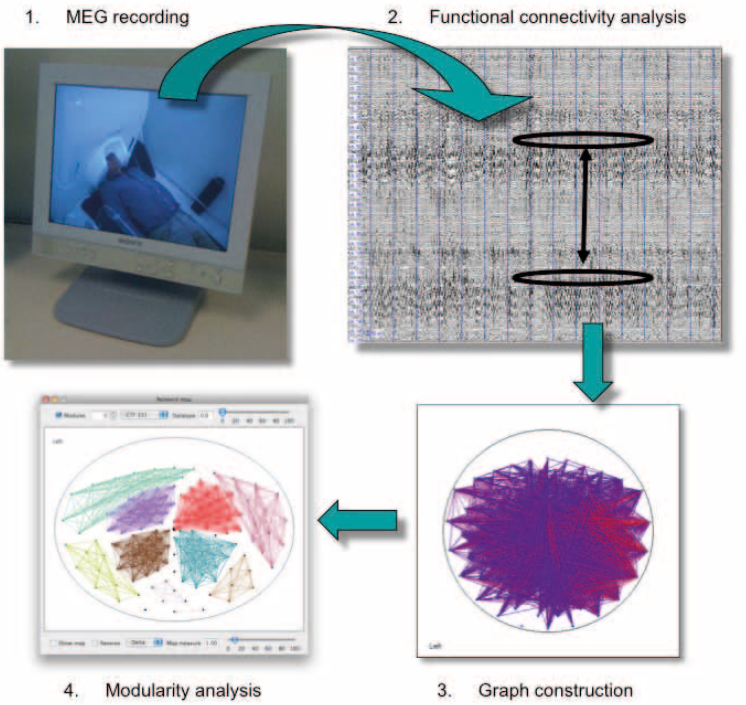

Figure 1. The multi-step procedure from recording MEG data to modularity analysis.

1. MEG recording

Magnetic fields were recorded while subjects were seated inside a magnetically shielded room (Vacuumschmelze GmbH, Hanau, Germany) using a 151-channel whole-head MEG system (CTF Systems Inc., Port Coquitlam, BC, Canada). Average distance between neighbouring sensors in this system was 3.1 cm. A third-order software gradient (61) was used after online band-pass filtering between 0.25 and 125 Hz. Sample frequency was 625 Hz. For technical reasons two channels had to be omitted, yielding 149 channels or sensors for analysis. Fields were measured during a task-free, eyes-closed condition. At the beginning and ending of the recording the head position relative to the coordinate system of the helmet was recorded by leading small alternating currents through three head position coils attached to the left and right pre-auricular points and the nasion on the subject's head. Head position changes during the recording up to approximately 1.5 cm were accepted. During the MEG recording, patients were instructed to close their eyes, stay awake, and to reduce eye movements. For the subsequent off-line processing the recordings were converted to ASCII files. For each subject care was taken to select four artifact-free epochs of 4096 samples by two of the investigators (WDH and CS), who were blinded to the diagnosis. Typical artifacts were due to (eye) movements, swallowing, dental prosthetics, or drowsiness. All further functional connectivity and graph theoretical analysis were performed with in-house developed software (BrainWave

version 0.8.68, CS. Latest version freely available on home.kpn.nl/stam7883/brainwave.html).

2. Functional connectivity analysis

Correlations between all pair-wise combinations of MEG channels were computed with the Synchronization Likelihood (SL). Mathematical details can be found in previous work (Stam and Dijk, 2002), (Montez *et al.*, 2006); here we give a brief description. The SL is a general measure of the correlation or synchronization between 2 time series, which is sensitive to linear as well as nonlinear interdependencies. The basic principle of the SL is to divide each time series into a series of 'patterns' (roughly, brief pieces of time series containing a few cycles of the dominant frequency) and to search for a recurrence of these patterns. The SL is then the probability that pattern recurrence in time series X coincides in time with pattern recurrence in time series Y. The end result of computing the SL for all pair-wise combinations of channels is a square matrix (with 149 rows and columns, equal to the number of MEG channels), where each entry contains the resulting SL value of the sensor pair. This matrix is called the *adjacency* or *connectivity* matrix.

3. Graph construction

Graphs are constructed using all information in the connectivity matrix. This results in fully connected, weighted (the connection strength between a sensor pair is their SL value), undirected (connections between nodes have no direction) 149 node-networks. For this study, we focussed on graph measures describing community structure in networks. The node strength (*s*), within-module degree and participation coefficient (see section below) were computed for all individual nodes. By averaging nodal values, global or regional values can be obtained for these measures. Since in our weighted graphs the *strength* of a node is determined by the sum of all its SL values, the node strength distribution of the entire network reveals the regions that are most strongly connected (*hub regions*).

4. Modularity analysis

To describe modularity in the whole-brain network we used a modification of the approach by Guimera and Nunes Amaral (Guimerà and Amaral, 2005; Newman and Girvan, 2004), adapted for weighted networks and identical to Stam et al. (Stam, 2010):

$$Q_m^w = \sum_{s=1}^{m} \frac{l_s}{L} - \left(\frac{d_s}{2L}\right)^2 \quad (1)$$

where m is the number of modules, l_s the sum of the weights of all links in module s, L is the total sum of all weights in the network, d_s is the sum of the strength of all vertices in module s. In short, the relation between intra- and intermodular connections determines

the strength of each module. For any given network partition, this measure describes the strength of the total modularity by summing the relative strength of all the modules in the network. A strongly modular network has modularity value close to 1, and in a network without modular organization it will approach 0. Finding the optimal modular organization in a network is a computationally intensive problem. One of the most effective methods to date is *simulated annealing* (Guimerà *et al.*, 2004; Guimerà and Amaral, 2005). This method was used to find the optimal way to divide the network into modules: initially, each of the *N* nodes was randomly assigned to one of *m* possible clusters, where *m* was taken as the square of *N*. At each step, one of the nodes was chosen at random, and assigned a different randomly chosen module number from the interval [1,*N*]. Modularity was calculated before and after this. The cost *C* was defined as $-Q_m^w$. The new partitioning was preserved with probability *p*:

$$p = \begin{cases} 1 & f\ C_f \leq C_i \\ e^{-\frac{C_f - C_1}{T}} & f\ C_f > C_i \end{cases}. \quad (2)$$

Here, C_f is final cost and C_i is initial cost. The temperature *T* was 1 initially, and was lowered once every 100 steps as follows: $T_{new} = 0.995\ T_{old}$. In total, the simulated annealing algorithm was run for 10^6 steps. The partition with the strongest modular organization was identified separately for each epoch of every person for all the different frequency bands, and subjected to further graph analysis.

Once the modular organization in a network has been determined, the topological role of individual nodes can be described in greater detail (Guimerà and Amaral, 2005): nodes can be mainly involved in communication with other nodes in the same module, but can also interact with other modules. This aspect is quantified by two properties: the *within-module degree* (Z_i), and the *participation coefficient* (*PC*). The within-module degree measures the connectivity of the node within the module compared to the other nodes in the same module, and thus describes the relative importance within the module. The weighted within module degree can be defined as follows:

$$z_i^w = \frac{k_i^w(m_i) - \bar{k}^w(m_i)}{\sigma^{k^w(m_i)}} \quad (3)$$

where m_i is the module containing node *i*, $k_i^w(m_i)$ is the within module degree of *i* (the sum of all links between *i* and all other nodes in m_i), and $\bar{k}^w(m_i)$ and $\sigma^{k^w(m_i)}$ are the respective mean and standard deviation of the within-module m_i degree distribution.

The participation coefficient expresses how strongly a node is connected to other modules, and the weighted version is defined as:

$$PC_i = 1 - \sum_{m \in M} \left(\frac{k_i^w(m)}{k_i^w} \right)^2 \quad (4)$$

where M is the set of modules, and $k_i(m)$ is the sum of all links between i and all nodes in module m. The within module degree and the participation coefficient both range from 0 to 1, and determine the identity of a node in the modular network structure:

- Provincial hubs: relatively many links within own module (high Z_i, low PC)
- Connector hubs: relatively many links to other modules (low Z_i, high PC)

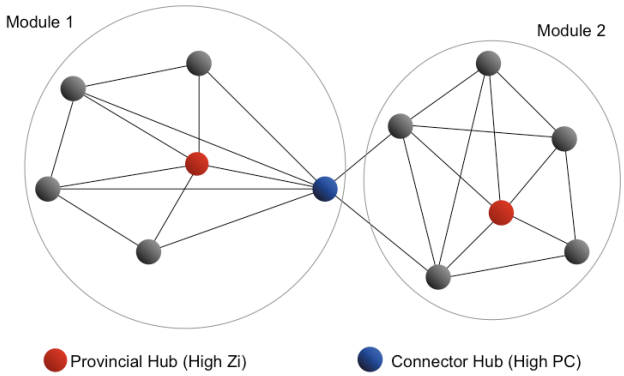

Figure 2. Modules and hub types. Modules are tight communities within a larger network. Provincial hubs, indicated in red, have many connections within their own module, while connector hubs, in blue, have relatively strong outward links.

In this study, node identities were determined by their relative values compared to the other nodes. To be able to describe group differences in these measures, global and regional mean Z_i and PC values were examined. For the latter analysis, nodes were assigned to five cortical regions (frontal, temporal, central, parietal, and occipital).

Statistical analysis

Statistical analysis was done with SPSS for Mac (version 18.0). All analyses were performed for each epoch separately for all different frequency bands, and prior to group comparison the four epochs per person were averaged. Since functional connectivity and graph measures showed Gaussian distributions, group differences were tested with independent sample t-tests. Regional Zi and PC analysis was performed with an ANOVA for repeated measures, using group as between-subject factor and cortical region as within-subject factor (Greenhouse-Geisser corrected). Correlations of graph measures with neuropsychological test scores in AD were assessed with Pearson's test. A significance level of $\alpha < 0.05$ was used for all tests.

RESULTS

Modularity – descriptive results

To get a first impression of modular organization, individual network modules were visualized. Comparing several different resting-state MEG epochs of the same person, modular structure was generally consistent. Often, three or four strongly clustered frontal or parietal modules were found, along with several weaker temporal and occipital ones. Modules were usually localized clusters of adjacent cortical areas, but also showed long-distance fragments. Inter-hemispheric modules were a frequent finding, especially bi-temporal. To demonstrate a representative example of group differences in modular organization of these functional networks, module head plots are shown for two matched subjects in the beta frequency band (figure 3).

The differences in distributions between the two persons are apparent; for example, while the healthy person shows strong parietal modules, they are absent in the AD patient. In the healthy control a long-distance, inter-hemispheric module with frontal, temporal, parietal and occipital nodes is visible.

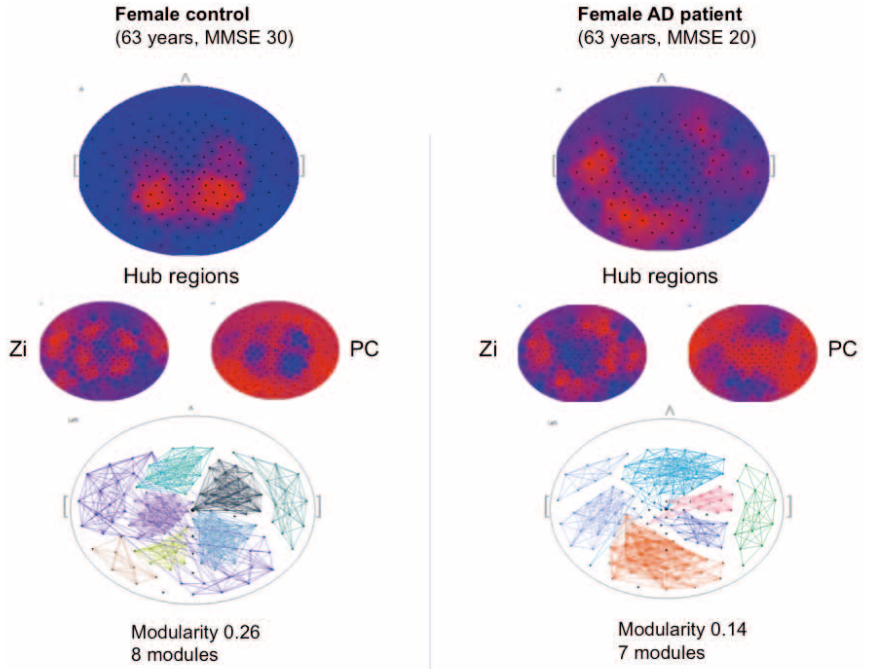

Figure 3. Head plots of network measure distributions and modules for two representative female subjects in the beta frequency band. Top view, top of each plot represents frontal region. Note the heterogeneous distribution of the different graph measures. Zi=within module degree, PC=participation coefficient.

Modularity – global results

Global modularity (Q) results are depicted in figure 4 (upper panel). Overall, modularity values were around 0.2, which is an indication of a weak modular network organization. Highest modularity was found in the beta band of the control group, while gamma band modularity was much lower in both groups. In patients with AD, delta and theta bands showed an increase, and beta and gamma bands showed a strong decrease in modularity. The number of modules (N_m) found in patient and control networks ranged between five and eleven. As figure 4 (lower panel) indicates, the AD group showed a loss of module count, strongest in higher frequency bands.

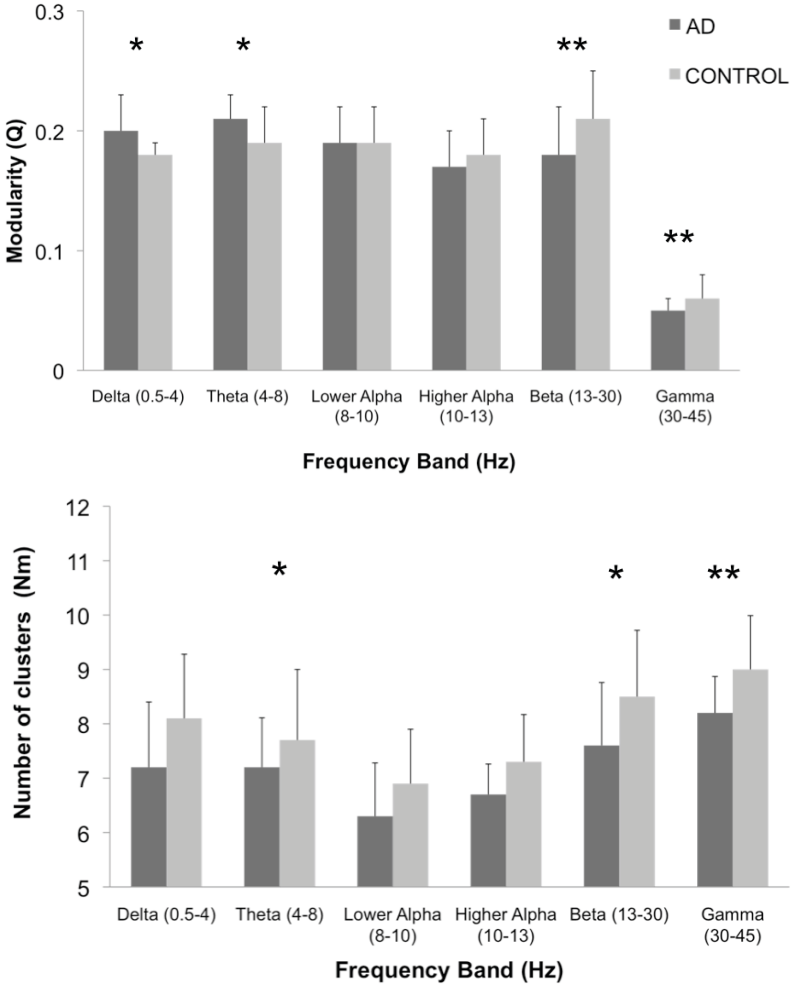

Figure 4. Main modularity results, AD versus controls (n=36). Upper panel shows changes in global modularity (Q) for all frequency bands. Lower panel shows changes in the mean number of modules (Nm) for all frequency bands. * $p < 0.05$, ** $p < 0.01$.

Modularity – Within module degree (Z_i)

A decrease of global intra-modular strength, as expressed by the average within module degree (*Zi*), was present in AD patients in the beta band only (see figure 5).

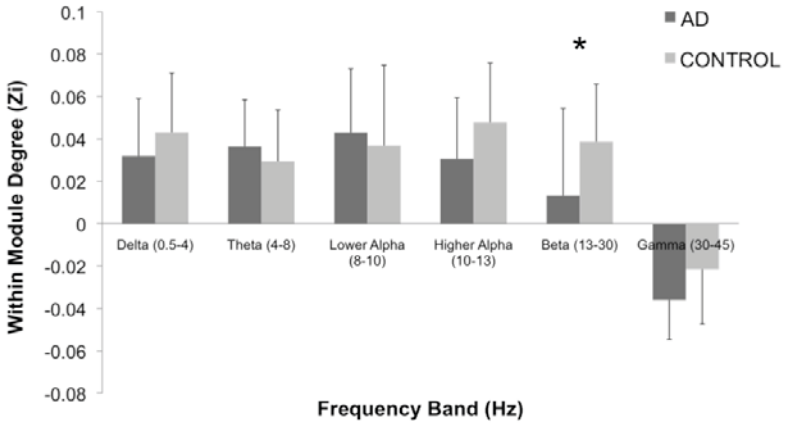

Figure 5. Within-module degree (Zi) comparisons for all frequency bands, AD versus controls (n=36). Error bars indicate standard deviations. * $p < 0.05$

Regional analysis of Zi in the beta band using ANOVA for repeated measures showed no main effect of group ($F[1,34] = 3.794$, $p = 0.060$) but one for region ($F[4,136] = 54.497$, $p < 0.001$). Moreover, we found a group*region interaction ($F[4,136] = 3.771$, $p = 0.040$). Intra-modular strength was highest in the parietal areas (see table 2).

Table 2. Regional synchronization likelihood (SL) and within module degree (Zi) values in the beta frequency band

Beta Band (13-30 Hz)		Central	Frontal	Occipital	Parietal	Temporal
SL	AD	0.014 (±0.003)	0.015 (±0.003)	0.017 (±0.002)	**0.018 (±0.004)**	0.015 (±0.001)
	C	0.017 (±0.003)	0.017 (±0.003)	0.016 (±0.002)	**0.020 (±0.004)**	0.016 (±0.002)
Zi	AD	-0.558 (±0.202)	0.154 (±0.154)	0.139 (±0.301)	**0.156 (±0.412)**	-0.113 (±0.110)
	C	-0.444 (±0.254)	0.227 (±0.101)	-0.029 (±0.233)	**0.422 (±0.304)**	-0.161 (±0.103)

Group means per cortical region of synchronization likelihood (SL) and within-module degree (Zi) in the beta frequency band, in AD patient and control group. Standard deviations are printed between parentheses. Note that the parietal region shows highest values for both measures (printed in bold), indicating hub status.

Modularity – Participation coefficient (PC)

Global inter-modular strength, as expressed by the participation coefficient (PC), decreased in the delta and theta frequency bands in AD, while the other bands did not show group differences (figure 6).

Regional analysis of PC in the delta band using ANOVA for repeated measures showed main effects of group ($F[1,34] = 8.488$, $p = 0.006$) and region ($F[4,136] = 30.876$, $p <$

0.001). There was no interaction between group and region, indicating a comparable decrease of PC across regions in AD patients. In the theta band we found a similar pattern, as there was a main effect of group ($F[1,34] = 6.506$, $p = 0.015$) and region ($F[4,136] = 24.889$, $p < 0.001$), but no group*region interaction.

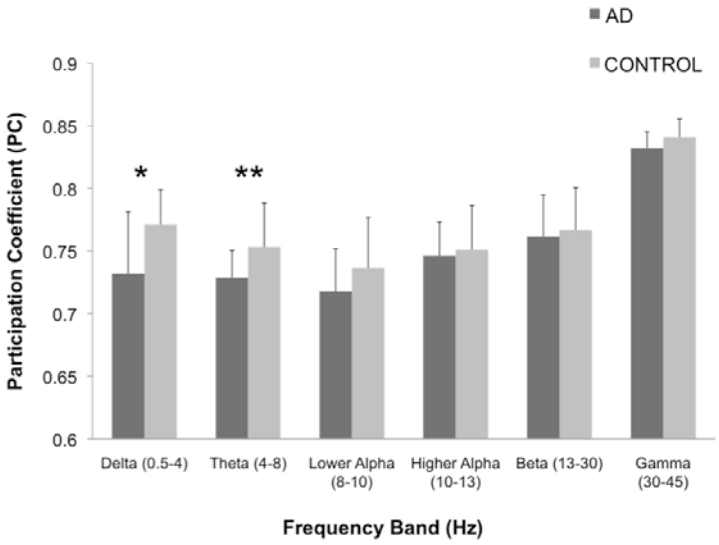

Figure 6. Participation coefficient (PC) comparisons for all frequency bands, AD versus controls (n=36). Error bars indicate standard deviations. * $p < 0.05$, ** $p < 0.01$.

Modularity and cognition

In the AD group, several remarkably strong correlations were found: delta band modularity and fluency ($r = -0.80$, $p < 0.01$), inter-modular strength (PC) and word recall ($r = 0.71$, $p < 0.01$), inter-modular strength and fluency ($r = 0.75$, $p < 0.01$), lower alpha band modularity and visual recognition ($r = -0.55$, $p < 0.05$) inter-modular strength and visual recognition ($r = 0.69$, $p < 0.01$), and inter-modular strength and fluency ($r = 0.72$, $p < 0.05$). Similar, consistent trends but no significant correlations were found in any of the other frequency bands.

DISCUSSION

The main message of this study is that the modular organization of large-scale spontaneous brain activity networks is disrupted in AD. Graph theoretical modularity analysis demonstrates weakening links within and, especially, between functional modules, correlating with cognitive dysfunction. Moreover, the vulnerability of the parietal region

in AD is confirmed by regional analyses. In the following paragraphs we will relate our findings to current literature and discuss methodological issues.

Describing resting-state functional modularity

In this exploratory study, we describe functional modularity in resting-state MEG data of AD patients and healthy controls. Although the methodology used in our study is different from the well-known characterization of resting-state networks (RSN) in fMRI data, the aim is similar: to describe functionally meaningful clusters or sub-networks in spontaneous brain activity. In fMRI literature, resting-state networks have been described consistently, indicating the existence of functional subgroups (Eguiluz *et al.*, 2005; Achard *et al.*, 2006; Damoiseaux *et al.*, 2006; De Luca *et al.*, 2006; Salvador *et al.*, 2005; Salvador *et al.*, 2008; van den Heuvel *et al.*, 2009). These sub-networks are usually identified using independent component analysis (ICA).

Several recent studies have also demonstrated the existence of non-random modular patterns in resting-state brain activity in healthy individuals (Meunier *et al.*, 2009; Fan *et al.*, 2010; van den Heuvel and Hulshoff Pol, 2010; Schwarz *et al.*, 2008; Ferrarini *et al.*, 2009). In general, caution should be used when investigating components of a complex system. Networks should preferably be examined both globally and locally, taking into account the relation between the whole network and its components. In this regard, an advantage of graph theoretical modularity algorithms is that connectivity within and especially *between* different modules and their role with regard to the rest of the network can be described more accurately. This seems a significant benefit, judging from the marked intermodular connectivity changes in AD patients in the present study.

Despite methodological differences, the few modularity-based studies so far have demonstrated similarities in the modular organization of large-scale brain networks. The number of modules we observed in our networks resembled what was found in previous fMRI studies; about five to seven large modules (He *et al.*, 2009; Meunier *et al.*, 2009; van den Heuvel *et al.*, 2008; Salvador *et al.*, 2005). Anatomical and structural imaging studies using graph theory reported five to ten modules on average (Hilgetag *et al.*, 2000; Chen *et al.*, 2008; Hagmann *et al.*, 2008). Since structural and functional networks in the brain are intimately related, functional modularity is probably constrained by the underlying structural connectivity (Bullmore *et al.*, 2009).

Using resting-state fMRI, Meunier et al. looked at differences of modular organization in two age groups of 18-33 and 62-76 years (Meunier *et al.*, 2009). Here, one of the main findings was that the pattern of inter-modular connections changed extensively, possibly reflecting normal human age-related brain changes.

The first MEG study investigating modularity of patient data with graph theoretical tools was performed in epilepsy patients (Chavez *et al.*, 2010). Using a similar modularity algorithm, (seizure free) resting-state differences were found in the theta-alpha band

range (5-14 Hz) between patients and controls. Like in the present study, main group differences were found in the inter-modular connections. Another very interesting recent study combining MEG recorded during a memory task and graph theoretical modularity investigated persons with Mild Cognitive Impairment (MCI) (Buldú *et al.,* 2011). While functional connectivity was slightly increased in the MCI group, overall modularity was lower, resembling the changes found in the present study. Although the comparison between resting-state and task paradigms should be made with caution, both studies suggest a link between modularity and cognition.

Neuronal synchronization between different brain areas is the prime candidate for the swift coordination of cognitive processes (Singer and Gray, 1995; Varela *et al.*, 2001; Fries, 2005). Since synchronization between neuronal assemblies is accomplished across a large spectrum of frequencies, a method with a sufficiently high temporal precision is essential. Combined with its decent spatial resolution and a relatively direct recording of neuronal activity compared to fMRI, MEG is therefore well suited for this task, especially regarding cortical sources (Pereda *et al.*, 2005).

With average modularity index values around 0.2, modularity was weak in both groups. Similarly, the absolute within-module degree (Zi) values were low in general and participation coefficient (PC) values were high, indicating that most nodes had extensive links outside their own module. These results might lead to the conclusion that resting-state functional modularity is weak. However, in our weighted networks all nodes are connected by definition, possibly including spurious links that might be primarily a reflection of noise or volume conduction instead of true synchronization. This might make the identification of the underlying modular organization more difficult, and overall modularity values lower. To avoid this, one could set a threshold, so that weak connections are discarded before graph analysis is performed (Stam *et al.*, 2006; de Haan *et al.*, 2009). However, setting a threshold is arbitrary and can even introduce new problems (van Wijk *et al.,* 2010). We therefore chose to use weighted networks without thresholds, preserving all information from the original connectivity matrices. Although this pragmatic choice affects the outcome, we believe that the observed group changes in our data cannot be explained by methodological bias in this regard.

Volume conduction remains an issue of concern in sensor-space EEG and MEG analysis. The reason for choosing SL as functional connectivity measure instead of one less sensitive to volume conduction, such as the Phase Lag Index (PLI), is threefold: first, since the PLI, as an extremely conservative measure, discards near-zero phase lag synchronization, it thereby also ignores genuine near-zero phase lag synchronization that is present. Since particularly adjacent regions can be synchronized with small phase lags, short-range synchronization might be underestimated. This might form a problem in particular when looking at modules, since they often contain adjacent regions and short-range synchronization. Second, although sensitivity to volume conduction might

influence modularity results, it is expected to influence both the AD patient group and the healthy control group similarly, and therefore it cannot explain group differences. Third, since the SL has been used more extensively in previous AD-related studies, it makes for an easier evaluation of this work with regard to existing literature.

Finally, the use of other modularity metrics might also result in different or additional findings, like hierarchical modularity or overlapping modules (Alexander-Bloch *et al.*, 2010; Lancichinetti and Fortunato, 2009; Palla *et al.*, 2005).

Modularity and cognition

The observed correlations between modularity measures and cognitive test scores indicate a possible significance of resting-state modularity with regard to cognitive function. This is in line with earlier studies, where structural and functional (resting-state and task-based) modularity has been linked to cognitive function (Hilgetag *et al.*, 2000; Salvador *et al.*, 2005; Kitzbichler *et al.*, 2011), healthy aging (Meunier *et al.*, 2009) and disease conditions (Chavez *et al.*, 2010; Buldu *et al.*, 2011). Although it is tempting to speculate about specific functional roles, modules may also serve less concrete (but no less important) purposes, like stimulating or inhibiting oscillatory activity in other frequency bands, or be a display of 'stationary' oscillatory activity. We did find several potentially meaningful correlations of global modularity measures with neuropsychological test scores. Directions of these correlations were consistent, and in line with our hypothesis: the observed group differences in AD modularity measures were related to a worse performance on these relevant cognitive tests. The finding that resting-state activity is related to task performance suggests the importance of 'default' functional network integrity for cognition. However, relating the distinct resting-state modules and their characteristics to specific cognitive domains, especially in individual subjects, requires further analysis.

Alzheimer's disease: a 'connector hub disease'?

The changes in global network modularity we found complement earlier studies that report loss of overall network structure in AD (He *et al.*, 2008; Supekar *et al.*, 2008; Stam *et al.*, 2009; de Haan *et al.*, 2009). The beta and gamma bands show a decrease both in modularity and in number of modules, but AD patients also show paradoxical modularity *increases* in the delta and theta bands. However, this can be explained by the strong loss of inter-modular connections in these bands (decrease of PC values). It is important to recognize that both increases *and* decreases in graph measure values can accompany sub-optimal cognitive conditions (Stam, 2010;Pievani *et al.*, 2011).

Disconnection syndromes result from either damage to the connections between areas or local damage in association regions (Geschwind, 1965; Catani and ffytche, 2005). Translated to network terms, one would expect primarily inter-modular damage

(decrease in connector hubs, or lower PC values) and possibly intra-modular damage (decrease in provincial hubs, or lower Zi values) in network hub regions. Our present findings in AD are in agreement with this prediction. The most striking finding of the regional graph analysis is the role of the parietal areas in AD in the beta band; according to their high strength and high within-module degree they serve as hub regions in the cortical network (see table 3). These findings are in line with the notion that the parietal association cortices serve as important integrative association areas (Mesulam, 1998). Structural, functional and metabolic vulnerability in AD of the parietal cortex has been demonstrated with various techniques (Iturria-Medina *et al.*, 2008; Gong *et al.*, 2009; Li *et al.*, 2009; Buckner *et al.*, 2005; Sperling *et al.*, 2009). In our study, the parietal hub areas were substantially weakened, confirming the vulnerability of the parietal region in AD. However, although intra-modular strength does show correlations with fluency in theta and beta bands, for cognition the *inter*-modular strength seems to play a larger role; there are more correlations with cognitive test scores (worse performance with lower PC), they are stronger, and the group differences in inter-modular strength are larger. Moreover, since the variability in PC was relatively small due to the methodological choice of using weighted, unthresholded networks, these results may even be underestimated. In this regard, connector hubs and thus global network integrity seem more important for adequate cognitive performance than local clustering. Strongest PC differences were found in delta and theta bands, suggesting that, while higher frequency bands are often associated with local processing, long-range low-frequency synchronization might be important for successful connector hub-mediated inter-modular connectivity.

The higher connectivity status of hub regions leading to greater vulnerability is a phenomenon that is encountered in many other complex networks like the World Wide Web, metabolic and email networks (Albert *et al.*, 2000; Jeong, 2004; Newman, 2003). Intuitively, a metabolic wear-and-tear or overload scenario of hub regions seems plausible, since they carry most network traffic. The overlap between hub regions and the default mode network suggests that these regions are not only the most highly connected, but also the most active ones (Buckner *et al.*, 2009). To evaluate this hypothesis, a better fundamental understanding of the relation between neural network connectivity, neuronal activity, and pathology is necessary. For this purpose, graph theoretical damage modeling can be a useful complementary bottom-up approach (Alstott *et al.*, 2009; Rubinov *et al.*, 2009; Stam *et al.*, 2009; Stam, 2010).

Conclusion

It becomes more and more evident that disruption of structural and functional brain connectivity plays a pivotal role in the onset of dementia (Stam, 2010). Graph theory allows us to go beyond classifying AD as a disconnection syndrome, providing more detail and meaning. Functional modules are theoretically plausible representations

of cognitive (sub-)processes, and therefore modularity analysis of MEG data seems a method with an appropriate spatiotemporal resolution to examine large-scale brain coordination. Even in the absence of specific cognitive tasks, this study demonstrates functional modularity changes in Alzheimer patients, ranging from local to long-range effects and from slow to fast brain activity. Intermodular communication seems to be particularly vulnerable in Alzheimer's disease, suggesting the relevance of a network perspective on dementia, and illustrating the potential of graph theoretical analysis to describe disconnection syndromes such as Alzheimer's disease in a more detail.

Acknowledgements

The authors thank Nicole Sistermans, Ellemarije Altena, Annelies van der Vlies and Sofie Boom for neuropsychological assessments, and Karin Plugge and Ndedi Sijsma for performing the MEG recordings.

REFERENCES

Achard S, Salvador R, Whitcher B, Suckling J, Bullmore E. 2006. A resilient, low-frequency, small-world human brain functional network with highly connected association cortical hubs. J Neurosci. Jan 4;26(1):63-72.

Achard S, Bullmore E. 2007. Efficiency and cost of economical brain functional networks. Plos Comput Biol. Feb 2;3(2):e17.

Albert R, Jeong H, Barabasi AL. 2000. Error and attack tolerance of complex networks. Nature. Jul 27;406(6794):378-82.

Alexander-Bloch AF, Gogtay N, Meunier D, Birn R, Clasen L, Lalonde F, et al. 2010. Disrupted modularity and local connectivity of brain functional networks in childhood-onset schizophrenia. Front Syst Neurosci. 4:147.

Alstott J, Breakspear M, Hagmann P, Cammoun L, Sporns O. 2009. Modeling the impact of lesions in the human brain. Plos Comput Biol. Jun;5(6):e1000408.

Barabasi AL, Albert R. 1999. Emergence of scaling in random networks. Science. Oct 15;286(5439):509-12.

Boccaletti S, Latora V, Moreno Y, Chavez M, Hwang D. 2006. Complex networks: Structure and dynamics. Physics Reports. 424(4-5):175 - 308.

Buckner RL, Snyder AZ, Shannon BJ, LaRossa G, Sachs R, Fotenos AF, et al. 2005. Molecular, structural, and functional characterization of alzheimer's disease: Evidence for a relationship between default activity, amyloid, and memory. J Neurosci. Aug 24;25(34):7709-17.

Buckner RL, Sepulcre J, Talukdar T, Krienen FM, Liu H, Hedden T, et al. 2009. Cortical hubs revealed by intrinsic functional connectivity: Mapping, assessment of stability, and relation to alzheimer's disease. J Neurosci. Feb 11;29(6):1860-73.

Buldú JM, Bajo R, Maestú F, Castellanos N, Leyva I, Gil P, et al. 2011. Reorganization of functional networks in mild cognitive impairment. PLoS One. 6(5).

Bullmore E, Sporns O. 2009. Complex brain networks: Graph theoretical analysis of structural and functional systems. Nat Rev Neurosci. Mar;10(3):186-98.

Bullmore E, Barnes A, Bassett DS, Fornito A, Kitzbichler M, Meunier D, Suckling J. 2009. Generic aspects of complexity in brain imaging data and other biological systems. Neuroimage. Sep;47(3):1125-34.

Catani M, ffytche DH. 2005. The rises and falls of disconnection syndromes. Brain. Oct;128(Pt 10):2224-39.

Celone KA, Calhoun VD, Dickerson BC, Atri A, Chua EF, Miller SL, et al. 2006. Alterations in memory networks in mild cognitive impairment and alzheimer's disease: An independent component analysis. J Neurosci. Oct 4;26(40):10222-31.

Chavez M, Valencia M, Navarro V, Latora V, Martinerie J. 2010. Functional modularity of background activities in normal and epileptic brain networks. Phys Rev Lett. Mar 19;104(11):118701.

Chen ZJ, He Y, Rosa-Neto P, Germann J, Evans AC. 2008. Revealing modular architecture of human brain structural networks by using cortical thickness from MRI. Cereb Cortex. Oct;18(10):2374-81.

Damoiseaux JS, Rombouts SA, Barkhof F, Scheltens P, Stam CJ, Smith SM, Beckmann CF. 2006. Consistent resting-state networks across healthy subjects. Proc Natl Acad Sci U S A. Sep 12;103(37):13848-53.

Delbeuck X, Van der Linden M, Collette F. 2003. Alzheimer's disease as a disconnection syndrome? Neuropsychol Rev. Jun;13(2):79-92.

Eguiluz VM, Chialvo DR, Cecchi GA, Baliki M, Apkarian AV. 2005. Scale-Free brain functional networks. Physical Review Letters. 94(1):18102.

Fair DA, Cohen AL, Power JD, Dosenbach NU, Church JA, Miezin FM, et al. 2009. Functional brain networks develop from a "local to distributed" organization. Plos Comput Biol. May;5(5):e1000381.

Fan Y, Shi F, Smith JK, Lin W, Gilmore JH, Shen D. 2011. Brain anatomical networks in early human brain development. Neuroimage. Feb 1;54(3):1862-71.

Ferrarini L, Veer IM, Baerends E, van Tol MJ, Renken RJ, van der Wee NJ, et al. 2009. Hierarchical functional modularity in the resting-state human brain. Hum Brain Mapp. Jul;30(7):2220-31.

Fodor JA. 1983. The modularity of mind: An essay on faculty psychology. MIT Press.

Fries P. 2005. A mechanism for cognitive dynamics: Neuronal communication through neuronal coherence. Trends Cogn Sci. Oct;9(10):474-80.

Geschwind N. 1965. Disconnexion syndromes in animals and man. I. Brain. Jun;88(2):237-94.

Gong G, He Y, Concha L, Lebel C, Gross DW, Evans AC, Beaulieu C. 2009. Mapping anatomical connectivity patterns of human cerebral cortex using in vivo diffusion tensor imaging tractography. Cereb Cortex. Mar;19(3):524-36.

Greicius MD, Srivastava G, Reiss AL, Menon V. 2004. Default-Mode network activity distinguishes alzheimer's disease from healthy aging: Evidence from functional MRI. Proc Natl Acad Sci U S A. Mar 30;101(13):4637-42.

Guimerà R, Sales-Pardo M, Amaral LA. 2004. Modularity from fluctuations in random graphs and complex networks. Phys Rev E Stat Nonlin Soft Matter Phys. Aug;70(2 Pt 2):025101.

Guimerà R, Amaral LA. 2005. Cartography of complex networks: Modules and universal roles. J Stat Mech 2005. Feb 1; (P02001):nihpa35573.

de Haan W, Pijnenburg YA, Strijers RL, van der Made Y, van der Flier WM, Scheltens P, Stam CJ. 2009. Functional neural network analysis in frontotemporal dementia and alzheimer's disease using EEG and graph theory. BMC Neurosci. 10:101.

Hagmann P, Cammoun L, Gigandet X, Meuli R, Honey CJ, Wedeen VJ, Sporns O. 2008. Mapping the structural core of human cerebral cortex. Plos Biol. 6(7):e159.

He Y, Chen Z, Evans A. 2008. Structural insights into aberrant topological patterns of large-scale cortical networks in alzheimer's disease. J Neurosci. Apr 30;28(18):4756-66.

He Y, Wang J, Wang L, Chen ZJ, Yan C, Yang H, et al. 2009. Uncovering intrinsic modular organization of spontaneous brain activity in humans. Plos One. 4(4):e5226.

Hilgetag CC, Burns GA, O'Neill MA, Scannell JW, Young MP. 2000. Anatomical connectivity defines the organization of clusters of cortical areas in the macaque monkey and the cat. Philos Trans R Soc Lond B Biol Sci. Jan 29;355(1393):91-110.

Humphries MD, Gurney K. 2008. Network 'small-world-ness': A quantitative method for determining canonical network equivalence. Plos One. 3(4):e0002051.

Iturria-Medina Y, Sotero RC, Canales-Rodríguez EJ, Alemán-Gómez Y, Melie-García L. 2008. Studying the human brain anatomical network via diffusion-weighted MRI and graph theory. Neuroimage. Apr 15;40(3):1064-76.

Jeong J. 2004. EEG dynamics in patients with alzheimer's disease. Clin Neurophysiol. Jul;115(7):1490-505.

Kaiser M, Martin R, Andras P, Young MP. 2007. Simulation of robustness against lesions of cortical networks. Eur J Neurosci. May;25(10):3185-92.

Kitzbichler MG, Henson RN, Smith ML, Nathan PJ, Bullmore ET. 2011. Cognitive effort drives workspace configuration of human brain networks. J Neurosci Jun 1;31(22):8259-70.

Lancichinetti A, Fortunato S. 2009. Community detection algorithms: A comparative analysis. Phys Rev E Stat Nonlin Soft Matter Phys. Nov;80(5 Pt 2):056117.

Leise EM. 1990. Modular construction of nervous systems: A basic principle of design for invertebrates and vertebrates. Brain Res Brain Res Rev. 15(1):1-23.

Lindeboom J, Schmand B, Tulner L, Walstra G, Jonker C. 2002. Visual association test to detect early dementia of the alzheimer type. J Neurol Neurosurg Psychiatry. Aug;73(2):126-33.

Li Y, Liu Y, Li J, Qin W, Li K, Yu C, Jiang T. 2009. Brain anatomical network and intelligence. Plos Comput Biol. May;5(5):e1000395.

De Luca M, Beckmann CF, De Stefano N, Matthews PM, Smith SM. 2006. Fmri resting state networks define distinct modes of long-distance interactions in the human brain. Neuroimage. Feb 15;29(4):1359-67.

Luteijn F, Ploeg FAE. Van der. 1982. Groninger Intelligentie Test (in Dutch). Lisse: Swets & Zeitlinger.

McKhann G, Drachman D, Folstein M, Katzman R, Price D, Stadlan EM. 1984. Clinical diagnosis of alzheimer's disease: Report of the NINCDS-ADRDA work group under the auspices of department of health and human services task force on alzheimer's disease. Neurology. Jul;34(7):939-44.

Mesulam MM. 1998. From sensation to cognition. Brain. Jun;121 (Pt 6):1013-52.

Meunier D, Achard S, Morcom A, Bullmore E. 2009. Age-Related changes in modular organization of human brain functional networks. Neuroimage. Feb 1;44(3):715-23.

Meunier D, Lambiotte R, Fornito A, Ersche KD, Bullmore ET. 2009. Hierarchical modularity in human brain functional networks. Front Neuroinformatics. 3:37.

Montez T, Linkenkaer-Hansen K, van Dijk BW, Stam CJ. 2006. Synchronization likelihood with explicit time-frequency priors. Neuroimage. Dec;33(4):1117-25.

Newman M. 2010. Networks : An introduction. New York: Oxford University Press.

Newman MEJ. 2003. The structure and function of complex networks. SIAM Review 45.

Newman MEJ, Girvan M. 2004. Finding and evaluating community structure in networks. Physical Review E. 69(2):26113.

Newman MEJ. 2006. Finding community structure in networks using the eigenvectors of matrices. Physical Review E. 74(3):36104.

Palla G, Derényi I, Farkas I, Vicsek T. 2005. Uncovering the overlapping community structure of complex networks in nature and society. Nature. Jun 9;435(7043):814-8.

Pereda E, Quiroga RQ, Bhattacharya J. 2005. Nonlinear multivariate analysis of neurophysiological signals. Prog Neurobiol. 77(1-2):1-37.

Pievani M, de Haan W, Wu T, Seeley WW, Frisoni GB. 2011. Functional network disruption in the degenerative dementias. Lancet Neurol. Sep;(10)9;829-43.

Rey A. 1964. L'examen clinique en psychologie. Paris: Presse Universitaire de France.

Rubinov M, Knock SA, Stam CJ, Micheloyannis S, Harris AW, Williams LM, Breakspear M. 2009. Small-World properties of nonlinear brain activity in schizophrenia. Hum Brain Mapp. Feb;30(2):403-16.

Rubinov M, Sporns O, van Leeuwen C, Breakspear M. 2009. Symbiotic relationship between brain structure and dynamics. BMC Neurosci.10:55.

Rubinov M, Sporns O. 2010. Complex network measures of brain connectivity: Uses and interpretations. Neuroimage. Sep;52(3):1059-69.

Salvador R, Suckling J, Coleman MR, Pickard JD, Menon D, Bullmore E. 2005. Neurophysiological architecture of functional magnetic resonance images of human brain. Cereb Cortex. Sep;15(9):1332-42.

Salvador R, Martínez A, Pomarol-Clotet E, Gomar J, Vila F, Sarró S, et al. 2008. A simple view of the brain through a frequency-specific functional connectivity measure. Neuroimage. Jan 1;39(1):279-89.

Schwarz AJ, Gozzi A, Bifone A. 2008. Community structure and modularity in networks of correlated brain activity. Magn Reson Imaging. Sep;26(7):914-20.

Singer W, Gray CM. 1995. Visual feature integration and the temporal correlation hypothesis. Annu Rev Neurosci. 18:555-86.

Sperling RA, Laviolette PS, O'Keefe K, O'Brien J, Rentz DM, Pihlajamaki M, et al. 2009. Amyloid deposition is associated with impaired default network function in older persons without dementia. Neuron. Jul 30;63(2):178-88.

Sporns O, Chialvo DR, Kaiser M, Hilgetag CC. 2004. Organization, development and function of complex brain networks. Trends Cogn Sci. Sep;8(9):418-25.

Sporns O. 2010. Networks of the brain. Cambridge, Mass.: The MIT Press.

Stam CJ, Dijk BWV. 2002. Synchronization likelihood: An unbiased measure of generalized synchronization in multivariate data sets. Physica D: Nonlinear Phenomena. 163(3-4):236 - 251.

Stam CJ, Jones BF, Manshanden I, van Cappellen van Walsum AM, Montez T, Verbunt JP, et al. 2006. Magnetoencephalographic evaluation of resting-state functional connectivity in alzheimer's disease. Neuroimage. Sep;32(3):1335-44.

Stam CJ, Reijneveld JC. 2007. Graph theoretical analysis of complex networks in the brain. Nonlinear Biomed Phys. 1(1):3.

Stam CJ, de Haan W, Daffertshofer A, Jones BF, Manshanden I, van Cappellen van Walsum AM, et al. 2009. Graph theoretical analysis of magnetoencephalographic functional connectivity in alzheimer's disease. Brain. Jan;132(Pt 1):213-24.

Stam CJ. 2010. Characterization of anatomical and functional connectivity in the brain: A complex networks perspective. Int J Psychophysiol. Sep;77(3):186-94.

Stam CJ. 2010. Use of magnetoencephalography (MEG) to study functional brain networks in neurodegenerative disorders. J Neurol Sci, Feb 15;289(1-2):128-34.

Supekar K, Menon V, Rubin D, Musen M, Greicius MD. 2008. Network analysis of intrinsic functional brain connectivity in alzheimer's disease. Plos Comput Biol. Jun;4(6):e1000100.

van den Heuvel MP, Stam CJ, Boersma M, Hulshoff Pol HE. 2008. Small-World and scale-free organization of voxel-based resting-state functional connectivity in the human brain. Neuroimage. Nov 15;43(3):528-39.

van den Heuvel MP, Mandl RC, Kahn RS, Hulshoff Pol HE. 2009. Functionally linked resting-state networks reflect the underlying structural connectivity architecture of the human brain. Hum Brain Mapp. Oct;30(10):3127-41.

van den Heuvel MP, Hulshoff Pol HE. 2010. Exploring the brain network: A review on resting-state fmri functional connectivity. Eur Neuropsychopharmacol. Aug;20(8):519-34.

van Wijk BC, Stam CJ, Daffertshofer A. 2010. Comparing brain networks of different size and connectivity density using graph theory. PLoS One. Oct;28;5(10).

Varela F, Lachaux JP, Rodriguez E, Martinerie J. 2001. The brainweb: Phase synchronization and large-scale integration. Nat Rev Neurosci. Apr;2(4):229-39.

Verhage, F. 1965. Intelligence and age in a dutch sample. Human Development. 8(4):238-45.

Vrba, J. 1999. Recent advances in biomagnetism : Proceedings of the 11th international conference on biomagnetism. Sendai, Japan: Tohoku University Press.

Watts DJ, Strogatz SH. 1998. Collective dynamics of 'small-world' networks. Nature. Jun 4;393(6684):440-2.

Node 6

Disruption of functional brain networks in Alzheimer's disease: what can we learn from graph spectral analysis of resting-state MEG?

Brain Connectivity 2012

W. de Haan*[a, b], W.M. van der Flier[b,c], H. Wang[d], P. Van Mieghem[d], P. Scheltens[b] and C.J. Stam[a]

[a.] Department of Clinical Neurophysiology and MEG, VU University Medical Center, PO Box 7057, 1007 MB, Amsterdam, The Netherlands

[b.] Alzheimer Center, Department of Neurology, VU University Medical Center, PO Box 7057 1007 MB, Amsterdam, The Netherlands

[c.] Department of Epidemiology and Biostatistics, VU University Medical Center, PO Box 7057, 1007 MB, Amsterdam, The Netherlands

[d.] Faculty of Electrical Engineering, Mathematics and Computer Science, Delft University of Technology, P.O Box 5031, 2600 GA Delft, The Netherlands

ABSTRACT

In Alzheimer's disease (AD), structural and functional brain network organization is disturbed. However, many of the present network analysis measures require *a priori* assumptions and methodological choices that influence outcome and interpretation. Graph *spectral* analysis is a more direct algebraic method to describe network properties, which might lead to more reliable results. In this study, graph spectral analysis was applied to magnetoencephalography (MEG) data to explore functional network integrity in AD. Sensor-level resting-state MEG was performed in 18 Alzheimer patients (age 67±9, 6 females) and 18 healthy controls (age 66±9, 11 females). Weighted, undirected graphs were constructed based on functional connectivity analysis using the Synchronization likelihood (SL), and graph spectral analysis was performed with a focus on network connectivity, synchronizability and node centrality. Main outcomes were a global loss of network connectivity and altered synchronizability in most frequency bands. Eigenvector centrality mapping (ECM) confirmed the hub status of the parietal areas, and demonstrated low centrality of the left temporal region in the theta band in AD patients that was strongly related to MMSE (global cognitive function test) score ($r=0.67$, $p=0.001$). Summarizing, graph spectral analysis is a theoretically solid approach that is able to detect disruption of functional network topology in AD. In addition to the previously reported overall connectivity losses and parietal area hub status, impaired network synchronizability and a clinically relevant left temporal centrality loss were found in AD patients. Our findings imply that graph spectral analysis is valuable for the purpose of studying altered brain network topology and dynamics in AD.

INTRODUCTION

In Alzheimer's disease (AD), the most prevalent form of dementia, imaging techniques have been successful in demonstrating local brain changes like atrophy, hypometabolism, and protein deposition, but these phenomena do not show a straightforward relation with the gradually progressing severity of cognitive symptoms in AD (Pievani et al., 2011). Since cognition depends heavily on efficient interaction *between* brain areas, changes in brain *network connectivity* might reflect cognitive decline more accurately. Both the investigation of the physical network wiring in the brain as well as the superimposed network *dynamics* ('functional' networks) may help to relate symptoms in AD to the underlying neurodegenerative processes.

In recent years graph theory has increasingly been used as a theoretical framework to describe brain network characteristics (Sporns, 2010). Graph theoretical studies in AD demonstrate disruption of large-scale brain network integrity (Stam et al., 2007; Supekar et al., 2008; He et al., 2009; de Haan et al., 2009; Stam et al., 2009; Lo et al., 2010; Sanz-Arigita et al., 2010). However, applying graph theoretical concepts to neuroscience also poses methodological dilemmas. A growing number of measures is being developed (Rubinov and Sporns, 2010), and although the reproducibility of graph measures is good (Deuker et al., 2009), varying definitions can bias outcomes and interpretations. For example, many graph measures are directly dependent on network size and density, demanding arbitrary normalization or thresholding procedures (van Wijk 2010).

A technique that is known in fields like mathematics, chemistry and engineering for its powerful characterization of network features is *Graph Spectral Analysis* (GSA) (Van Mieghem, 2011). In short, GSA investigates the *spectrum* of a network, which is the set of *eigenvectors* and corresponding *eigenvalues* that is mathematically derived from the adjacency or Laplacian matrix of the network. The spectrum contains considerable information about relevant network properties such as connectivity levels and resilience to damage, but also provides measures directly related to network dynamics, such as the spread of information throughout a network (Bonacich and Lloyd, 2001; Van Mieghem et al., 2009). Since interaction between distant brain regions is essential for cognition, dynamical efficiency is probably an important aspect of large-scale brain network topology (Arenas et al., 2008). Two graph spectral measures described in this study, the spectral gap and eigenratio, make predictions about the dynamical behavior in a network based on its topology. Another, relatively familiar graph spectral measure is the *eigenvector centrality* (EC) which is used to identify highly connected 'hub' regions in networks (Bonacich, 2007; Lohmann et al., 2010). Since hub region vulnerability has repeatedly been reported in AD (Buckner et al., 2005; Stam et al., 2009), the further exploration of hub structure is very relevant, as it could point towards an explanation for this fundamental pathophysiologic phenomenon.

The deterministic nature of graph spectral analysis and its solid theoretical background might make it a promising complement to the commonly used graph measures. We set out to investigate AD-related changes in five spectral measures describing network topology and hub status. To evaluate the clinical value of this approach, the relation of regional eigenvector centrality to cognitive test scores was also examined. Our hypothesis was that, in addition to the previously reported loss of functional network connectivity, graph spectral measures would be able to detect impaired network synchronizability. Also, we expected to find parietal hub region vulnerability and a corresponding decrease of regional EC values in AD.

MATERIALS AND METHODS

Patients and controls

The study involved 18 patients with a diagnosis of probable AD according to the NINCDS-ADRDA criteria (McKhann et al., 1984) who were recruited from the Alzheimer Centre of the VU University Medical Center. AD patients were assessed according to a standard diagnostic workup, which involved history taking, physical and neurological examination, an interview with a spouse or close family member, neuropsychological assessment, blood tests, MRI of the brain, and EEG. The diagnosis was made in a consensus meeting in which all the available clinical data were considered by a multidisciplinary team. Exclusion criteria for this study were active psychiatric or neurologic disease, or a MMSE score below 16. Eighteen healthy controls, often spouses of patients, were included as well. No structural (MRI) scans of the control subjects were made, but they were screened by a neurologist and underwent the same neuropsychological test battery as the patients. In both groups use of psychoactive medication was incidentally reported: antidepressants (specific serotonine reuptake inhibitors and tricyclic antidepressants, AD n=3: controls n=1) and sleep medication (benzodiazepines, AD n=1: controls n=2). Since AD patients were diagnosed shortly before the MEG recording was performed, few of them already used cholinesterase inhibitors (galantamine, n=2). Most frequent comorbidities were hypertension (AD n=6; controls n=3) and diabetes mellitus type 2 (AD n=4: controls n=0). Main subject characteristics are summarized in table 1.

Global cognitive functioning was assessed with the Mini Mental State Examination (MMSE) (Folstein et al., 1983). Level of education was classified according to the system of Verhage ranging from 1 to 7 (low to highly educated) (Verhage, 1965). The Local Research Ethics Committee approved the study and all participants gave written informed consent. Subjects and recordings were identical to a recent graph theoretical study focusing on modularity (de Haan et al., 2011).

Table 1. Subject characteristics. Data are represented as mean±SD unless indicated otherwise. N= number of subjects, M=males, F=females, MMSE=mini mental state examination. Education score is based on Verhage index (Verhage F, 1965).

	Controls	Alzheimer patients	
N	18	18	
Age	66±9	67±9	p = 0.82
Gender (M/F)	7/11	12/6	p = 0.16
MMSE	29±1	23±1	p < 0.001
Education	5±1	5±1	p = 0.89

MEG recording and post-processing

Magnetic fields were recorded while subjects were seated inside a magnetically shielded room (Vacuumschmelze GmbH, Hanau, Germany) using a 151-channel whole-head MEG system (CTF Systems Inc., Port Coquitlam, BC, Canada). A third-order software gradient (Vrba and Robinson, 2001) was used after online band-pass filtering between 0.25 and 125 Hz. Sample frequency was 625 Hz. For technical reasons two channels had to be omitted, leaving 149 channels for analysis. Subjects were measured during a no-task, eyes-closed condition. At the beginning and at the ending of the recording the head position relative to the coordinate system of the helmet was recorded by leading small alternating currents through three head position coils attached to the left and right pre-auricular points and the nasion on the subject's head. Head position changes during the recording up to approximately 1.5 cm were accepted. During the MEG recording, subjects were instructed to close their eyes, stay awake, and reduce eye movements. In addition, we instructed subjects to just let their minds wander, and certainly not to perform specific cognitive tasks such as counting.

Typical artifacts were due to (eye) movements, swallowing, dental prosthetics, or drowsiness. For each subject, care was taken to select four artifact-free epochs of 4096 samples (approximately 6.5 seconds) by two of the investigators (WDH and CS), who were blinded to the diagnosis. All further analyses were performed in the following frequency bands: delta (0.5-4 Hz), theta (4-8 Hz), lower alpha (8-10 Hz), higher alpha (10-13 Hz), beta (13-30 Hz) and gamma (30-45 Hz). All functional connectivity and graph analyses were performed for each epoch separately, and prior to statistical analysis the four epoch results of each person were averaged.

All functional connectivity and subsequent graph spectral analyses were performed with in-house developed software (BrainWave version 0.8.68, CS. Software available at: http://home.kpn.nl/stam7883/brainwave.html). Graph spectral measures described below were implemented using an open access JAVA library called JAMA (http://www.cs.princeton.edu/introcs/95linear/Eigenvalues.java.html)

Functional connectivity analysis

Correlations between all pair-wise combinations of MEG channels were computed with the Synchronization Likelihood (SL). Mathematical details can be found in previous work (Stam and Dijk, 2002; Montez et al., 2006), and in the supplemental material; here we give a brief description. The SL is a general measure of the correlation or synchronization between two time series, which is sensitive to linear as well as nonlinear interdependencies. The basic principle of the SL is to divide each time series into a series of 'patterns' (roughly, brief pieces of time series containing a few cycles of the dominant frequency) and to search for a recurrence of these patterns. The SL is then the probability that pattern recurrence in time series X coincides in time with pattern recurrence in time series Y. The end result of computing the SL for all pair-wise combinations of channels is a square matrix (with 149 rows and columns, equal to the number of MEG channels), where each entry contains the resulting SL value of the sensor pair. This matrix is called the *weighted* (connections strengths or *weights* are included) *adjacency* or *connectivity matrix A*. Note that any connectivity measure could be used for this purpose. Since all connections in our network are bidirectional, the adjacency matrix is symmetrical along its diagonal axis.

Graph Spectral Analysis

In this section, we give a brief explanation of the concepts and measures used in this study; for a more extensive technical background, please see (Van Mieghem, 2011; Bonacich and Lloyd, 2001; Brouwer and Haemers, 2011; Newman, 2007; Farkas et al., 2001). The multi-step procedure from MEG recording to spectral analysis is summarized in figure 1.

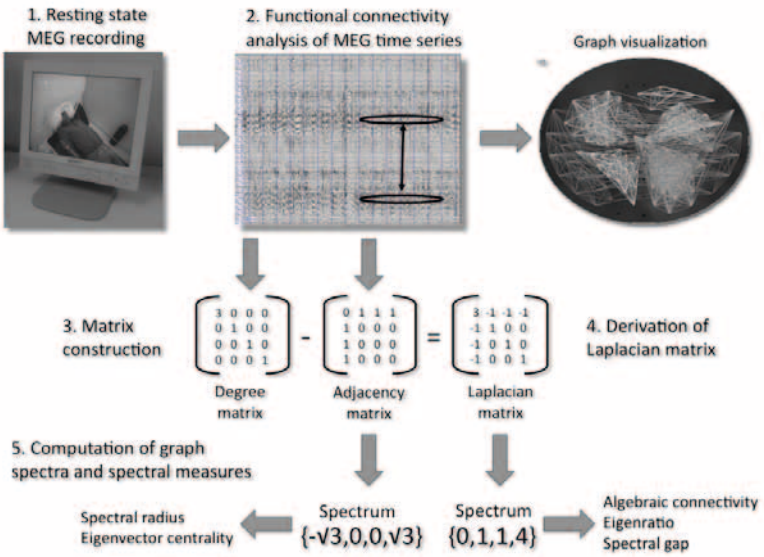

Figure 1. Multi-step procedure from MEG recording to the computation of graph spectral measures. For this study brain activity was recorded in an eyes-close resting-state condition. Functional connectivity analysis was performed on 4 time segments (ca. 6.5 seconds) per person. Subsequently, weighted functional brain networks were formed, and from the corresponding adjacency matrices the Laplacian matrices were constructed. For each network, from both the adjacency and Laplacian matrices the spectrum was calculated, and the eigenvalues from these spectra were used to compute various spectral measures. Spectral measures were then used in statistical analysis to compare group averages and correlation with cognition. Note that once a network is constructed, its eigenvectors and eigenvalues will be determined.

Graph spectral measures are derived from the adjacency or *Laplacian matrix Q*. This is done by subtracting the adjacency matrix from the *degree matrix* Δ (Q=Δ-A), which is the diagonal matrix with the nodal degrees (equal to the rowsum of the adjacency matrix); see figure 1 for an example. The Laplacian matrix can be regarded as way to combine both connectivity and degree information (all relevant information) in the same matrix. Both the adjacency and Laplacian matrix can be written in terms of their eigenvectors and corresponding eigenvalues, e.g. $A=XAX^T$, where the matrix X consists of all eigenvectors in columns and the diagonal matrix A contains the corresponding eigenvalues. The spectral information (X and A) thus contains the same information as the topology, or adjacency matrix (Van Mieghem, 2011). The spectrum of a graph can be regarded as a unique 'fingerprint'. Especially the different eigenvalues contain precise information about network properties, and can be used to quantitatively classify network topologies. Here, we briefly describe four graph spectral measures that contain meaningful information about the network as a whole (two derived from the adjacency matrix, two from the Laplacian matrix) and one measure with a more local focus.

Global graph analysis

The **spectral radius** λ is the largest eigenvalue of the adjacency matrix, and obeys $2L/N \leq \lambda \leq d_{max}$, where N and L are the number of links and nodes and d_{max} is the maximum degree in the graph (Van Mieghem, 2011). For a fixed size N of the network, the larger λ is, the more links L, and the better connected the network (Brouwer and Haemers,; Dvorák and Mohar, 2010). The inverse of the spectral radius equals the epidemic threshold in a network (Van Mieghem et al., 2009), and is proportional to the synchronization threshold of a network (Restrepo et al., 2005). It is also related to *kappa*, the ratio of the average squared degree and the average degree.

The **spectral gap** describes how fast a dynamic process in a network will converge to the steady state (Van Mieghem, 2011). It is equal to the difference between the two largest eigenvalues of the adjacency matrix. Please note that the spectral gap and the eigenratio (introduced below) are graph spectral measures that deal with synchronized states of a *network*, as opposed to the underlying synchronization measure between nodes (SL in this case) that is used to determine the connectivity matrix.

The **algebraic connectivity**, introduced by Fiedler in 1973, measures how difficult it is to tear a network apart. If the network is fully connected, the algebraic connectivity is greater than 0. The magnitude of the algebraic connectivity can also be regarded as a measure for network 'robustness'. The algebraic connectivity is equal to the second-smallest eigenvalue of the Laplacian matrix (Fiedler, 1973; Mohar, 1991; Van Mieghem, 2011).

The **eigenratio** expresses the stability of a synchronized state in a dynamical network. It is the ratio of the largest and the second-smallest eigenvalue of the Laplacian matrix. The smaller it is the more stable the network synchronization (Arenas et al., 2008). In this study we use its inverse (1/eigenratio) to get a value between 0 and 1.

Regional graph analysis

The **eigenvector centrality (EC)** is a measure of the relative importance (or hub status) of a node within a network (Bonacich and Lloyd, 2001; Bonacich, 2007). The most straightforward method to identify hubs is by their *degree centrality*, which assigns hub status to nodes with the highest number of connections (or highest sum of all weighted connections). However, this measure only takes a node's direct connections into account. Popular alternative centrality measures that have a wider scope are the *betweenness centrality* and *closeness centrality*; they also have some drawbacks however, such as their dependency on path length and considerable computational demands (Rubinov et al., 2009; Rubinov and Sporns, 2011). In contrast, the defining characteristic of the eigenvector centrality is that it takes into account both the degree of a node and the degrees of its neighbors. It therefore recognizes the fact that having important nodes as immediate neighbors makes a node more important in the network. Actually,

the largest eigenvector component *i* is a 'dynamic' degree, where 'dynamic' refers to all walks in the graph that traverse the node *i*. Eigenvector centrality x_i for node *i* is the i^{th} component of the eigenvector corresponding to the largest eigenvalue of the adjacency matrix, and is equal to:

$$x_i = \frac{1}{\lambda} \sum_{j=1}^{N} A_{ij} x_j \qquad [1]$$

where *l* is the largest eigenvalue of the adjacency matrix, *N* is the total number of nodes, and *A* is the adjacency matrix of the network. Note that x_i is proportional to sum of weights of all nodes connected to it. EC is calculated per node, but we averaged values over ten sensor groups (left and right frontal, temporal, central, parietal and occipital) to obtain a centrality distribution at a larger-scale.

Statistical analysis

The statistical analysis was performed with SPSS for Mac (version 18.0). Normal distribution of all measures was tested with Kolmogorov-Smirnov tests. For testing group differences in spectral radius, spectral gap, algebraic connectivity and eigenratio we performed independent sample t-tests and non-parametric Mann Whitney U tests, which produced very similar results. We analyzed regional EC results using ANOVA for repeated measures (Greenhouse-Geisser corrected) with group as between-subjects factor, and hemisphere (left and right) and sensor region (frontal, central, temporal, parietal and occipital) as within-subjects factors. Gender was included as covariate. Correlations of the regional eigenvector centrality values with MMSE scores were evaluated with Pearson's test. Analyses were performed for all frequency bands separately. For all tests a significance level of $\alpha \leq 0.05$ was used, no correction for multiple comparisons was applied.

RESULTS

Global graph analysis

The spectral radius was generally lower in AD patients, but this difference reached significance only in the gamma band ($p < 0.01$, see figure 2). This indicates a higher network synchronizability threshold in the gamma band.

The spectral gap was lower in AD patients in all frequency bands except for the theta band, which was only significant in the gamma band ($p < 0.01$, see figure 3). This indicates that functional network dynamics in the gamma band will take longer to reach a steady, synchronized state in AD.

The algebraic connectivity in AD patients was lower in the lower alpha ($p < 0.05$), beta ($p < 0.01$) and gamma bands ($p < 0.01$, see figure 4). No differences were found in the remaining three bands. The decrease in multiple frequency bands can be interpreted as a loss of overall connectivity in AD.

The eigenratio was lower in the theta band ($p < 0.05$), and higher in the gamma band ($p < 0.01$) in AD when compared to controls (see figure 5). No differences were found in the other frequency bands. This implies that overall network synchronizability decreases in the theta band, but increases in the gamma band in AD.

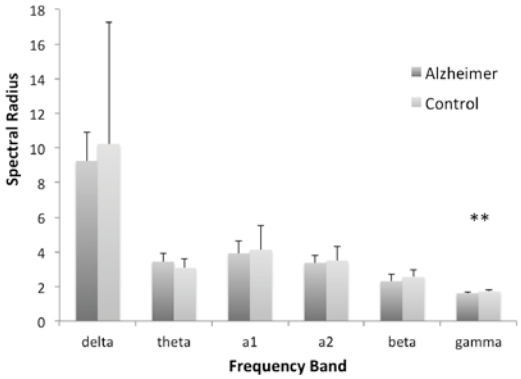

Figure 2. Spectral radius results for the different frequency bands. Error bars indicate standard deviation. AD = Alzheimer patient group, C = control group. a1 = lower alpha band, a2 = higher alpha band. ** $p < 0.01$ (uncorrected).

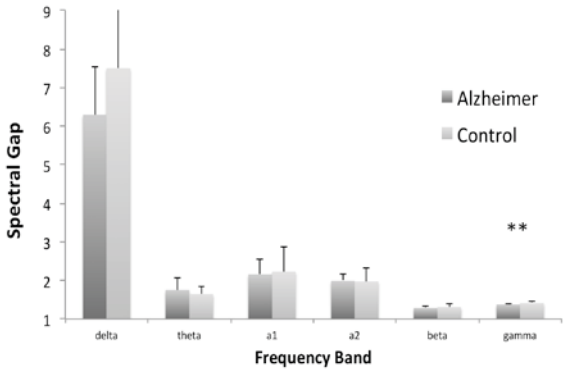

Figure 3. Spectral gap results for the different frequency bands. Error bars indicate standard deviation. AD = Alzheimer patient group, C = control group. a1 = lower alpha band, a2 = higher alpha band. ** $p < 0.01$ (uncorrected).

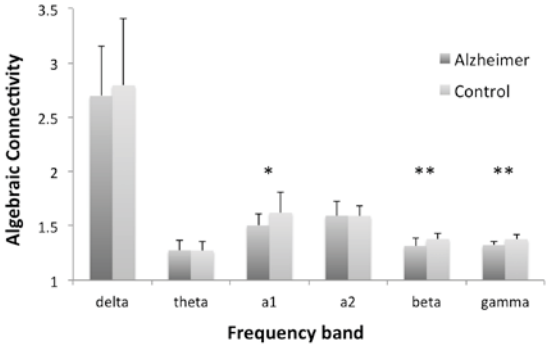

Figure 4. Algebraic connectivity results for the different frequency bands. Error bars indicate standard deviation. AD = Alzheimer patient group, C = control group. a1 = lower alpha band, a2 = higher alpha band. * $p < 0.05$, ** $p < 0.01$ (uncorrected).

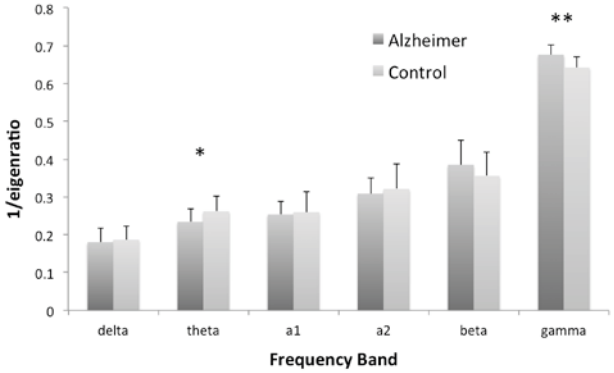

Figure 5. Eigenratio results for the different frequency bands. Note that the depicted results are based on the inverse of the original eigenratio (1/eigenratio) to obtain a value between 0 and 1. Error bars indicate standard deviation. AD = Alzheimer patient group, C = control group. a1 = lower alpha band, a2 = higher alpha band. * $p < 0.05$, ** $p < 0.01$ (uncorrected).

Regional graph analysis

ANOVA for repeated measures of regional EC results (see table 2) showed no main effect of group, but did show a main effect of region in all bands except for the delta band. In the gamma band a main effect of hemisphere was found, but no effects were found in any of the other frequency bands. Moreover, higher alpha and gamma bands showed region*hemisphere interactions, indicating dissimilar regional differences for each hemisphere in those bands. Region*group interactions were found in the theta and beta band, as well as a hemisphere*group interaction in the beta band, pointing to changes in EC distribution in AD.

Table 2. Eigenvector centrality - ANOVA for repeated measures results. Repeated measures ANOVA analysis for eigenvector centrality (EC) averaged per sensor region (frontal, temporal, central, parietal and occipital sensors in both hemispheres). A Greenhouse-Geisser correction was applied to the degrees of freedom of the ANOVA. P-values are uncorrected. Significant effects are printed in bold.

	Between subjects	**Within Subjects**					
	Group	**Region**	**Hemisphere**	**Region * hemisphere**	**Region* group**	**Hemisphere * group**	**Region* hemisphere*group**
Delta	F[1,33] = 0.24 p = 0.63	F[4,132] = 1.23 p = 0.30	F[4,132] = 0.16 p = 0.90	F[4,132] = 0.66 p = 0.56	F[4,132] = 1.32 p = 0.27	F[4,132] = 0.17 p = 0.68	F[4,132] = 2.15 p = 0.11
Theta	F[1,33] = 1.08 p = 0.31	**F[4,132] = 3.96 p = 0.019**	F[4,132] = 1.00 p = 0.32	F[4,132] = 0.31 p = 0.77	**F[4,132] = 3.12 p = 0.04**	F[4,132] = 0.44 p = 0.83	F[4,132] = 0.02 p = 0.99
Lower alpha	F[1,33] = 0.52 p = 0.48	**F[4,132] = 3.21 p = 0.04**	F[4,132] = 3.57 p =0.07	F[4,132] = 1.06 p = 0.37	F[4,132] = 1.74 p = 0.18	F[4,132] = 0.37 p = 0.55	F[4,132] = 1.31 p = 0.28
Higher alpha	F[1,33] = 0.64 p = 0.43	**F[4,132] = 5.63 p = 0.01**	F[4,132] = 0.73 p = 0.40	**F[4,132] = 4.44 p = 0.01**	F[4,132] = 2.12 p = 0.13	F[4,132] = 0.38 p = 0.54	F[4,132] = 0.14 p = 0.89
Beta	F[1,33] = 0.64 p = 0.43	**F[4,132] = 3.17 p = 0.046**	F[4,132] = 0.03 p = 0.87	F[4,132] = 0.25 p = 0.78	**F[4,132] = 3.96 p = 0.02**	**F[4,132] = 4.90 p = 0.03**	F[4,132] = 0.77 p = 0.47
Gamma	F[1,33] = 0.54 p = 0.47	**F[4,132] = 4.47 p = 0.02**	**F[4,132] = 7.49 p = 0.01**	**F[4,132] = 8.30 p = 0.001**	F[4,132] = 1.24 p =0.30	F[4,132] = 1.03 p = 0.32	F[4,132] = 0.35 p = 0.78

In figure 6, the regional EC averages in all frequency bands are displayed. In most bands, EC was highest in the parietal sensors, confirming the previously reported hub status of this region (Buckner et al., 2005; Tomasi and Volkow, 2011). In this band, temporal sensor EC values were relatively low in both groups, and were even lower in AD patients. This indicates a diminishing network role of those regions in the AD patients in the theta band. In the beta band, parietal EC values were lower in AD while temporal and particularly occipital values were higher. In the gamma band, the hemispherical differences were marked, with lower frontal EC but higher EC values in the sensors over the left posterior hemisphere.

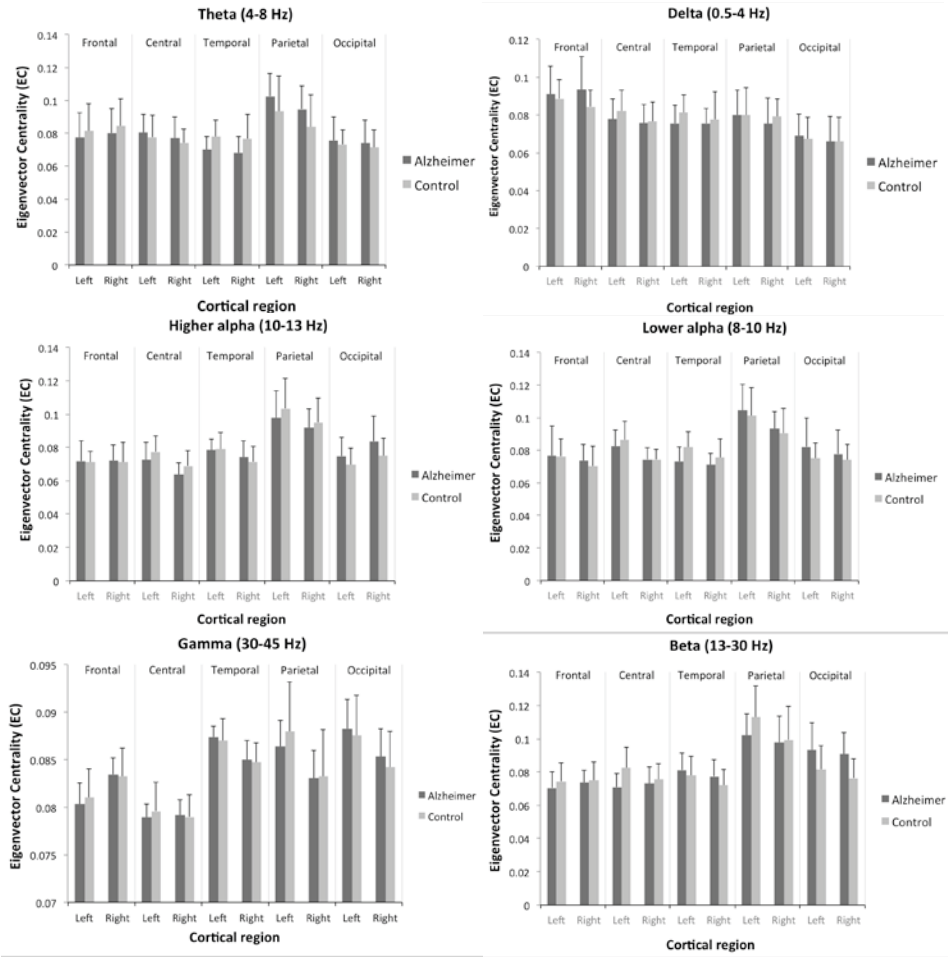

Figure 6. Regional sensor space ECM results for all frequency bands, Alzheimer patients versus control subjects. Error bars indicate standard deviation.

Eigenvector centrality and cognition

Finally, we assessed correlations between regional EC values and MMSE score for the different frequency bands. The results are displayed in table 3.

The left temporal regional EC in the theta band was strongly associated with MMSE score in AD patients ($r = 0.67$, $p = 0.001$) (see figure 7). In the other bands, left temporal EC showed the same trend but with weaker, non-significant correlations. Right central EC in the theta band was negatively correlated to MMSE score in AD patients ($r = -0.66$, $p = 0.003$), but not in the other bands.

In the lower alpha band, the pattern of EC values and changes in AD was similar. In the gamma band, right parietal EC and MMSE were strongly correlated ($r = 0.68$, $p = 0.009$).

Table 3. Relation between eigenvector centrality and MMSE in AD patients. Pearson's bivariate correlations between regional eigenvector centrality (EC) values in ten sensor regions and mini mental examination (MMSE) score (AD patient group). Significant findings are printed in bold; * $p < 0.05$, ** $p < 0.01$ (uncorrected).

EC	Delta	Theta	Lower Alpha	Higher Alpha	Beta	Gamma
Left Frontal	0.03	-0.02	-0.25	-0.25	0.09	-0.18
Right Frontal	-0.30	0.05	-0.09	-0.28	-0.01	-0.29
Left Central	0.09	0.27	-0.14	0.15	-0.05	-0.14
Right Central	-0.42	**-0.66****	-0.26	-0.16	-0.04	-0.16
Left Temporal	0.21	**0.67****	**0.55***	0.38	0.25	0.26
Right Temporal	0.13	-0.02	0.16	0.04	0.03	-0.21
Left Parietal	0.14	0.32	0.47	0.21	-0.33	-0.07
Right Parietal	-0.06	-0.39	0.08	0.17	-0.06	**0.62****
Left Occipital	0.22	0.19	0.00	0.02	0.12	0.30
Right Occipital	0.22	-0.04	-0.18	0.12	0.02	0.23

DISCUSSION

In this first application of graph spectral analysis (GSA) to MEG patient data, we show that this technique is able to detect changes in resting-state functional network integrity of early-stage Alzheimer patients. Main outcomes are a general loss of network integrity in the AD patients, especially in the higher frequency bands, and a distinct pattern of regional connectivity changes that correlate with cognitive impairment. These findings are generally in line with previous literature and our hypotheses, although a few discrepancies were encountered as well.

Global network topology

The decreases in algebraic connectivity and spectral radius in several frequency bands in the AD patient group can be interpreted as a loss of network robustness and deviation from the optimal configuration for dynamic processing. This agrees with related graph theoretical studies in AD so far (He et al., 2009; Stam, 2010), and supports the notion that in AD, functional disconnection between regions is taking place, leading to suboptimal cognitive processing. The finding that these different methods point in the same direction provides a degree of validation. Results of topological and spectral graph measures cannot be compared directly, but the decrease of algebraic connectivity can be taken as a stronger and theoretically sounder sign of network breakdown than the previously reported loss of small-world network structure. In the spectral approach no prior model (e.g. Watts and Strogatz, 1998), normalization of graph measures (e.g. clustering coef-

ficient and path length) through comparison with random surrogate networks, or other additional methodological choices are required.

Theoretically, the relation between network topology and network synchronizability is not straightforward (Arenas et al., 2008), and increased network stability might also be pathological, for example by contributing to epileptic seizures. The prevalence of epilepsy in AD patients is higher than in the healthy population, and it is thought to be directly related to neurodegenerative pathophysiological processes (Palop and Mucke, 2009; Larner, 2010). The observed eigenratio decrease (increase of 1/eigenratio in figure 5) in the gamma band in AD indeed suggests higher network synchronization stability in AD. In the theta band, the eigenratio *in*creases in AD patients, suggesting lower network synchronization stability in this band. This shift, opposite to the gamma band findings, could also point to different network functions of the frequency bands, or to cross-frequency coupling effects; the theta-gamma band relation with regard to memory processes has been repeatedly described, and is very relevant in AD, where memory impairment is often the main symptom. On the other hand, the observed spectral gap decrease in the AD gamma band indicates that reaching a synchronized state will be harder for the network. This finding supports loss of large-scale network synchronizability in AD.

Regional eigenvector centrality

In the present study, parietal sensors had the largest EC values in almost all frequency bands, characterizing them as main hub regions. This is in line with previous findings (Stam et al., 2009; Lo et al., 2010; Tomasi and Volkow, 2011), and with the presumed integrative function of the parietal association areas (Mesulam, 1998). In a recent fMRI study, EC was applied to resting-state voxel-based fMRI networks of healthy subjects to explore differences between individuals in various satiety states (Lohmann et al., 2010). Besides confirming the hub status of the posterior cortical area, Lohmann et al stress advantages like the parameter- and assumption-free nature of eigenvector centrality, as well as its computational efficiency compared to other centrality algorithms when investigating very large networks.

An intriguing recent insight that has come from network analysis in AD is that hub regions (especially parietal) are selectively vulnerable, and overlap strongly with regions of amyloid deposition, hypometabolism and atrophy (Buckner et al., 2005; Drzezga et al., 2011). The vulnerability of parietal hub areas was reflected in our ECM findings by a parietal EC decrease in higher frequency bands and an increase in lower bands, i.e. a loss of high frequency centrality. In addition, a notable regional EC change in AD took place in the theta band in both temporal areas, which already have a relatively low EC in healthy controls. On the one hand this might be a sign of the known (medio-) temporal atrophy and dysfunction in AD, and fit the observed decrease in theta band

synchronizability. However, if a major part of the temporal connections are to and from the vulnerable parietal hub areas, the EC decrease may be mainly due to the weakening parietal hub nodes. Thus, a possible explanation of this difference is the more indirect character of EC compared to degree centrality.

The striking correlation that was found in the theta band between left temporal EC and MMSE score (see table 3 and figure 7) suggests that the drop in network centrality of the left temporal region in AD patients reflects the severity of cognitive symptoms. Overall, only few clear correlations were found between regional EC and MMSE score, even without correction for multiple testing. Nevertheless, the temporal lobe association in the theta band is remarkably strong, and might hold most promise as a functional (bio-)marker of AD progression. It is well known that changes in theta activity are among the earliest neurophysiological signs to accompany AD, and in previous studies left temporal lobe characteristics specifically have been suggested as AD disease progression markers (Fernandez et al., 2003; Osipova et al., 2005; Gianotti et al., 2007).

Limitations and future directions

Several potential limitations of this study should be taken into account. First of all, methodological choices might have influenced our outcome measures and subsequent interpretations: the use of resting-state data, the influence of volume conduction in MEG sensor space analysis, and epoch selection. Another limitation could be our choice for the SL as functional connectivity measure. Although we think it is the most appropriate measure for our purpose given earlier SL-based studies, different functional connectivity measures could lead to different results. The influence of coupling measures on subsequent graph analysis results has not yet been investigated in a systematic way, but since a similar pattern of functional connectivity loss has been reported using different measures, we feel confident that the observed group differences cannot be explained by this choice. In this exploratory study, we opted for several commonly used and well-understood graph spectral measures that describe relevant properties with concern to brain network analysis. However, other measures, for example describing network clustering properties, might be of special interest in future studies (Bialonski and Lehnertz, 2006). Also, it would be interesting to compare the findings obtained in this study with graph spectral results based on different functional connectivity measures, task-based datasets or disease conditions.

From a more clinical perspective, several possible limiting factors might have been present: modest sample size, comorbidity, disease heterogeneity and the use of psychoactive medication, as described in the method section. However, since the occurrence of these phenomena were infrequent and distributed across both groups, it is not likely that they had a large influence on the observed group differences. Persons possessing any of these factors were not identified as outliers.

Conclusion

Graph spectral analysis detects changes in resting-state functional network integrity of mild to moderate Alzheimer patients. The changes in AD patients point towards less efficient network configuration for dynamic processing. Moreover, the relation between loss of temporal lobe centrality and cognitive impairment in AD indicates potential value for tracking disease course. These clinically relevant results, based on a solid, computationally efficient theoretical background that does not require *a priori* assumptions or arbitrary parameter settings, make graph spectral analysis in our opinion a valid approach for exploring brain network integrity.

Acknowledgements

The authors thank Lieke Smits, Nicole Sistermans, Ellemarije Altena, Annelies van der Vlies and Sofie Boom for neuropsychological assessments, and Karin Plugge and Ndedi Sijsma for performing the MEG recordings.

REFERENCES

Arenas A, Díaz-Guilera A, Kurths J, Moreno Y, Zhou C. 2008. Synchronization in complex networks. Physics Reports 469(3):93-153.

Bialonski S and Lehnertz K. 2006. Identifying phase synchronization clusters in spatially extended dynamical systems. Phys Rev E 74: 051909.

Bonacich P, Lloyd P. 2001. Eigenvector-Like measures of centrality for asymmetric relations. Social Networks 23(3):191-201.

Bonacich P. 2007. Some unique properties of eigenvector centrality. Social Networks 29(4):555-64.

Brouwer AE, Haemers WH. *Spectra of graphs*. Electronic Book. Available at http://www.win.tue.nl/.aeb/ipm.pdf

Buckner RL, Snyder AZ, Shannon BJ, LaRossa G, Sachs R, Fotenos AF, et al. 2005. Molecular, structural, and functional characterization of alzheimer's disease: Evidence for a relationship between default activity, amyloid, and memory. J Neurosci 25(34):7709-17.

Deuker L, Bullmore ET, Smith M, Christensen S, Nathan PJ, Rockstroh B, Bassett DS. 2009. Reproducibility of graph metrics of human brain functional networks. Neuroimage 47(4):1460-8.

Drzezga A, Becker JA, Van Dijk KR, Sreenivasan A, Talukdar T, Sullivan C, et al. 2011. Neuronal dysfunction and disconnection of cortical hubs in non-demented subjects with elevated amyloid burden. Brain 134 (pt. 6): 1635-46.

Dvorák Z, Mohar B. 2009. Spectral radius of finite and infinite planar graphs and of graphs of bounded genus. Journal of Combinatorial Theory, Series B Vol. 47, 1096.

Farkas IJ, Derényi I, Barabási AL, Vicsek T. 2001. Spectra of "real-world" graphs: Beyond the semicircle law. Phys Rev E Stat Nonlin Soft Matter Phys 64(2 Pt 2):026704.

Fernandez A, Arrazola J, Maestu F, Amo C, Gil-Gregorio P, Wienbruch C, Ortiz T. 2003. Correlations of hippocampal atrophy and focal low-frequency magnetic activity in alzheimer disease: Volumetric MR imaging-magnetoencephalographic study. American Journal of Neuroradiology 24(3):481.

Fiedler M. 1973. Algebraic connectivity of graphs. Czechoslovak Mathematical Journal 23(2):298-305.

Folstein MF, Folstein SE, McHugh PR, Fanjiang G. 1983. Mini-Mental state examination (MMSE). Arch Gen Psychiatry 40:812.

Gianotti LRR, Kunig G, Lehmann D, Faber PL, Pascual-Marqui RD, Kochi K, Schreiter-Gasser U. 2007. Correlation between disease severity and brain electric LORETA tomography in alzheimer's disease. Clinical Neurophysiology 118(1):186-96.

de Haan W, Pijnenburg YA, Strijers RL, van der Made Y, van der Flier WM, Scheltens P, Stam CJ. 2009. Functional neural network analysis in frontotemporal dementia and alzheimer's disease using EEG and graph theory. BMC Neurosci 10:101.

de Haan W, van der Flier WM, Koene T, Smits LL, Scheltens P, Stam CJ. 2012.

Disrupted modular brain dynamics reflect cognitive dysfunction in Alzheimer's disease. Neuroimage 59(4):3085-93.

He Y, Chen Z, Gong G, Evans A. 2009. Neuronal networks in alzheimer's disease. Neuroscientist 15(4):333-50.

Larner AJ. 2010. Mar. Epileptic seizures in AD patients. Neuromolecular Med 12(1):71-7.

Lo CY, Wang PN, Chou KH, Wang J, He Y, Lin CP. 2010. Diffusion tensor tractography reveals abnormal topological organization in structural cortical networks in alzheimer's disease. J Neurosci 30(50):16876-85.

Lohmann G, Margulies DS, Horstmann A, Pleger B, Lepsien J, Goldhahn D, et al. 2010. Eigenvector centrality mapping for analyzing connectivity patterns in FMRI data of the human brain. Plos One 5(4):e10232.

McKhann G, Drachman D, Folstein M, Katzman R, Price D, Stadlan EM. 1984. Clinical diagnosis of alzheimer's disease: Report of the NINCDS-ADRDA work group under the auspices of department of health and human services task force on alzheimer's disease. Neurology 34(7):939-44.

Mesulam MM. 1998. From sensation to cognition. Brain 121 (Pt 6):1013-52.

Mohar B. 1991. The laplacian spectrum of graphs. Graph Theory, Combinatorics, and Applications 2:871-98.

Montez T, Linkenkaer-Hansen K, van Dijk BW, Stam CJ. 2006. Synchronization likelihood with explicit time-frequency priors. Neuroimage 33(4):1117-25.

Newman MEJ. 2007. The mathematics of networks. The New Palgrave Encyclopedia of Economics.

Osipova D, Ahveninen J, Jensen O, Ylikoski A, Pekkonen E. 2005. Altered generation of spontaneous oscillations in alzheimer's disease. Neuroimage 27(4):835 - 841.

Palop JJ, Mucke L. 2009. Epilepsy and cognitive impairments in Alzheimer disease. Arch Neurol 66(4):435-40.

Restrepo JG, Ott E, Hunt BR. 2005. Onset of synchronization in large networks of coupled oscillators. Phys Rev E 71:036151.

Rubinov M, Knock SA, Stam CJ, Micheloyannis S, Harris AW, Williams LM, Breakspear M. 2009. Small-World properties of nonlinear brain activity in schizophrenia. Hum Brain Mapp 30(2):403-16.

Rubinov M, Sporns O. 2010. Complex network measures of brain connectivity: Uses and interpretations. Neuroimage 52(3):1059-69.

Rubinov M, Sporns O. 2011. Weight-Conserving characterization of complex functional brain networks. Neuroimage 56(4):2068-79.

Sanz-Arigita EJ, Schoonheim MM, Damoiseaux JS, Rombouts SA, Maris E, Barkhof F, et al. 2010. Loss of 'small-world' networks in alzheimer's disease: Graph analysis of FMRI resting-state functional connectivity. Plos One 5(11):e13788.

Sporns O. 2010. *Networks of the brain.* Cambridge, Mass.: The MIT Press.

Stam CJ, Dijk BWV. 2002. Synchronization likelihood: An unbiased measure of generalized synchronization in multivariate data sets. Physica D: Nonlinear Phenomena 163(3-4):236 - 251.

Stam CJ, Jones BF, Nolte G, Breakspear M, Scheltens P. 2007. Small-World networks and functional connectivity in alzheimer's disease. Cereb Cortex 17(1):92-9.

Stam CJ, de Haan W, Daffertshofer A, Jones BF, Manshanden I, van Cappellen van Walsum AM, et al.. 2009. Graph theoretical analysis of magnetoencephalographic functional connectivity in alzheimer's disease. Brain 132(Pt 1):213-24.

Stam CJ. 2010. Characterization of anatomical and functional connectivity in the brain: A complex networks perspective. Int J Psychophysiol 77(3):186-94.

Supekar K, Menon V, Rubin D, Musen M, Greicius MD. 2008. Network analysis of intrinsic functional brain connectivity in alzheimer's disease. Plos Comput Biol 4(6):e1000100.

Tomasi D, Volkow ND. 2011. Functional connectivity hubs in the human brain. Neuroimage 57(3);908-17.

Van Mieghem P, Omic JS, Kooij RE. 2009. Virus Spread in Networks. IEEE/ACM Transaction on Networking, Vol. 17, No. 1, February, pp 1-14.

Van Mieghem P. 2011. *Graph spectra for complex networks.* Cambridge Univ Press.

van Wijk BC, Stam CJ, Daffertshofer A. 2010. Comparing brain networks of different size and connectivity density using graph theory. Plos One 5(10):e13701.

Verhage, F. 1965. Intelligence and age in a dutch sample. Human Development 8(4):238-45.

Vrba J, Robinson SE. 2001. Signal processing in magnetoencephalography. Methods 25(2):249-71.
Watts DJ, Strogatz SH. 1998. Collective dynamics of 'small-world' networks. Nature 393(6684):440-2.

Node 7

Activity Dependent Degeneration Explains Hub Vulnerability in Alzheimer's Disease

PLoS Computational Biology 2012

Willem de Haan*[a, b], Katherine Mott[a], Elisabeth C.W. van Straaten[a], Philip Scheltens[b] and Cornelis J. Stam[a]

[a.] Department of Clinical Neurophysiology and MEG, VU University Medical Center, PO Box 7057, 1007 MB, Amsterdam, The Netherlands

[b.] Alzheimer Center, Department of Neurology, VU University Medical Center, PO Box 7057 1007 MB, Amsterdam, The Netherlands

ABSTRACT

Brain connectivity studies have revealed that highly connected 'hub' regions are particularly vulnerable to Alzheimer pathology: they show marked amyloid-β deposition at an early stage. Recently, excessive local neuronal activity has been shown to increase amyloid deposition. In this study we use a computational model to test the hypothesis that hub regions possess the highest level of activity and that hub vulnerability in Alzheimer's disease is due to this feature. Cortical brain regions were modeled as neural masses, each describing the average activity (spike density and spectral power) of a large number of interconnected excitatory and inhibitory neurons. The large-scale network consisted of 78 neural masses, connected according to a human DTI-based cortical topology. Spike density and spectral power were positively correlated with structural and functional node degrees, confirming the high activity of hub regions, also offering a possible explanation for high resting state Default Mode Network activity. 'Activity dependent degeneration' (ADD) was simulated by lowering synaptic strength as a function of the spike density of the main excitatory neurons, and compared to random degeneration. Resulting structural and functional network changes were assessed with graph theoretical analysis. Effects of ADD included oscillatory slowing, loss of spectral power and long-range synchronization, hub vulnerability, and disrupted functional network topology. Observed transient increases in spike density and functional connectivity match reports in Mild Cognitive Impairment (MCI) patients, and may not be compensatory but pathological. In conclusion, the assumption of excessive neuronal activity leading to degeneration provides a possible explanation for hub vulnerability in Alzheimer's disease, supported by the observed relation between connectivity and activity and the reproduction of several neurophysiologic hallmarks. The insight that neuronal activity might play a causal role in Alzheimer's disease can have implications for early detection and interventional strategies.

AUTHOR SUMMARY

An intriguing recent observation is that deposition of the amyloid-β protein, one of the hallmarks of Alzheimer's disease, mainly occurs in brain regions that are highly connected to other regions. To test the hypothesis that these 'hub' regions are more vulnerable due to a higher neuronal activity level, we examined the relation between brain connectivity and activity in a computational model of the human brain. Furthermore, we simulated progressive damage to brain regions based on their level of activity, and investigated its effect on the structure and dynamics of the remaining brain network. We show that brain hub regions are indeed the most active ones, and that by damaging net-

works according to regional activity levels, we can reproduce not only hub vulnerability but a range of phenomena encountered in actual neurophysiological data of Alzheimer patients as well: loss and slowing of brain activity in Alzheimer, loss of synchronization between areas, and similar changes in functional network organization. The results of this study suggest that excessive, connectivity dependent neuronal activity plays a role in the development of Alzheimer, and that the further investigation of factors regulating regional brain activity might help detect, elucidate and counter the disease mechanism.

INTRODUCTION

Like many other complex networks, the human brain contains parts that are better connected to the rest than others: 'hub' regions. Evidence is increasing that a collection of brain hub regions forms a 'structural core' or 'connectivity backbone' that facilitates cognitive processing [1,2,3]. Brain hub regions are mainly located in heteromodal association cortices (which integrate information coming from primary cortices), and show a striking overlap with the Default Mode Network [4,5]. Furthermore, their function has been related to fundamental cognitive features such as consciousness, memory, and IQ [6-10]. The central role and large responsibility of hub network regions has an obvious downside: hub damage can have a dramatic impact on network integrity [11,12]. One of the most intriguing recent insights in this regard has emerged from network-related studies in the field of Alzheimer's disease (AD): cortical hub areas turn out to be exceptionally vulnerable to amyloid deposition, hypometabolism and, eventually, atrophy [13-15]. This fascinating link between connectivity and susceptibility to AD pathology deserves further study: what could be causing the hub vulnerability?

The prevailing amyloid-cascade hypothesis of AD states that interstitial amyloid-beta proteins exert a toxic effect on surrounding neurons and synapses, thereby disturbing their function and eventually causing dementia [16]. However, this theory does not provide an explanation for the selective vulnerability of highly connected hub areas. Could an activity-driven mechanism, i.e. hub areas suffering most damage *due to* their higher connectivity *and* activity level have any legitimacy? Chronic, excessive metabolic demand can lead to tissue damage in many organs, and the human brain has extraordinary energy demands. Furthermore, major AD risk factors such as age, ApoE genotype, vascular damage and female gender have all been linked to an increased burden on neuronal metabolism, activity and plasticity [17-19]. Recently, direct evidence was presented that excessive neuronal and/or synaptic activity leads to amyloid deposition [20,21,22]. However, whether this relation between neuronal activity and AD pathology exists in humans, and whether hub regions are indeed the most active areas of the brain

has not yet been explored. We speculated that an 'activity dependent degeneration' scenario, in which hub regions are preferentially affected due to high neuronal activity levels, could be a plausible disease mechanism.

To test this hypothesis, a model is required that incorporates both large-scale connectivity as well as (micro-scale) neuronal activity. The macroscopic level is needed to provide a realistic structural human brain topology, including hub regions. Topological maps are well within reach nowadays, since an increasing amount of imaging data describing the human *connectome* is becoming available [1,23,24]. Imposed on this structural framework, a realistic representation of network dynamics is required. For this purpose, so-called *neural mass models* (NMMs) can be employed [25-27]. Here, each neural mass reflects activity in a brain region by representing a large population of interconnected excitatory and inhibitory neurons, characterized by an average membrane potential and spiking density. Multiple neural masses can be coupled according to any desired structural topology (e.g. human anatomical data) to form a dynamic brain model, which can then be employed to investigate the relationship between connectivity and neuronal activity [28-30].

Structural (anatomical) connectivity and functional (dynamical) connectivity are strongly related, but not always in a straightforward way [5,31-33]. It has been shown that macroscopic models of mammalian brain networks combined with graph theoretical analysis may explain the topology of functional networks at various time scales [34-36]. To simulate disease, macroscopic models and graph theory have been used to predict the structural and functional consequences of various types of lesions on brain networks [11,12,30]. Similarly, the gradually progressive neuronal damage of neurodegenerative processes such as AD can be modeled using this approach, and analyzed with graph theoretical tools [14,37-39]. The novel aspect of the present study is that the degenerative damage is based on neuronal activity itself.

In short, by simulating neuronal dynamics on a network that is modeled on a realistic human cortical connectivity structure we explore the relation between large-scale connectivity and neuronal activity in normal and abnormal conditions. In the present study we use this approach to a) establish that cortical hub regions, *because* of their high connectivity, possess the highest intrinsic neuronal activity levels, and b) demonstrate that 'Activity Dependent Degeneration' (ADD), in which brain connectivity is damaged based on local neuronal activity levels, may serve as a computational model of AD that offers a potential explanation for hub vulnerability.

RESULTS

Experiment 1: relation between connectivity and activity

To assess whether the most highly connected cortical regions also showed the highest levels of neuronal activity, we plotted spike density and total power for all regions against the structural degree of nodes (figure 1A). The group of 13 regions with the highest ('very high' category in the figure) structural degree were defined as hubs; the remaining 65 regions were labeled as non-hubs. In non-hubs, spike density actually showed a weak negative relation with structural degree, but in hubs clearly higher levels were found compared to non-hubs ($p<0.01$). Furthermore, the total power of hubs was significantly higher than that of non-hubs ($p<0.0001$). Figure 1B shows the same relations, but now plotted for all regions, and for three different initial coupling strengths. When S=1.5, the correlations between structural degree and spike density (r=0.35) and structural degree and total power (r=0.94) indicate that especially the link between structural degree and total power is strong. For higher coupling strengths between the NMMs (S=2.0), a strong positive correlation between structural degree and spike density was observed as well (r=0.86). Thus, although coupling strength has an influence on these results, overall the positive relation between structural connectivity and neuronal activity is apparent.

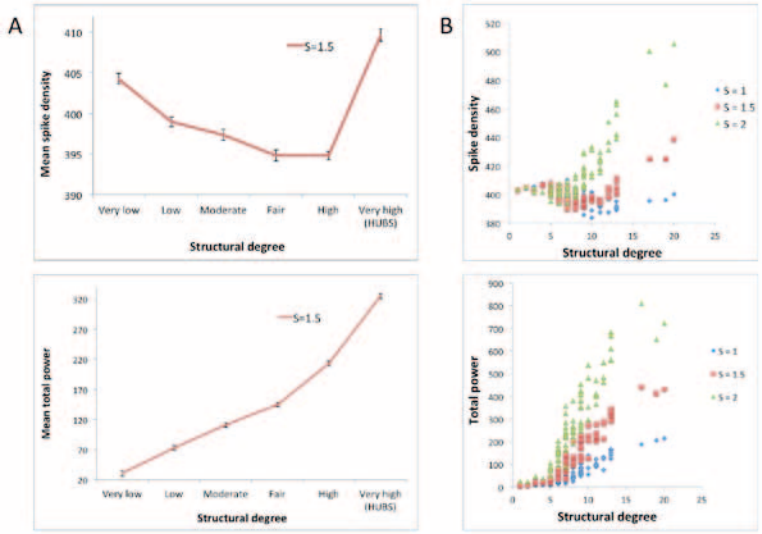

Figure 1: Relation between structural degree and neuronal activity
A: Six bins with ascending mean structural degrees are plotted against their average spike density and total power values. Nodes in the 'very high' degree bin were defined as hubs. Coupling strength (S) between neural masses was set to 1.5. Error bars indicate standard deviation within each bin. **B**: Similar plots as in the left panel, but for every region individually, and for three different coupling strengths S (see Supporting information, section 3).

Since activity level might also be influenced by a nodes functional role rather than its structural connectivity status, we performed comparisons between structural and functional degree (sum of all weighted *functional* connections of a node) of all nodes for the common frequency bands (delta 0-4 Hz, theta 4-8 Hz, lower alpha 8-10 Hz, higher alpha 10-13 Hz, beta 13-30 Hz, gamma 30-45 Hz). Results of this analysis and of direct comparisons between functional degree and neuronal activity are reported in Supporting information section 1. In most bands, clear positive correlations were found, demonstrating that functional hub regions generally have high neuronal activity levels as well. Table 1 shows all 78 regions ranked by structural degree, with their functional degree, total power and spike density levels.

Table 1. Cortical regions; degree of connectivity and level of activity.

Cortical region	*Structural degree*	*Functional degree**		*Spike density*	*Total power*
Precuneus R	20	0.034	±0.004	435	420
Precuneus L	19	0.034	±0.003	426	408
Middle Occipital Gyrus L	17	0.033	±0.004	428	447
Superior Frontal Gyrus, medial R	13	0.035	±0.004	395	228
Calcarine fissure and surrounding cortex L	13	0.035	±0.004	408	296
Middle Temporal Gyrus L	13	0.034	±0.004	404	275
Superior Occipital Gyrus R	13	0.032	±0.005	410	342
Calcarine fissure and surrounding cortex R	13	0.032	±0.005	412	352
Precentral Gyrus L	13	0.031	±0.005	403	312
Lingual Gyrus R	12	0.032	±0.004	403	203
Superior Frontal Gyrus, medial L	12	0.032	±0.005	395	226
Middle Occipital Gyrus R	12	0.031	±0.004	404	285
Precentral Gyrus R	12	0.03	±0.004	398	278
Postcentral Gyrus L	11	0.033	±0.004	396	227
Superior Frontal Gyrus, dorsal L	11	0.032	±0.005	396	242
Postcentral Gyrus R	11	0.031	±0.004	395	261
Superior Frontal Gyrus, dorsal R	11	0.03	±0.005	396	234
Superior Temporal Gyrus R	10	0.034	±0.004	397	127
Supplementary motor area R	10	0.034	±0.005	398	188
Cuneus R	10	0.034	±0.004	398	276
Superior Occipital Gyrus.L	10	0.027	±0.004	398	264
Insula L	9	0.035	±0.006	395	143
Inferior Temporal Gyrus L	9	0.033	±0.004	395	184
Lingual Gyrus L	9	0.033	±0.005	398	205
Supplementary motor area L	9	0.032	±0.005	397	131

Supramarginal Gyrus R	9	0.032	±0.005	393	175
Angular gyrus R	9	0.03	±0.006	391	200
Middle Temporal Gyrus R	9	0.03	±0.005	393	177
Fusiform Gyrus L	9	0.03	±0.005	395	167
Superior Parietal Gyrus R	9	0.029	±0.005	393	207
Middle Frontal Gyrus, R	9	0.029	±0.004	400	61
Inferior Frontal Gyrus, orbital part L	9	0.028	±0.006	398	130
Anterior Cingulate and paracingulate Gyri L	9	0.028	±0.006	395	140
Cuneus L	9	0.028	±0.004	397	86
Superior Frontal Gyrus, medial orbital R	8	0.033	±0.004	393	109
Angular gyrus L	8	0.032	±0.005	392	232
Superior Parietal Gyrus L	8	0.03	±0.004	395	163
Inferior Frontal Gyrus, opercular part.R	8	0.029	±0.006	400	64
Superior Frontal Gyrus, orbital part L	8	0.028	±0.005	395	122
Superior Temporal Gyrus L	8	0.028	±0.004	402	74
Middle Frontal Gyrus L	8	0.028	±0.005	394	123
Temporal Pole: middle temporal gyrus R	8	0.026	±0.005	396	113
Paracentral Lobule L	8	0.026	±0.005	399	101
Anterior Cingulate and paracingulate gyri R	8	0.026	±0.004	394	143
Fusiform Gyrus R	8	0.024	±0.005	394	145
Superior Frontal Gyrus, medial orbital L	7	0.032	±0.003	390	120
Median Cingulate and paracingulate gyri R	7	0.031	±0.005	402	69
Inferior Occipital Gyrus L	7	0.03	±0.005	397	127
Paracentral Lobule R	7	0.029	±0.005	403	63
Inferior Frontal Gyrus, opercular part L	7	0.028	±0.006	405	31
Supramarginal Gyrus L	7	0.028	±0.006	398	75
Gyrus Rectus L	7	0.027	±0.004	394	63
Rolandic operculum L	7	0.027	±0.005	398	110
Inferior Frontal Gyrus, triangular part L	7	0.027	±0.004	396	101
Superior Frontal Gyrus, orbital part R	7	0.026	±0.004	405	37
Inferior Parietal L	7	0.026	±0.004	402	42
Inferior Temporal Gyrus R	7	0.015	±0.003	394	109
Inferior Occipital Gyrus R	6	0.031	±0.004	409	23
Olfactory cortex R	6	0.025	±0.004	396	134
Parahippocampal Gyrus L	6	0.025	±0.006	404	47
Temporal Pole: middle temporal gyrus L	6	0.025	±0.004	402	45
Inferior Parietal R	6	0.025	±0.005	394	112
Median Cingulate and paracingulate gyri L	6	0.024	±0.004	405	43
Parahippocampal Gyrus R	6	0.023	±0.005	399	60
Rolandic operculum R	6	0.023	±0.003	410	35
Posterior cingulate Gyrus L	6	0.021	±0.003	404	43

Inferior Frontal Gyrus triangular part R	6	0.02	±0.005	404	45
Inferior Frontal Gyrus, orbital part R	5	0.024	±0.006	404	31
Insula R	5	0.021	±0.004	404	17
Temporal Pole: superior temporal gyrus L	5	0.018	±0.003	405	29
Middle Frontal Gyrus, orbital part L	5	0.017	±0.004	390	163
Posterior Cingulate Gyrus R	5	0.013	±0.002	397	225
Middle Frontal Gyrus, orbital part R	4	0.022	±0.004	406	19
Gyrus Rectus R	4	0.014	±0.002	405	29
Olfactory cortex L	4	0.013	±0.003	400	37
Temporal Pole: superior temporal gyrus R	3	0.017	±0.003	403	17
Heschl Gyrus L	2	0.012	±0.002	405	9
Heschl Gyrus R	1	0.012	±0.002	403	6

List of human cortical regions included in the model, ranked in order of descending structural degree. Regions printed in bold were classified as hub regions. * Functional degree is based on broadband (0.5 – 45 Hz) functional connectivity. S (coupling strength) was set at 1.5; different values of S produced different absolute values but no changes in functional degree rank. T (time delay) was kept constant at 0.002 s for all experiments (see Supporting information, section 2). Averaged values and standard deviations over 20 runs of the NMM.

Experiment 2: Activity Dependent Degeneration (ADD)

Effect of ADD on structural network integrity

Since, according to our hypothesis, ADD lowers connectivity based on activity level, it was expected to disrupt both structural and functional networks. First we investigated the effect of ADD on the structural network, and whether it had different effects on hubs versus non-hub regions. In ADD, every time-unit represents a small amount of damage to the system, so as to simulate gradual, cumulative degeneration. However, the amount of real, absolute time that is required for these successive steps is not known. Time as presented in these figures should therefore not be interpreted as days or years, but as arbitrary units of undetermined length. Figure 2A shows the decrease of the structural connectivity for three time points in all regions. The normalized node strength, which is the ratio of the node strength after ADD over the original node strength, is plotted for different time points. At baseline (T=0, not shown) normalized node strength is 1 by definition. Over time node strength decreases, and, as hypothesized, particularly in hub nodes, illustrated by the declining slope of the lines. The difference in normalized node strength between hubs and non-hubs is highly significant for all time points shown ($p<0.001$). On the contrary, in the random degeneration (RD) model, there was no difference between hubs and non-hubs in normalized node strength over time (see figure 2B).

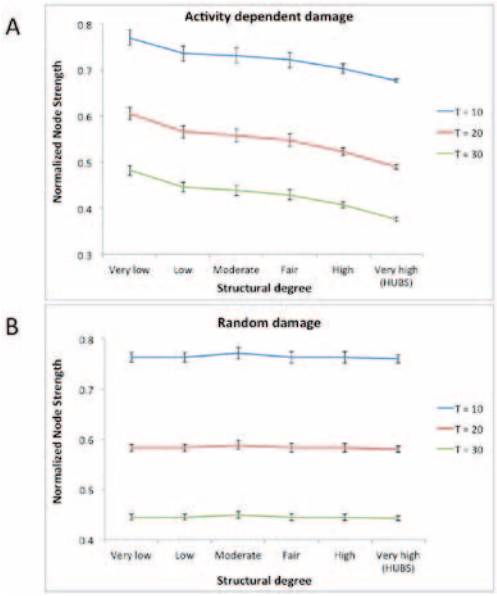

Figure 2: Effect of ADD on structural degree
A: All cortical regions binned according to initial structural degree from low to high values, and their average normalized node strengths at different stages of activity dependent degeneration (ADD). T = time. Error bars indicate standard error of the mean. B: All cortical regions binned according to initial structural degree from low to high values, and their average normalized node strengths at different stages of random degeneration (RD). T = time. Error bars indicate standard error of the mean.

Effect of ADD on neuronal activity

Next, we studied the effect of ADD on network dynamics. When visually inspecting the model-generated data it was apparent that there were notable changes in oscillation amplitude over time. The power spectrum of hub regions initially showed much higher alpha power than in non-hub areas, and a surprising slightly lower alpha peak frequency (see Supporting information section 4). As expected, total power decreased over time (see figure 3A). Hubs started at a higher mean power level ($p<0.0001$), but declined more rapidly than non-hubs, reaching bottom levels at approximately the same moment. Loss of total power in the ADD model was stronger than in RD, especially in hubs; for all time points (except T=0) hub power under ADD was significantly lower than under the RD regime ($p<0.01$). The initial positive relation between structural degree and total power disappeared accordingly (see figure 3B). We subsequently performed a similar analysis for spike density changes over time due to ADD and RD (see figure 4A and 4B). At T=0, the spike density in hubs was higher than in non-hubs ($p=0.01$). In the early stage, we found an unexpected rise of spike density in both ADD and RD, which was stronger in hubs (maximum spike density increase was larger, $p<0.0001$). However, the maximum spike density in hubs under ADD was reached significantly earlier than in non-hubs (average T=52 versus T=60, $p<0.0001$), while peaks were reached at similar times under RD.

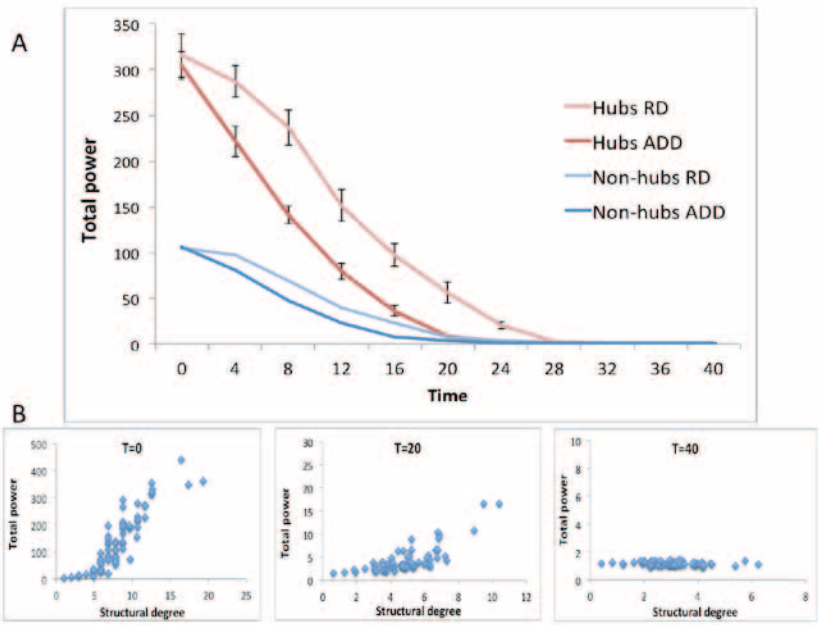

Figure 3: Effect of ADD on total power
A: Average total power of hub and non-hub regions plotted over time, for both the ADD and RD procedure. Error bars indicate standard error of the mean. B: Correlation between structural degree and total power for all regions at different time points during ADD.

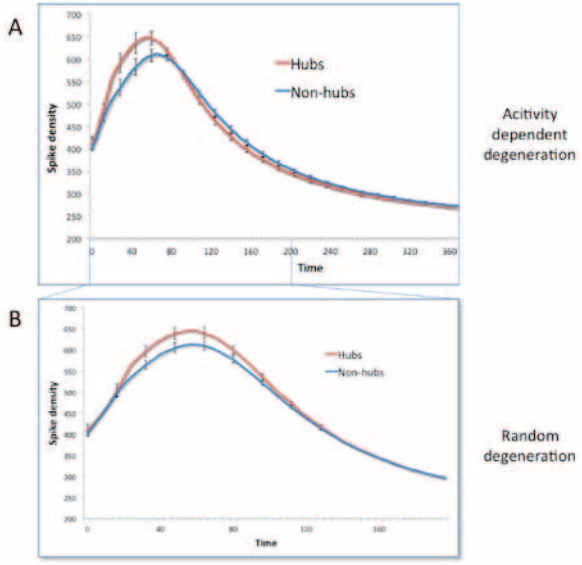

Figure 4: Effect of ADD on spike density
A: Average level of spike density during ADD is plotted for hubs and non-hubs. Error bars indicate standard deviations. B: Average level of spike density during RD is plotted for hubs and non-hubs. Error bars indicate standard deviations.

Effect of ADD on functional network topology

Since we expected ADD to affect functional network topology as well, we examined changes over time in the synchronization likelihood, as well as basic graph measures like average clustering coefficient, characteristic path length, and modularity. Since data generated by the NMM is most reliable in the alpha band, and AD-related functional network changes have most consistently been found in the lower alpha band, we report just the results of this representative band in figure 5. Like spike density, functional connectivity strength first increased before a rapid breakdown occurred, which reached bottom level at around the same time point as total power (described above). The average clustering coefficient decreased, while the characteristic path length fluctuated around the same level through the ADD process (although hubs and non-hubs showed different behavior during the first phase, see figure 5). The ratio between these two measures became smaller, indicating that the balance between global and local connectivity and thus the small-world network topology was disturbed and had become more random. Global modular organization, as expressed by Newman's index, decreased before reaching a stable, lower level.

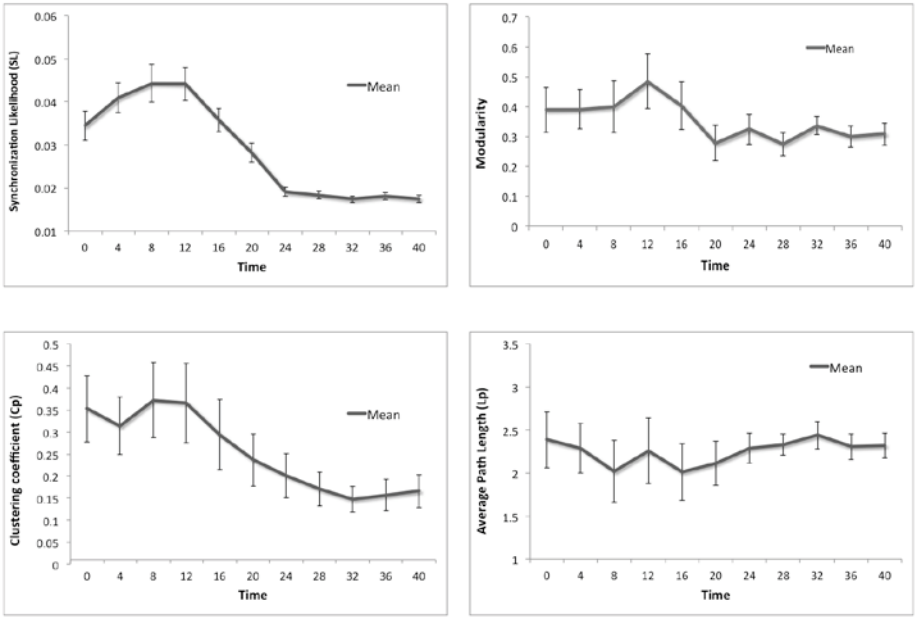

Figure 5: Effect of ADD on functional connectivity and network topology.
Mean levels of synchronization likelihood, modularity, clustering coefficient and path length during ADD are plotted for hubs and non-hubs. Error bars indicate standard deviations.

DISCUSSION

In this study we used a computational model with 78 dynamic neural masses coupled according to realistic human cortical topology to investigate the relation between connectivity and neuronal activity. We find that cortical hub regions have the highest level of intrinsic activity, and that the minimal assumption of higher local neuronal activity leading to more severe neurodegeneration can predict a range of AD hallmarks observed in patient data such as oscillatory slowing, a subsequent increase and breakdown of functional connectivity, and a loss of functional network integrity. These results suggest an 'activity dependent degeneration' (ADD) hypothesis of AD, and below we will discuss our findings and possible consequences in greater detail.

Hub status and activity level

Our first aim was to find out whether the level of activity in a region is related to its degree of structural connectivity. An expected positive correlation was indeed found in repeated experiments across all degrees of connectivity (see figures 1, 3, and 4): structural hub regions possess the highest average power and spike densities. As can be judged from figure 1, an exception is the relation between structural connectivity and spike density for low values of NMM coupling (S). This result indicates that the relation between connectivity and activity might be more complex than we expected. Nevertheless, similar analysis performed using functional connectivity results (see figure S1) led to clear positive correlations in the large majority of cases. It should further be noted that there is no unique definition of hub status, and in this experiment (and the rest of the study) we adhered to the pragmatic choice of taking a selection of nodes (n=13) with the highest structural degree. However, since connectivity and activity are clearly positively related in regions with higher structural degrees, we do not believe that a different hub definition would have led to a different interpretation.

Still, although high neuronal activity in hub regions was a solid finding that might have been expected intuitively, it should ultimately be verified in experimental data. As can be judged from table 1, many Default Mode Network (DMN)-related regions possess a high degree of connectivity *and* activity. The well-documented high resting-state activity level of the DMN is therefore in line with our findings [5]; however, instead of being attributed to ongoing cognitive processing or mental phenomena like introspection, high resting-state activity in the DMN might actually be (partially) explained by the underlying degree of structural and functional connectivity

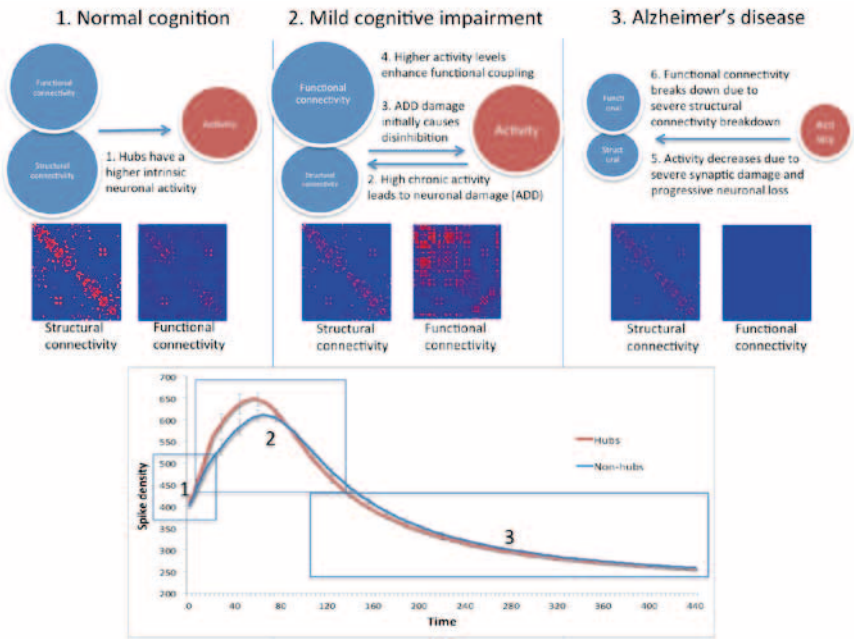

Figure 6: The relation between connectivity and activity at different stages of ADD.
The proposed relation between connectivity and activity is summarized for three different stages of ADD. Structural hubs have a higher baseline intrinsic activity, making them most susceptible to ADD. The second phase might represent the 'Mild Cognitive Impairment' (MCI) stage; structural connectivity declines steadily, but functional connectivity, power and spike density initially increase, leading to a pathologic spiral of increasing activity and metabolic burden in progressively weaker neurons. In the third "AD" phase, the damaged neurons and decreasing structural connectivity can no longer support the high demands, and the network collapses.

Activity dependent degeneration (ADD)

Based on the findings in our first experiment, we expected that ADD would probably preferentially target hub regions, since they possessed the highest level of activity. Analyses of both structural and functional connectivity changes due to ADD seem to be in agreement with this expectation (see figures 2-5). Furthermore, total (or absolute) power decreases rapidly, largely accounted for by weakening of hub regions, and the initial correlation between degree and power is lost (figure 3). Thus, large-scale brain connectivity loses its efficient 'hub' topology in ADD, like in AD.

Surprisingly, the steady loss of power is accompanied by an initial rise of spike density on average (see figure 4), before a final oscillatory slowing sets in. This effect is stronger in hubs; spike density rises more quickly, reaches its peak rate sooner, and seems to slow down more rapidly. One explanation for the increase in spike density observed in our results is neuronal disinhibition. In fundamental neuroscience disinhibition is a well-known phenomenon and it is widely accepted that inhibitory interneurons have a large influence on oscillatory behavior [40]. Besides damaging excitatory connections, ADD

impairs connectivity to and from inhibitory neurons within the neural masses, and the resulting loss of inhibition seems to be a dominant influence on spike density in the first stage. This then leads to a vicious spiral of increasing activity, more activity-dependent damage, etc. until the weakening network can no longer support an increase in spike density (the inter-mass excitatory coupling weakens substantially, which leads to breakdown of the system, see also figure 6). The eventual spike density decrease due to ADD resembles the oscillatory slowing known from AD neurophysiologic literature [41,42].

Several authors have argued for a prominent role of neuronal disinhibition in AD pathophysiology: for example, Gleichmann et al. propose a process they call 'homeostatic disinhibition', which is based on a different underlying mechanism but might explain the higher prevalence of epilepsy that is seen in AD, reduced gamma band activity, and, interestingly, the increase in neuronal activity as measured by fMRI [43]. Schmitt argues that AD is accompanied by a loss of inhibition that leads to alterations in calcium homeostasis and excitotoxicity, respectively [44]. Olney et al. hypothesize that a disinhibition syndrome caused by hypoactive NMDA receptors triggers excitotoxic activity and widespread neurodegeneration [45]. Palop & Mucke suggest that amyloid itself causes dysfunction of inhibitory interneurons causing an increase in neuronal activity [46,47], possibly also accounting for the higher prevalence of epileptic activity in AD [48]. Kapogiannis & Mattson review reports that in aging excitatory imbalance is due to a decrease in GABA-ergic signaling, and that this mechanism is exacerbated in AD [19].

An early but transient rise was also found in functional connectivity results (see figure 5), and interestingly, this is in line with experimental data of Mild Cognitive Impairment (MCI) patients, where increased functional connectivity levels are often interpreted as a compensatory mechanism [49-52]. However, this increase of functional connectivity has not been directly related to cognitive improvement, and according to our model, it might well be a part of the degeneration process itself.

Finally, the ADD induced changes in functional network topology, such as the weakening of small-world structure and modularity (see figure 5), are in line with recent findings in resting-state EEG and MEG studies in AD [14,39,53-55]. In recent years, brain disconnectivity and disturbed network topology has been observed in an increasing number of disorders (for example schizophrenia, multiple sclerosis, brain tumor, autism, epilepsy) [56-59]. It is conceivable that different disease mechanisms and types of network damage (for example extensive non-hub network damage) could lead to a similar situation of hub overload and decay. Computational models like the one described here could be employed to investigate various underlying pathologies and to examine the differences between them. Several recent studies support the notion that node properties such as degree and centrality may play a crucial role in the pathophysiology of degenerative brain disease [60-62].

Alzheimer's disease: consequence of excessive hub activity?

The results of this study suggest that hub regions are vulnerable due to their intrinsically high activity level. The assumption of activity dependent degeneration leads to hub vulnerability along with many neurophysiologic features of AD (i.e. as found in quantitative EEG and MEG literature). A recently conducted large fMRI study demonstrated that highly connected cortical regions like the precuneus are even stronger hubs in females than in males: could this perhaps explain the higher levels of early amyloid deposition ánd the higher prevalence of AD in women [63,64]? The computational model used in this study offers a possible mechanism by which excessive neuronal activity in hubs might lead to the observed macro-scale disruption of brain connectivity and dynamics in AD.

In addition to the presumed role of disinhibition mentioned in the previous paragraph, a prominent role of excessive neuronal activity in AD pathogenesis has been suggested before: several studies have demonstrated a direct link between neuronal activity and the development of amyloid plaques in transgenic mice [20,21,22]. Regions that are most active during resting-state show the most outspoken AD-related pathology [4,5,13]. Excessive hippocampal activity is related to cortical thinning in non-demented elderly persons, is present in MCI patients, and is related to neurodegeneration in AD [49,65,66]. Finally, known risk factors for AD such as genetic profile, age, vascular damage, or common comorbidities like sleep disorders and epilepsy, all predispose to excessive activity and a subsequent burden on metabolism and plasticity [17,18,66-68]. On the other hand, protective factors like high level of education and sustained cognitive activity might relieve the burden on hub regions due to frequent activation of task-related circuits, and accompanying DMN *de*activation. Summarizing, vulnerability of cortical hub regions due to their high activity levels may be aggravated or alleviated by the presence of one or more predisposing or protective factors, respectively (see figure 7).

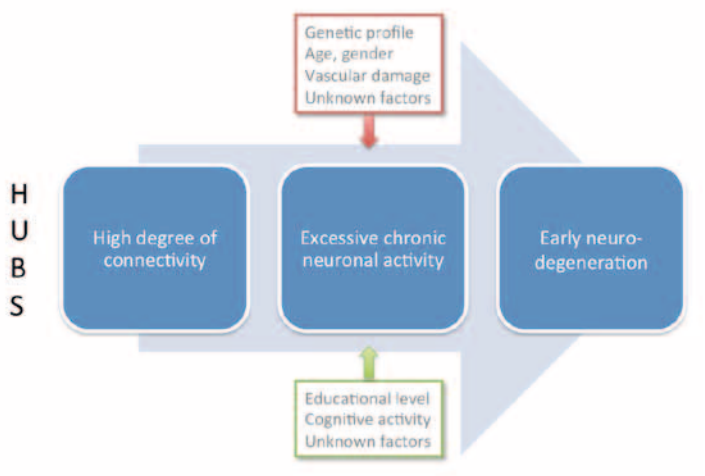

Figure 7: The role of excessive neuronal activity in Alzheimer's disease.
Excessive neuronal activity might be a common pathway through which many of the known risk factors enlarge the chance to develop Alzheimer pathology. Hub regions are most likely to display activity-dependent pathology, since they have the highest intrinsic neuronal activity (which is further amplified in the initial phase of ADD).

This line of reasoning implies that changes in brain activity and connectivity are already involved in the very early stages of AD pathology. In this regard, it is interesting to note that an increasing number of studies show that changes in activity and functional connectivity can be detected before cognitive complaints arise or pathological levels of amyloid are detected with PET and CSF analysis [18,69-73].

Although activity dependent degeneration is quite different from amyloid-induced damage, they need not be mutually exclusive: chronic, excessive activity might lead to amyloid deposition, which in turn causes aberrant activity and neuronal damage: a pathological cycle with different stages (see also figure 6). Relatively small increases of extracellular amyloid-beta can increase neuronal activity, especially in neurons with low activity, whereas higher levels cause synaptic depression [74,75]. Palop and Mucke emphasize the role of inhibitory interneuron dysfunction, leading to hypersynchronization [47]. In conclusion, although these studies provide compelling evidence for a prominent role of neuronal activity, our predictions that hub regions might form the weakest links in AD pathogenesis should be tested in further studies.

Modeling Alzheimer's disease

Several recent studies use similar computational modeling approaches to examine AD related neurophysiological phenomena: Bhattacharya et al. focus on thalamo-cortico-thalamic circuitry and its relation with alpha band power in AD [38]. By varying the synaptic strengths in the thalamic module of the model they find that especially the connectivity of synaptic inhibitory neurons in the thalamus has a large influence on

alpha power and frequency. Pons et al. use a neural mass model and human EEG data to investigate the influence of structural pathways on functional connectivity in the aging brain and pre-clinical stages of AD [37]. Findings in line with our present results are the higher functional connectivity values in MCI and the relation between structural and functional connectivity. An increase in functional connectivity and network randomness during a memory task was found by Buldú et al. in a MEG study of MCI patients [76]. Interestingly, the authors also provide a network degeneration model which might explain these observations. The combination of neural mass modeling and graph theory was used in a recent study from our group [36]. This study explores the manifestation of modularity in developing networks and investigates the effect of more acute lesions on network dynamics. The gradual recovery of functional network characteristics that was observed after lesions raises the question whether and to what extent similar mechanisms play a role in neurodegenerative damage; this should be subject of further study. To describe functional network modularity, the same algorithm and heuristic was used as in the present study. The computational models used in these studies provide a framework to address different questions and hypotheses concerning brain disease, e.g. different functional lesions. A novel aspect of the approach in the present study is that a single hypothesis (ADD) is proposed as main pathophysiological mechanism of AD. Comparison to a 'random degeneration' (RD) model provides further support for the ADD hypothesis, but does not rule out the possibility that other plausible degenerative models exist.

Methodological issues

Various methodological choices might have affected our results, and should be taken into account when interpreting them. First, although the DTI-derived connectivity matrix that served as the basis of our model is in our opinion a solid overall large-scale representation of human cortical connectivity, it was based on data of healthy young adults [24]. Since AD mainly affects the aging population, and since it has been shown that structural connectivity is altered during aging [77], results might have been different if structural connectivity data of older subjects had been implemented. However, the major hub regions seem largely independent of age, justifying our approach that mainly focuses on hub versus non-hub differences. Furthermore, we now know that AD affects many people below the age of 65, and that AD pathology is presumably already present for decades before initial symptoms appear. In a similar way we expect that individual variability in structural connectivity will not have had a major influence on our present approach, since major hub regions appear to be consistent across studies [3,64]. Although the computational model used here could be refined in many ways, e.g. by implementing a larger number of regions, assigning different weights to structural connections, using DSI-derived data, correcting for spatial scale and/or DTI biases, or by

using more elaborate and detailed graph analysis, we believe that this would not have affected our main outcome dramatically, since comparing characteristics of hub and non-hub cortical regions does not necessarily require a high level of detail. By keeping the model and hypotheses as simple as possible, it might be easier to discover or test underlying basic principles and mechanisms of degeneration.

The main motivation to use an NMM network of this size was the observation that topographical maps and atlases of the human cerebral cortex of this order of magnitude are quite common in macroscopic structural and functional connectivity studies (for an overview, please refer to [39,56-58]. Also, since EEG and MEG studies have comparable network sizes (21-300 sensors), this is a fairly realistic spatial resolution for NMM-generated dynamics. Two relevant references are recent computational modeling studies by Deco et al. [27] and Pons et al. [37].

Varying the structural coupling strength S in our neural mass model can lead to different results, and therefore we have reported its influence on our outcomes. Similarly, the arbitrary 'loss'-rate parameter of the ADD function will affect the speed of the degeneration process. However, since we were mainly concerned with a topological 'hub versus non-hub' comparison, the absolute rate of degeneration was of minor importance for this study. Moreover, loss-rates were equally applied to *all* connections; network *distribution* was not selectively influenced by these parameters.

Future directions

Observations from this study that could be explored further include ADD-induced changes in structural network topology, the relation between spike density and anatomical region, and the lower alpha peak frequency in hub regions (see Text S1 section 4). Predictions from our model, especially the close link between local neuronal activity and large-scale connectivity should be verified in longitudinal clinical studies, preferably of normal aging as well as patients with subjective memory complaints (SMC), Mild cognitive impairment (MCI) and AD. To assess structural and functional connectivity as well as large-scale neuronal activity, a combination of DTI and MEG might be the most appropriate method. Source space analysis of MEG data may help to develop topologically accurate neural mass models. On a fundamental level, the relation between neuronal connectivity, activity and pathology should be further explored in animal models. Interestingly, the relation between regional activity and large-scale functional connectivity has recently also addressed with respect to schizophrenia [78,79]. In both studies it is argued that more knowledge of this relation is essential for understanding mechanisms of altered functional connectivity, and this is very much in line with the main message of this study. Different disease conditions may have specific causes or patterns in which this relationship is harmed, but at the same time universal principles may apply that can help us gain more insight in a range of neuropsychiatric disorders.

Conclusion

In this study we used a neural mass model with DTI-based human topology to demonstrate that brain hub regions possess the highest levels of neuronal activity. Moreover, 'Activity dependent degeneration' (ADD), a damage model motivated by this observation, generates many AD-related neurophysiologic features such as oscillatory slowing, disruption of functional network topology and hub vulnerability. Early-stage, transient rises of firing rate and functional connectivity in ADD matches observations in pre-clinical AD patients, suggesting that this chain of events is not compensatory, but pathological. Overall, the results of this study favor a central role of neuronal activity and connectivity in the development of Alzheimer's disease.

MATERIALS AND METHODS

In this study we simulated neurophysiologic activity of 78 Neural Mass Models embedded in a realistic structural cortical network topology to evaluate hypotheses about the relation between (structural and functional) connectivity and neuronal activity. The output of this model provides information about the neuronal activity level in the form of average voltage and spike density per region, and generates EEG-like data that can be subjected to further spectral, functional connectivity and graph theoretical analysis. Hypotheses about brain pathophysiology can be tested by artificially damaging structural or dynamical properties of the brain model. The outline of the analysis procedure employed in this study is depicted in figure 8.

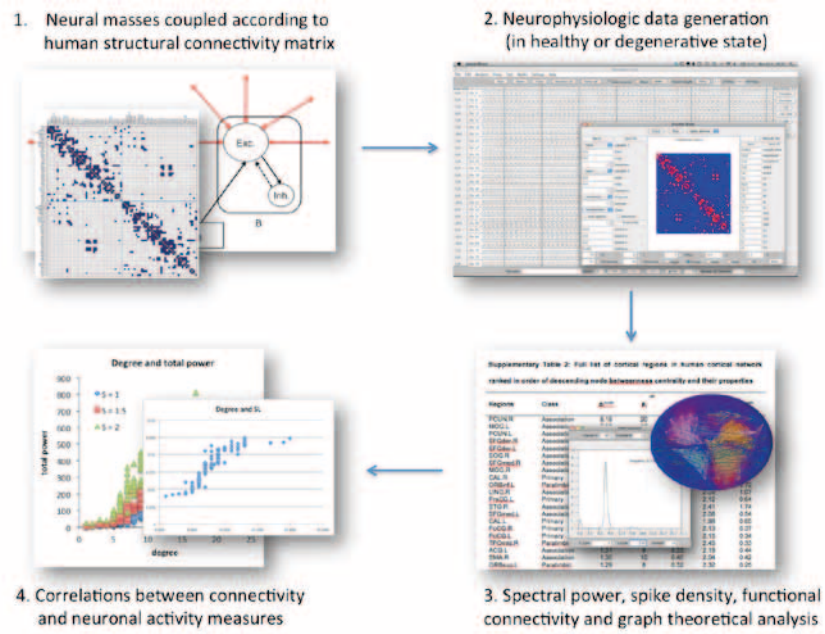

Figure 8: Outline of the consecutive steps in the experimental procedure.
Multi-step procedure from the simulation of realistic human neurophysiological activity to analyzing and correlating connectivity and activity results.

Network dynamics: the Neural Mass Model

We used a model of interconnected neural masses, where each neural mass represents a large population of connected excitatory and inhibitory neurons generating an EEG or MEG like signal. The model was recently employed in two other graph theoretical studies [30,36]. The basic unit of the model is a neural mass model (NMM) of the alpha rhythm [26,80,81]. This model considers the average activity in relatively large groups of interacting excitatory and inhibitory neurons. Spatial effects (i.e. distance) are ignored

in this model; brain topology is introduced later by coupling several NMMs together. The average membrane potential and spike density of the excitatory neurons of each of the NMMs separately were the multichannel output related to neuronal activity that was subject to further analysis. All neural mass model parameters and functions are summarized and explained in Supporting information, section 3 (see also figure S4 and table S1).

Structural network topology of neural mass model

A diffusion tensor imaging (DTI) based study by Gong et al. published in 2009 that focused on large-scale structural connectivity of the human cortex resulted in a connectivity matrix of 78 cortical regions [24,82]. The connectivity matrix was implemented in our model software, and used as topological framework for the 78 coupled NMMs. Coupling between two NMMs, if present, was always reciprocal, and excitatory. Note that at the start of the simulation, the coupling strength between all NMM pairs (S) was identical, and the only difference between the cortical regions (or NMMs) was their degree of connectivity to other neural masses (cortical regions). Since the coupling strength S was an arbitrarily chosen parameter, repeated analyses were performed with different values of this variable (see for example figure 3).

Activity dependent degeneration (ADD)

For the present study the model was extended to be able to deal with activity dependent evolution of connection strength between multiple coupled NMMs. Activity dependent degeneration (ADD) was realized by lowering the 'synaptic' coupling strength as a function of the spike density of the main excitatory neurons. For each neural mass the spike density of the main excitatory population is stored in a memory buffer that contains the firing rates of the last 20 steps in the model. Step size depends on the sample frequency. At each new iteration, the highest spike density value of the last 20 sample steps is determined and designated as maxAct. From maxAct a loss is determined according to the following relation:

$$loss = \exp^{-0.01 \max Act} \tag{1}$$

Since maxAct is non-negative, loss will be a number between 0 and 1. Next, the coupling values C1 (connections between main excitatory population and inhibitory population), C2 (connections between inhibitory population and main excitatory population), Pt (thalamic input to main excitatory population) and S (structural coupling strength between neural masses) are all multiplied by loss to obtain their new lower values. To assess the specificity of ADD, results were compared with a random degeneration (RD) model in which the *maxAct* variable was discarded, so damage was equally applied to all

regions, regardless of their level of activity. The effects of ADD and RD were measured by changes in total power (local average membrane potential) and spike density, and these two measures were used as representations of neuronal activity in further analyses. Note that the time scale of the data generated by the model is equal to normal brain activity and EEG/MEG data, but that the ADD and RD procedures have a more abstract time scale. The exact duration of the degenerative procedures was not considered relevant to our present focus on the relation between connectivity and activity, but could be considered to reflect a length that is representative of a neurodegenerative process, spanning years to decades (see figures 3-5). The computational model was programmed in Java and implemented in the in-house developed program BrainWave (v0.9.04), written by C.J. Stam (latest version available for download at http://home.kpn.nl/stam7883/brainwave.html).

Spectral analysis

Since spectral analysis is a common neurophysiological procedure that provides clinically relevant information in neurodegenerative dementia, we included this in our experiments. Fast Fourier transformation of the EEG-like oscillatory output signal was used to calculate for all separate regions the total power (absolute broadband power, 0-70 Hz) as well as the absolute power in the commonly used frequency bands delta (0.5-4 Hz), theta (4-8 Hz), lower alpha (8-10 Hz), higher alpha (10-13 Hz), beta (13-30 Hz) and gamma (30-45 Hz).

Functional connectivity analysis

To quantify large-scale synchronization as a measure of interaction between different cortical areas, we used the Synchronization likelihood (SL), which is sensitive to both linear and non-linear coupling [83,84]. SL was calculated for all frequency bands, and the matrix containing all pairwise SL values served as the basis for all further graph theoretical analyses of functional network characteristics.

Graph theoretical analysis

Graph theoretical properties of the structural DTI network that were relevant for our hub study such as node degree, betweenness centrality, and local path length were published in the original article by Gong et al [24]. One new measure we introduced was the 'normalized node strength', which is the ratio of the structural degree of a node after activity dependent damage over its original degree. This measure was used to track structural connectivity loss and to compare the loss of degree in hubs and non-hubs. For functional network analysis, connectivity matrices were subjected to topographical analysis. The functional degree of a node is defined as the sum of all its link weights [85]. Averaging the functional degree over all nodes gives the overall functional degree of a

network. To match the functional network to the given structural network (minimizing effects of graph size and density), we constructed a binary, unweighted matrix that was obtained after using a threshold that resulted in a network with an average degree of 8, close to that of the structural network (which was 8.1). All graph theoretical measures used in this study are summarized in table 2, for more exact definitions please refer to [14,85]. For functional modularity analysis, we used Newman's modularity metric combined with a simulated annealing process (previously described in [55, 86]).

Table 2. Graph theoretical definitions

Measure		Description
Degree	k	Number of connections of a node. Average for all nodes in a network produces the average degree K.
Node strength (or weighted degree)	k^w	Sum of all connection weights of a node.
Clustering coefficient	Cp	Number of directly connected neighbors of a node divided by the maximally possible number of interconnected neighbors. The mean of this value for all nodes gives the average clustering coefficient; a measure of local integration.
Path length	Lp	Shortest number of steps from one node to another. Average over all possible shortest paths is the characteristic path length of a network; a measure of global integration.
Gamma	γ	Normalized average clustering coefficient, obtained by dividing Cp by the average Cp of a set randomized networks of the same size and density.
Lambda	λ	Normalized characteristic path length, obtained by dividing Lp by the characteristic Lp of a set randomized networks of the same size and density.
Modularity	Q	Expresses the strength of the modular character of a network.

Glossary of graph theoretical measures used in this study. For exact definitions, please refer to [14,85].

Statistical analysis

For the baseline, pre-ADD analysis in experiment 1 and 2, the data-generating procedure using the model was repeated twenty times to obtain a representative amount of data. On each run the subsequent spectral, functional connectivity and graph theoretical analysis was performed, and then all results of these twenty runs were averaged prior to further statistical analysis. Regional results were visualized using 6 bins ascending in structural degree, each containing 13 regions. All 13 regions in the bin with the highest mean degree were classified as hubs. Standard deviations of bins are displayed as error bars. For bivariate correlations Pearson's test was used.

Acknowledgements

The authors would like to thank Gaolang Gong and Alan C. Evans for their valuable comments, and for making available their DTI-based structural connectivity data.

REFERENCE LIST

1. Stam CJ, de Haan W, Daffertshofer A, Jones BF, Manshanden I, et al (2009) Graph theoretical analysis of magnetoencephalographic functional connectivity in Alzheimer's disease. Brain 132: 213-224.
2. Gong G, He Y, Concha L, Lebel C, Gross DW, et al (2009) Mapping anatomical connectivity patterns of human cerebral cortex using in vivo diffusion tensor imaging tractography. Cereb Cortex 19: 524-536.
3. Ponten SC, Daffertshofer A, Hillebrand A, Stam CJ (2010) The relationship between structural and functional connectivity: graph theoretical analysis of an EEG neural mass model. Neuroimage 52: 985-994.
4. Stam CJ (2010) Characterization of anatomical and functional connectivity in the brain: a complex networks perspective. Int J Psychophysiol 77: 186-194.
5. Lopes da Silva FH, Hoeks A, Smits H, Zetterberg LH (1974) Model of brain rhythmic activity. Biological Cybernetics 15: 27-37.
6. Zetterberg LH, Kristiansson L, Mossberg K (1978) Performance of a model for a local neuron population. Biological cybernetics 31: 15-26.
7. Stam CJ, Pijn JP, Suffczynski P, Lopes da Silva FH (1999) Dynamics of the human alpha rhythm: evidence for non-linearity? Clin Neurophysiol 110: 1801-1813.
8. Ursino M, Zavaglia M, Astolfi L, Babiloni F (2007) Use of a neural mass model for the analysis of effective connectivity among cortical regions based on high resolution EEG recordings. Biological cybernetics 96: 351-365.
9. Deuker L, Bullmore ET, Smith M, Christensen S, Nathan PJ, et al (2009) Reproducibility of graph metrics of human brain functional networks. Neuroimage 47: 1460-1468.
10 Whitlow CT, Casanova R, Maldjian JA (2011) Effect of resting-state functional MR imaging duration on stability of graph theory metrics of brain network connectivity. Radiology 259: 516.
11. Schuuring D (1988) Modelleren en simuleren van epileptische activiteit. Master thesis, University of Twente, the Netherlands.
12. de Haan W, van der Flier WM, Koene T, Smits LL, Scheltens P, Stam CJ (2011) Disrupted modular brain dynamics reflect cognitive dysfunction in Alzheimer's disease. Neuroimage Nov 30. [Epub ahead of print]

SUPPORTING INFORMATION

1 Relation between functional degree and total power

Since activity level might also be influenced by a node's functional role rather than its structural connectivity status, we performed direct comparisons between functional degree (sum of all weighted *functional* connections of a node) and total power in the common frequency bands (see figure S1). Except for delta and higher alpha, most bands showed strong positive correlations. The beta band showed a remarkably strong correlation (r=0.96). These results suggest that functional hub regions generally have high neuronal activity levels as well, as would be expected intuitively.

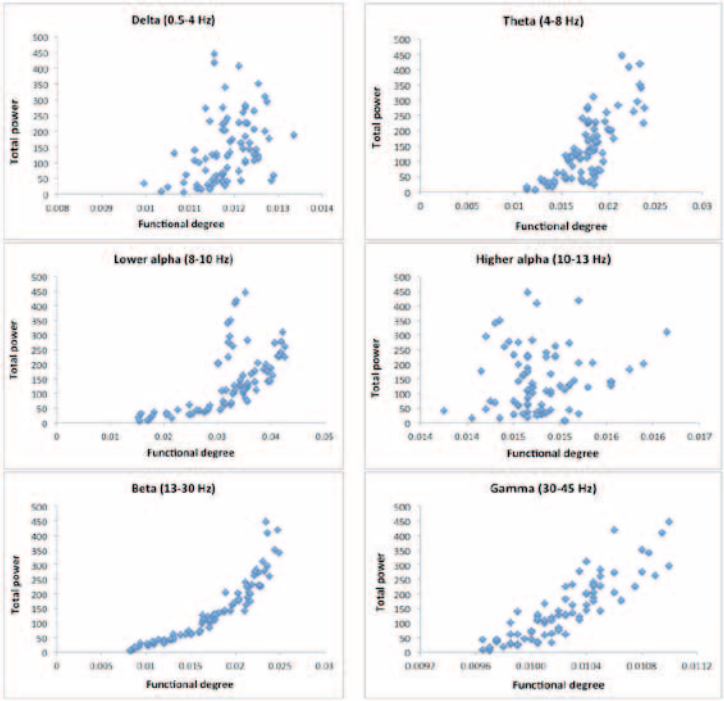

Figure S1: Correlation between functional degree and total power in all frequency bands.

2 Relation between structural and functional degree

Before examining the relationship between connectivity and activity, we wished to assess if structural and functional connectivity in our brain model was related; i.e. if structural hubs could also be characterized as functional hubs. Therefore, global functional network properties of model simulation data were first investigated. Functional networks all showed small-world organization and weak to moderate modularity in all frequency bands, resembling human MEG data (not shown) [1,12]. Subsequently, we visually compared the structural and broadband functional connectivity matrices (see figure S2). Although not identical, the two matrices evidently share similar connectivity patterns.

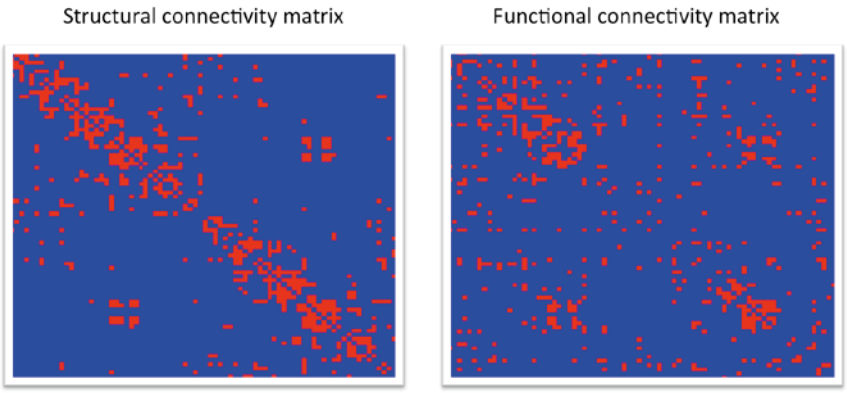

Figure S2: Relation between structural and functional connectivity
Left panel: matrix of the structural connections between all 78 cortical regions, adapted from Gong et al. [24]. Red squares indicate the presence of a connection. Since all connections are bidirectional, the matrix is symmetrical over its diagonal axis. Right panel: matrix of functional connections acquired using the synchronization likelihood (SL) as coupling measure (broadband frequency range: 0.5-45 Hz), and thresholding all pairwise SL values to obtain a graph with the same average degree (K=8) as the structural connectivity matrix to the left.

To quantify the relation between network structure and function we compared the structural and functional degree for all regions in different frequency bands (see figure S3). In all bands a positive correlation can be observed, indicating that structural hubs are also functional hubs in those frequency ranges. The strongest relation was found in the beta band ($r = 0.85$, $p < 0.001$).

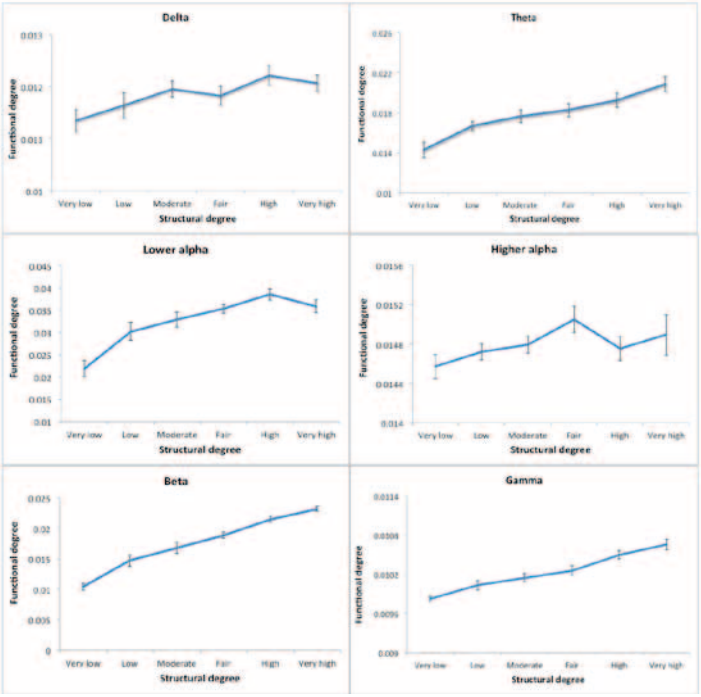

Figure S3: Relation between structural and functional degree in all frequency bands. Error bars depict standard deviations within each bin after 20 simulated runs.

3 Network dynamics: the Neural Mass Model

We used a model of interconnected neural masses, where each neural mass represents a large population of connected excitatory and inhibitory neurons generating an EEG or MEG like signal. The model was described in Ponten et al. and Stam et al. [3,4]. The basic unit of the model is a neural mass model (NMM) of the alpha rhythm [5,6]. The same model was used in a previous study on bifurcation phenomena of the alpha rhythm [7]. As previously described, this model considers the average activity in relatively large groups of interacting excitatory and inhibitory neurons. Spatial effects are ignored in this model; we will introduce topological effects by coupling several NMMs together. The excitatory and inhibitory populations of each NMM are characterized by their average membrane potentials $V_e(t)$ and $V_i(t)$, and by their pulse densities, i.e., the proportion of cells firing per unit time $E(t)$ and $I(t)$. Static non-linear functions $S_E(x)$ and $S_I(x)$ relate the potentials $V_e(t)$ and $V_i(t)$ to the corresponding pulse densities $E(t)$ and $I(t)$. The excitatory post-synaptic potential (EPSP) and inhibitory post-synaptic potential (IPSP) are modeled by the impulse responses $h_e(t)$ and $h_i(t)$. The constants C_1 and C_2 describe the coupling from excitatory to inhibitory and from inhibitory to excitatory populations respectively. $P(t)$ is the pulse density of an input signal to the excitatory population. Following Zetterberg et al. [6] the following impulse responses were used:

$$h(t) = A[\exp(-at) - \exp(-bt) \quad \text{for} \quad t \geq 0$$
$$h(t) = 0 \quad \text{for} \quad t < 0. \qquad (1)$$

For $h_e(t)$ the parameter values were: $A = 1.6$ mV, $a = 55$ s^{-1}, $b = 605$ s^{-1}. For $h_i(t)$ the parameter values were: $A = 32$ mV, $a = 27.5$ s^{-1}, $b = 55$ s^{-1}. The sigmoid function relating the average membrane potential, V_m, to the impulse density was also taken from Zetterberg et al. [6]:

$$S[V_m - V_d] = g \cdot \exp[q(V_m - Vd)] \quad \text{for} \quad V_m \leq V_d$$
$$S[V_m - V_d] = g[2 - \exp(q(V_d - V_m))] \quad \textit{for} \quad V_m > V_d \qquad (2)$$

Here the parameter values used were: $q = 0.34$ mV^{-1}, $V_d = 7$ mV, $g = 25$ s^{-1}. For the coupling constants we used $C_1 = 32$ and $C_2 = 3$ [5]. A schematic representation is shown in Figure S4A. The activity (spiking rate and power) of the excitatory population in an NMM is largely determined by excitatory input (from the thalamus, but also from other NMMs). All model parameters are summarized in Table S1. The impulse response and sigmoid functions are shown in Figure S4C.

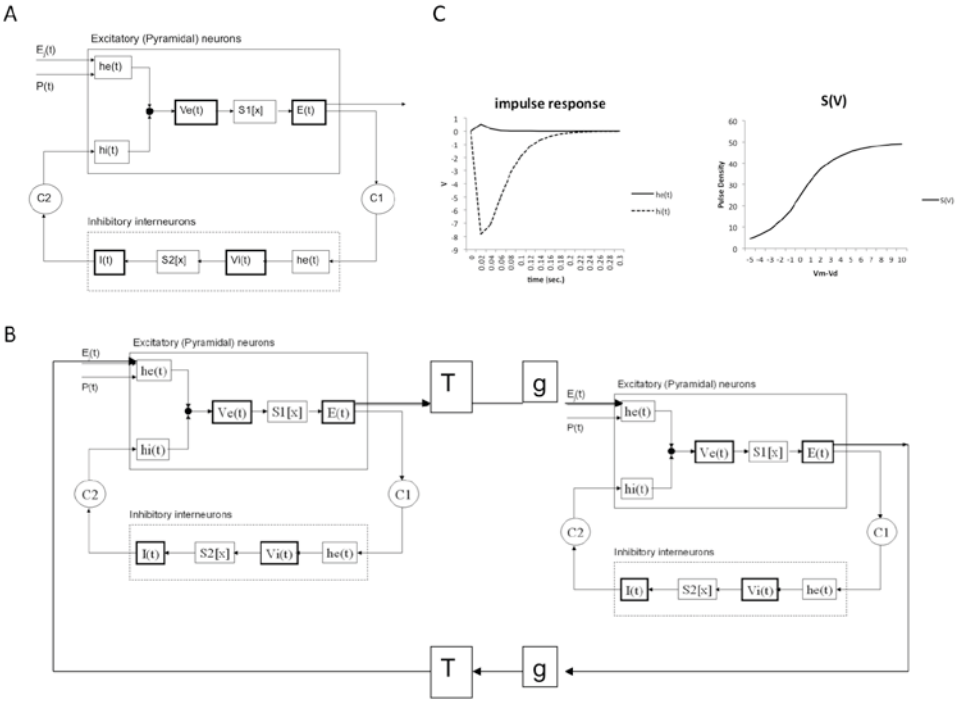

Figure S4A: Schematic presentation of single neural mass model.
The upper rectangle represents a mass of excitatory neurons, the lower rectangle a mass of inhibitory neurons. The state of each mass is modeled by an average membrane potential [Ve(t) and Vi(t)] and a pulse density [E(t) and I(t)]. Membrane potentials are converted to pulse densities by sigmoid functions S1[x] and S2[x]. Pulse densities are converted to membrane potentials by impulse responses he(t) and

hi(t). C1 and C2 are coupling strengths between the two populations. P(t) and Ej(t) are pulse densities coming from thalamic sources or other cortical areas respectively.

Figure S4B: Coupling of two neural mass models.

Two masses are coupled via excitatory connections. These are characterized by a fixed delay T and a strength g.

Figure S4C: Essential functions of the model.

The upper left panel shows the excitatory [he(t)] and inhibitory [hi(t)] impulse responses of Eq. 1. The upper right shows the sigmoid function relating average membrane potential to spike density (Eq. 2).

The average membrane potential of the excitatory neurons $V_e(t)$ of each of the NMMs separately was the multichannel output. The sample frequency was 500 Hz. In the present study each run consisted of 4096 samples (±8 s). Amount of data selected for analysis was based on previous studies and literature on reproducibility of graph theoretical results [9,10]. The adjacency matrix at the end of each run was subjected to topographical analysis. These parameters go back to a large number of studies with this lumped model, and ultimately to the original model of Lopes da Silva [5].

The final model consisted of 78 of the NMMs as described above, which were coupled together based on the structural DTI network results from Gong et al. [24]. Coupling between two NMMs, if present, was always reciprocal, and excitatory. The output E(t) of the main excitatory neurons of one NMM was used as the input for the impulse response he(t) of the excitatory neurons of the second NMM; the output E(t) of the second module was coupled to the impulse response he(t) of the excitatory neurons of the first NMM. Following Ursino et al. [87] we used a time delay (T × sample time, with n an integer, $0 < T < 21$) and a gain factor. In the present study, n and gain were set to 1 for all connections. A schematic illustration of the coupling between two NMMs is shown in Figure 1B. For the present study the model was extended in order to be able to deal with activity dependent degeneration of connection strength between multiple coupled NMMs. Coupling strength between neural masses was initially set at the same level for all connections; different levels were tested (S=1, S=1.5, S=2; see figure 3). For the present study the model was extended in order to be able to deal with activity dependent evolution of connection strength between multiple coupled NMMs. Activity dependent degeneration (ADD) was realized by lowering the 'synaptic' coupling strength as a function of the spike density of the main excitatory neurons. For each neural mass the spike density of the main excitatory population is stored in a memory buffer that contains the firing rates of the last 20 steps in the model. Step size depends on the sample frequency. At each new iteration, the highest spike density value of the last 20 sample steps is determined and designated as maxAct. From maxAct a loss is determined according to the following relation:

$$loss = \exp^{-0.01 \max Act} \tag{3}$$

Since maxAct is non-negative, loss will be a number between 0 and 1. Next, the coupling values C1 (connections between main excitatory population and inhibitory population), C2 (connections between inhibitory population and main excitatory population), Pt (thalamic input to main excitatory population) and S (*structural* coupling strength between neural masses) are all multiplied by loss to obtain their new lower values.

The model was programmed in Java and implemented in the program BrainWave (version 0.9.04, written by C.J. Stam, available on home.kpn.nl/stam7883). The Java code was based on the Pascal source code described by Schuuring [11].

Table 8.S1. Overview of model parameters.

Symbol	Interpretation	Value
EQUATIONS 1 AND 2; FIGURE 1		
t	Sample time	0.002 s
$P(t)$	Subcortical input level to each neural mass	550 spikes s^{-1}
Noise	Random fluctuations around average level of $P(t)$	1.0
$A\,h_e(t)$	Amplitude of the EPSP	1.6 mV
$A\,h_i(t)$	Amplitude of the IPSP	32 mV
$a\,h_e(t)$	Shape parameter of EPSP	55 s^{-1}
$b\,h_e(t)$	Shape parameter of EPSP	605 s^{-1}
$a\,h_i(t)$	Shape parameter of IPSP	275 s^{-1}
$b\,h_i(t)$	Shape parameter of IPSP	55 s^{-1}
g	Parameter of sigmoid function that relates membrane potential to impulse density	25 s^{-1}
q	Parameter of sigmoid function that relates membrane potential to impulse density	0.34 mV^{-1}
V_{d1}	Threshold potential used in the sigmoid function that relates membrane potential to impulse density for main population of excitatory neurons	7 mV
V_{d2}	Threshold potential used in the sigmoid function that relates membrane potential to impulse density for inhibitory neurons	7 mV
C_1	Connection strength between main population of excitatory neurons and inhibitory neurons	32
C_2	Connection strength between inhibitory neurons and main population of excitatory neurons	3
Gain	Gain factor for the coupling between different neural masses	1
T	Time delay for the coupling between neural masses	0.002 s

4 Relation between structural degree and alpha peak frequency

An additional observation in our experiments is that hub regions have a slightly *lower* alpha peak in their power spectrum, as is shown in figures S5 and S6.

It might be possible that a high structural connectivity slows regions down, however this finding should be verified in neurophysiological experiments. NB: the mu rhythm, which is a variation of the alpha rhythm that is present in cortical regions that are not seen as hub regions, is indeed faster than the dominant posterior alpha rhythm.

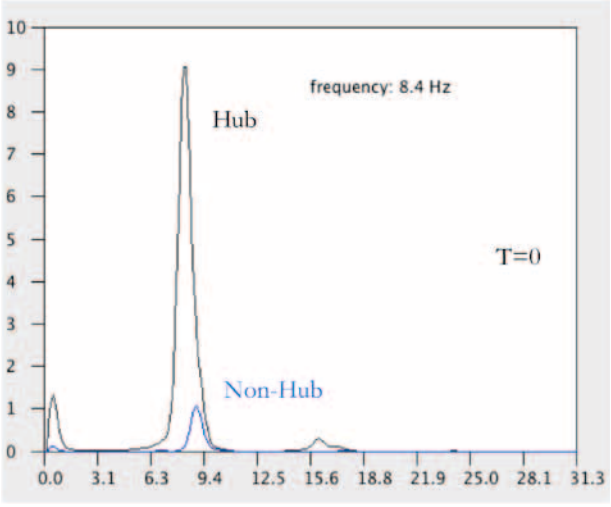

Figure S5: Power spectrum of hubs.
Power spectrum of a hub region (precuneus) in black, and a non-hub region in blue. Note the difference in power, but also the lower alpha peak of the hub region.

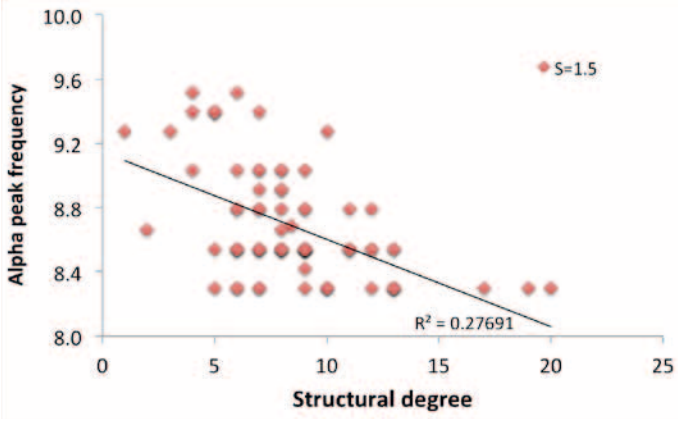

Figure S6: Alpha peak frequency in hubs.
The alpha peak frequency of all cortical regions plotted against their structural degree. A negative correlation can be observed (r=-0.53). Hubs (the 13 regions with highest structural degree) have a significantly lower alpha peak ($p<0.001$) compared to non-hubs.

REFERENCES

1. Hagmann P, Cammoun L, Gigandet X, Meuli R, Honey CJ, et al (2008) Mapping the structural core of human cerebral cortex. PLoS Biol 6: e159.
2. Zamora-López G, Zhou C, Kurths J (2010) Cortical hubs form a module for multisensory integration on top of the hierarchy of cortical networks. Front Neuroinformatics 4.
3. van den Heuvel MP, Sporns O (2011) Rich-Club Organization of the Human Connectome. J Neurosci 31:15775.
4. Buckner RL, Snyder AZ, Shannon BJ, LaRossa G, Sachs R, et al (2005) Molecular, structural, and functional characterization of Alzheimer's disease: evidence for a relationship between default activity, amyloid, and memory. J Neurosci 25: 7709-7717.
5. Raichle ME, Snyder AZ (2007) A default mode of brain function: a brief history of an evolving idea. Neuroimage 37: 1083-90; discussion 1097-9.
6. van den Heuvel MP, Stam CJ, Kahn RS, Hulshoff Pol HE (2009) Efficiency of functional brain networks and intellectual performance. J Neurosci 29: 7619-7624.
7. Vanhaudenhuyse A, Noirhomme Q, Tshibanda LJF, Bruno MA, Boveroux P, et al (2010) Default network connectivity reflects the level of consciousness in non-communicative brain-damaged patients. Brain 133: 161.
8. Li Y, Liu Y, Li J, Qin W, Li K, et al (2009) Brain anatomical network and intelligence. PLoS Comput Biol 5: e1000395.
9. Sestieri C, Corbetta M, Romani GL, Shulman GL (2011) Episodic Memory Retrieval, Parietal Cortex, and the Default Mode Network: Functional and Topographic Analyses. J Neurosci 31:12, 4407.
10. Yeo A, Arden R, Jung E (2011) Alzheimers disease and intelligence. Curr Alzheimer Res 8:4, 345-353.
11. Honey CJ, Sporns O (2008) Dynamical consequences of lesions in cortical networks. Hum Brain Mapp 29: 802-809.
12. Alstott J, Breakspear M, Hagmann P, Cammoun L, Sporns O (2009) Modeling the impact of lesions in the human brain. PLoS Comput Biol 5: e1000408.
13. Buckner RL, Sepulcre J, Talukdar T, Krienen FM, Liu H, et al (2009) Cortical hubs revealed by intrinsic functional connectivity: mapping, assessment of stability, and relation to Alzheimer's disease. J Neurosci 29: 1860-1873.
14. Stam CJ, de Haan W, Daffertshofer A, Jones BF, Manshanden I, et al (2009) Graph theoretical analysis of magnetoencephalographic functional connectivity in Alzheimer's disease. Brain 132: 213-224.
15. Lo CY, Wang PN, Chou KH, Wang J, He Y et al (2010) Diffusion tensor tractography reveals abnormal topological organization in structural cortical networks in Alzheimer's disease. J Neurosci 30: 16876-16885.
16. Hardy J, Selkoe DJ (2002) The amyloid hypothesis of Alzheimer's disease: progress and problems on the road to therapeutics. Science 297: 353.
17. Mesulam MM (2000) A plasticity-based theory of the pathogenesis of Alzheimer's disease. Ann N Y Acad Sci 924: 42-52.
18. Kramer G, van der Flier WM, de Langen C, Blankenstein MA, Scheltens P et al (2008) EEG functional connectivity and ApoE genotype in Alzheimer's disease and controls. Clin Neurophysiol 119: 2727-2732.
19. Kapogiannis D, Mattson MP (2010) Disrupted energy metabolism and neuronal circuit dysfunction in cognitive impairment and Alzheimer's disease. The Lancet Neurology .

20. Bero AW, Yan P, Roh JH, Cirrito JR, Stewart FR, et al (2011) Neuronal activity regulates the regional vulnerability to amyloid-β deposition. Nat Neurosci 14: 750-756.
21. Walker LC, Jucker M (2011) Amyloid by default. Nat Neurosci 14(6):669-70.
22. Cirrito JR, Yamada KA, Finn MB, Sloviter RS, Bales KR et al (2005) Synaptic activity regulates interstitial fluid amyloid-beta levels in vivo. Neuron 48:913-22.
23. Iturria-Medina Y, Sotero RC, Canales-Rodríguez EJ, Alemán-Gómez Y, Melie-García L (2008) Studying the human brain anatomical network via diffusion-weighted MRI and Graph Theory. Neuroimage 40: 1064-1076.
24. Gong G, He Y, Concha L, Lebel C, Gross DW, et al (2009) Mapping anatomical connectivity patterns of human cerebral cortex using in vivo diffusion tensor imaging tractography. Cereb Cortex 19: 524-536.
25. Wilson HR, Cowan JD (1972) Excitatory and inhibitory interactions in localized populations of model neurons. Biophys J 12: 1-24.
26. Lopes da Silva FH, Hoeks A, Smits H, Zetterberg LH (1974) Model of brain rhythmic activity. Biol Cybern 15: 27-37.
27. Deco G, Jirsa VK, Robinson PA, Breakspear M, Friston K (2008) The dynamic brain: from spiking neurons to neural masses and cortical fields. PLoS Comput Biol 4: e1000092.
28. Sotero RC, Trujillo-Barreto NJ, Iturria-Medina Y, Carbonell F, Jimenez JC (2007) Realistically coupled neural mass models can generate EEG rhythms. Neural Comput 19: 478-512.
29. Stam CJ (2010) Characterization of anatomical and functional connectivity in the brain: a complex networks perspective. Int J Psychophysiol 77: 186-194.
30. Ponten SC, Daffertshofer A, Hillebrand A, Stam CJ (2010) The relationship between structural and functional connectivity: graph theoretical analysis of an EEG neural mass model. Neuroimage 52: 985-994.
31. Damoiseaux JS, Greicius MD (2009) Greater than the sum of its parts: a review of studies combining structural connectivity and resting-state functional connectivity. Brain Struct Funct 213: 525-533.
32. Honey CJ, Thivierge JP, Sporns O (2010) Can structure predict function in the human brain? Neuroimage 52:766-76.
33. Honey CJ, Kötter R, Breakspear M, Sporns O (2007) Network structure of cerebral cortex shapes functional connectivity on multiple time scales. Proc Natl Acad Sci 104: 10240.
34. Zhou C, Zemanová L, Zamora-Lopez G, Hilgetag CC, Kurths J (2007) Structure--function relationship in complex brain networks expressed by hierarchical synchronization. New J Phys 9: 178.
35. Honey CJ, Sporns O, Cammoun L, Gigandet X, Thiran JP, et al (2009) Predicting human resting-state functional connectivity from structural connectivity. Proceedings of the National Academy of Sciences 106: 2035.
36. Stam CJ, Hillebrand A, Wang H, Van Mieghem P (2010) Emergence of modular structure in a large-scale brain network with interactions between dynamics and connectivity. Front Comput Neurosci 4.
37. Pons AJ, Cantero JL, Atienza M, Garcia-Ojalvo J (2010) Relating structural and functional anomalous connectivity in the aging brain via neural mass modeling. Neuroimage 52: 848-861.
38. Bhattacharya BS, Coyle D, Maguire LP (2011) Alpha and theta rhythm abnormality in Alzheimer's disease: a study using a computational model. Adv Exp Med Biol 718: 57-73.
39. Pievani M, de Haan W, Wu T, Seeley WW, Frisoni GB (2011) Functional network disruption in the degenerative dementias. Lancet Neurol 10:829-43.
40. Buzsáki G (2006) Rhythms of the Brain. Oxford University Press, USA.
41. Jeong J (2004) EEG dynamics in patients with Alzheimer's disease. Clin Neurophysiol 115: 1490-1505.

42. de Haan W, Stam CJ, Jones BF, Zuiderwijk IM, van Dijk BW et al (2008) Resting-state oscillatory brain dynamics in Alzheimer disease. J Clin Neurophysiol 25:4, 187-93.
43. Gleichmann M, Chow VW, Mattson MP (2011) Homeostatic Disinhibition in the Aging Brain and Alzheimer's Disease. J Alzheimers Dis 24: 15-24.
44. Schmitt HP (2005) Neuro-modulation, aminergic neuro-inhibition and neuro-degeneration. Draft of a comprehensive theory for Alzheimer's disease. Med Hypotheses 65, 1106-1119.
45. Olney JW, Wozniak DF, Farber NB (1997) Excitotoxic neurodegeneration in Alzheimer disease. Arch Neurol 54:1234-40.
46. Palop JJ, Mucke L (2009) Epilepsy and cognitive impairments in Alzheimer disease. Arch Neurol 66: 435.
47. Palop JJ, Mucke L (2010) Amyloid-beta-induced neuronal dysfunction in Alzheimer's disease: from synapses toward neural networks. Nat Neurosci 13: 812-818.
48. Larner AJ (2010) Epileptic seizures in AD patients. Neuromolecular Med 12: 71-77.
49. Dickerson BC, Salat DH, Greve DN, Chua EF, Rand-Giovannetti E, et al (2005) Increased hippocampal activation in mild cognitive impairment compared to normal aging and AD. Neurology 65: 404.
50. Qi Z, Wu X, Wang Z, Zhang N, Dong H, et al (2010) Impairment and compensation coexist in amnestic MCI default mode network. Neuroimage 50: 48-55.
51. Maestú F, Yubero R, Moratti S, Campo P, Gil-Gregorio P, et al (2011) Brain Activity Patterns in Stable and Progressive Mild Cognitive Impairment During Working Memory as Evidenced by Magnetoencephalography. J Clin Neurophysiol 28: 202.
52. Liang P, Wang Z, Yang Y, Jia X, Li K (2011) Functional Disconnection and Compensation in Mild Cognitive Impairment: Evidence from DLPFC Connectivity Using Resting-State fMRI. PLoS One 6: e22153.
53. Stam CJ, Jones BF, Nolte G, Breakspear M, Scheltens P (2007) Small-world networks and functional connectivity in Alzheimer's disease. Cereb Cortex 17: 92-99.
54. Stam CJ (2010) Use of magnetoencephalography (MEG) to study functional brain networks in neurodegenerative disorders. J Neurol Sci 289:1-2, 128-34.
55. de Haan W, van der Flier WM, Koene T, Smits LL, Scheltens P et al (2012) Disrupted modular brain dynamics reflect cognitive dysfunction in Alzheimer's disease. Neuroimage 59:3085-93.
56. Stam CJ, Reijneveld JC (2007) Graph theoretical analysis of complex network in the brain. Nonlinear Biomed Phys 1:3.
57. Bassett DS, Bullmore ET (2009) Human brain network in health and disease. Curr Opin Neurol 22:340-7.
58. van den Heuvel MP, Hulshoff Pol HE (2010) Exploring the brain network: a review on resting-state fMRI connectivity. Eur Neuropsychopharmacol 20:519-34
59. Stam CJ, van Straaten EC (2012) The organization of physiological brain networks. Clin Neurophysiol 123:1067-87
60. Warren JD, Rohrer JD, Hardy J (2012) Disintegrating brain networks: from syndromes to molecular nexopathies. Neuron 73:1060-2.
61. Zhou J, Gennatas ED, Kramer JH, Miller BL, Seeley WW (2012) Predicting regional neurodegeneration from the healthy brain functional outcome. Neuron 73:1216-27.
62. Raj A, Kuceyeski A, Weiner M (2012) A network diffusion model of disease progression in dementia. Neuron 73:1204-15.
63. Corder EH, Ghebremedhin E, Taylor MG, Thal DR, Ohm TG et al (2004) The biphasic relationship between regional brain senile plaque and neurofibrillary tangle distributions: modification by age, sex, and APOE polymorphism. Ann N Y Acad Sci 1019: 24-28.

64. Tomasi D, Volkow ND (2011) Functional connectivity hubs in the human brain. Neuroimage 57:908-17.
65. Putcha D, Brickhouse M, O'Keefe K, Sullivan C, Rentz D et al (2011) Hippocampal hyperactivation associated with cortical thinning in Alzheimer's disease signature regions in non-demented elderly adults. J Neurosci 31:17680-8.
66. Noebels J (2011) A perfect storm: Converging paths of epilepsy and Alzheimer's dementia intersect in the hippocampal formation. Epilepsia 52: 39-46.
67. Filippini N, MacIntosh BJ, Hough MG, Goodwin GM, Frisoni GB, et al (2009) Distinct patterns of brain activity in young carriers of the APOE-varepsilon4 allele. Proc Natl Acad Sci 106: 7209.
68. Kang JE, Lim MM, Bateman RJ, Lee JJ, Smyth LP, et al (2009) Amyloid-β dynamics are regulated by orexin and the sleep-wake cycle. Science 326: 1005.
69. Sperling RA, Laviolette PS, O'Keefe K, O'Brien J, Rentz DM, et al (2009) Amyloid deposition is associated with impaired default network function in older persons without dementia. Neuron 63:178-188.
70. Hedden T, Van Dijk KR, Becker JA, Mehta A, Sperling RA, et al (2009) Disruption of functional connectivity in clinically normal older adults harboring amyloid burden. J Neurosci 29:12686-12694.
71. Sheline YI, Morris JC, Snyder AZ, Price JL, Yan Z, D'Angelo G, Liu C, Dixit S, Benzinger T, Fagan A, Goate A, Mintun MA (2010) APOE4 allele disrupts resting state fMRI connectivity in the absence of amyloid plaques or decreased CSF Ab42. J Neurosci 30:17035-40.
72. Drzezga A, Becker JA, Van Dijk KR, Sreenivasan A, Talukdar T, et al (2011) Neuronal dysfunction and disconnection of cortical hubs in non-demented subjects with elevated amyloid burden. Brain 134:1635-46.
73. Machulda MM, Jones DT, Vemuri P, McDade E, Avula R, et al (2011) Effect of APOE {varepsilon}4 Status on Intrinsic Network Connectivity in Cognitively Normal Elderly Subjects. Arch Neurol 68:1131-6.
74. Puzzo D, Privitera L, Leznik E, Fà M, Staniszewski A, et al (2008) Picomolar amyloid-β positively modulates synaptic plasticity and memory in hippocampus. J Neurosci 28:14537-45.
75. Abramov E, Dolev I, Fogel H, Ciccotosto GD, Ruff E et al (2009) Amyloid-β as a positive endogenous regulator of release probability at hippocampal synapses. Nat Neurosci 12:1567-1576.
76. Buldú JM, Bajo R, Maestú F, Castellanos N, Leyva I et al (2011) Reorganization of functional networks in mild cognitive impairment. PLoS One 6:5, e19584
77. Gong G, Rosa-Neto P, Carbonell F, Chen ZJ, He Y et al (2009) Age- and gender-related differences in the cortical anatomical network. J Neurosci 29:15684-93.
78. Bassett DS, Nelson BG, Mueller BA, Camchong J, Lim KO (2012) Altered resting state complexity in schizophrenia. Neuroimage 59:2196-207
79. Zalesky A, Fornito A, Egan GF, Pantelis C, Bullmore ET (2011) The relationship between regional and inter-regional functional connectivity deficits in schizophrenia. Hum Brain Mapp doi: 10.1002/hbm.21379
80. Zetterberg LH, Kristiansson L, Mossberg K (1978) Performance of a model for a local neuron population. Biol Cybern 31:15-26.
81. Stam CJ, Pijn JP, Suffczynski P, Lopes da Silva FH (1999) Dynamics of the human alpha rhythm: evidence for non-linearity? Clin Neurophysiol 110:1801-1813.
82. Tzourio-Mazoyer N, Landeau B, Papathanassiou D, Crivello F, Etard O, et al (2002) Automated anatomical labeling of activations in SPM using a macroscopic anatomical parcellation of the MNI MRI single-subject brain. Neuroimage 15:273-289.

83. Stam CJ, Dijk BWV (2002) Synchronization likelihood: an unbiased measure of generalized synchronization in multivariate data sets. Physica D: Nonlinear Phenomena 163: 236 - 251.
84. Montez T, Linkenkaer-Hansen K, van Dijk BW, Stam CJ (2006) Synchronization likelihood with explicit time-frequency priors. Neuroimage 33: 1117-1125.
85. Rubinov M, Sporns O (2010) Complex network measures of brain connectivity: uses and interpretations. Neuroimage 52: 1059-1069.
86. Guimerà R, Sales-Pardo M, Amaral LAN (2007) Classes of complex networks defined by role-to-role connectivity profiles. Nat Phys 3: 63-69.
87. Ursino M, Zavaglia M, Astolfi L, Babiloni F (2007) Use of a neural mass model for the analysis of effective connectivity among cortical regions based on high resolution EEG recordings. Biol cybern 96:3, 351-365

Node 8

Functional network disruption in the degenerative dementias

Lancet Neurology 2011

Michela Pievani, PhD;[1] Willem de Haan, MD;[2] Tao Wu, MD;[3] William W Seeley, MD;[4] Giovanni B Frisoni, MD.[1]

[1]IRCCS Centro San Giovanni di Dio, Fatebenefratelli, Brescia, Italy

[2]Alzheimer Center, Department of Neurology, VU University Medical Center, Amsterdam, The Netherlands

[3]Beijing Institute of Geriatrics, Xuanwu Hospital, Capital Medical University, Beijing, China

[4]Memory and Aging Center, Department of Neurology, University of California, San Francisco, CA, USA

ABSTRACT

Despite considerable advances towards understanding the molecular pathophysiology of the neurodegenerative dementias, the mechanisms linking molecular changes to neuropathology and the latter to clinical symptoms remain largely obscure. Connectivity is a distinctive feature of the brain and the integrity of functional network dynamics is critical for normal functioning. A better understanding of network disruption in the neurodegenerative dementias may help bridge the gap between molecular changes, pathology and symptoms. Recent findings on functional network disruption as assessed with "resting-state" or intrinsic connectivity fMRI and EEG/MEG show distinct patterns of network disruption across the major neurodegenerative diseases. These network abnormalities are relatively specific to the clinical syndromes, and in Alzheimer's disease and frontotemporal dementia network disruption tracks the pattern of pathological changes. These findings may have a practical impact on diagnostic accuracy, allowing earlier detection of neurodegenerative diseases even at the pre-symptomatic stage, and tracking of disease progression.

INTRODUCTION

Historically, clinicians have recognized patients with neurodegenerative dementias based on their clinical symptoms. In recent years, basic science advances have allowed researchers to re-categorize these diseases based on molecular phenotype, i.e. which toxic, misfolded disease protein aggregates are observed in the brain post-mortem, such as beta amyloid (Aβ) and hyperphosphorylated tau (HP-tau) in Alzheimer's Disease (AD); tau, TAR DNA-binding protein of 43 kDa (TDP-43), or fused in sarcoma (FUS) in frontotemporal dementia (FTD), and alpha-synuclein in Parkinson's Disease (PD) and Dementia with Lewy Bodies (DLB).[1] These pathological changes are considered early events in a cascade that begins at the synaptic and neuronal levels and ultimately leads to the clinical syndrome. Within this temporal window, quantifiable biological, imaging, and physiological markers of pathology have been identified that can be considered *in vivo* intermediate phenotypes. Such surrogate markers of pathology can clarify disease pathophysiology, i.e. link the molecular phenotype to clinical symptoms and have the potential to facilitate earlier, more accurate diagnosis and monitoring of disease progression. In AD, PET amyloid ligands enable *in vivo* mapping of cerebral Aβ deposition,[2] whereas structural MRI has been shown to reflect HP-tau-related neurodegeneration.[3] These biomarkers have recently been incorporated into the new AD diagnostic criteria.[4,5] In disorders such as PD, FTD and DLB, structural biomarkers have clarified disease

pathophysiology by showing patterns of atrophy associated with histopathology on the one hand,[6-8] and clinical symptoms on the other (Table 1).[8,9]

Table 1. Connectivity as an intermediate phenotype in the degenerative dementias

	Alzheimer's disease	**Frontotemporal degeneration (behavioural variant)**	**Parkinson's disease**	**Dementia with Lewy bodies**
Molecular phenotype	β-Amyloid—distributed throughout neocortex; hyperphosphorylated tau—medial temporal lobe	Tau, TDP-43, or FUS—frontal cortex, anterior temporal cortex, striatum, amygdala, and thalamus	α-Synuclein—brainstem (dorsal motor nucleus of the vagus nerve, locus coeruleus, and substantia nigra)	α-Synuclein—brainstem (dorsal motor nucleus of the vagus nerve, locus coeruleus, and substantia nigra)
Intermediate phenotypes				
Molecular imaging	Widespread diffuse neocortical amyloid ligand uptake on PET	NA	NA	NA
Connectivity	Default-mode-network disruption on task-free functional MRI/EEG/MEG	Salience network disruption	Basal ganglia–thalamocortical loop abnormalities	NA
Structural imaging	Atrophy in the medial temporal lobe	Atrophy in the anterior cingulate cortex, frontoinsula, frontal pole, temporal pole, striatum, thalamus, and amygdala	Mild atrophy in the frontal and temporal cortices, and basal ganglia	Atrophy in the substantia nigra, midbrain, hypothalamus, basal forebrain, and amygdala
Clinical phenotype	Episodic memory loss	Social–emotional deficits	Motor impairment (tremor, rigidity, bradykinesia, and postural instability)	Hallucinations, parkinsonism, fluctuations in cognition, and motor impairment

TDP-43=TAR DNA-binding protein of 43 kDa. FUS=fused in sarcoma. NA=not available. EEG=electroencephalography. MEG=magnetoencephalography.

Localization-based approaches (such as *in vivo* mapping of molecular changes and neurodegeneration) have helped build much of the current knowledge regarding disease pathophysiology. These approaches, however, are less suited to investigate neuronal/synaptic dysfunction, which is thought to underlie cognitive and functional deficits. Because brain functions rely on the integrity of dynamic communication between interconnected brain regions and circuits, a network perspective accounting for such interactions has the potential to provide novel and meaningful intermediate phenotypes of pathology (Table 1). Prevalent views on the relationship between symptoms and pathology in AD help illustrate this notion (Figure 1). In typical AD, the progression

of symptoms follows a relatively stereotyped order which mirrors the topographic progression of HP-tau:[10] episodic memory loss occurs first (hippocampus and medial temporal lobe, posterior cingulate cortex), followed by semantic memory loss (lateral temporal cortex), aphasic, apraxic, and visuospatial symptoms (frontal, temporal, and parietal neocortex), and finally motor and visual deficits (sensorimotor and occipital cortex). Although atypical variants exist,[11] this orderly progression may reflect incremental spread throughout interconnected regions within large-scale networks, and ultimate spread into adjacent or upstream regions.

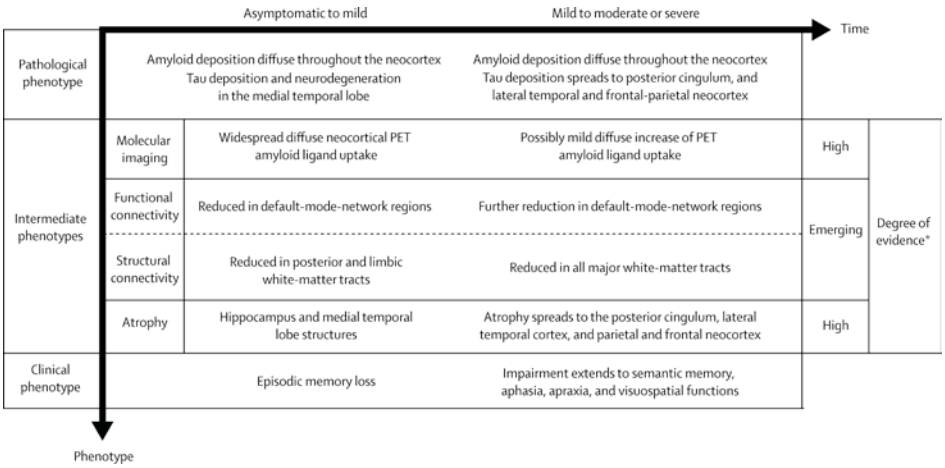

Figure 1: The pathophysiological framework of Alzheimer's disease: connectivity as an intermediate phenotype between pathology and symptoms
*Evidence that intermediate phenotypes are associated with pathological or clinical phenotypes.

The brain can be viewed as a complex neural network consisting of structurally and functionally interconnected regions at multiple scales (Panel 1).[12] At the macroscopic level, neural networks can be investigated non-invasively in health and disease with functional MRI and neurophysiological techniques (electro- and magneto-encephalography, EEG and MEG).[13,14] The aim of this review is to provide a comprehensive overview of findings on functional network disruption in the most prevalent neurodegenerative dementias. Although several excellent reviews have addressed functional networks disruption in AD and in psychiatric conditions,[15-20] here we summarize studies across multiple neurodegenerative dementias. By including FTD, PD dementia and DLB, we highlight functional network similarities and differences among conditions that share common mechanisms (toxic protein aggregation and neuronal loss) but have distinct clinical phenotypes. Toward this aim, resting-state "task-free" functional imaging and neurophysiological studies will be reviewed. Because our primary goal is to review functional methods that are broadly applicable across neurodegenerative diseases, we

have omitted task-activation studies, which require the design of disease-specific experiments (for a review of its applications in AD, see Dickerson 2007),[21] as well as studies of gray matter structural covariance.[22,23]

Techniques to investigate network integrity

fMRI, EEG and MEG techniques enable researchers to investigate large-scale neural networks at different spatial and temporal resolutions. Functional connectivity between brain regions is measured at a spatial resolution as low as 2-3 millimeters using fMRI and at about 5-30 millimeters with EEG/MEG. fMRI and neurophysiological techniques contrast most sharply in their temporal and spatial resolutions, which differ by three orders of magnitude (seconds *versus* milliseconds). Structural connectivity within networks can be measured at a spatial resolution of 3-6 millimeters using diffusion tensor imaging (DTI).

Task-free fMRI

Task-free fMRI allows functional network mapping at high spatial resolution. Resting-state or so-called "intrinsic connectivity" fMRI is used to measure spontaneous low frequency (<0·08-0·1 Hz) fluctuations in the blood oxygen level dependent (BOLD) signal while subjects lie quietly in the scanner and perform no specific task.[24] The BOLD signal reflects changes in the ratio between oxy- and deoxy-haemoglobin following neuronal activity, therefore resting fMRI provides an *indirect* marker of neuronal function on a time scale of seconds. Functional connectivity is defined by temporal correlations (over minutes of data acquisition) of the BOLD signal between spatially distinct regions.[24]

Resting-state networks can be identified with several analytical methods, including "seed" or region-of-interest based methods and independent component analysis (ICA).[24] Region-of-interest based approaches measure the temporal correlation between an *a priori* selected brain region and all other brain voxels. The choice of the seed region is investigator driven and depends on the goals of the analysis. This approach identifies a network of brain areas ("nodes"; Panel 1) functionally connected with the seed region. ICA is a data-driven method that does not require *a priori* hypotheses about the regions of interest. This approach enables identification of multiple networks consisting of spatially independent and temporally correlated regions.[25] Several networks have been consistently identified with either method (Figure 2):[26] the default mode network (DMN), a posterior cingulate cortex-precuneus/medial temporal/lateral temporoparietal/medial frontal network that often deactivates during cognitively demanding tasks;[27] bilateral executive-control networks made up of lateral frontal-parietal nodes;[28] the salience network, an anterior cingulate/frontoinsular system with links to limbic and subcortical autonomic control centers,[28] a dorsal attentional system embedded in high frontoparietal sensorimotor association regions,[29] and networks related to primary vi-

sual, auditory, and sensorimotor regions.[26] One area of active work concerns how many brain networks can be meaningfully outlined at the group and single-subject levels with these methods.

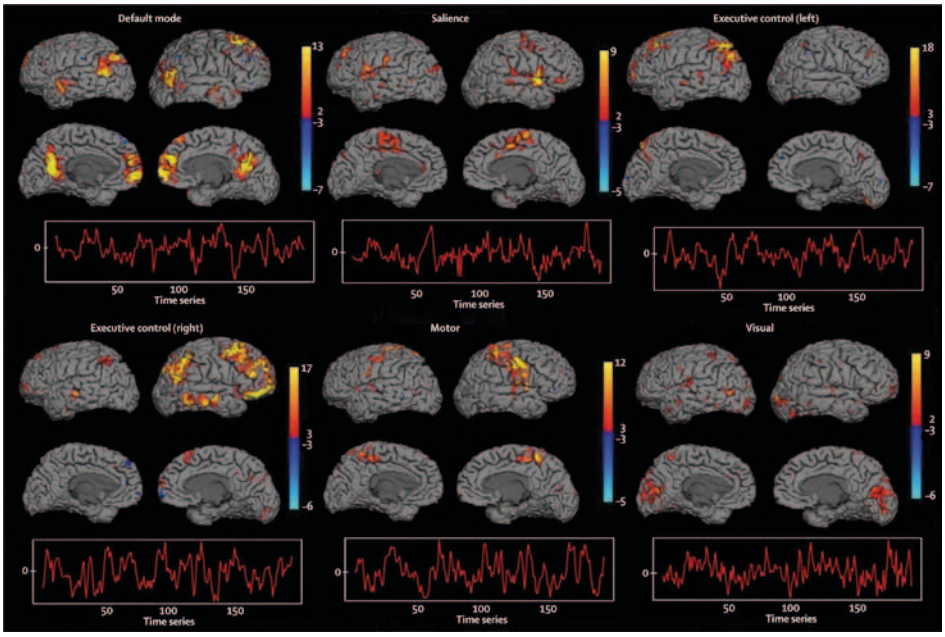

Figure 2 Functional connectivity on resting-state fMRI in healthy people
Independent-component-analysis-derived resting-state fMRI networks (default mode, salience, left and right executive control, visual, and motor networks) [26–28] of a healthy man aged 33 years.
Red-to-yellow colours show the strength of each voxel's connectivity to overall component time series.
fMRI=functional MRI.

In the absence of an experimental task, these networks show a tight spatial correspondence with the neuronal circuits activated during cognitive, emotional, and sensorimotor tasks.[30] Moreover, connectivity strength within these networks "at rest" has been related to cognitive and emotional state,[28,31] further supporting resting-state fMRI as a tool to investigate symptoms and deficits in the context of disease. Functional networks can also be investigated within a graph theoretical framework (see section 2.4) by defining brain regions as the network nodes (e.g., through atlas-based or functional brain parcellation) and the temporal correlation strengths between node pairs as the weighted edges.

Task-free EEG and MEG

Task-free EEG and MEG allow functional network mapping at high temporal resolution. These techniques represent a complementary approach to studying resting-state networks is based on the synchrony of spontaneous electrical and magnetic activity

of the brain. Oscillating neuronal assemblies are assumed to reflect cognitive processing,[32] and generate a fluctuating electromagnetic field that can be detected with scalp electrodes. EEG detects the electrical component of this field with a high temporal resolution (millisecond range) and provides a *direct* reflection of (large-scale) neuronal activity. Factors that limit the use of EEG are the relatively modest spatial resolution and the difficulty recording subcortical sources of activity. In this regard, MEG provides an important step forward. MEG records the very weak magnetic field around the brain (±100-1000 femtoTesla), which requires advanced equipment including superconducting quantum devices and a magnetically shielded room, but offers clear advantages including higher spatial resolution (±5 millimeters), less artifact interference, and a shorter set-up time without electrodes.[33] The EEG and MEG signals are usually analyzed in separate frequency bands: delta (between 0-4 Hz), theta (4-8 Hz), alpha (8-13 Hz), beta (13-30 Hz) and gamma (30-45 Hz).

Oscillatory synchronization between different brain regions can be quantified with several procedures. Coherence, one of the most popular synchronization measures, describes the linear similarity between two EEG/MEG time-series at a given frequency.[34] Examples of more advanced markers of functional coupling are the Synchronization Likelihood, which is sensitive to both linear and non-linear interdependencies between EEG/MEG signals, and the Phase Lag Index, which overcomes the problem of volume conduction, whereby neighboring electrodes detect common sources, spuriously increasing synchronization.[13] Functional networks can be constructed by taking signals recorded at different regions as network nodes, and their mutual synchronization as connection strengths (Figure 3).[13] Subsequently, these networks can be analyzed using graph theoretical algorithms, as outlined in the section 2.4.

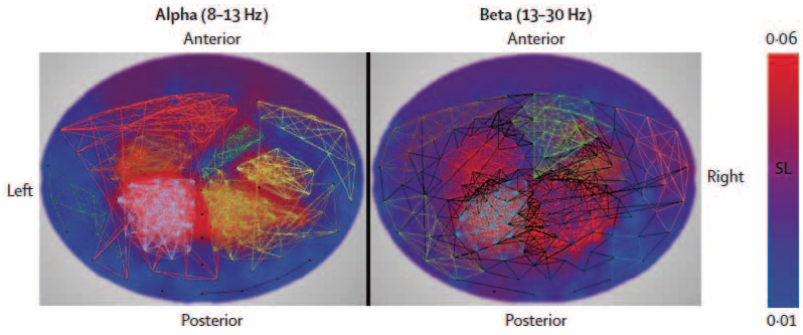

Figure 3 Functional connectivity on resting-state MEG in healthy people
Headplot showing functional MEG network of a healthy woman aged 63 years in the alpha (8–13 Hz) and beta (13–30 Hz) frequency ranges.13 Coloured lines show diff erent functional subnetworks (modules), black lines represent their interconnections (only shown in beta-band example). Background colours show connectivity strength (red are hub—ie, highly connected—regions). MEG=magnetoencephalography. SL=synchronisation likelihood.[13]

Diffusion tensor imaging

Diffusion tension imaging provides markers of structural connectivity. Brain regions with synchronous BOLD signal, electrical or magnetic fluctuations often (but not always) feature some form of direct physical connection. DTI assesses the structural integrity of brain connections (i.e. axons and fiber tracts) by measuring changes in the diffusion of water molecules through tissues.[35] Two markers of structural integrity are commonly investigated: fractional anisotropy, a marker of white matter (WM) fiber disruption (loss of fiber coherence, demyelination, axonal loss), and mean diffusivity, a marker for cell density.[35] Axial and radial diffusivity may provide more specific markers of axonal damage and demyelination.[35] Common methods to investigate structural disruption are voxel-wise, DTI tractography and ROI-based techniques.[35] DTI tractography may be preferable on an individual subject basis, allowing one to reconstruct and visualize specific WM connections between cortical nodes (Figure 4).[36] Graph theoretical analysis can be used to build structural networks and study their topology, in a way similar to that used to investigate resting-state fMRI and EEG/MEG-derived functional networks.

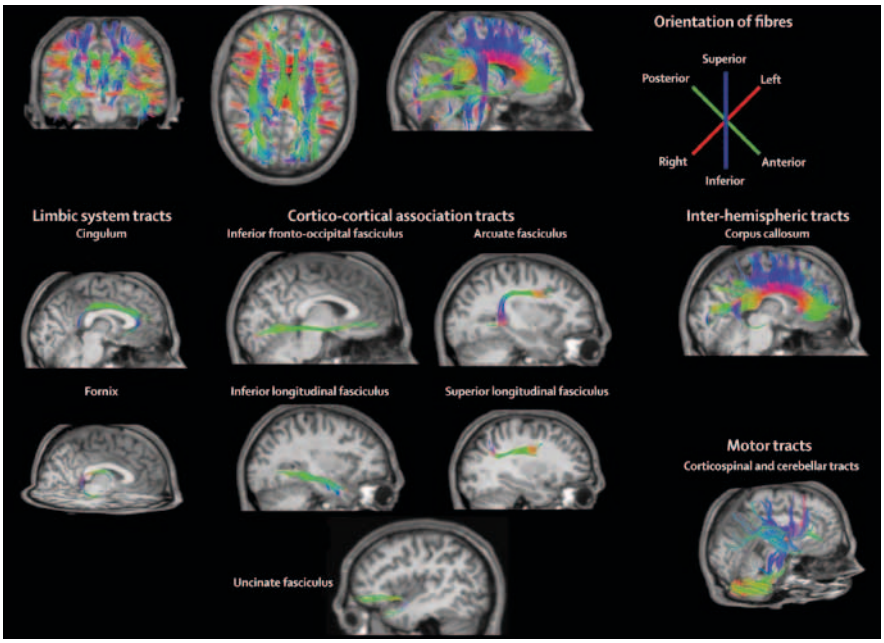

Figure 4 Structural connectivity assessed with diff usion tensor imaging in a healthy man aged 33 years. Diffusion tensor imaging tractography shows long (mainly visible in sagittal view as green and blue colour-coded fi bres) and short (mainly visible in axial and coronal views as red colour-coded fibres) white-matter connections (top row). Specific tracts can be identified that subserve distinct cognitive and non-cognitive functions. The fornix and cingulum are mainly associated with memory and emotional processing, cortico-cortical association and intra-hemispheric tracts are associated with a broad range of cognitive processes, and the corticospinal and cerebellar tracts are generally involved in motor disorders.[36]

Network organisation

Graph theory provides a framework for exploring brain network organization in normal and pathological conditions.[13,14,37] Graph theoretical analysis to fMRI, EEG/MEG and DTI data can model the whole brain as a single network and investigate its properties such as network structure, modularity, and robustness to damage (Panel 2).[14] The healthy human brain is thought to be organized into a 'small-world' topology,[38] a network architecture that combines an efficient balance between local (short range) and global (long range) connectivity. This small-world configuration is considered better suited for information transfer and thus presumably for cognitive processing than the topology of 'random' or 'regular' networks.[39] Graph theory can also extract functional sub-networks ('modules') and quantify interactions between them by using data-driven modularity algorithms.[40] Another area of graph theory is devoted to the investigation of highly connected ('hub') nodes, since these regions are critical for network integrity (Panel 2).

Increasing evidence suggests that functional and structural network properties are related to development,[41] age and cognition.[42-44] Older (mean age of 67) vs. Young (mean age of 24) adults show a distinct modular organization of the brain, the former with greater con-

nectivity between posterior and central regions, and the latter showing higher connectivity between fronto-cingulo-parietal modules.[42] In addition, IQ score has been negatively correlated with global functional connectivity (characteristic path length) in young adults,[43] and the structural efficiency of networks has been negatively associated with age, and positively correlated with processing speed, visuospatial and executive functions.[44]

Functional networks and clinical impairment

Imaging and lesion studies have led to valuable insights into the functional anatomy of the brain, and localization principles are vital to the clinical neurologist. As outlined in the introduction, however, localization-based perspectives often fail to explain the complex interrelationship between neurodegenerative pathology and clinical symptoms. Even 'focal' lesions like stroke (e.g. 'strategic' infarction), brain tumour or traumatic brain injury can cause widespread disturbance of functional connectivity and unexpected cognitive symptoms that can be explained by a variety of lesion locations.[45-47] There is also increasing evidence that local damage can change the overall network structure in a way that can lead to pathological hypersynchronization and epilepsy.[48] In an elegant simulation study,[49] the effect of focal brain lesions on the patterns of functional connectivity was investigated by simulating lesions at different brain locations. The study showed that focal lesions located in the precuneus, medial anterior cingulate cortex, temporo-parietal junction, or superior frontal cortex produced widespread and pronounced changes in functional connectivity with intra-hemispheric and contralateral regions. Conversely, lesions to the visual or motor cortex had limited effects on global connectivity.[49] Neurodegenerative processes, characterised by gradual and selective spreading of pathology across brain regions, might cause a progressive targeted network injury, leading to specific "disconnection syndromes" and progressive cognitive dysfunction.[50,51] The difference between most neurodegenerative diseases and neurological disorders due to focal lesions is that in the latter case networks are affected at random, with no specific topographic and chronological pattern, whereas in the former case networks are affected with a relatively stereotyped sequence. Network analysis may therefore help to explain the link between local damage, long-range disconnection, and more widespread physiological and clinical dysfunction. Literature in this emerging field is still scarce but already points to intriguing new hypotheses.

Alzheimer's disease

AD results from deposition of Aβ in the neocortex and HP-tau in the entorhinal cortex and hippocampus.[52,53] More recent evidence suggests that even earlier HP-tau-related neurofibrillary changes may occur in the brainstem dorsal raphe nucleus or the locus ceruleus.[54] In humans HP-tau pathology is associated with memory deficits,[55] whereas Aβ deposition is not directly related to cognition,[55] but shows topographical correspondence with the DMN.[56] Moreover, the sequence of functional and structural disruption within

and between DMN regions is reminiscent of the spread of tau pathology. Buckner et al. mapped *in vivo* PIB-PET Aβ deposition in patients with AD and cortical hubs in healthy controls and showed that regions of high Aβ deposition in patients largely overlap with DMN cortical hubs in the healthy brain, especially the posterior cingulate cortex.[56] Disruption of DMN regions in AD has been consistently reported by resting-state fMRI studies using ICA or seed-based methods.[57-61] Similar changes have been reported in subjects with mild cognitive impairment, a condition which is believed to often represent pre-clinical AD.[62-64] Early DMN functional disruption in AD involves the medial temporal lobe and posterior cingulate cortex/precuneus,[57,58,62,63] subsequently worsening and extending to the lateral parietal and medial frontal regions with increasing disease severity.[59] Structural connectivity disruption follows a similar pattern: the posterior WM tracts, connecting the hippocampus/medial temporal lobe with the posterior cingulate cortex and the limbic regions, are affected first,[65-67] whereas frontal WM tracts (genu of corpus callosum, anterior cingulum) are minimally affected, except for the uncinate and arcuate fasciculi, which connect temporal to frontal cortex.[66-68] Electrophysiological studies are consistent with fMRI studies in reporting a reduction of cortico-cortical connectivity in AD. EEG and MEG analyses have shown reduced connectivity between long distance fronto-parietal and fronto-temporal regions in the alpha and beta frequency bands.[69-71] These frequency bands show good topographic correspondence with the DMN and the greatest correlation between EEG power and DMN fMRI fluctuations.[72,73]

When tau pathology has extended through the entire network, cognitive deficits generally involve multiple domains and patients will have developed overt AD. Therefore the breakdown of this network due to neurodegeneration may track progression to dementia. In subjects with mild cognitive impairment, preliminary evidence indicates that reduced DMN connectivity is a significant predictor of conversion to AD independently of global atrophy.[74] Interestingly, the predictive value of DMN connectivity was no longer significant when memory performance was taken into account,[74] suggesting that functional connectivity changes are related to memory deficits.

In addition to reduced DMN connectivity, increased intrinsic connectivity has been reported by several resting-state fMRI studies between frontal-parietal regions.[59,61,63] The basis for these connectivity increases remains unclear; although some authors suggest that they represent compensatory mechanisms,[59,61,63] there is as yet no evidence that such changes improve cognition. An alternative explanation is that damage to one network enhances connectivity within regions that normally feature an anti-correlated relationship with the damaged network.[58]

Graph theoretical analysis of network organization in AD has shown a loss of small-world structure toward a more 'random' network topology,[75-78] indicated by a reduction in the clustering coefficient values,[75,76,78] and lower characteristic path length.[75,77,78] The topography of network abnormalities assessed with this technique is in line with previous

studies, showing reduced connectivity in the hippocampus and posterior parietal regions with fMRI,[76,77] and in the alpha (8-10Hz) and beta (13-30Hz) frequency bands with MEG.[75,78] In addition, Stam et al. have shown greater 'hub' vulnerability in AD, as simulated targeted attacks to highly connected nodes better explained the network changes observed in the alpha frequency band than 'random' removal of nodes.[75] A single study has assessed structural network connectivity, reporting abnormal network topology in AD.[79]

Frontotemporal dementia

FTD refers to a group of clinical syndromes associated with underlying frontotemporal lobar degeneration (FTLD) pathology. Three major clinical syndromes are recognized: a behavioural variant (bvFTD), which presents with social-emotional dysfunction, and two primary progressive aphasia (PPA) subtypes, the semantic and nonfluent/agrammatic variants.[80] A high proportion of FTLD cases present associated motor neuron disease. A third PPA subtype, the logopenic variant, has been included in the recently revised diagnostic criteria,[81] although many patients with this variant show underlying AD at autopsy. FTLD pathology, in turn, can be divided into three major molecular classes based on the underlying disease protein: tau (FTLD-tau), TDP-43 (FTLD-TDP), or FUS (FTLD-FUS).[80] For some clinical syndromes, such as semantic variant PPA and FTD with motor neuron disease, the underlying FTLD molecular class can be predicted with good confidence during life.[82,83] For other syndromes, such as bvFTD, existing criteria do not reliably predict the underlying molecular pathology.[83]

Recent work has revealed that bvFTD syndrome, like typical AD, reflect the progressive degeneration of a specific large-scale network, the "salience network".[6,84] This network is involved in processing emotionally significant stimuli and is inversely correlated with the DMN in task-free settings,[28] leading Seeley and colleagues to predict that bvFTD and AD would feature divergent network connectivity patterns.[85] This hypothesis was subsequently tested using task-free fMRI and ICA analysis of the DMN and salience networks in patients with bvFTD and AD.[58] The study identified divergent patterns in the two clinical groups, with reduced salience network connectivity and increased DMN connectivity in bvFTD and the opposite pattern in AD.[58] In addition, reduced salience network connectivity in bvFTD patients was associated with greater disease severity.[58] A score incorporating DMN and salience network connectivities better discriminated between the two clinical groups than did either network alone,[58] suggesting that network-based patterns which are sensitive to decreases and increases may prove more specific to a given disease. Studies of structural connectivity in bvFTD support the disruption of specific frontal-temporal WM tracts, such as the bilateral uncinate and anterior cingulate tracts.[66,86] The FTD language syndromes (PPAs) have not yet been directly investigated with resting-state network mapping, however atrophy-mapping studies suggest that they are likewise associated with degeneration of specific networks.[84] DTI studies indeed

support the disruption of specific WM tracts within the PPA-targeted networks.[86,87] Neurophysiological literature on functional networks in FTLD is almost non-existent. One resting-state EEG study assessed functional connectivity in AD, FTLD, and persons with subjective memory complaints, and failed to find group differences.[88] A subsequent MEG study of network organization in FTD patients however showed changes in the opposite direction to that observed in AD patients, towards an overly regular and ordered topology.[78] This intriguing contrast aligns with resting-state fMRI results in AD and FTD[58] to suggest that these disorders may exert divergent effects on large-scale networks (Figure 5)[89] and that these effects may help distinguish these disorders during life.

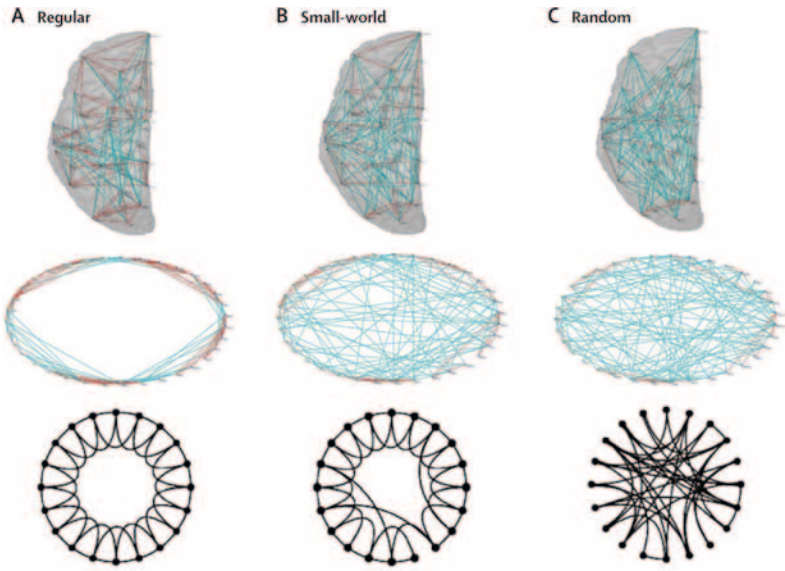

Figure 5 Schematic representation of a small-world brain functional network and of simulated regular and random networks with 35 nodes and 120 connections. Regular networks (A) have many connections between neighbouring regions (red lines) and few connections with distant nodes (light blue lines). Small-world networks (B) have fewer local connections and more long-distance connections. Random networks (C) have few local connections and many connections between distant regions. Each network is shown overlaid onto a standard template (top row) and in schematic representation (middle row). Nodes represent 35 cortical points of the left hemisphere drawn from the automated anatomical labeling template, and edges represent functionally connected nodes. The real-world network was extracted from a single person, the corresponding regular (A) and random (C) networks were simulated with the Brain Connectivity Toolbox.[89] The corresponding theoretical Watts–Strogatz network models are also shown (bottom row). Adapted from Watts and Strogatz[38] by permission of Macmillan Publishers Ltd.

Whether the underlying FTD molecular class can be identified by its impact on network-specific connectivity, however, remains unknown. Considering the role of anatomy (rather than the specific misfolded protein) in driving the clinical syndrome, there is reason to suspect that anatomically based methods (including resting-state network mapping) may struggle to reliably differentiate patients with bvFTD due to FTLD-tau vs.

FTLD-TDP vs. FTLD-FUS, for example. On the other hand, it remains possible that to date bvFTD remains an overly inclusive clinical syndrome. If so, further clinical or anatomical differentiation may improve our ability to predict pathology during life.[90,91]

Parkinson's Disease and Dementia with Lewy bodies

PD and DLB are two neurodegenerative syndromes associated with deposition of alpha-synuclein-containing Lewy bodies and Lewy neurites within brainstem, limbic, and cortical neurons.[92] In spite of a common molecular substrate, PD and DLB syndromes show important differences with regard to the timing and severity of symptoms.[93] A proportion of patients with PD develop dementia in later disease stages (Parkinson disease dementia, PDD), clinically resembling DLB.[93]

Available evidence suggests that PD and DLB are associated with distinct patterns of functional network dysfunction, namely increased basal ganglia-thalamocortical connectivity in PD and reduced global and local cortico-cortical connectivity in patients with dementia. The basal ganglia-thalamocortical loop includes the striatum, globus pallidus, thalamus, subthalamic nucleus, and substantia nigra; and cortical motor areas (primary motor cortex, supplementary motor area, premotor cortex).[94] Resting-state fMRI studies of this network have consistently reported increased connectivity between the basal ganglia and motor regions in PD patients.[95-98] These network abnormalities were normalised after levodopa administration.[95,98] In addition, *reduced* connectivity within this network has been reported by resting-state fMRI studies between the putamen and parietal and motor areas.[95,96] Resting-state EEG/MEG studies reported increased connectivity, in the alpha and beta (8-30 Hz) frequency ranges, between the subthalamic nucleus and the motor cortex,[99] and cortico-cortically.[100] A resting-state MEG study of patients in early, drug-naive stages showed an increase in alpha band (8-10 Hz) cortico-cortical functional connectivity that expanded towards other frequency bands (4-30 Hz range) with increasing disease severity.[101] Increased connectivity affected both global and local connections and was associated with motor deficits.[100,101] Less clear is whether levodopa administration and deep brain stimulation normalise these abnormalities, as one study showed a normalization of connectivity after intervention in association with motor improvement,[100] and another showed a further increase in connectivity.[99] In PDD, preliminary studies indicate a different pattern, with decreased functional connectivity reminiscent of the changes in AD.[102] In DLB, the most consistent finding is a reduction of global cortico-cortical coherence in the alpha (8-13Hz) frequency band.[103-105] A MEG study specifically assessed coherence in long (anterior and posterior) and short (lateral and medial) cortico-cortical connections, reporting more pronounced loss of connectivity in long- than short-distance connections in this frequency band.[103] Inconsistent changes have been reported in the delta (0·5-4Hz) frequency range.[104,105]

In PD and DLB, a clear correspondence between structural and functional connectivity changes in specific networks is difficult to draw, in part because DLB has yet to be linked to a particular network detectable with resting-state fMRI.[106] DTI demonstrates microstructural abnormalities in the basal ganglia of PD patients.[107-109] but evidence of structural disconnection within this circuit is limited.[109,110] Reduced connectivity in the frontal and parietal association tracts has been reported but without detecting a clear pattern of WM involvement.[111-113] PD patients who develop dementia show a specific involvement of the posterior cingulum compared with both PD and controls.[114,115] In DLB, the most consistent finding is a reduction of connectivity in the inferior longitudinal fasciculus,[114,116-118] which connects the posterior temporal and occipital visual cortices, a finding in line with the occurrence of visual hallucinations in these patients.[116] In addition, DLB patients show reduced connectivity between fronto-temporal and fronto-occipital regions compared to controls.[114,118] This pattern of WM disruption is overall similar to that detected in patients with PDD,[114] and AD,[118] but damage in the visual association areas is more pronounced in DLB than in other dementias.[114,118] Because these studies were based on patients diagnosed on clinical grounds, whereas DLB and AD pathologies often co-occur at autopsy,[119] it is perhaps not surprising that efforts to date show significant overlap in the patterns of network disruption in DLB and AD.[103,114,116,118]

Graph theory studies of network organization in PD, PDD and DLB are scarce. One study investigated motor circuits connectivity in PD, reporting abnormal basal ganglia-thalamocortical connectivity in line with previous fMRI studies,[120] and another study showed reduced global efficiency in PD.[121]

Neurobiological and clinical implications of network disruption

Research findings reviewed here demonstrate that functional neuroimaging is able to detect distinct patterns of network disruption across the major neurodegenerative diseases (Table 2). These networks are relatively specific to the clinical profiles and may represent intermediate phenotypes between pathology and clinical syndromes. In AD, the topography of Aβ deposition overlaps with the DMN, broadly defined, whereas HP-tau pathology is most prominent within a DMN subnetwork devoted to episodic memory.[122] In FTD, the salience network is profoundly disrupted in the behavioural variant. In PD, alpha-synuclein pathology affects the cortico-striatal motor loops. In DLB, forebrain alpha-synuclein deposition has not been matched to a specific network with resting-state techniques, but neuropathological evidence supports an ascent through the brainstem to the limbic and cortical regions associated with clinical symptoms.[92] Disruption of ascending brainstem projection systems may soon prove detectable with network-based methods.[123]

Important network differences have emerged from comparisons between PD, PDD and DLB, with an opposite EEG-pattern of connectivity associated with dementia onset

(increased *versus* decreased connectivity). Interestingly, PDD and DLB changes were less severe though similar to those of AD with respect to the involvement of long-distance connections, although molecular *in vivo* and post-mortem studies do not support an Alzheimer's etiology.[119,124] With regard to long-distance connections, hub regions may play a key role.[125] Posterior parietal regions are among the brain regions with the highest connectivity, consistent with their role as multimodal association areas.[126] Damage to heteromodal association hub regions, as seen prominently in AD,[56,75] may prove particularly disruptive by dis-integrating unimodal and polymodal representations that normally converge at hubs after being processed in secondary and association cortices.[126] In PD cognitive symptoms are generally milder than in AD, and pathology targets the motor circuits, whose damage may have more restricted effects on whole brain connectivity.[49] Future studies will likely elucidate whether the relatively preserved cognition in PD is explained by the relative sparing of cortical hub regions until late disease stages.[115]

Table 2. Connectivity disruption in the degenerative dementias

	Alzheimer's disease	**Frontotemporal degeneration (behavioural variant)**	**Parkinson's disease**	**Dementia with Lewy bodies**
Functional connectivity				
Resting-state functional MRI	Reduced connectivity—default mode network	Reduced connectivity—salience network	Increased connectivity—basal ganglia–thalamocortical loops; normalisation after levodopa administration	Insufficient evidence
Resting-state EEG/MEG	Reduced connectivity—alpha and beta (8–30 Hz) range between long-distance fronto-parietal and fronto-temporal regions	Insufficient evidence	Increased connectivity—alpha and beta (8–30 Hz) range locally and globally	Reduced connectivity—alpha (8–13 Hz) range locally and globally
Structural connectivity (diffusion tensor imaging)	Reduced connectivity—posterior and limbic white-matter tracts	Reduced connectivity—anterior white-matter tracts	No change in the major white-matter tracts	Reduced connectivity—visual pathway
Network organisation	Change towards a different topology—small-world to random; hub vulnerability	Change towards a different topology—small-world to regular	Insufficient evidence	No evidence

EEG=electroencephalography. MEG=magnetoencephalography.

From a clinical perspective, further pursuit of network-based strategies may lead to the development of sensitive and specific biomarkers for diagnostic, prognostic, and disease-monitoring purposes. Although the reviewed studies were conducted at the group level, preliminary data about the sensitivity/specificity of network-derived markers seem promising. In AD, two studies have explored the accuracy of resting fMRI derived-markers to discriminate between AD patients and healthy elderly, reporting a sensitivity of 85% and a specificity of 77% using DMN connectivity,[57] and a sensitivity of 72% and a specificity of 78% using the clustering coefficient.[76] In the study by Zhou and colleagues,[58] the combination of DMN and salience network activity allowed 100% separation of AD and FTD, although the performance of these measures remains to be tested in independent patient samples. Task-free fMRI and EEG/MEG techniques also offer practical advantages over existing biomarkers, such as PET and cerebrospinal fluid sampling. In general, these techniques are non-invasive and safe. Task-free fMRI data can be obtained in eight minutes and added to the structural MRI most patients receive as part of a routine dementia evaluation, creating minimal new costs for data acquisition. Moreover, fMRI and EEG/MEG can be repeated as often as necessary (within clinical trials, for example), without radioactivity exposure concerns. On the other hand, some practical limitations that might limit the clinical implementation of these techniques in the short period should be mentioned. The expertise to analyse these data is yet limited to few centres and the analysis itself is time-consuming.

CONCLUSIONS AND FUTURE DIRECTIONS

Brain connectivity studies allow questions to be addressed that have so far escaped a convincing answer. For example, what is the mechanism whereby in AD the deposition of Aβ and HP-tau takes place in largely distinct but highly interconnected hub regions? Why damage to the whole network subsequently ensues? Similar questions apply to alpha-synuclein in DLB and tau, TDP-43, and FUS in FTD. Several working models for network-based molecular pathogenesis have begun to emerge. One parsimonious account contends that misfolded disease proteins first spread intraneuronally, like prions, by inducing misfolding of adjacent normally folded (or unfolded) proteins.[127-130] This process may then move from pre- to post-synaptic cells via one of several transmission modes.[127] Evidence supporting a prion-like mechanism has come from cellular and rodent models of tau, alpha-synuclein, and Aβ disorders,[127-129] as well as from patients with PD who received transplanted dopaminergic neurons from fetal donors only to develop Lewy bodies within those neurons a few years after transplantation.[130] Other models emphasize the role of network-based dysregulation of excitation-inhibition balance (especially at the local microcircuit level),[131] disruption of activity- or connectivity-based

inter-neuronal trophic factor support,[132] and the long-term metabolic demands of high synaptic plasticity and turnover.[133,134] These accounts need not be considered mutually exclusive and each presents a potential therapeutic target for exploration.

Finally, although the mechanisms noted above are built around the idea that networks constrain and determine the anatomical disease pattern, apparent network-based spread could emerge, in a network-independent manner, if individual nodes within each target network possessed differential vulnerability to the disease process, leading those nodes to succumb sequentially according to their vulnerability. These mechanistic considerations raise the question of whether neurodegenerative diseases should be considered primary diseases of networks. Alternatively, networks might be damaged and disrupted in these illnesses without representing the most relevant primary target. One ecumenical framework might suggest that these diseases begin by targeting selectively vulnerable, region-specific neuron classes, such that early-stage disease is best considered a primary "neuron-opathy". Next, the disease may spread within local microcircuitry, producing accentuated damage within the site of initial injury. Long-range disease spread, during a next phase, might be uniquely constrained by the long-range connectivity profile of the early-affected neurons and microcircuits, such that later-stage disease is most accurately regarded as a "network-opathy" and will require or benefit from treatments that target mechanisms of network-based disease propagation.

The analysis of functional networks is a multi-step procedure, in which methodological choices and assumptions must be made. The choice of the post-processing techniques such as artifact reduction, filtering, normalization, and nuisance variable regression can influence the results. Both ICA and seed-based analysis of fMRI data have technical and practical limitations that remain to be addressed and have been outlined in a recent review.[135] Similarly, graph theoretical network investigation requires methodological decisions that can bias outcomes and conclusions. For example, appropriate statistical thresholding for network definition and extraction remains a critical issue for this approach.[14] In addition, it is important to recognize that the spatial resolution of present EEG/MEG recording techniques poses limitations on the measurement of deep brain neuronal activity and therefore on the interpretation of the results.[33] Finally, data about the sensitivity, specificity and reliability of task-free fMRI and EEG/MEG data are still limited.[136] However, despite these important limitations, recent brain connectivity studies using different recording techniques and analytical approaches show converging results,[137] suggesting that a more cohesive view of brain (dys)function in dementia may arise from the study of networks.

In broad terms, the study of functional network disruption in the degenerative dementias is in its infancy. Some conditions, such as AD, have been widely investigated with the described approaches. Other illnesses, such as PDD and DLB, as well as FTD language variants, largely remain to be explored. In PD and DLB, a disease-specific ICA networks

has not yet been identified with task-free fMRI , but recent work suggests a link to a basal ganglia network, anti-correlated with the DMN, which might be affected in these disorders.[123] Similarly, graph theoretical approaches may be used to assess functional changes in the PD spectrum. In addition, novel and more sophisticated approaches such as Bayesian network modelling may provide additional markers of connectivity by assessing causal relationships between nodes. Preliminary findings from the analysis of DMN with this method in AD look promising.[138]

In the coming years, technical improvements will help refine the topography of network degeneration. In addition, a complete understanding of network organization will require knowledge of how brain structure influences brain function, and *vice versa*. Strictly speaking, functional connectivity is unrelated to anatomy, i.e. functionally connected regions may show no direct structural connection, although the presence of structural connectivity generally implies functional connectivity.[139,140] For some brain regions, a functional connection might be established by intermediate regions or through a common source that drives activity in both regions. Efforts are under way to integrate structural and functional connectivity into a common framework. Important advances are expected from a recently funded $40M NIH project, which aims to identify the brain network architecture by using advanced diffusion imaging with fMRI and EEG/MEG recordings (The Human Connectome Project; http://www.humanconnectomeproject.org/).

How might increasing focus on functional brain networks lead to more effective dementia therapies? The first hope relates to patient categorization, and AD provides an illustrative example. Among healthy older persons without cognitive impairment, high levels of brain Aβ are suspected to represent preclinical AD.[141] Pinpointing presymptomatic, Aβ-associated network disruption, as reported in several recent studies,[142,143] might identify a subgroup most likely to benefit from a disease-modifying pharmacological treatment. Similarly, network analysis may provide sensitive markers of preclinical FTD (e.g., in gene mutation carriers) and help to distinguish patients on the PD-DLB spectrum. Other approaches may seek to recalibrate networks directly. Phase I trials of deep brain and transcranial magnetic stimulation targeting cognitive circuits have shown improvement of network-wide metabolic function or cognitive function in patients with AD.[144,145] Finally, task-free fMRI and neurophysiological methods provide attractive candidates for longitudinal, disease-monitoring biomarkers due to the safe and repeatable nature of these techniques. Whether these methods will prove successful in detecting and monitoring clinical change is a question that awaits future studies. In light of cross-sectional correlations between network connectivity strength and clinical severity,[58,59] cautious optimism seems justified.

Search strategy and selection criteria

References for this Review were identified through searches of PubMed with the search terms "network", "network dysfunction", "connectivity", "resting state functional MRI", "electroencephalography, "magnetoencephalography", "diffusion tensor imaging", "tractography", "dementia", "neurodegenerative disorders", "frontotemporal dementia", "Alzheimer", "mild cognitive impairment", "Parkinson", "Lewy bodies dementia", "stroke", "tumour" from 1986 until June, 2011. In addition, articles were identified through searches of the references of articles. Only papers published in English were reviewed. The final list of publications was selected by the authors on the basis of relevance to the topic.

REFERENCES

1. Taylor JP, Hardy J, Fischbeck KH. Toxic proteins in neurodegenerative disease. *Science* 2002; **296**: 1991-5.
2. Ikonomovic MD, Klunk WE, Abrahamson EE, et al. Post-mortem correlates of in vivo PiB-PET amyloid imaging in a typical case of Alzheimer's disease. *Brain* 2008; **131**: 1630–45.
3. Whitwell JL, Josephs KA, Murray ME, et al. MRI correlates of neurofibrillary tangle pathology at autopsy: a voxel-based morphometry study. *Neurology* 2008; **71**: 743-9.
4. McKhann GM, Knopman DS, Chertkow H, et al. The diagnosis of dementia due to Alzheimer's disease: Recommendations from the National Institute on Aging-Alzheimer's Association work-groups on diagnostic guidelines for Alzheimer's disease. *Alzheimers Dement* 2011; **7**: 263-9.
5. Albert MS, Dekosky ST, Dickson D, et al. The diagnosis of mild cognitive impairment due to Alzheimer's disease: Recommendations from the National Institute on Aging-Alzheimer's Association workgroups on diagnostic guidelines for Alzheimer's disease. *Alzheimers Dement* 2011; **7**: 270-9.
6. Seeley WW, Crawford R, Rascovsky K, et al. Frontal paralimbic network atrophy in very mild behavioral variant frontotemporal dementia. *Arch Neurol* 2008; **65**: 249-55.
7. Whitwell JL, Josephs KA. Voxel-based morphometry and its application to movement disorders. *Parkinsonism Relat Disord* 2007; **13** (Suppl 3): S406-16.
8. Whitwell JL, Weigand SD, Shiung MM, et al. Focal atrophy in dementia with Lewy bodies on MRI: a distinct pattern from Alzheimer's disease. *Brain* 2007; **130**: 708-19.
9. Du AT, Schuff N, Kramer JH, et al. Different regional patterns of cortical thinning in Alzheimer's disease and frontotemporal dementia. *Brain* 2007; **130**: 1159-66.
10. Frisoni GB, Fox NC, Jack CR Jr, Scheltens P, Thompson PM. The clinical use of structural MRI in Alzheimer disease. *Nat Rev Neurol* 2010; **6**: 67-77.
11. Alladi S, Xuereb J, Bak T, et al. Focal cortical presentations of Alzheimer's disease. *Brain* 2007; **130**: 2636-45.
12. Sporns O. The human connectome: a complex network. *Ann N Y Acad Sci* 2011; **1224**: 109-25.
13. Stam CJ. Use of magnetoencephalography (MEG) to study functional brain networks in neurodegenerative disorders. *J Neurol Sci* 2010; **289**: 128-34.
14. Bullmore E, Sporns O. Complex brain networks: graph theoretical analysis of structural and functional systems. *Nat Rev Neurosci* 2009; **10**: 186-98.

15. Zhang D, Raichle ME. Disease and the brain's dark energy. *Nat Rev Neurol* 2010; **6**: 15-28.
16. Sperling RA, Dickerson BC, Pihlajamaki M, et al. Functional alterations in memory networks in early Alzheimer's disease. *Neuromolecular Med* 2010; **12**: 27-43.
17. Bokde AL, Ewers M, Hampel H. Assessing neuronal networks: understanding Alzheimer's disease. *Prog Neurobiol* 2009; **89**: 125-33.
18. Sorg C, Riedl V, Perneczky R, Kurz A, Wohlschläger AM. Impact of Alzheimer's disease on the functional connectivity of spontaneous brain activity. *Curr Alzheimer Res* 2009; **6**: 541-53.
19. Dickerson BC, Sperling RA. Large-scale functional brain network abnormalities in Alzheimer's disease: insights from functional neuroimaging. *Behav Neurol* 2009; **21**: 63-75.
20. Guye M, Bettus G, Bartolomei F, Cozzone PJ. Graph theoretical analysis of structural and functional connectivity MRI in normal and pathological brain networks. *MAGMA* 2010; **23**: 409-21.
21. Dickerson BC. Advances in functional magnetic resonance imaging: technology and clinical applications. *Neurotherapeutics* 2007; **4**: 360-70.
22. He Y, Chen Z, Evans A. Structural insights into aberrant topological patterns of large-scale cortical networks in Alzheimer's disease. *J Neurosci* 2008; **28**: 4756-66.
23. Yao Z, Zhang Y, Lin L, Zhou Y, Xu C, Jiang T; Alzheimer's Disease Neuroimaging Initiative. Abnormal cortical networks in mild cognitive impairment and Alzheimer's disease. *PLoS Comput Biol* 2010; **6**: e1001006. doi:10.1371/journal.pcbi.1001006.
24. Fox MD, Raichle ME. Spontaneous fluctuations in brain activity observed with functional magnetic resonance imaging. *Nat Rev Neurosci* 2007; **8**: 700-11.
25. Beckmann CF, DeLuca M, Devlin JT, Smith SM. Investigations into resting-state connectivity using independent component analysis. *Philos Trans R Soc Lond B Biol Sci* 2005; **360**: 1001-13.
26. Damoiseaux JS, Rombouts SA, Barkhof F, et al. Consistent resting-state networks across healthy subjects. *Proc Natl Acad Sci USA* 2006; **103**: 13848-53.
27. Buckner RL, Andrews-Hanna JR, Schacter DL. The brain's default network: anatomy, function, and relevance to disease. *Ann N Y Acad Sci* 2008; **1124**: 1-38.
28. Seeley WW, Menon V, Schatzberg AF, et al. Dissociable intrinsic connectivity networks for salience processing and executive control. *J Neurosci* 2007; **27**: 2349-56.
29. Fox MD, Snyder AZ, Vincent JL, Corbetta M, Van Essen DC, Raichle ME. The human brain is intrinsically organized into dynamic, anticorrelated functional networks. *Proc Natl Acad Sci USA* 2005; **102**: 9673-8.
30. Smith SM, Fox PT, Miller KL, et al. Correspondence of the brain's functional architecture during activation and rest. *Proc Natl Acad Sci USA* 2009; **106**, 13040–5.
31. Hampson M, Tokoglu F, Sun Z, et al. Connectivity-behavior analysis reveals that functional connectivity between left BA39 and Broca's area varies with reading ability. *Neuroimage* 2006; **31**: 513-9.
32. Varela F, Lachaux JP, Rodriguez E, Martinerie J. The brainweb: phase synchronization and large-scale integration. *Nat Rev Neurosci* 2001; **2**: 229-39.
33. Ioannides AA. Magnetoencephalography as a research tool in neuroscience: state of the art. *Neuroscientist* 2006; **12**: 524-44.
34. Nunez PL, Srinivasan R, Westdorp AF, et al. EEG coherency. I: Statistics, reference electrode, volume conduction, Laplacians, cortical imaging, and interpretation at multiple scales. *Electroencephalogr Clin Neurophysiol* 1997; **103**: 499-515.
35. Johansen-Berg H, Behrens TEJ. Diffusion MRI: From Quantitative Measurement to In vivo Neuroanatomy. Elsevier, London, 2009.

36. Catani M, Thiebaut de Schotten M. A diffusion tensor imaging tractography atlas for virtual in vivo dissections. *Cortex* 2008; **44**: 1105-32.
37. Reijneveld JC, Ponten SC, Berendse HW, Stam CJ. The application of graph theoretical analysis to complex networks in the brain. *Clin Neurophysiol* 2007; **118**: 2317-31.
38. Watts DJ, Strogatz SH. Collective dynamics of 'small-world' networks. *Nature* 1998; **393**: 440-2.
39. Bassett DS, Bullmore E. Small-world brain networks. *Neuroscientist* 2006; **12**: 512-23.
40. Ferrarini L, Veer IM, Baerends E, et al. Hierarchical functional modularity in the resting-state human brain. *Hum Brain Mapp* 2009; **30**: 2220-31.
41. Power JD, Fair DA, Schlaggar BL, Petersen SE. The development of human functional brain networks. *Neuron* 2010; **67**: 735-48.
42. Meunier D, Achard S, Morcom A, Bullmore E. Age-related changes in modular organization of human brain functional networks. *Neuroimage* 2009; **44**: 715-23.
43. van den Heuvel MP, Stam CJ, Kahn RS, Hulshoff Pol HE. Efficiency of functional brain networks and intellectual performance. *J Neurosci* 2009; **29**: 7619-24.
44. Wen W, Zhu W, He Y, et al. Discrete neuroanatomical networks are associated with specific cognitive abilities in old age. *J Neurosci* 2011; **31**: 1204-12.
45. Bosma I, Reijneveld JC, Klein M, et al. Disturbed functional brain networks and neurocognitive function in low-grade glioma patients: a graph theoretical analysis of resting-state MEG. *Nonlinear Biomed Phys* 2009; **3**: 9. doi:10.1186/1753-4631-3-9.
46. Wang L, Yu C, Chen H, et al. Dynamic functional reorganization of the motor execution network after stroke. *Brain* 2010; **133**: 1224-38.
47. Castellanos NP, Paúl N, Ordóñez VE, et al. Reorganization of functional connectivity as a correlate of cognitive recovery in acquired brain injury. *Brain* 2010; **133**: 2365-81.
48. Ponten SC, Bartolomei F, Stam CJ. Small-world networks and epilepsy: graph theoretical analysis of intracerebrally recorded mesial temporal lobe seizures. *Clin Neurophysiol* 2007; **118**: 918-27.
49. Alstott J, Breakspear M, Hagmann P, Cammoun L, Sporns O. Modeling the impact of lesions in the human brain. *PLoS Comput Biol* 2009; **5**: e1000408. doi:10.1371/journal.pcbi.1000408.
50. Delbeuck X, Van der Linden M, Collette F. Alzheimer's disease as a disconnection syndrome? *Neuropsychol Rev* 2003; **13**: 79-92.
51. Saper CB, Wainer BH, German DC. Axonal and transneuronal transport in the transmission of neurological disease: potential role in system degenerations, including Alzheimer's disease. *Neuroscience* 1987; **23**: 389-98.
52. Thal DR, Rüb U, Orantes M, Braak H. Phases of Ab-deposition in the human brain and its relevance for the development of AD. *Neurology* 2002; **58**: 1791-800.
53. Braak H, Braak E. Neuropathological stageing of Alzheimer-related changes. *Acta Neuropathol* 1991; **82**: 239–59.
54. Braak H, Del Tredici K. The pathological process underlying Alzheimer's disease in individuals under thirty. *Acta Neuropathol* 2011; **121**: 171-81.
55. Mormino EC, Kluth JT, Madison CM, et al. Episodic memory loss is related to hippocampal-mediated beta-amyloid deposition in elderly subjects. *Brain* 2009; **132**: 1310-23.
56. Buckner RL, Sepulcre J, Talukdar T, et al. Cortical hubs revealed by intrinsic functional connectivity: mapping, assessment of stability, and relation to Alzheimer's disease. *J Neurosci* 2009; **29**: 1860-73.
57. Greicius MD, Srivastava G, Reiss AL, Menon V. Default-mode network activity distinguishes Alzheimer's disease from healthy aging: evidence from functional MRI. *Proc Natl Acad Sci USA* 2004; **101**: 4637-42.

58. Zhou J, Greicius MD, Gennatas ED, et al. Divergent network connectivity changes in behavioural variant frontotemporal dementia and Alzheimer's disease. *Brain* 2010; **133**: 1352-67.
59. Zhang HY, Wang SJ, Liu B, et al. Resting brain connectivity: changes during the progress of Alzheimer disease. *Radiology* 2010; **256**: 598-606.
60. Wang L, Zang Y, He Y, et al. Changes in hippocampal connectivity in the early stages of Alzheimer's disease: evidence from resting state fMRI. *Neuroimage* 2006; **31**: 496-504.
61. Zhang HY, Wang SJ, Xing J, et al. Detection of PCC functional connectivity characteristics in resting-state fMRI in mild Alzheimer's disease. *Behav Brain Res* 2009; **197**: 103-8.
62. Sorg C, Riedl V, Mühlau M, et al. Selective changes of resting-state networks in individuals at risk for Alzheimer's disease. *Proc Natl Acad Sci U S A* 2007; **104**: 18760-5.
63. Qi Z, Wu X, Wang Z, et al. Impairment and compensation coexist in amnestic MCI default mode network. *Neuroimage* 2010; **50**: 48-55.
64. Gili T, Cercignani M, Serra L, et al. Regional brain atrophy and functional disconnection across Alzheimer's disease evolution. *J Neurol Neurosurg Psychiatry* 2011; **82**: 58-66.
65. Pievani M, Agosta F, Pagani E, et al. Assessment of white matter tract damage in mild cognitive impairment and Alzheimer's disease. *Hum Brain Mapp* 2010; **31**: 1862-75.
66. Zhang Y, Schuff N, Du AT, et al. White matter damage in frontotemporal dementia and Alzheimer's disease measured by diffusion MRI. *Brain* 2009; **132**: 2579-92.
67. Acosta-Cabronero J, Williams GB, Pengas G, Nestor PJ. Absolute diffusivities define the landscape of white matter degeneration in Alzheimer's disease. *Brain* 2010; **133**: 529-39.
68. Sexton CE, Kalu UG, Filippini N, Mackay CE, Ebmeier KP. A meta-analysis of diffusion tensor imaging in mild cognitive impairment and Alzheimer's disease. *Neurobiol Aging* 2010; published online Jul 7.
69. Stam CJ, Montez T, Jones BF, et al. Disturbed fluctuations of resting state EEG synchronization in Alzheimer's disease. *Clin Neurophysiol* 2005; **116**: 708-15.
70. Babiloni C, Ferri R, Binetti G, et al. Fronto-parietal coupling of brain rhythms in mild cognitive impairment: a multicentric EEG study. *Brain Res Bull* 2006; **69**: 63-73.
71. Stam CJ, Jones BF, Manshanden I, et al. Magnetoencephalographic evaluation of resting-state functional connectivity in Alzheimer's disease. *Neuroimage* 2006; **32**: 1335-44.
72. Mantini D, Perrucci MG, Del Gratta C, Romani GL, Corbetta M. Electrophysiological signatures of resting state networks in the human brain. *Proc Natl Acad Sci U S A* 2007; **104**: 13170-5.
73. Jann K, Kottlow M, Dierks T, Boesch C, Koenig T. Topographic electrophysiological signatures of FMRI Resting State Networks. *PLoS One* 2010; **5**: e12945. doi:10.1371/journal.pone.0012945.
74. Petrella JR, Sheldon FC, Prince SE, Calhoun VD, Doraiswamy PM. Default mode network connectivity in stable vs progressive mild cognitive impairment. *Neurology* 2011; **76**: 511-7.
75. Stam CJ, de Haan W, Daffertshofer A, et al. Graph theoretical analysis of magnetoencephalographic functional connectivity in Alzheimer's disease. *Brain* 2009; **132**: 213-24.
76. Supekar K, Menon V, Rubin D, Musen M, Greicius MD. Network analysis of intrinsic functional brain connectivity in Alzheimer's disease. *PloS Comput Biol* 2008; **4**: e1000100. doi:10.1371/journal.pcbi.1000100.
77. Sanz-Arigita EJ, Schoonheim MM, Damoiseaux JS, et al. Loss of 'small-world' networks in Alzheimer's disease: graph analysis of FMRI resting-state functional connectivity. *PLoS One* 2010; **5**: e13788. doi:10.1371/journal.pone.0013788.
78. deHaan W, Pijnenburg YA, Strijers RL, et al. Functional neural network analysis in frontotemporal dementia and Alzheimer's disease using EEG and graph theory. *BMC Neurosci* 2009; **10**: 101. doi:10.1186/1471-2202-10-101.

79. Lo CY, Wang PN, Chou KH, Wang J, He Y, Lin CP. Diffusion tensor tractography reveals abnormal topological organization in structural cortical networks in Alzheimer's disease. *J Neurosci* 2010; **30**: 16876-85.
80. Mackenzie IR, Rademakers R, Neumann M. TDP-43 and FUS in amyotrophic lateral sclerosis and frontotemporal dementia. *Lancet Neurol* 2010; **9**: 995-1007.
81. Gorno-Tempini ML, Hillis AE, Weintraub S, et al. Classification of primary progressive aphasia and its variants. *Neurology* 2011; **76**: 1006-14.
82. Josephs KA, Hodges JR, Snowden JS, et al. Neuropathological background of phenotypical variability in frontotemporal dementia. *Acta Neuropathol* 2011; published online May 26.
83. Rohrer JD, Geser F, Zhou J, et al. TDP-43 subtypes are associated with distinct atrophy patterns in frontotemporal dementia. *Neurology* 2010; **75**: 2204-11.
84. Seeley WW, Crawford RK, Zhou J, Miller BL, Greicius MD. Neurodegenerative diseases target large-scale human brain networks. *Neuron* 2009; **62**: 42-52.
85. Seeley WW, Allman JM, Carlin DA, et al. Divergent social functioning in behavioral variant frontotemporal dementia and Alzheimer disease: reciprocal networks and neuronal evolution. *Alzheimer Dis Assoc Disord* 2007; **21**: S50-7.
86. Whitwell JL, Avula R, Senjem ML, et al. Gray and white matter water diffusion in the syndromic variants of frontotemporal dementia. *Neurology* 2010; **74**: 1279-87.
87. Agosta F, Henry RG, Migliaccio R, et al. Language networks in semantic dementia. *Brain* 2010; **133**: 286-99.
88. Pijnenburg YA, Strijers RL, Made YV, van der Flier WM, Scheltens P, Stam CJ. Investigation of resting-state EEG functional connectivity in frontotemporal lobar degeneration. *Clin Neurophysiol* 2008; **119**: 1732-8.
89. Rubinov M, Sporns O. Complex network measures of brain connectivity: uses and interpretations. *Neuroimage* 2010; **52**: 1059-69.
90. Whitwell JL, Jack CR Jr, Parisi JE, et al. Imaging Signatures of Molecular Pathology in Behavioral Variant Frontotemporal Dementia. *J Mol Neurosci* 2011; published online May 10.
91. Josephs KA, Whitwell JL, Knopman DS, et al. Two distinct subtypes of right temporal variant frontotemporal dementia. *Neurology* 2009; **73** : 1443-50.
92. Braak H, Del Tredici K, Rüb U, de Vos RA, Jansen Steur EN, Braak E. Staging of brain pathology related to sporadic Parkinson's disease. *Neurobiol Aging* 2003; **24**: 197-211.
93. McKeith IG, Dickson DW, Lowe J, et al. Diagnosis and management of dementia with Lewy bodies: third report of the DLB Consortium. *Neurology* 2005; **65**: 1863-72.
94. Alexander GE, DeLong MR, Strick PL. Parallel organization of functionally segregated circuits linking basal ganglia and cortex. *Annu Rev Neurosci* 1986; **9**: 357-81.
95. Wu T, Long X, Wang L, et al. Functional connectivity of cortical motor areas in the resting state in Parkinson's disease. *Hum Brain Mapp* 2010; published online Aug 25. doi:10.1002/hbm.21118.
96. Helmich RC, Derikx LC, Bakker M, Scheeringa R, Bloem BR, Toni I. Spatial remapping of cortico-striatal connectivity in Parkinson's disease. *Cereb Cor*tex 2010; **20**: 1175-86.
97. Baudrexel S, Witte T, Seifried C, et al. Resting state fMRI reveals increased subthalamic nucleus-motor cortex connectivity in Parkinson's disease. *Neuroimage* 2011; **55**: 1728-38.
98. Kwak Y, Peltier S, Bohnen NI, Müller ML, Dayalu P, Seidler RD. Altered resting state cortico-striatal connectivity in mild to moderate stage Parkinson's disease. *Front Syst Neurosci* 2010; **4**: 143. doi:10.3389/fnsys.2010.00143.
99. Litvak V, Jha A, Eusebio A, et al. Resting oscillatory cortico-subthalamic connectivity in patients with Parkinson's disease. *Brain* 2011; **134**: 359-74.

100. Silberstein P, Pogosyan A, Kühn AA, et al. Cortico-cortical coupling in Parkinson's disease and its modulation by therapy. *Brain* 2005; **128**: 1277-91.
101. Stoffers D, Bosboom JL, Deijen JB, Wolters ECh, Stam CJ, Berendse HW. Increased cortico-cortical functional connectivity in early-stage Parkinson's disease: an MEG study. *Neuroimage* 2008; **41**: 212-22.
102. Bosboom JL, Stoffers D, Wolters ECh, Stam CJ, Berendse HW. MEG resting state functional connectivity in Parkinson's disease related dementia. *J Neural Transm* 2009; **116**: 193-202.
103. Franciotti R, Iacono D, Della Penna S, et al. Cortical rhythms reactivity in AD, LBD and normal subjects: a quantitative MEG study. *Neurobiol Aging* 2006; **27**: 1100-9.
104. Andersson M, Hansson O, Minthon L, Rosén I, Londos E. Electroencephalogram variability in dementia with lewy bodies, Alzheimer's disease and controls. *Dement Geriatr Cogn Disord* 2008; **26**: 284-90.
105. Kai T, Asai Y, Sakuma K, Koeda T, Nakashima K. Quantitative electroencephalogram analysis in dementia with Lewy bodies and Alzheimer's disease. *J Neurol Sci* 2005; **237**: 89-95.
106. Galvin JE, Price JL, Yan Z, Morris JC, Sheline YI. Resting bold fMRI differentiates dementia with Lewy bodies vs Alzheimer disease. *Neurology* 2011; **76**: 1797-803.
107. Péran P, Cherubini A, Assogna F, et al. Magnetic resonance imaging markers of Parkinson's disease nigrostriatal signature. *Brain* 2010; **133**: 3423-33.
108. Vaillancourt DE, Spraker MB, Prodoehl J, et al. High-resolution diffusion tensor imaging in the substantia nigra of de novo Parkinson disease. *Neurology* 2009; **72**: 1378-84.
109. Yoshikawa K, Nakata Y, Yamada K, Nakagawa M. Early pathological changes in the parkinsonian brain demonstrated by diffusion tensor MRI. *J Neurol Neurosurg Psychiatry* 2004; **75**: 481-4.
110. Menke RA, Scholz J, Miller KL, et al. MRI characteristics of the substantia nigra in Parkinson's disease: a combined quantitative T1 and DTI study. *Neuroimage* 2009; **47**: 435-41.
111. Gattellaro G, Minati L, Grisoli M, et al. White matter involvement in idiopathic Parkinson disease: a diffusion tensor imaging study. *AJNR Am J Neuroradiol* 2009; **30**: 1222-6.
112. Karagulle Kendi AT, Lehericy S, Luciana M, Ugurbil K, Tuite P. Altered diffusion in the frontal lobe in Parkinson disease. *AJNR Am J Neuroradiol* 2008; **29**: 501-5.
113. Zhang K, Yu C, Zhang Y, et al. Voxel-based analysis of diffusion tensor indices in the brain in patients with Parkinson's disease. *Eur J Radiol* 2011; **77**: 269-73.
114. Lee JE, Park HJ, Park B, et al. A comparative analysis of cognitive profiles and white-matter alterations using voxel-based diffusion tensor imaging between patients with Parkinson's disease dementia and dementia with Lewy bodies. *J Neurol Neurosurg Psychiatry* 2010; **81**: 320-6.
115. Matsui H, Nishinaka K, Oda M, Niikawa H, Kubori T, Udaka F. Dementia in Parkinson's disease: diffusion tensor imaging. *Acta Neurol Scand* 2007; **116**: 177-81.
116. Kantarci K, Avula R, Senjem ML, et al. Dementia with Lewy bodies and Alzheimer disease: neurodegenerative patterns characterized by DTI. *Neurology* 2010; **74**: 1814-21.
117. Ota M, Sato N, Ogawa M, et al. Degeneration of dementia with Lewy bodies measured by diffusion tensor imaging. *NMR Biomed* 2009; **22**: 280-4.
118. Kiuchi K, Morikawa M, Taoka T, et al. White matter changes in dementia with Lewy bodies and Alzheimer's disease: A tractography-based study. *J Psychiatr Res* 2011; published online Feb 9.
119. Burack MA, Hartlein J, Flores HP, Taylor-Reinwald L, Perlmutter JS, Cairns NJ. In vivo amyloid imaging in autopsy-confirmed Parkinson disease with dementia. *Neurology* 2010; **74**: 77-84.
120. Wu T, Wang L, Chen Y, Zhao C, Li K, Chan P. Changes of functional connectivity of the motor network in the resting state in Parkinson's disease. *Neurosci Lett* 2009; **460**: 6-10.

121. Skidmore F, Korenkevych D, Liu Y, He G, Bullmore E, Pardalos PM. Connectivity brain networks based on wavelet correlation analysis in Parkinson fMRI data. *Neurosci Lett* 2011; **499**: 47-51.
122. Andrews-Hanna JR, Snyder AZ, Vincent JL, et al. Disruption of large-scale brain systems in advanced aging. *Neuron* 2007; **56**: 924-35.
123. Robinson S, Basso G, Soldati N, et al. A resting state network in the motor control circuit of the basal ganglia. *BMC Neurosci* 2009; **10**: 137. doi:10.1186/1471-2202-10-137.
124. Gomperts SN, Rentz DM, Moran E, et al. Imaging amyloid deposition in Lewy body diseases. *Neurology* 2008; **71**: 903-10.
125. Achard S, Salvador R, Whitcher B, Suckling J, Bullmore E. A resilient, low-frequency, small-world human brain functional network with highly connected association cortical hubs. *J Neurosci* 2006; **26**: 63-72.
126. Mesulam MM. From sensation to cognition. *Brain* 1998; **121**: 1013-52.
127. Frost B, Diamond MI. Prion-like mechanisms in neurodegenerative diseases. *Nat Rev Neurosci* 2010; **11**: 155-9.
128. Clavaguera F, Bolmont T, Crowther RA, et al. Transmission and spreading of tauopathy in transgenic mouse brain. *Nat Cell Biol* 2009; **11**: 909-13.
129. Eisele YS, Obermüller U, Heilbronner G, et al. Peripherally applied Abeta-containing inoculates induce cerebral beta-amyloidosis. *Science* 2010; **330**: 980-2.
130. Angot E, Steiner JA, Hansen C, Li JY, Brundin P. Are synucleinopathies prion-like disorders? *Lancet Neurol* 2010; **9**: 1128-38.
131. Palop JJ, Chin J, Roberson ED, et al. Aberrant excitatory neuronal activity and compensatory remodeling of inhibitory hippocampal circuits in mouse models of Alzheimer's disease. *Neuron* 2007; **55**: 697–711.
132. Wu C, Cui B, He L, Chen L, Mobley WC. The coming of age of axonal neurotrophin signaling endosomes. *J Proteomics* 2009; **72**: 46-55.
133. Mesulam MM. Neuroplasticity failure in Alzheimer's disease: bridging the gap between plaques and tangles. *Neuron* 1999; **24**: 521-9.
134. Buckner RL, Snyder AZ, Shannon BJ, et al. Molecular, structural, and functional characterization of Alzheimer's disease: evidence for a relationship between default activity, amyloid, and memory. *J Neurosci* 2005; **25**: 7709-17.
135. Cole DM, Smith SM, Beckmann CF. Advances and pitfalls in the analysis and interpretation of resting-state FMRI data. *Front Syst Neurosci* 2010; **4**: 8. doi:10.3389/fnsys.2010.00008.
136. Zuo XN, Kelly C, Adelstein JS, Klein DF, Castellanos FX, Milham MP. Reliable intrinsic connectivity networks: test-retest evaluation using ICA and dual regression approach. *Neuroimage* 2010; **49**: 2163-77.
137. Stevenson IH, Körding KP. On the similarity of functional connectivity between neurons estimated across timescales. *PLoS One* 2010; **5**: e9206. doi:10.1371/journal.pone.0009206.
138. Wu X, Li R, Fleisher AS, Reiman EM, Guan X, Zhang Y, Chen K, Yao L. Altered default mode network connectivity in alzheimer's disease-A resting functional MRI and bayesian network study. *Hum Brain Mapp* 2011; published online Jan 21. doi:10.1002/hbm.21153.
139. Honey CJ, Sporns O, Cammoun L, et al. Predicting human resting-state functional connectivity from structural connectivity. *Proc Natl Acad Sci USA* 2009; **106**: 2035-40.
140. Damoiseaux JS, Greicius MD. Greater than the sum of its parts: a review of studies combining structural connectivity and resting-state functional connectivity. *Brain Struct Funct* 2009; **213**: 525-33.

141. Pike KE, Savage G, Villemagne VL, et al. Beta-amyloid imaging and memory in non-demented individuals: evidence for preclinical Alzheimer's disease. *Brain* 2007; **130**: 2837-44.
142. Sperling RA, Laviolette PS, O'Keefe K, et al. Amyloid deposition is associated with impaired default network function in older persons without dementia. *Neuron* 2009; **63**: 178–88.
143. Drzezga A, Becker JA, Van Dijk KR, et al. Neuronal dysfunction and disconnection of cortical hubs in non-demented subjects with elevated amyloid burden. *Brain* 2011; **134**: 1635-46.
144. Laxton AW, Tang-Wai DF, McAndrews MP, et al. A phase I trial of deep brain stimulation of memory circuits in Alzheimer's disease. *Ann Neurol* 2010; **68**: 521-34.
145. Cotelli M, Calabria M, Manenti R, et al. Improved language performance in Alzheimer disease following brain stimulation. *J Neurol Neurosurg Psychiatry* 2011; **82**: 794-7.

Panel 1: Glossary of basic network concepts

Network
A mathematical representation of a complex system made of a finite number of nodes and links. Many real-world complex systems, such as biological, social, and neuronal systems, can be modelled as networks.

Node
A basic network element.

Link (or edge)
A connection between two nodes.

Neural network
A complex system whose node and links are represented by neurons and their connections. Neural networks can be defined at many scales: microscopic (neurons and synapses), meso-scale (neural assembles and circuitry), and macro-scale (anatomical regions and fibre tracts). Connections can be either structural or functional. Node choice largely depends on the technique used. Common choices for imaging and neurophysiological techniques are grey-matter regions and electrodes.

Functional connectivity
The presence of functional connections between nodes (eg, synchronous neuronal oscillations). Functionally connected nodes might have no direct physical connection.

Structural connectivity
The presence of physical connections between nodes (eg, fibre tracts).

Module
Subset of network nodes with high internal connectivity.

Panel 2: Glossary of graph theory terms

Graph
A visual representation of a network.

Graph theory
A branch of mathematics investigating network characteristics such as topology (ie, network structure), cost, efficiency, and robustness.

Degree
The total number of connections (edges) of a node. Can be averaged over the whole network to obtain a global measure of connection density or so-called wiring cost.

Hub
A highly connected node (ie, with a high degree). These nodes are relevant for efficient network communication, and damage to these nodes might be especially disruptive for network integrity.

Clustering coefficient
The interconnectedness of a node's immediate neighbours (note that neighbouring nodes need not be anatomically proximal). Clustering coefficient values can be averaged over a region to obtain a measure of local connectivity.

Path length
The travel distance (number of intermediate links) from one node to another. Path lengths between all nodes in a network can be averaged to obtain the characteristic path length, which is a measure of global connectivity.

Small-world network
A network topology characterised by a high clustering coeffi cient coupled with a low characteristic path length. Investigators presume this network structure is optimum for efficient communication between regions, and it can be found in many real-world systems, including neural networks.

Random network
A network topology characterised by a lower clustering coeffi cient and a smaller characteristic path length than small-world networks.

Efficiency
The inverse of the characteristic path length, which is thought of as a measure of information processing capability.

Robustness
Resilience of a network against damage to nodes or links. This property is infl uenced by factors such as the degree, clustering coefficient, and the presence of hubs.

Modularity
Extent to which a network can be described as a set of interconnected subnetworks (modules). Modular networks are often efficient and robust, and many real-world networks (including neural networks) can be thought of as modular.

Node 9

Summary

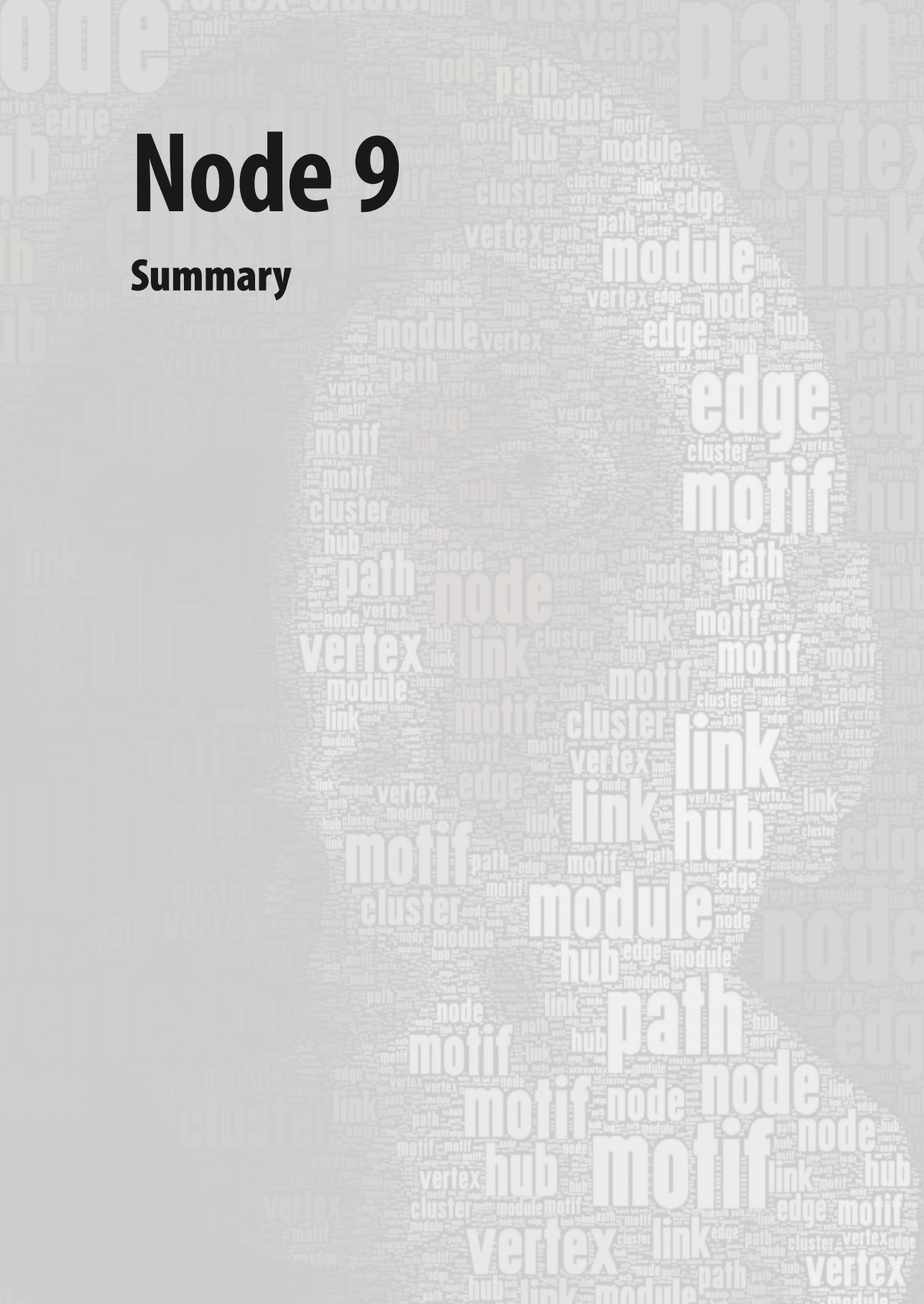

SUMMARY

In **module 1** Alzheimer's disease (AD), the most prevalent type of neurodegenerative dementia, is introduced as a rapidly increasing problem in our aging population. A thorough understanding of the disease mechanism is lacking, and no effective cure exists. An essential aspect of cognitive processing is particularly poorly understood: the role of brain *dynamics*. Greater knowledge of how cognitive processes are coordinated in the brain might clarify the complex relation between observed structural brain damage and clinical symptoms in AD.

The first step is to capture and describe large-scale brain dynamics in a reliable way. To provide a short background, basic neurophysiologic principles are outlined, ranging from single neuron action potentials to synchronization between large groups of neurons. The concept of functional connectivity is introduced as a method to describe interaction between brain regions, and EEG & MEG are discussed as neurophysiological data acquisition techniques. A short, focused overview of the existing neurophysiological literature in AD is provided. When describing large-scale brain dynamics, we find out that the brain is a complex dynamical system. Complex network theory is introduced as a method to interpret complex systems, and to explain how changes in network structure relate to changes in network function. It is argued that the application of concepts from network theory to neuroscientific patient data could help to better relate both structural and dynamical brain changes to cognitive symptoms.

To conclude this section, the aims and outline of this thesis are listed.

In **module 2**, we report that resting-state brain activity as measured by MEG relative power is altered in a wide range of frequencies and different cortical regions in AD. The overall observed diffuse slowing of brain activity is in agreement with existing EEG literature, and adds more detail by demonstrating the regional heterogeneity in dynamical changes. However, since this approach does not take into account interaction between different regions, increases and decreases are hard to interpret. A large-scale network perspective is desired.

Module 3 starts with a description of functional network structure in resting-state EEG data, and shows that different types of dementia lead to different types of network disturbance: both AD and FTD patients demonstrate a loss of balance between local and global network connectivity ('small-worldness'), but in opposite directions. This difference might reflect different underlying pathology, which could lead to useful diagnostic tests in the future. Next, an MEG study in AD patients is reported to show network disruption in more detail: again, a loss of small-world structure and a shift towards a more random network organization is observed. AD-related network damaged is also compared to two theoretical damage models: one of random damage, and one where highly connected hub regions are preferentially damaged. The last model resembles the damage in AD most, which suggests that hubs are especially vulnerable in AD. After

these demonstrations of local and global functional network damage, the third study in this section deals with an intermediate terrain where sub-networks or modules are investigated. In AD, a loss of modularity, a vulnerability of the parietal hub region, and a particular vulnerability of *inter*modular connections is found, which correlates with cognitive impairment. These studies illustrate a relevant relation between brain connectivity and impaired cognition.

Module 4 takes a different, more algebraic approach to describe network properties. Graph spectral analysis has proven its usefulness in other research areas, and has several methodological advantages compared to topological graph theory. With graph spectral techniques, we again detect large-scale network connectivity changes in AD, as well as differences in robustness and network synchronizability. Hub status of regions is examined again using eigenvector centrality, and the earlier reported hub status of the parietal region is confirmed.

The observed hub vulnerability in AD is an intriguing finding, and since a link between hub regions and amyloid deposition was reported, as well as a direct influence of excessive neuronal activity on amyloid deposition, we hypothesized that the high connectivity level of hubs requires a high level of activity, and that this chronic, high activity of hubs makes them susceptible to degeneration. In short, we speculated that dynamics might have a *causal* role in AD pathogenesis.

To test this hypothesis, a computational neural mass model that is based on realistic human brain topography and dynamics was employed. We demonstrate in **Module 5** that brain hubs are indeed the most active regions, and that when regions are damaged based on their level of activity, model-generated data shows many neurophysiological hallmarks of AD, such as oscillatory slowing and a loss of functional connectivity and functional network disruption. These findings suggest that excessive neuronal activity indeed plays a significant role in AD pathogenesis.

In this module a review of relevant recent literature discusses the important role of brain connectivity for our understanding of neurodegenerative dementias. Subsequently, the main outcomes of the studies in this thesis are summarized, and interpreted with regard to the original aims of this thesis and existing literature. This is followed by a discussion of the most relevant methodological considerations. In the final paragraphs, recommendations for future research are provided, and the section ends with a more personal view on the potential usefulness of the approach followed in this thesis.

Node 10

General discussion

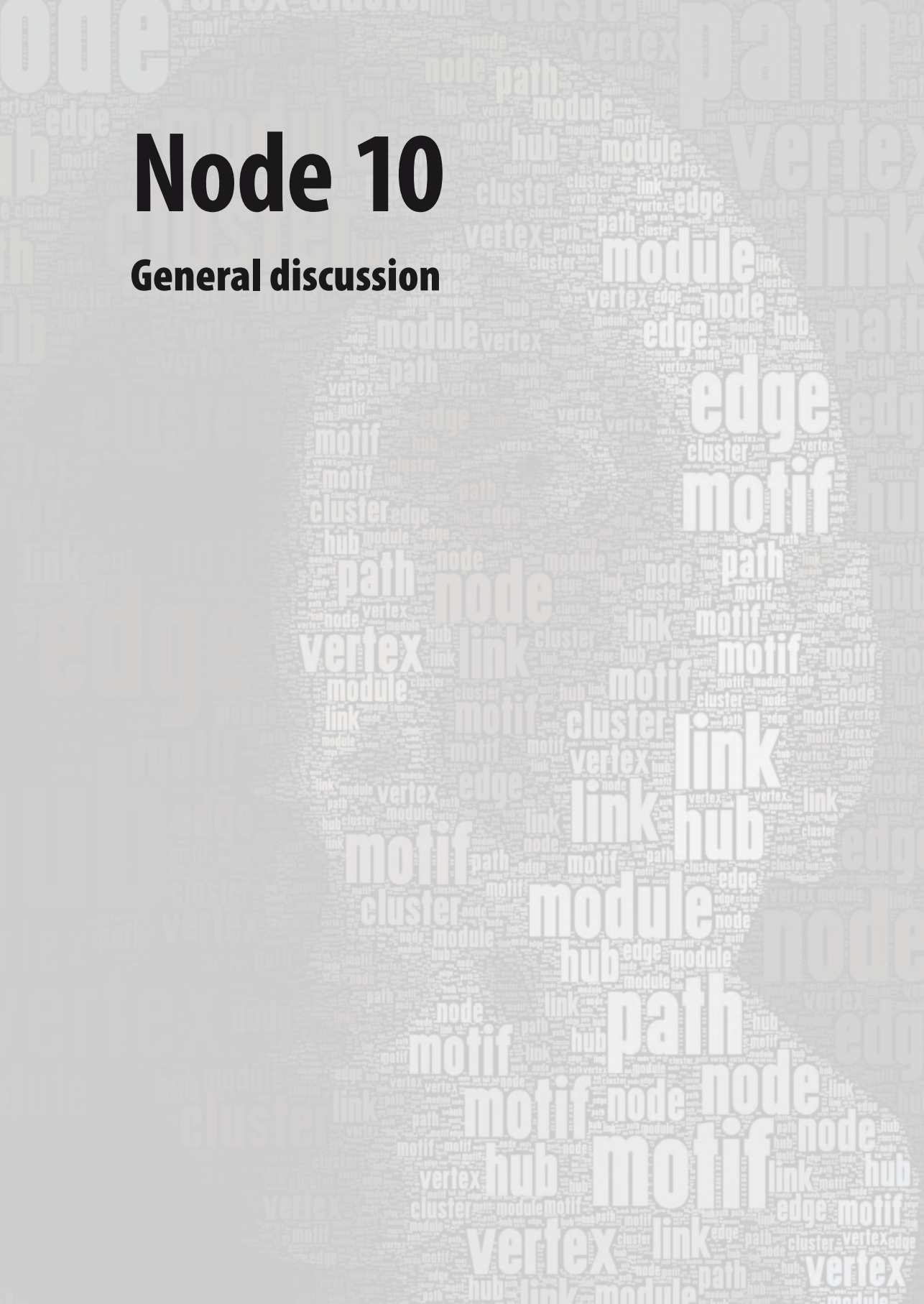

GENERAL DISCUSSION

Main findings

The main aim of this dissertation is to explore the role of cerebral functional network topology in Alzheimer's disease (AD). For this purpose, macro-scale functional network disruption in AD is described using neurophysiological data acquisition techniques (EEG/MEG) and concepts from modern network theory. Consequently, a relation between changes in network organization, cognitive status and structural damage is investigated. The overall conclusion of this thesis is that further examination the role of disturbed brain network activity and connectivity in dementia is significant: our study results suggest that this novel perspective will expand our understanding of cognitive disease mechanisms. In the following paragraphs, arguments for this conclusion will be discussed.

Key findings corresponding to the original aims of this thesis:

- Functional network topology is altered in AD at different scales: global network integrity decreases, communication between functional sub-networks or modules is disturbed, and highly connected network hub regions are especially vulnerable to damage. AD patients have a less robust and efficient system to maintain the fast and flexible brain dynamics that are required for cognitive processing. By representing a level between structural pathology and cognitive impairment, functional network analysis may also provide new clues about the disease mechanism itself.
- Diiferent forms of dementia (AD and FTD) show dissimilar functional network disruption, suggesting that network analysis can detect and discriminate different underlying pathophysiological mechanisms.
- Functional network integrity markers correlate with cognitive status as measured by neuropsychological testing, indicating the potential clinical relevance of altered functional network organization in dementia.
- Computational modeling results strongly support an activity-driven neurodegeneration hypothesis of AD, which could have major implications for future research, diagnostic and therapeutic strategies.

Factors considered important for evaluating the functional network approach in this thesis are explanatory power, practical feasibility and reliability of the analyses, as well as the ability to generate new hypotheses for future research. Therefore, this discussion is divided into three parts: first, an interpretation of functional network disruption in AD including a hypothesis about the disease mechanism is provided. Next, an overview is presented of the most relevant methodological choices and pitfalls. Finally, potential future directions are briefly outlined before reaching the final conclusive statements. While in the original articles most issues have been discussed in detail, here the key

aspects are highlighted in order to provide a more coherent overview of the value of graph theoretical functional network analysis in Alzheimer's disease.

Alzheimer's disease: system failure?

Functional network disruption at multiple scales

Graph theory is applied to brain networks of very different spatiotemporal resolutions and sizes [13,34,35]. These different levels of detail each offer an incomplete, limited perspective on the working human brain, but are all integrated into a single system [36-39]. The contribution of EEG and MEG to our understanding of this system is a description of fast, large-scale brain dynamics. While the temporal resolution of EEG and MEG is very high, its spatial resolution is less precise. However, it is unlikely that descriptions of individual neurons or small neuronal assemblies would be the best level of detail to appreciate the overall coordination of brain-wide distributed cognitive processes. Based on literature, meaningful cognition-related dynamics in the brain often span multiple brain regions, and take place in the order of milliseconds. Therefore, investigating the relation between neurophysiologic activity of large-scale cortical regions and cognitive performance seems a justified approach.

The main neurophysiological hallmark of AD found in literature is the diffuse, gradual slowing of oscillatory brain dynamics, expressed for example by changes in spectral power [5]. We show in Node 3 that there is a substantial regional heterogeneity in this oscillatory slowing: posterior regions are more strongly affected, and different frequency bands show different patterns, a finding that has been replicated in a recent EEG study [76]. Since we know that brain regions are not functionally isolated compartments, but highly integrated systems that influence each other, the observed heterogeneity in power change does not necessarily point to local characteristics, but probably also reflects interaction patterns within the whole system. Based on regional power analysis, it is impossible to discover which factor is the main cause of regional heterogeneity. We therefore need to explore *inter*regional communication (or functional connectivity) to shed more light on the reasons behind these changes in AD.

The loss of global and regional synchronization in AD, as expressed by several functional connectivity measures, confirms previous studies and indicates that interregional communication is changing as well [10,40]. Furthermore, frequency band-specific changes signify that functional connectivity is disturbed at various time scales in AD. Although interesting, the observed changes in functional connectivity are not self-explanatory. By describing connectivity disruption within the framework of network theory, AD-related changes in brain dynamics become more meaningful. To focus on disrupted network topology at different levels, we have opted to investigate network disruption at three

scales: global measures that describe overall network characteristics, intermediate measures that describe communities or sub-networks, and measures that describe individual node roles. Of course, these different network scales are closely related, and without any of them an incomplete picture would appear.

In Nodes 4 and 5, we have shown that global functional network architecture is disrupted in AD. According to the Watts & Strogatz model, an optimal balance between local and global connectivity is considered to be the most effective network configuration for information processing [19]. In AD, we see that particularly the loss of local functional clustering leads to a disturbance of this balance, resulting in a more random network structure. This quantifiable 'loss of structure' makes sense; it is not just disconnectivity, but also less *efficient* connectivity; AD as a *disorganization* syndrome. The more dependent a network is on circulation of information and fast dynamics, the more its structure will influence its performance. In this regard, the brain seems even more highly dependent on network integrity than for example telecommunication or infrastructure systems, and thus network efficiency, as expressed by the Watts & Strogatz model, may form a key feature. Nevertheless, it is also important to realize that although the Watts & Strogatz model represents a revolutionary step forward, it is not the ultimate network benchmark. For example, degree distribution, modularity, cost, growing processes and hierarchy are important network features that are not explained by this model. Just as the 'small-worldness', or balance between integration and segregation, is important [41], the relation between ordered and chaotic dynamics or wiring cost and efficiency might be equally important [22,39]. In other words: although we find a loss of functional network efficiency in AD, it is probably not the whole story.

Whereas global network measures show important overall characteristics, measures that focus on specific elements or parts give additional information. Within the global brain network, many parallel cognitive abilities are somehow maintained. Higher cognitive functions make use of both local, specialized processing and long-range distributed interaction [77]. Different regions that are required for a certain cognitive task might thus form a temporary collective assembly with a common goal. For example, a temporary link between neuronal assemblies in the occipital and temporal lobe might be needed to perform a task that requires visual recognition. Translated to graph theoretical terms, f*unctional modules* might be plausible candidates to describe these temporary collaborative sub-networks [26,49, 79]. Modularity has been an influential concept in various scientific fields [42,78]. In our work, we adhere to the graph theoretical definition. As argued in de discussion section of Node 6, detecting modules can be compared to the description of so-called 'resting-state networks' (RSN) in fMRI. The aim is similar: to describe functional regions or groups. As there a many different methods to identify modules or RSNs, results must always be interpreted with caution: different methods yield different results, a module might not reflect a specific *cognitive* function,

and the relation between different sub-networks or a module and the entire network might be just as important. For this last reason, graph theoretical modularity has an advantage over methods like independent component analysis (ICA) that are used for RSN detection, since the graph theoretical approach accurately quantifies the connectivity *between* modules. In fact, we show that *inter*modular connectivity might be more informative with regard to AD-related cognitive impairment than the *intra*modular connectivity. Further exploration of modular characteristics therefore may clarify the regional coordination of cognitive processes.

As network nodes constitute basic elements of any graph or network, their definition in a specific context determines how the graph theoretical analysis results should eventually be interpreted [41]. In neurophysiological studies, nodes usually consist of large regions, containing millions of neurons. Within one node, many lower-level networks and circuits may exist, and two separate nodes may have a completely different 'internal' organization. Nevertheless, the role of these heterogeneous regions in a network can still point to important large-scale connectivity characteristics. The best example of this may be nodal differences in degree: the identification of hubs in brain networks has become a major subject in network-related brain research. In AD, we have shown that hub regions weaken, particularly those that connect different modules, and this has catastrophic consequences for the entire network integrity. Hub node vulnerability, and the observation that hub regions show a large overlap with AD-related pathology, can be considered a fundamental 'connectopathic' phenomenon in need of an explanation.

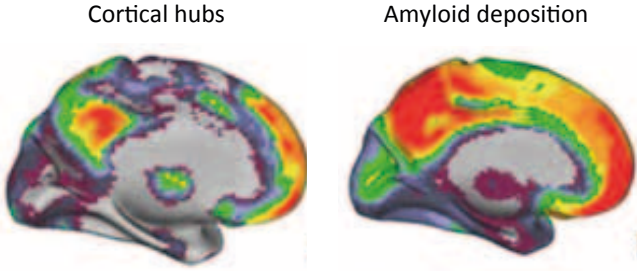

Figure 1. The striking overlap between cortical hub regions and amyloid deposition in Alzheimer patients. Source: Buckner et al., J Neurosci 29:6, 1860-73.

Summarizing, in AD brain networks are disrupted at different scales in time and space: overall functional organization, as expressed by small-world indicators and graph spectral measures, becomes more random and less efficient. Moreover, clustering decreases, functional modules weaken, and connections *between* modules weaken. Third, influential functional nodes (hubs) lose their power, and many other nodal characteristics change in AD. These results are interrelated: when hubs lose influence, overall efficiency in the network goes down, and structure becomes less clear. Although AD-related net-

work literature is still scarce, these main findings have been reported repeatedly now in both structural and functional studies [30,43-46,80]. Therefore, we can conclude that AD is characterized by structural *and* functional brain network disruption.

Functional networks and cognition

Increasing evidence is showing that there is a strong relationship between structural and functional brain networks and cognitive status. Brain networks alter during childhood [13,47,48], keep changing throughout life [4,49], and are influenced by experience and learning [50]. Impaired levels of consciousness, as in sleep or coma, are associated with differences in network structure [51-53]. Furthermore, IQ has been directly linked to network efficiency [54-56], and network properties seem to be inheritable to a considerable degree [57]. Finally, in various neurological disease conditions, networks show marked changes as cognition deteriorates [46,58-60]. These results provide compelling evidence for a strong relation between overall brain network structure and cognition, but do not address the question why specific cognitive domains are preferably impaired in AD. Therefore, the relation between specific network characteristics and cognitive domains should be investigated.

In our studies, we repeatedly found frequency band specific correlations between cognitive test scores and network measures (see Module 3). In Node 6 we demonstrate correlations between various modularity measures and specific cognitive functions that are typically impaired in AD. This is a fascinating finding, but the detection of these relationships is still not sufficient to pinpoint cognitive domains to specific patterns of connectivity. In this regard, it might be tempting to speculate about the exact cognitive function of a certain module, like memory or attention. Similar to resting-state networks, network modules or clusters have been linked to cognitive domains before [61,62]. However, modules found in resting-state EEG or MEG data might also be a reflection of non-specific neuronal coordination, or perhaps even of irrelevant stationary brain activity. Although this first investigation of the relation between modularity and cognition looks promising, many more aspects can be examined, like for example module size, dynamics, structure, and hierarchy. Furthermore, since individual nodes represent entire cortical regions in EEG and MEG networks, they too might show specific relations to certain cognitive traits. And while these single nodes might not be sufficient to explain complex cognitive abilities, their dysfunction might on the other hand certainly disrupt cognition. Therefore, their relation to cognition should be further investigated in future studies.

Diagnosis and prognosis

Even in specialized dementia centers that have the possession over new diagnostic techniques like PET and CSF analysis, the definite diagnosis of specific dementia types can

be far from easy. At present the gold standard is pathological examination post-mortem, and even here so-called 'mixed-pathology' (for example containing both amyloid deposition and vascular damage) is frequently encountered, frustrating a comfortable distinction between different forms of dementia [81]. The magnitude of variability and mismatch between the clinical picture and pathology in individuals is striking, and to make matters worse, many forms of dementia also show overlapping clinical symptoms. Even AD and FTD, two of the most common types of neurodegenerative dementia, can pose profound diagnostic difficulties. In FTD, imaging, cognitive and neurophysiological examinations can remain within the normal range for a long time. Whereas in AD slowing of background patterns, decrease of the alpha peak and loss of functional connectivity are common findings by now, no such signs have been identified for FTD. A previous study of functional connectivity in FTD showed no clear changes [63]. However, it is conceivable that while overall functional connectivity levels remain stable, network organization changes. Therefore, graph theoretical analysis might be able to find group differences and thereby enlarge diagnostic certainty during life. Besides diagnostic accuracy and early detection, functional networks might be used as disease monitoring and perhaps even prognostic indices. However, a strong relation of brain network measures with cognition and cognitive impairment does not automatically imply that graph measures will serve as powerful diagnostic or prognostic biomarkers.

From the amount of individual variability and overlap between individuals and groups we encountered in our graph analysis results, we can not expect to find highly sensitive and specific diagnostic indicators. In our results, we did find reasonable ROC-curve results for regional relative power in AD patients, comparable to the discriminative power of presently used neurophysiologic tests, but not strong enough to improve the present diagnostic markers.

An interesting observation was the number of differences we found between global functional network measures in AD and FTD groups. In AD, the shift of the functional network organization towards a more random type, was mainly caused by a decrease of local clustering, as expressed by the clustering coefficient. In contrast, FTD network organization changed in an opposing way, resulting in a more 'ordered' topology with relatively higher local clustering. A recent fMRI-based study by Zhou et al. showed similar results [64]. The finding that overall network structure becomes more random in AD, while it becomes more ordered in FTD also points toward an important fundamental notion: both in- and decreases in graph measure values can accompany pathological states. Since for example the balance between clustering coefficient and path length expresses a presumably ideal situation for information processing, deviations from this balance in both directions are considered less optimal. However, the observed differences were not strong and consistent enough for clinical use.

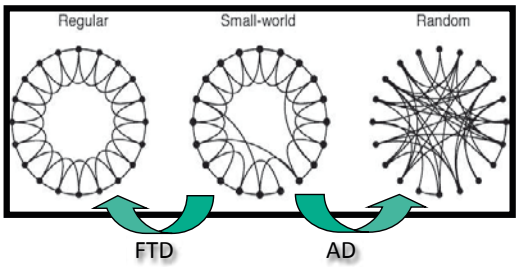

Figure 2. Three typical graph examples, based on the Watts & Strogatz model. Regular networks have high local connectivity, but low global connectivity. Random networks have opposite characteristics. Small-world network represent an optimal balance between these two extremes. The green arrows indicate the opposite shifts in network structure in AD and FTD.

Since MEG is a patient friendly, relatively fast and non-invasive technique, it would make a useful clinical tool in the diagnostic work-up of AD. In a recent review, Zamrini et al. argue for a more prominent role of MEG [65]. It can well be that more refined graph analysis, task-based data and longitudinal analysis can improve diagnostic power; this should be subject of further studies.

The graph spectrum

One reason for incorporating techniques that have proven their use in other fields might be specific desired qualities, such as a strong classification power. The identification of unique but consistent properties of individual brain networks could be of great importance for diagnostic and monitoring purposes. The use of alternative graph theoretical approaches becomes more relevant when there are limitations or methodological problems with the present ones. Although topological graph measures have initiated the explosion of network related studies, several practical issues have been raised by now, such as thresholding, normalization and measure selection (see also the Methodological Issues section below).

Graph *spectral* analysis is known for its strong classification power, and has the advantage over the 'traditional' topological graph measures that its use requires less arbitrary choices [66]. Moreover, different graph spectral measures are less intercorrelated, and therefore carry more unique, independent network information [28]. The notion that some of the spectral measures are closely related to the efficiency of dynamic processes on networks, such as synchronizability and information circulation, might form another advantage for our specific interest, since not many traditional graph measures are directly related to dynamical processes on networks. *Network synchronizability* based on the graph spectrum should not be confused with levels of synchronization between nodes, as described by functional connectivity measures: it is a *global* network feature. The topology of a structural network determines the ease and stability of global network synchronization, and we examine these same qualities in relation to the functional

MEG-derived network topology. Results of the two synchronizability measures reported in Node 7, the spectral gap and the eigenratio, indeed point towards altered functional network synchronizability.

One of the main findings of Node 5 was the hub vulnerability in AD. Since graph spectral analysis offers efficient ways to examine hub structure in networks, we implemented eigenvector centrality computations in our analysis. This analysis confirmed the strong hub status of the parietal regions, and showed an interesting strong correlation between the loss of left temporal centrality and MMSE score, implying the clinical relevance of these findings. On the other hand, hub distribution was not completely similar to earlier degree centrality based analyses, which illustrates the fact that different definitions and algorithms lead to different results, requiring caution when interpreting study outcomes.

Although graph spectral analysis showed several clear group differences, confirming topological analysis results, strong classification power was not possible based on the present resting state MEG data. Reasons for this might have been the amount of noise in neurophysiological data compared to other complex systems, the method chosen to obtain the underlying connectivity matrix, or the relatively modest network size (n=151). Of course, it should also be emphasized that the selection of graph spectral measures was motivated but inevitably arbitrary. Nevertheless, it is promising that with this completely different method significant group differences can be found, and that they are in line with results obtained using the more standard topological graph approach. In summary, the results so far and the theoretical benefits of graph spectral analysis justify additional investigation. Different methodological choices might be made, and different graph spectral measures or datasets may be investigated.

Early detection of Alzheimer's disease

In AD research, early detection is an important topic for obvious reasons: more clarity for patients and caregivers, anticipation and more efficient organization of care, and furthermore it seems that interventional studies are most promising at an early stage. It is presumed that dementia pathophysiology is present in the brain for decades before initial symptoms appear, so much progress could be made here. The dominant amyloid-cascade theory of AD states that problems start with local cellular processes, gradually spreading across the brain. And indeed, in particular amyloid-beta and tau levels in the brain and CSF have turned out to be fairly reliable early predictors of AD. However, the amyloid-based hypotheses do not offer an explanation for the vulnerability of specific brain areas in AD, do not predict the disease course, have an unclear link with risk factors and cognitive status, and interventions based on this hypothesis are disappointing. In short, it is not a very likely final theory of the AD disease mechanism. Hypotheses that

offer a more satisfying explanation of the non-random spread of pathology and its link to cognition should be taken seriously.

Figure 3 depicts the presumed time course in which different biomarkers of dementia become abnormal. Note that in this model, biomarkers are either structural or clinical; markers of brain dynamics are missing. However, since cellular damage occurs within neurons and synapses, their function is inevitably altered. This means that accurate assessment of changes in brain dynamics might contribute to the early detection of dementia. But at what stage will this be possible; only after profound structural damage is done? Increasing evidence suggests the opposite: functional connectivity is already disturbed at a very early stage, before cognitive symptoms arise, and even before notable amyloid deposition can be detected with PET or CSF analysis [67,68]. This does not only imply that changes in brain dynamics might lead to early detection, but also leads to the question whether dynamics are a *consequence* or *cause* of structural damage in the first place. In either case, early detection of functional changes might become an important topic in AD research over the next years.

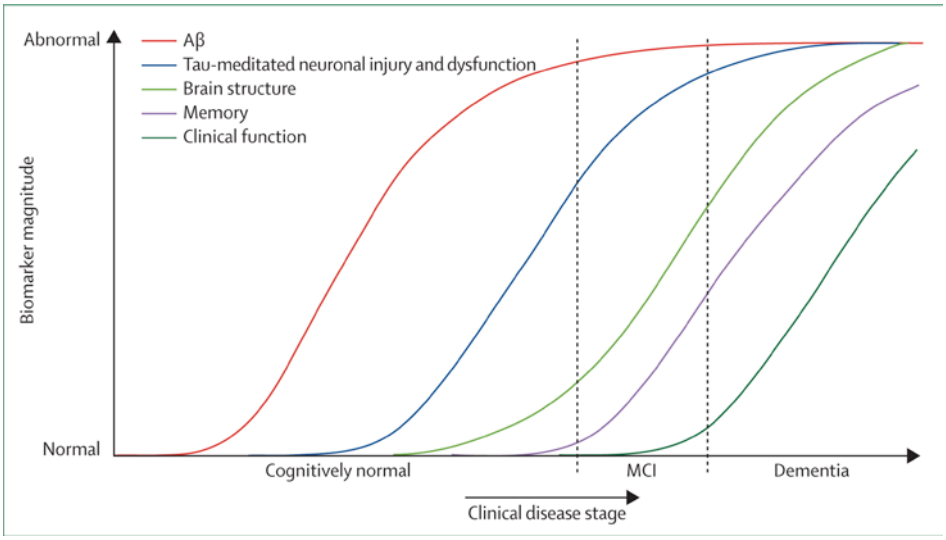

Figure 3. Timeline of presumed biomarker conversion during the development of dementia. Note that markers of brain dynamics are not incorporated in this scheme. Source: Jack et al, Lancet Neurology 2010, 9(1):119-128

Could it be that dynamical disturbance *precedes and causes* structural brain damage? There is support for this view from several angles:

- In many complex systems, dynamic activity can cause structural damage and global network dysfunction.
- In many human organs, chronic excessive activity can lead to pathologic damage, e.g. due to high metabolic demands and oxidative stress.

- Brain dynamics and functional connectivity are altered in people at risk for or in early-stage AD [43,67,68,82,88-95,97,100].
- For the major risk factors of AD (age, ApoE status), direct associations with altered levels of brain activity have been reported [86,87,96,98,99]
- Experimental animal studies show that excessive neuronal activity directly increases interstitial amyloid-beta concentration [70,71].

The potentially causal role of excessive brain dynamics in AD is explored in Node 8. In the following section, this hypothesis will be discussed further.

Activity dependent degeneration

While the accurate description of changes in brain network organization in patients may be an effective strategy for distinguishing groups or diagnosing disease, the observed changes do not necessarily *explain* underlying causes of cognitive (dys-)function. Abnormal patterns of network disruption may lead to new hypotheses of AD pathophysiology, but may be hard to recognize within rich and complex datasets, and even harder to interpret. Also, to test causal mechanisms, direct interference with the brain is usually required, and in humans this is only rarely a viable option. For these purposes, computational network modeling studies may form a fitting complementary approach. Brain network models allow for endless manipulation and hypothesis testing: the effect of disease processes on brain networks can be simulated and investigated. The results of this approach can subsequently be used to make realistic predictions about pathophysiology, to be verified in patient data.

In Node 5 we described a loss of functional network structure in AD patients. To find out if the network damage could be explained by a simple principle, we tested two different damage models: a 'random error' and a 'targeted attack' model. In the targeted attack model, high degree nodes were damaged more strongly. We found that the targeted attack model better explained the AD-related network damage, which led us to conclude that AD somehow preferably targeted hub regions. Whatever made hubs different than other regions, besides their high level of connectivity, could be a potential clue about the disease mechanism.

An obvious feature of hub regions could be high levels of activity and energy demand, but this has never been reported. The only support for this notion was the high spontaneous activity levels of the well-known Default Mode network, which shows a large amount of overlap with cortical hub regions [69]. But, even if hubs *would* be more active, a pathological effect of this activity needs to be explained. Recently, an AD-related pathologic effect of excessive levels of neuronal activity (increasing amyloid-beta concentration) was described in transgenic mice [70,71]. If the hub vulnerability phenomenon, the early connectivity changes and high activity of hub regions, and the evidence of excessive neuronal damage leading to neurodegeneration could be com-

bined in a single coherent model, this might serve as an elegant explanation for hub vulnerability in AD.

For this purpose, a computational neural mass model was developed that combines realistic structural connectivity (DTI-based) with EEG-like brain dynamics. The model simulates brain activity, and this activity can be analyzed in the same way as real data. An additional feature of the model is that it can be 'damaged' by a disease-simulating algorithm and that its output also includes spike density, a direct neuronal activity measure. Thus, in this computational model connectivity and activity is combined in a way that allows for testing our hypothesis, and therefore we implemented the 'activity dependent degeneration' (ADD) procedure (see Node 8). The main idea behind this was that excessive activity would make hubs vulnerable to AD, and we tested this by demonstrating that hubs were indeed the most active regions, and that by damaging the network according to activity level, we could reproduce all major common neurophysiological AD characteristics like oscillatory slowing, loss of power and functional coupling. Furthermore, the transient increase in spike density and functional connectivity is in line with reports of increased activity in MCI, and implies that this is not a compensatory phenomenon, as is often suggested, but a pathologic one. In addition, ADD offers a possible explanation of the high levels of DMN activity. In healthy persons, the DMN is *de*activated during cognitive tasks, and high DMN levels are only present in resting state conditions. In AD, this task-dependent deactivation is impaired, and DMN activity stays high [82].

The outcome of this study suggests that activity-dependent degeneration plays a causal role in the AD disease mechanism. However, it is still possible that other damage models might produce similar findings. Alternative damage models can be implemented. On the other hand, it could also be that the ADD-principle is not specific for AD, but a general damage mechanism that also contributes to other disorders. To investigate the specificity of the ADD process, we compared it to a random damage model, but it is still conceivable that alternative models lead to similar findings. Progressive non-hub damage, and subsequent re-routing of network activity might for example also cause hub region 'overload'. Finally, the neural mass model we used could have been made more detailed, for example by adding higher resolution structural connectivity matrices, or directed links, which could also enhance the reliability and accuracy of the model. It is however important to emphasize that the level of detail in the model also depends on the hypothesis that is tested: for our global 'hub versus non-hub' comparison, more detail might not be required, and even potentially distracting.

The predictions made by this study should eventually be verified in experimental studies. Since direct investigation and manipulation of neuronal activity is easier in rodents, assessing detailed connectivity and activity data might be more feasible. In human studies, longitudinal EEG/MEG data combined with other structural (MRI/DTI),

functional (fMRI) and metabolism/pathology (PET) techniques may provide more indirect support for the ADD hypothesis. Suppose there is truth in ADD, this could have wide implications for AD research: therapeutic strategies that are aimed at influencing neuronal activity might be a new target. This could be realized in different ways: for example, anti-epileptic medication can protect against neuronal hyperactivity and its consequences. Based on recent findings of a beneficial effect of levetiracitam (Keppra) on hippocampal hyperactivity and memory performance in transgenic mice, a recent study in amnestic MCI patients has shown similar results in humans [72]. Non-pharmaceutical approaches could be transcranial magnetic stimulation (TMS), transcranial direct durrent stimulation (tDCS), or deep brain stimulation (DBS). DBS is already applied successfully in depression, Parkinson's disease and obsessive-compulsive disorder, and a small recent phase I trial in AD patients showed interesting results [73]. For monitoring the effects on neuronal dynamics and functional connectivity of any of these therapies, EEG/MEG-based functional network analysis would be a valid option.

Capturing dynamic networks: methodological issues

In the multi-step procedure ranging from the recruitment of patients to the interpretation of the analysis results many methodological decisions have to be made, and these choices can have a substantial influence on the final outcome. For a better interpretation of the findings in this thesis, our key methodological decisions and alternative possibilities are discussed in this section.

Subject selection

For clinical studies, patients were recruited from the VU University Alzheimer Center. Dementia patients were required to have a recent diagnosis of mild-to-moderate Alzheimer disease according to the NINCDS-ADRDA criteria [2]. Healthy persons who were willing to participate, often spouses of patients, underwent an extensive cognitive test battery to confirm their normal cognitive status. Although care was taken to ensure that patient and control groups were matched with regard to age, other factors made the group more heterogeneous. For example, gender was not equally distributed in all groups (although not significantly different), while recently gender-specific effects on network parameters have been reported [3,4]. Furthermore, people with psychiatric or neurologic comorbidity were excluded, but we did include individuals with different types of psychoactive medication and cardiovascular disease. However, medication use and comorbidity was modest and equally distributed in both groups, and the populations in these studies were regarded to be representative for a tertiary memory clinic.

In our EEG study persons with subjective cognitive complaints (SMC) have been used as control group. One might argue that this can lead to underestimation of group differences, since persons with SMC have been shown to have a higher risk to eventually

develop dementia. There are, however, also good reasons to use this control group: first of all, they have had the same thorough diagnostic work-up as the dementia patients (including brain imaging), which gives more confidence about their normal cognitive status than 'healthy' persons that have only had neuropsychological testing. Moreover, since we would like our results to be valuable for eventual clinical use, persons with SMC form a very appropriate control group, since any potential marker that gives a clear distinction between dementia patients and persons with SMC is of value.

Neurophysiological data recording and post-processing

A principal decision is the amount of EEG/MEG data that is selected for analysis. Recordings often last at least 30 minutes, but final analysis in these studies was usually performed on 4 segments with a length of approximately 10 seconds per epoch. There are several reasons for this:

Artifacts. Every recording contains artifacts ranging from eye blinks, swallowing, movement, drowsiness or technical artifacts. The most efficient way to exclude artifacts is visual analysis by an experienced researcher, who is blinded to the diagnosis. Because of drowsiness, epochs were selected from the first minutes of the recording. This is particularly relevant in AD patients, where drowsiness occurs more often.

Reliability. Functional connectivity and graph theoretical analysis was always performed on each time segment separately, and then averaged over the 4 segments per person to obtain a representative average. This allows for consistent averages, and enough data to reliably extract measures in all frequency bands [5]. In a recent MEG study, test-retest reliability was found to be adequate [6].

Data reduction. For simpler measures, entire datasets can be analyzed fast, but for more complex network measures such as modularity or coupling measures like the SL, computation time can increase rapidly.

Another fundamental matter is the selection of frequency bands, instead of a broadband or very narrow band analysis. Based on neurophysiological literature, in which different frequency bands have been identified by their different behavior and relation to cognitive processes, we decided to adhere to the commonly used bands: delta (0.5-4 Hz), theta (4-8 Hz), lower alpha (8-10 Hz), higher alpha (10-13 Hz), beta (13-30 Hz) and gamma (30-45 Hz). This division allows for a more meaningful interpretation and comparison with previous literature [83,84]. Although alternative choices may produce different results, of importance is that a wide range of frequencies is studied, since cognition may require the whole spectrum. Another branch of research is devoted to cross-frequency coupling, i.e. the interaction *between* different frequencies in the brain, like the theta-gamma rhythm binding in working memory [7].

Functional connectivity measures

While the characterization of functional connectivity in the brain is a research area on its own, in this thesis it forms the basis on which graph theoretical network analysis is built. In general, since different coupling measures produce different connectivity matrices, they influence subsequent graph analysis results. Therefore, observed group differences based on a connectivity matrix derived from SL as coupling measure might not have been found using PLI and vice versa. To ascertain the robustness of results in this regard, various coupling measures could be compared. The influence of different functional connectivity measures on graph theoretical measures has not yet been investigated in a systematic way, and this is certainly a desirable future step. For most studies in this thesis, we used the Synchronization Likelihood (SL) as functional connectivity measure. The SL is a general measure of the correlation or synchronization between two time series, which is sensitive to linear as well as nonlinear interdependencies [8,9]. In previous years, it has been used in many clinical studies [10-14].

One of the most troublesome dilemma's in neurophysiological studies is volume conduction, which refers to the fact that different EEG or MEG sensors are likely to pick up signals from the same underlying sources, which can lead to an overestimation of synchronization and thus confound graph results. To tackle this dilemma, different strategies have been developed. One example is the Phase Lag Index (PLI) used in the MEG study in Node 5 [15]. The PLI discards any (near-) zero phase lag synchronization, and is thus not sensitive to volume conduction. However, with this it also discards meaningful small phase lag coupling. For graph methods that focus on clustering and modularity, this feature is a disadvantage: many true short range-links are ignored. At this moment, there is no perfect solution yet, although recent studies show that moving functional connectivity analysis from 'sensor space' (the signal as measured at the sensor) to 'source space' (the activity as estimated in the underlying source) may help to overcome this problem [16].

Once the mean level of functional connectivity between all network nodes (in our case EEG/MEG sensors) is established, this information can be combined into the connectivity matrix, on which all further network analysis is based. Therefore, the reliability of the connectivity matrix is of great importance. Since different underlying functional connectivity measures can be used to construct the matrix (e.g. SL and PLI), different connectivity matrices can be derived from the same data. This influences the final outcome, and to increase the reliability of their interpretation, the original underlying research question or particular topic of interest should be guiding the specific choices, and different functional connectivity measures should be compared to ascertain consistency.

Graph theoretical analysis

Modern complex network theory, including the application of graph theory to complex networks, is under constant development [17,18]. Since the seminal papers by Watts & Strogatz and Barabási & Albert, many new methods and measures have been proposed [19-21]. The clustering coefficient and characteristic path length, two basic properties proposed by Watts & Strogatz, have already undergone many adaptations and variations. For instance, the characteristic path length of a network is the average of the shortest path lengths between all node pairs. However, when a graph has disconnected points, this would mean the path length would approximate infinity. To solve this, one can take the mean of al inversed path lengths. But now, a higher path length value reflects a *shorter* path, which is quite counterintuitive (unless it is termed 'nodal efficiency' [22]). Therefore, taking the inverse of this number again produces a more intuitive path length value. There are more path length definitions, and some network scientists distrust the use of this measure in functional networks, because links between nodes, and therefore path lengths based on these links, could reflect an indirect interaction. These different views could be interpreted as signs of flexibility, but also of ambiguity in the network approach, and this methodological issue applies to other situations as well.

For instance, in the studies presented here we make use of both weighted and unweighted graph measures, i.e. with and without taking the connection weights between nodes into account. Many graph measures have both weighted and unweighted variants. Although weighted networks preserve more information from the original connectivity matrix, they possibly also contain noisy, spurious links and link weights. Since it is often impossible to separate noise from true connectivity, this will influence results. Although several approaches have been developed to tackle this problem, there is no perfect solution yet. One strategy is to convert the weighted connectivity matrix into a binary, unweighted matrix by applying a threshold and setting link weights below the threshold to 0 and those above to 1. The network now has become binary, and by discarding link weights there is a loss of information. In addition, the problem of using a threshold is that setting its height is arbitrary: with a low threshold there may still be many noisy links, and with a high threshold true connections might be erroneously ignored. Even more problematic, since many graph measures directly depend on network size and density, the threshold height itself influences the results [23]. To explore the size of this effect, a range of thresholds could be examined (see for example [24]). When graph theoretical results are then found to be similar for different thresholds, the amount of distortion by thresholding might become acceptable.

Once the underlying connectivity matrix is determined, there is a wide range of graph theoretical measures that can be employed, and many of them have been described in this thesis. The development and application of new graph measures in neuroscience provides ample choice, but it also raises the question which (versions of) measures

are the most appropriate or reliable ones. An illustrative example is modularity, where various algorithms exist that have different advantages [25-27]. Most graph measures are designed to describe a certain global, regional, or nodal characteristic of network topology, and therefore appear to be very specific and well defined. That this is not necessarily the case is illustrated by a recent study, which shows that graph theoretical measures that are supposed to describe different aspects of a graph (e.g. clustering and path length) can be strongly correlated [28]. This indicates that further studies to assess the consistency and reliability of various graph theoretical measures are needed.

Graph comparison

As the previous paragraphs show, graph theoretical analysis results depend on methodological choices. However, since networks are often ultimately compared between groups, the absolute values of graph measures might be less important than relative in- or decreases. Unfortunately, comparing networks can in fact complicate matters even further: for example, if a disease weakens connections, the resulting network will not only change in configuration but also in size and density. The different size leads to different graph results, so if the comparison should only be between network topology of groups, size and density should be similar. This has been the approach in several of our studies: networks of both groups were thresholded in such a way that the resulting graphs were at least equal in average degree (k), allowing for comparisons between network topology only. On the other hand, one might argue that the decrease of network size, and all its consequences for graph measure values is part of the disease, and should not be ignored by leveling the networks. This last option has become more attractive since it was shown that using a fixed k-based threshold is not optimal, since the influence of degree and density depends on the underlying graph topology, which is often not known a priori [23]. The authors also show that another often-used approach, which consists of normalizing graphs by comparing them to a large set of random surrogate networks, may even increase the sensitivity to differences in degree and density and yield spurious results.

To circumvent several of these methodological dilemmas, we investigated the possibilities of graph spectral analysis (see module 4). Since graph spectral measures are fully determined once the connectivity matrix is known, it can be considered a more parameter-free way of describing networks. The previously mentioned graph metric correlation study by Li et al. also found graph spectral measures to be more independent of each other, thus containing unique topological information. However, further studies are needed to assess reliability.

Methods, measures and hypotheses…

In this relatively new field, methodological 'gold standards' still have to be defined. Fortunately, regardless of the various methods used in this thesis, and of the diverse techniques combined with graph theoretical analysis in present literature, the major

part of AD-related studies show converging results [29,30]. This indicates that although the methodological issues described above deserve our interest, the graph theoretical approach still allows us to discern robust, relevant patterns of change in AD. Nevertheless, considering the rapidly growing availability of graph theoretical measures and methods, future studies that systematically compare different methods will become very important.

Whether a certain method will be suited also strongly depends on the specific research question or hypothesis: for example, when examining clustering and modularity, the use of the PLI to derive the connectivity matrix may not be advisable due to its relative underestimation of true near-zero phase lag synchronization, as was discussed in Node 6. Thus, instead of applying every available graph measure to every imaginable situation, a major challenge will be to ask the right questions, formulate sharp hypotheses, and then make a motivated decision about the optimal graph theoretical strategy to test them.

Future directions

With the improving quality of imaging and neurophysiological techniques and the growing collection of graph theoretical tools, it seems that many new ways to investigate functional network disruption in AD are within reach. A few of the most interesting and practically feasible directions are summed up below.

Clinical questions

Longitudinal studies in healthy persons, MCI patients and patients that suffer from any form of neurodegenerative dementia could be very helpful in tracking functional network changes over time. For **monitoring therapeutic efficacy**, pharmaceutical or non-pharmaceutical, a similar approach can be used. For **early detection** studies, functional network analysis of healthy ApoE4 carriers or persons with subjective memory complaints may be an interesting next step. To **relate functional network changes to brain structure and pathology**, EEG/MEG results should be combined with MRI, DTI and PET. Besides resting-state studies, cognitive **task-based paradigms** can probably increase our understanding of the coordination of cognitive processes. The i**nvestigation of patients with reversible cognitive deficits,** like in delirium or depression, could be informative. Stronger network **classification** procedures are highly desired, and graph spectral analysis could play a role here.

Methodological considerations

A systematic investigation of the **influence of different functional connectivity measures on graph analysis results** is an important next step, since this will make interpretation of network studies more reliable and meaningful. To be able **to describe direction and causality in functional network**, the development of functional cou-

pling measures that are able to describe the influence of one node over another would be required. Furthermore, in our frequency band specific analysis, interaction between different frequencies is not accounted for, while this **cross frequency coupling** might be very relevant for cognitive processing. Instead of using the EEG/MEG signal as measured by the sensor for further analysis (sensor space), it is also possible to estimate source locations, and thus produce a more three-dimensional '**source space'** image of functional network dynamics. An example of this approach is the recent study by Hillebrand et al., which illustrated that using beamformer techniques, MEG data could be projected on a standardized anatomical template [16].

Conceptual challenges

The Watts & Strogatz model was a breakthrough in describing the overall efficiency of networks, but the balance between integration and segregation is only one aspect of many. A big challenge will be **to implement major brain network features like small-worldness, modularity, scale-free degree distributions and hierarchy in one theoretical framework**, so that network changes that are observed in disease conditions may be interpreted better. For this purpose, successful models in different research fields might be helpful, and **collaboration with other complex system sciences** like economics, sociology or telecommunication may prove an effective strategy to find new, vital insights.

Conclusion

"There are billions of neurons in our brains, but what are neurons? Just cells. The brain has no knowledge until connections are made between neurons. All that we know, all that we are, comes from the way our neurons are connected."

Tim Berners-Lee
Inventor of the World Wide Web

The quote above is not from a leading neuroscientist, but from someone with an entirely different background. One might object to the level of conviction with which he makes a statement outside his field of expertise. Others may argue that these kinds of alternative perspectives are exactly what we need in neuroscience: there seems to be no shortage of human brain connectivity data, but there is a lack of bright ideas about how to deduce fundamental principles and mechanisms from this rapidly growing mass of information.

In many complex system research fields, the perception that connectivity is a crucial part of a system's performance, has inspired years or even decades of research, enabling major developments. In our increasingly connected society, many modern day phenomena such as international travel, economical trade, telecommunication, internet and social networking all require knowledge of connectivity and network organization. Here, the large body of mathematical literature on network structure and function provides a versatile and solid theoretical background. In recent years, complex network theory has discovered shared fundamental motifs and principles between many very distinct systems.

In dementia research, connectivity analysis of the brain does not play a large role yet with regard to evaluation of cognitive function. Present etiological hypotheses, diagnostic and prognostic criteria and interventional strategies are primarily based on structural, pathological abnormalities such as protein deposition and atrophy. Unfortunately, there is a substantial discrepancy between the severity of pathological damage and cognitive impairment in many individual cases, and the specific spread of pathology during neurodegenerative dementia only correlates with cognitive performance on a global level. Interestingly, one of the best structural correlates of cognitive impairment in Alzheimer's disease is synaptic loss [1]; another clue that more insight in brain connectivity will help us to understand and predict cognitive symptoms.

Of course, Tim Berners-Lee is not really the first person to point out the importance of connectivity in the brain. In a longstanding historic debate about the localization of cognitive function, great scientists such as Flourens, Wernicke, Cajal, Sherrington,

Lashley, Hebb, Varela, Edelman and Tononi have convincingly argued for a system-level approach to cognition [85]. Unfortunately, effective tools to observe and interpret cognitive mechanisms directly in living humans have been lacking so far. However, due to the technical advances in neuroscience and recent breakthroughs in modern network theory, we might be getting closer to a tipping point, where accurate descriptions and interpretations of distributed brain function come within our reach, and where many old questions and ideas about cognitive (dys)function can finally be addressed with more precision.

At first, the application of concepts from network theory seems a complicating, abstract step away from biomedical reality. But the brain *is* a complex network, and should thus be studied with the appropriate tools. The main theme of this thesis is that approaching the brain as a network, and dementia as network failure, could contribute substantially to bridging the gap in our understanding between structural brain damage and cognitive symptoms in dementia. Cognition is a distributed, dynamical process, and cognitive impairment is too. In a highly connected complex system, local damage often has global implications, and global dysfunction cannot be understood from a local perspective.

One might argue that the aims of this thesis have not been very specific. This observation is justified, but in this very new research field having a wide scope might be a smarter strategy than trying to answer very specific research questions that later turn out to be misguided questions in the first place. Another rightful remark might be that our conclusion that a network perspective on dementia is useful is rather premature: the outcomes of these studies have not yet led directly to better diagnostic or prognostic tests, or to a substantially improved understanding of the causes of cognitive impairment in dementia. At this point, we must acknowledge that there is plenty of room for improvement: there are several tough methodological issues, the observed group differences are not strong enough to produce sensitive diagnostic markers, and the relation between functional network features and cognition is not yet clear. However, it would be naive to expect that one or several of these major challenges would be resolved in the short time span of a few years. At this stage, finding the right tools and approaches to grasp the complexity of the brain is the most important goal. This dissertation is more about new options than about final answers.

The power of network theory in neuroscience is not just the interpretation of functional brain networks, but applies in a much broader sense: for instance, it can be a powerful theoretical framework for exploring the symbiotic relation between brain structure and dynamics, combining results of different imaging/recording techniques, and bridging the gap between the micro- an macroscopic levels at which the brain is being investigated [74, 75]. And, as mentioned before, the translation of successful strategies in other complex network fields to neuroscience can be aided by having

modern network theory as a common language and reference point. Inspired by other fields, more and more neuroscientists that are searching for straightforward underlying principles to describe the staggering complexity of the brain now seem to recognize the potential of network analysis, and perhaps this is the reason for the recent increase of network-related brain studies (see figure below).

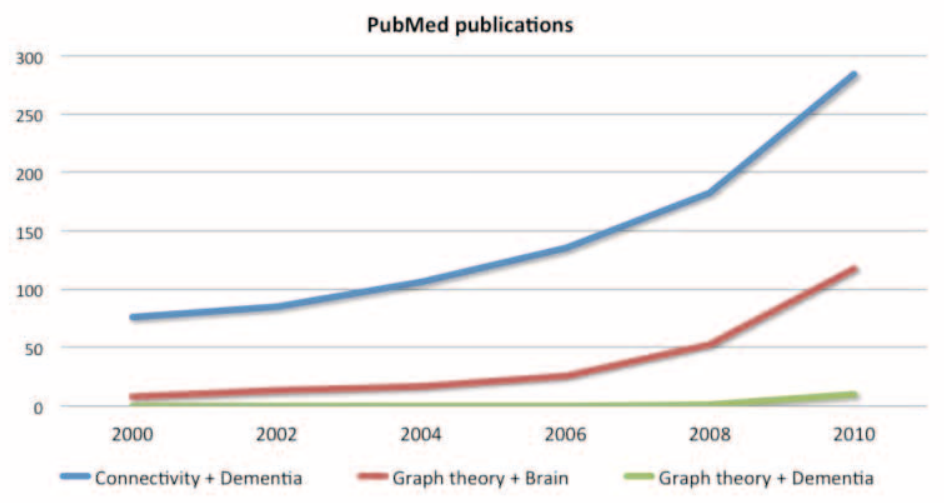

Figure 5 The number of brain connectivity, network and dementia related publications reported in the PubMed database in the last ten years, based on different combinations of keywords.

Hopefully, with this increased interest in brain connectivity, the realization that coordinated brain *dynamics* might be the missing link between pathology and clinical symptoms will re-emerge again among AD-researchers. Presently, the strong focus on structural, pathological approaches seems to distract many researchers from the fact that neuronal activity, although essential for cognitive processing, is largely neglected in AD research. However, brain structure and dynamics are so closely related that trying to study them in isolation will not lead to a complete understanding of cognitive impairment. Hopefully, the combination of graph theory and neurophysiological techniques presented in this dissertation can contribute in bringing about a shift of focus towards the underestimated role of brain activity and connectivity in dementia research.

REFERENCE LIST

1 Selkoe DJ (2002) Alzheimer's disease is a synaptic failure. Science 298: 789-791.

2 McKhann G, Drachman D, Folstein M, Katzman R, Price D, Stadlan EM (1984) Clinical diagnosis of Alzheimer's disease: report of the NINCDS-ADRDA Work Group under the auspices of Department of Health and Human Services Task Force on Alzheimer's Disease. Neurology 34: 939-944.

3 Schoonheim MM, Hulst HE, Landi D, Ciccarelli O, Roosendaal SD, et al (2011) Gender-related differences in functional connectivity in multiple sclerosis. Multiple Sclerosis Journal .

4 Gong G, Rosa-Neto P, Carbonell F, Chen ZJ, He Y, Evans AC (2009) Age-and gender-related differences in the cortical anatomical network. The Journal of Neuroscience 29: 15684-15693.

5 Niedermeyer E, Da Silva FHL (2005) Electroencephalography: basic principles, clinical applications, and related fields. Lippincott Williams & Wilkins.

6 Deuker L, Bullmore ET, Smith M, Christensen S, Nathan PJ, et al (2009) Reproducibility of graph metrics of human brain functional networks. Neuroimage 47: 1460-1468.

7 Canolty RT, Knight RT (2010) The functional role of cross-frequency coupling. Trends Cogn Sci 14: 506-515.

8 Stam CJ, Dijk BWV (2002) Synchronization likelihood: an unbiased measure of generalized synchronization in multivariate data sets. Physica D: Nonlinear Phenomena 163: 236 - 251.

9 Montez T, Linkenkaer-Hansen K, van Dijk BW, Stam CJ (2006) Synchronization likelihood with explicit time-frequency priors. Neuroimage 33: 1117-1125.

10 Stam CJ, Jones BF, Manshanden I, van Cappellen van Walsum AM, Montez T, et al (2006) Magnetoencephalographic evaluation of resting-state functional connectivity in Alzheimer's disease. Neuroimage 32: 1335-1344.

11 Stoffers D, Bosboom JL, Deijen JB, Wolters ECh, Stam CJ, Berendse HW (2008) Increased cortico-cortical functional connectivity in early-stage Parkinson's disease: an MEG study. Neuroimage 41: 212-222.

12 Wendling F, Ansari-Asl K, Bartolomei F, Senhadji L (2009) From EEG signals to brain connectivity: a model-based evaluation of interdependence measures. J Neurosci Methods 183: 9-18.

13 Boersma M, Smit DJ, de Bie HM, Van Baal GC, Boomsma DI, et al (2010) Network analysis of resting state EEG in the developing young brain: Structure comes with maturation. Hum Brain Mapp .

14 Buldú JM, Bajo R, Maestú F, Castellanos N, Leyva I, et al (2011) Reorganization of functional networks in mild cognitive impairment. PLoS One 6: e19584.

15 Stam CJ, de Haan W, Daffertshofer A, Jones BF, Manshanden I, et al (2009) Graph theoretical analysis of magnetoencephalographic functional connectivity in Alzheimer's disease. Brain 132: 213-224.

16 Hillebrand A, Barnes GR, Bosboom JL, Berendse HW, Stam CJ (2011) Frequency-dependent functional connectivity within resting-state networks: An atlas-based MEG beamformer solution. Neuroimage .

17 Boccaletti S, Latora V, Moreno Y, Chavez M, Hwang D- (2006) Complex networks: Structure and dynamics. Physics Reports 424: 175 - 308.

18 Newman MEJ (2003) The structure and function of complex networks. SIAM Review 45 .

19 Watts DJ, Strogatz SH (1998) Collective dynamics of 'small-world' networks. Nature 393: 440-442.

20 Barabasi AL, Albert R (1999) Emergence of scaling in random networks. Science 286: 509-512.

21 Rubinov M, Sporns O (2010) Complex network measures of brain connectivity: uses and interpretations. Neuroimage 52: 1059-1069.

22 Achard S, Bullmore E (2007) Efficiency and cost of economical brain functional networks. PLoS Comput Biol 3: e17.
23 van Wijk BC, Stam CJ, Daffertshofer A (2010) Comparing brain networks of different size and connectivity density using graph theory. PLoS One 5: e13701.
24 Stam CJ, Jones BF, Nolte G, Breakspear M, Scheltens P (2007) Small-world networks and functional connectivity in Alzheimer's disease. Cereb Cortex 17: 92-99.
25 Guimerà R, Amaral LA (2005) Cartography of complex networks: modules and universal roles. J Stat Mech 2005: nihpa35573.
26 Alexander-Bloch AF, Gogtay N, Meunier D, Birn R, Clasen L, et al (2010) Disrupted modularity and local connectivity of brain functional networks in childhood-onset schizophrenia. Front Syst Neurosci 4: 147.
27 Schwarz AJ, Gozzi A, Bifone A (2008) Community structure and modularity in networks of correlated brain activity. Magn Reson Imaging 26: 914-920.
28 Li C, Wang H, de Haan W, Stam CJ, Van Mieghem P (2011) The correlation of metrics in complex networks with applications in functional brain networks. Journal of Statistical Mechanics: Theory and Experiment 2011: P11018.
29 Stam CJ (2010) Use of magnetoencephalography (MEG) to study functional brain networks in neurodegenerative disorders. J Neurol Sci 289: 128-134.
30 He Y, Chen Z, Gong G, Evans A (2009) Neuronal networks in Alzheimer's disease. Neuroscientist 15: 333-350.
31 Geschwind N (2010) Disconnexion syndromes in animals and man: Part I. 1965. Neuropsychol Rev 20: 128-157.
32 Catani M, ffytche DH (2005) The rises and falls of disconnection syndromes. Brain 128: 2224-2239.
33 Delbeuck X, Van der Linden M, Collette F (2003) Alzheimer's disease as a disconnection syndrome? Neuropsychol Rev 13: 79-92.
34 Bonifazi P, Goldin M, Picardo MA, Jorquera I, Cattani A, et al (2009) GABAergic hub neurons orchestrate synchrony in developing hippocampal networks. Science 326: 1419-1424.
35 van den Heuvel MP, Stam CJ, Boersma M, Hulshoff Pol HE (2008) Small-world and scale-free organization of voxel-based resting-state functional connectivity in the human brain. Neuroimage 43: 528-539.
36 van den Heuvel MP, Mandl RC, Kahn RS, Hulshoff Pol HE (2009) Functionally linked resting-state networks reflect the underlying structural connectivity architecture of the human brain. Hum Brain Mapp 30: 3127-3141.
37 Damoiseaux JS, Greicius MD (2009) Greater than the sum of its parts: a review of studies combining structural connectivity and resting-state functional connectivity. Brain Struct Funct 213: 525-533.
38 Honey CJ, Sporns O, Cammoun L, Gigandet X, Thiran JP, et al (2009) Predicting human resting-state functional connectivity from structural connectivity. Proceedings of the National Academy of Sciences 106: 2035.
39 Stam CJ (2010) Characterization of anatomical and functional connectivity in the brain: a complex networks perspective. Int J Psychophysiol 77: 186-194.
40 Berendse (2000) Magnetoencephalographic analysis of cortical activity in Alzheimer's disease: a pilot study. Clinical neurophysiology 111: 604-612.
41 Sporns O (2010) Networks of the brain. Cambridge, Mass.: The MIT Press.
42 Fodor JA (1983) The modularity of mind: An essay on faculty psychology. The MIT Press.

43 Buckner RL, Snyder AZ, Shannon BJ, LaRossa G, Sachs R, et al (2005) Molecular, structural, and functional characterization of Alzheimer's disease: evidence for a relationship between default activity, amyloid, and memory. J Neurosci 25: 7709-7717.

44 Sanz-Arigita EJ, Schoonheim MM, Damoiseaux JS, Rombouts SA, Maris E, et al (2010) Loss of 'small-world' networks in Alzheimer's disease: graph analysis of FMRI resting-state functional connectivity. PLoS One 5: e13788.

45 Supekar K, Menon V, Rubin D, Musen M, Greicius MD (2008) Network analysis of intrinsic functional brain connectivity in Alzheimer's disease. PLoS Comput Biol 4: e1000100.

46 Pievani M, de Haan W, Wu T, Seeley WW, Frisoni GB (2011) Functional network disruption in the degenerative dementias. The Lancet Neurology .

47 Fair DA, Cohen AL, Power JD, Dosenbach NU, Church JA, et al (2009) Functional brain networks develop from a "local to distributed" organization. PLoS Comput Biol 5: e1000381.

48 Power JD, Fair DA, Schlaggar BL, Petersen SE (2010) The development of human functional brain networks. Neuron 67: 735-748.

49 Meunier D, Achard S, Morcom A, Bullmore E (2009) Age-related changes in modular organization of human brain functional networks. Neuroimage 44: 715-723.

50 Bassett DS, Wymbs NF, Porter MA, Mucha PJ, Carlson JM, Grafton ST (2011) Dynamic reconfiguration of human brain networks during learning. Proceedings of the National Academy of Sciences 108: 7641.

51 Koenis MMG, Romeijn N, Piantoni G, Verweij I, Van der Werf YD, et al (2011) Does sleep restore the topology of functional brain networks? Hum Brain Mapp .

52 Kar S, Routray A, Nayak BP (2010) Functional network changes associated with sleep deprivation and fatigue during simulated driving: Validation using blood biomarkers. Clin Neurophysiol .

53 Vanhaudenhuyse A, Noirhomme Q, Tshibanda LJF, Bruno MA, Boveroux P, et al (2010) Default network connectivity reflects the level of consciousness in non-communicative brain-damaged patients. Brain 133: 161.

54 Li Y, Liu Y, Li J, Qin W, Li K, et al (2009) Brain anatomical network and intelligence. PLoS Comput Biol 5: e1000395.

55 van den Heuvel MP, Stam CJ, Kahn RS, Hulshoff Pol HE (2009) Efficiency of functional brain networks and intellectual performance. J Neurosci 29: 7619-7624.

56 Song M, Zhou Y, Li J, Liu Y, Tian L, et al (2008) Brain spontaneous functional connectivity and intelligence. Neuroimage 41: 1168-1176.

57 Smit DJ, Boersma M, van Beijsterveldt CE, Posthuma D, Boomsma DI, et al (2010) Endophenotypes in a Dynamically Connected Brain. Behav Genet .

58 Reijneveld JC, Ponten SC, Berendse HW, Stam CJ (2007) The application of graph theoretical analysis to complex networks in the brain. Clin Neurophysiol 118: 2317-2331.

59 Stam CJ, Reijneveld JC (2007) Graph theoretical analysis of complex networks in the brain. Nonlinear Biomed Phys 1: 3.

60 Bassett DS, Bullmore ET (2009) Human brain networks in health and disease. Curr Opin Neurol 22: 340-347.

61 Salvador R, Suckling J, Coleman MR, Pickard JD, Menon D, Bullmore E (2005) Neurophysiological architecture of functional magnetic resonance images of human brain. Cereb Cortex 15: 1332-1342.

62 He Y, Wang J, Wang L, Chen ZJ, Yan C, et al (2009) Uncovering intrinsic modular organization of spontaneous brain activity in humans. PLoS One 4: e5226.

63 Pijnenburg YA, Strijers RL, Made YV, van der Flier WM, Scheltens P, Stam CJ (2008) Investigation of resting-state EEG functional connectivity in frontotemporal lobar degeneration. Clin Neurophysiol 119: 1732-1738.

64 Zhou J, Greicius MD, Gennatas ED, Growdon ME, Jang JY, et al (2010) Divergent network connectivity changes in behavioural variant frontotemporal dementia and Alzheimer's disease. Brain .

65 Zamrini E, Maestu F, Pekkonen E, Funke M, Makela J, et al (2011) Magnetoencephalography as a Putative Biomarker for Alzheimer's Disease. International journal of Alzheimer's disease 2011: 280289.

66 Van Mieghem P (2011) Graph Spectra for Complex Networks. Cambridge Univ Pr.

67 Drzezga A, Becker JA, Van Dijk KR, Sreenivasan A, Talukdar T, et al (2011) Neuronal dysfunction and disconnection of cortical hubs in non-demented subjects with elevated amyloid burden. Brain .

68 Sheline YI, Morris JC, Snyder AZ, Price JL, Yan Z, et al (2010) APOE4 allele disrupts resting state fMRI connectivity in the absence of amyloid plaques or decreased CSF Aβ42. J Neurosci 30: 17035-17040.

69 Buckner RL, Sepulcre J, Talukdar T, Krienen FM, Liu H, et al (2009) Cortical hubs revealed by intrinsic functional connectivity: mapping, assessment of stability, and relation to Alzheimer's disease. J Neurosci 29: 1860-1873.

70 Cirrito JR, Yamada KA, Finn MB, Sloviter RS, Bales KR, et al (2005) Synaptic activity regulates interstitial fluid amyloid-[beta] levels in vivo. Neuron 48: 913-922.

71 Bero AW, Yan P, Roh JH, Cirrito JR, Stewart FR, et al (2011) Neuronal activity regulates the regional vulnerability to amyloid-β deposition. Nat Neurosci 14: 750-756.

72 Bakker A, Krauss GL, Albert MS, Speck CL, Jones LR et al (2012) Reduction of hippocampal hyperactivity improves cognition in amnestic mild cognitive impairment Neuron 74(3):467-74.

73 Laxton AW, Tang-Wai DF, McAndrews MP, Zumsteg D, Wennberg R, et al (2010) A phase I trial of deep brain stimulation of memory circuits in Alzheimer's disease. Ann Neurol 68: 521-534.

74 Rubinov M, Sporns O, van Leeuwen C, Breakspear M (2009) Symbiotic relationship between brain structure and dynamics. BMC Neurosci 10: 55.

75 Bullmore E, Barnes A, Bassett DS, Fornito A, Kitzbichler M, et al (2009) Generic aspects of complexity in brain imaging data and other biological systems. Neuroimage 47: 1125-1134.

76 de Waal H, Stam CJ, de Haan W, van Straaten EC, Scheltens P, van der Flier WM (2011) Young Alzheimer patients show distinct regional changes of oscillatory brain dynamics. Neurobiol Aging. Nov 25.

77 Kandel ER (2000) Principles of neural science. McGraw-Hill, New York.

78 Simon HA (1962) The architecture of complexity. Proc. Am. Philos. Soc. 106, 467-482.

79 Varela F (2001) The brainweb: phase synchronization and large-scale integration. Nat Rev Neurosci 2:4, 229-39.

80 Xie T, He Y (2011) Mapping the Alzheimer's brain with connectomics. Front Psychiatry. 2:77.

81 Schneider JA, Arvanitakis Z, Leurgans SE, Bennett DA (2009) The neuropathology of probable Alzheimer disease and mild cognitive impairment. Ann Neurol. Aug;66(2):200-8.

82 Pihlajamäki M, Sperling RA (2009) Functional MRI assessment of task-induced deactivation of the default mode network in Alzheimer's disease and at-risk older individuals. Behav Neurol. 21(1):77-91.

83 Basar E, Güntekin B (2008) A review of brain oscillations in cognitive disorders and the role of neurotransmitters. Brain Res 1235, 172-93.

84 Jeong J (2004) EEG dynamics in patients with Alzheimer's disease. Clin Neurophysiol 115:7, 1490-505.
85 Stam K, Douw L, de Haan W (2010) Hersenweb: wat moderne netwerktheorie ons leert over de werking van de hersenen. Prometheus/Bert Bakker, Amsterdam. Dutch.
86 Kramer G, van der Flier WM, de Langen C, Blankenstein MA, Scheltens P, Stam CJ (2008) EEG functional connectivity and ApoE genotype in Alzheimer's disease and controls. Clin Neurophysiol. Dec;119(12):2727-32.
87 Beason-Held LL (2011) Dementia and the default mode. Curr Alzheimer Res 8:4, 361-5
88 Celone KA, Calhoun VD, Dickerson BC, Atri A, Chua EF, Miller SL, DePeau K, Rentz DM, Selkoe DJ, Blacker D, Albert MS, Sperling RA (2006) Alterations in memory networks in mild cognitive impairment and Alzheimer's disease: an independent component analysis. J Neurosci. Oct 4;26(40):10222-31.
89 Maestu F, Baykova E, Ruiz JM, Montejo P, Montenegro M, Llanero M, Solesio E, Gil P, Yubero R, Paul N, Pozo F, Nevado A (2011) Increased biomagnetic activity in healthy elderly with subjective memory complaints. Clin Neurophysiol. 2011 Mar;122(3):499-505.
90 Prichep LS, John ER, Ferris SH, Rausch L, Fang Z, Cancro R, Torossian C and Reisberg B (2006) Prediction of longitudinal cognitive decline in normal elderly with subjective complaints using electrophysiological imaging. Neurobiol Aging 27:3, 471-81
91 Prichep LS (2007) Quantitative EEG and electromagnetic brain imaging in aging and in the evolution of dementia. Ann N Y Acad Sci 1097, 156-67
92 Buldú JM, Bajo R, Maestú F, Castellanos N, Leyva I, Gil P, Sendiña-Nadal I, Almendral JA, Nevado A, Del-Pozo F and Boccaletti S (2011) Reorganization of functional networks in mild cognitive impairment. PLoS One 6:5, e19584
93 Criado JR, Amo C, Quint P, Kurelowech L and Otis SM (2006) Using magnetoencephalography to study patterns of brain magnetic activity in Alzheimer's disease. Am J Alzheimers Dis Other Demen 21:6, 416-23
94 Dickerson BC, Salat DH, Greve DN, Chua EF, Rand-Giovannetti E, Rentz DM, Bertram L, Mullin K, Tanzi RE, Blacker D, Albert MS, Sperling RA (2005) Increased hippocampal activation in mild cognitive impairment compared to normal aging and AD. Neurology. Aug 9;65(3):404-11.
95 Filippini N, MacIntosh BJ, Hough MG, Goodwin GM, Frisoni GB, Smith SM, Matthews PM, Beckmann CF, Mackay CE (2009) Distinct patterns of brain activity in young carriers of the APOE-epsilon4 allele. Proc Natl Acad Sci U S A. Apr 28;106(17):7209-14.
96 Heise V, Filippini N, Ebmeier KP, Mackay CE (2011) The APOE ε4 allele modulates brain white matter integrity in healthy adults. Mol Psychiatry. Sep;16(9):908-16.
97 Jagust W (2009) Amyloid + activation = Alzheimer's? Neuron 63:2,141-3
98 Kapogiannis D, Mattson MP (2011) Disrupted energy metabolism and neuronal circuit dysfunction in cognitive impairment and Alzheimer's disease. Lancet Neurol. Feb;10(2):187-98.
99 Machulda MM, Jones DT, Vemuri P, McDade E, Avula R, Przybelski S, Boeve BF, Knopman DS, Petersen RC, Jack CR Jr (2011) Effect of APOE ε4 status on intrinsic network connectivity in cognitively normal elderly subjects. Arch Neurol. Sep;68(9):1131-6.
100 Sperling RA, Laviolette PS, O'Keefe K, O'Brien J, Rentz DM, Pihlajamaki M, Marshall G, Hyman BT, Selkoe DJ, Hedden T, Buckner RL, Becker JA, Johnson KA (2009) Amyloid deposition is associated with impaired default network function in older persons without dementia. Neuron. Jul 30;63(2):178-88.

NEDERLANDSE SAMENVATTING

'In a network state of mind' - de rol van cerebrale functionele netwerk topologie bij de ziekte van Alzheimer

In **module 1** wordt de ziekte van Alzheimer (AD) geïntroduceerd als een snel groeiend probleem in onze vergrijzende bevolking. Een fundamenteel begrip van het ziektemechanisme ontbreekt, en tot op heden bestaat er geen doeltreffende behandeling. Het is onduidelijk hoe de geobserveerde structurele schade aan het brein exact samenhangt met de achteruitgang in cognitieve vermogens, en nieuwe invalshoeken die meer samenhang kunnen aanbrengen zijn gewenst. Het is opvallend dat onderzoek naar de rol van hersen*activiteit* bij dementie relatief klein is, terwijl dit een onmisbaar onderdeel is van een gezonde cognitie. Meer kennis over de coördinatie van lokale en globale cognitieve processen, en de verstoring hiervan bij de ziekte van Alzheimer, kan bijdragen aan een beter begrip van de ziekte, en aan nieuwe diagnostische en therapeutische strategieën.

Om dit doel te verwezenlijken is de eerste stap het nauwkeurig en betrouwbaar beschrijven van hersenactiviteit. In deze thesis wordt gebruikt gemaakt van neurofysiologische technieken, omdat zij een goede balans bieden tussen nauwkeurigheid en belasting voor de patiënt. Om een achtergrond te schetsen worden enkele neurofysiologische basisbegrippen besproken, zoals actiepotentialen, oscillaties en synchronisatie. Het begrip *functionele connectiviteit* wordt geïntroduceerd als methode voor het beschrijven van de interactie tussen hersengebieden, en de neurofysiologische meettechnieken elektro-encefalografie (EEG) en magneto-encefalografie (MEG) worden besproken. Een motivatie voor het gebruik van spontane, taak-vrije data ten opzichte van taak-gerichte data wordt gegeven, en tot slot volgt een kort overzicht van de rol van neurofysiologische literatuur in dementie tot nu toe.

Het doorgronden van de complexe patronen van activiteit en functionele connectiviteit vormt een grote uitdaging. In plaats van de hersenen te beschouwen als een verzameling afzonderlijke, gespecialiseerde gebieden, leggen we de nadruk op de hersenen als systeem; hoe efficiënt en robuust is het netwerk als geheel? Grafentheorie wordt geïntroduceerd als een methode om uit te leggen hoe wijzigingen in de netwerkstructuur betrekking hebben op wijzigingen in netwerkfunctie. Betoogd wordt dat de toepassing van concepten uit grafentheorie op neurofysiologische data kan helpen om dementie beter te begrijpen. Dit leidt vervolgens tot de algemene doelstelling van deze dissertatie:

het beschrijven van veranderingen in functionele hersennetwerk organisatie bij de ziekte van Alzheimer met behulp van neurofysiologische technieken en moderne netwerktheorie, alsmede de relatie hiervan met de onderliggende pathologie en bijbehorende klinische symptomen van AD.

In **module 2** rapporteren we dat hersenactiviteit, beschreven met behulp van MEG metingen, bij patiënten met Alzheimer vertraagt. Dit was reeds geruime tijd bekend uit EEG onderzoek, maar in MEG data is nauwkeuriger te zien dat de vertraging verschilt per corticaal gebied. De oscillatoire activiteit van verschillende gebieden lijken dus in wisselende mate te worden beïnvloedt door het ziekteproces. Echter, de gebruikte methode houdt geen rekening met de (vermoedelijk eveneens veranderende) interactiviteit *tussen* verschillende regio's, hetgeen een incompleet beeld oplevert. Een meer samenhangend 'netwerkperspectief' zou wellicht kunnen helpen om de patronen van afwijkende hersenactiviteit en hersenfunctie bij de ziekte van Alzheimer beter te begrijpen.

Module 3 beschrijft de globale functionele netwerkstructuur op basis van EEG metingen in gezonde mensen, patiënten met de ziekte van Alzheimer en patiënten met fronto-temporale dementie (FTD). Graaf theoretische analyse laat zien dat de verschillende vormen van dementie leiden tot andere soorten netwerkverstoring: zowel AD als FTD vertonen een verlies van evenwicht tussen lokale en globale netwerkconnectiviteit, maar in tegengestelde richtingen. Dit verschil suggereert verschillende onderliggende hersenfunctiestoornissen, een gegeven dat tot meer begrip en nieuwe diagnostische tests kan leiden.

In de volgende studie wordt netwerkverstoring bij AD patiënten in meer detail weergeven met behulp van MEG: wederom wordt een verlies van optimale netwerkstructuur waargenomen. AD-gerelateerde netwerkschade wordt daarnaast ook vergeleken met twee theoretische schademodellen: 'random error' of willekeurige netwerkschade, en een 'targeted attack' scenario waar vooral de sterk verbonden 'hub' gebieden worden beschadigd. Dit laatste model weerspiegelt de veranderingen in AD het best, hetgeen suggereert dat –om de een of andere reden – de sterk verbonden hersengebieden kwetsbaar zijn.

Na deze focus op globale netwerkschade en de rol van afzonderlijke gebieden, wordt vervolgens gekeken naar een tussenliggend niveau: dat van sub-netwerken oftewel modules. In AD wordt een verlies van globale modulariteit, kwetsbaarheid van de pariëtale hub-module, en vooral een sterke beschadiging van *inter*modulaire verbindingen gevonden, welke ook correleren met de sterkte van aanwezige cognitieve stoornissen. Deze studies illustreren een relevante relatie tussen verstoorde functionele netwerken en cognitieve symptomen.

Module 4 illustreert een alternatieve methode om netwerkeigenschappen te beschrijven: graaf spectrale analyse. Deze methode heeft zijn nut in andere onderzoeksterreinen bewezen, en heeft als methodologische voordelen ten opzichte van de eerder beschreven aanpak dat de netwerkeigenschappen minder arbitraire parameters hebben, en dat een aantal eigenschappen specifiek betrekking hebben op dynamische processen in netwerken . Met behulp van deze techniek detecteren we opnieuw verlies van efficientie in de netwerken van AD patiënten, evenals verschillen in robuustheid en

informatie circulatie. De graad van verbondenheid van regio's wordt met behulp van 'eigenvector-centraliteit' onderzocht, en de eerder beschreven centrale rol van de sterk verbonden pariëtale regio wordt hier nogmaals bevestigd. De links temporale regio is opvallend kwetsbaar, en dit hangt samen met slechtere MMSE scores.

De waargenomen 'hub'-kwetsbaarheid in AD (module 3) is een intrigerende maar nog onverklaarde bevinding. Aangezien in recente studies een relatie tussen hub-status en mate van amyloïd-depositie in corticale gebieden werd gelegd, en er onlangs een directe invloed van overmatige neuronale activiteit op amyloïd-depositie is gerapporteerd, veronderstelden we dat de hoge connectiviteit van hub gebieden een gemiddeld hoge activiteit vereist, en dat de chronische, hogere activiteit van sterk verbonden corticale gebieden ze gevoelig maakt voor degeneratie. Kortom, we speculeerden dat excessieve dynamiek zelf mogelijk een *oorzakelijke* rol in de AD pathogenese zou kunnen hebben.

Om deze hypothese te testen ontwikkelden we een computationeel model dat gebaseerd is op realistische hersenconnectiviteit en -dynamiek. We laten zien in **Module 5** dat hersenhubs inderdaad ook de meest actieve regio's zijn, en dat wanneer regio's worden beschadigd aan de hand van hun activiteitsniveau, de door het model gegenereerde schade veel kenmerken van AD-gerelateerde schade vertoont, zoals globale vertraging, verlies van functionele connectiviteit, en vergelijkbare functionele netwerk verstoring. Dit suggereert dat excessieve neuronale activiteit inderdaad een rol in het ontstaan van Alzheimer speelt.

Module 6 begint met een review van relevante netwerk-gerelateerde literatuur in dementia, waarin net als in Module 3 wordt betoogd dat functionele netwerk verstoring verschilt tussen de diverse vormen van dementia, hetgeen consequenties kan hebben voor de diagnostiek, prognostiek en therapie van dementie. Vervolgens bespreekt deze sectie de belangrijkste resultaten van dit proefschrift, en probeert deze in een breder kader te plaatsen. Terugkijkend naar de doelstelling van dit project kan worden geconcludeerd dat het beschrijven van verstoorde hersennetwerken bij dementie een aantal nieuwe gezichtspunten oplevert, zoals het verlies van een efficiënte functionele netwerkstructuur, verlies van modulariteit, de verschillende typen netwerkschade bij AD en FTD, en de kwetsbaarheid van sterk verbonden gebieden in AD. Deze conclusie wordt gevolgd door een bespreking van relevante methodologische kwesties zoals volume conductie en obstakels in de graaf-theoretische analyse. Daarnaast worden enkele concrete suggesties voor toekomstig onderzoek gedaan, en de algemene discussie eindigt met een beschouwing van het mogelijke nut van de aanpak in deze thesis, en een pleidooi voor dit type onderzoek bij dementie.

DANKWOORD

In de eerste plaats wil ik alle patiënten en vrijwilligers die hebben meegewerkt aan dit onderzoeksproject hartelijk danken; uw inzet heb ik zeer gewaardeerd!

Beste Kees, een kleine zes jaar geleden woonde ik een voordracht van je bij over – de toen nog compleet onbekende – netwerkanalyse van EEG data. Ik herinner me dat ik niet alles helemaal kon volgen, maar dat ik wel meteen het gevoel kreeg dat hier iemand echt met iets innovatiefs en avontuurlijks bezig was. In de afgelopen jaren is dit gevoel van bewondering alleen maar verder gegroeid. Ik ken niemand die op zo'n indrukwekkende en creatieve manier de kennis van verschillende vakgebieden aan elkaar koppelt, met ideeën die de gemiddelde neuroloog draaiduizelig achterlaten, en die doorgewinterde technici voorzien van het nodige biologisch gezonde verstand. Niet-lineaire dynamica en moderne netwerktheorie koppelen aan klinische neurofysiologie is één ding, maar ook nog je eigen software hiervoor ontwikkelen en het geheel begrijpelijk kunnen uitleggen aan spartelende promovendi is wat anders! Ik voel me vereerd dat ik onder de hoede van één van de grondleggers van deze tak van onderzoek een bijdrage heb mogen leveren, en voel me nu ook een beetje baanbrekend. Ik hoop van harte dat we in de toekomst opnieuw kunnen samenwerken, en dat ik dan ook eens een keer een heel goed idee krijg.

Beste Philip, waar sommigen jaren hard moet nadenken om een beetje grip te krijgen op netwerken, zijn anderen geboren netwerkers. Jouw humor, enthousiasme en visie zijn aanstekelijk, en ik heb geregeld meegemaakt op congressen dat mensen een beetje glazig uit hun ogen begonnen te kijken als ik iets vertelde over de MEG, om vervolgens enthousiast op te veren als ik noemde dat ik in 'the Scheltens group' zat. Ik ben je erg dankbaar voor het geschonken vertrouwen om dit project te kunnen uitvoeren, en natuurlijk om deel te mogen zijn van je swingende team. De afgelopen jaren waren zonder twijfel de leukste uit mijn carrière tot nu toe, en alle geboden kansen hebben zich rechtstreeks uitbetaald bij het tot stand komen van dit proefschrift; van de laptop waarop het is getypt tot de auteurs waarmee je me in contact hebt gebracht. De afgelopen jaren hebben me ervaringen gebracht die ik niet snel zal vergeten, varierend van het gezamenlijk vertolken van Schubert liederen (weet dat ik hier nog steeds videomateriaal van bezit!) tot het 's avonds cocktails sippen in Honolulu.

Beste Wiesje, naast 'Occam's Razor', het principe dat uit een aantal mogelijke hypothesen degene met de minste aannames de voorkeur heeft, zou ik graag 'Wiesje's Razor' willen introduceren: als je denkt dat je stuk staat als een huis voordat Wiesje ernaar heeft gekeken, maak je een gevaarlijke aanname! Jouw analytische scherpte en kritische blik

worden alom – zeg maar gerust - gevreesd, en ik kan daar nog veel van leren. Daarnaast vind ik het indrukwekkend om te zien hoe je bij het begeleiden van deze dynamische groep onderzoekers met uiteenlopende projecten én persoonlijkheden het overzicht en overwicht weet te behouden. En... ik heb natuurlijk zeer genoten van onze muzikale uitstapjes!

Ik zou graag de leden van de leescommissie hartelijk willen danken voor de moeite die zij nemen om dit proefschrift te evalueren en de verdediging ervan bij te wonen: prof. dr. S.A.R.B. Rombouts, prof. dr. M.J. van Putten, prof. dr. J.J. Heimans, dr. F. Maestu, dr. Y.A.L. Pijnenburg, en dr. M. van den Heuvel.

Maria 'heeee buurman' Boersma, netwerk-buddy van het eerste uur: hoewel we elkaar de laatste tijd minder hebben gezien, hebben wij voor mijn gevoel de meeste netwerk-inhoudelijke discussies gevoerd, waarbij jij uiteindelijk vaak nog nét een kritische vraag op wist te werpen die ik alleen nog maar kon pareren met: "misschien moeten we dat nog eens met Kees bespreken...".

Hanneke, fijn dat jij mij samen met Maria mentaal wil ondersteunen als paranimf, maar waar is mijn poster-koker eigenlijk gebleven?

Alle VUmc netwerk-pioniers! Linda, Menno, Eelco, Kim, Edwin, Prejaas, Bernadette en nog vele anderen... We kennen allemaal het moedeloze gevoel als de clustering coefficient en padlengte weer iets heel anders doen dan we hadden verwacht, maar we komen er wel uit! Later zullen ze ons wegbereiders noemen!

Iedereen bij het Alzheimercentrum (teveel om op te noemen)**: bedankt!**

Alle medewerkers van de afdeling **klinische neurofysiologie**, in het bijzonder Bob van Dijk en Arjan Hillebrand, hartelijk dank voor jullie inzet en ondersteuning op technisch en organisatorisch vlak!

Onze netwerk-broeders van de **TU Delft**: prof. Piet Van Mieghem en zijn groep met Huijuan Wang, Dajie Liu, Cong Li…ons contact was voor mij erg interessant en leerzaam en heeft een paar mooie publicaties opgeleverd!

Alle **neuropsychologen** die heben meegewerkt aan dit project: Sietske (nog bedankt trouwens voor de promotie to-do list, zonder deze was ik nu waarschijnlijk nog niet eens begonnen!), Lieke, Annelies, Ellemarije, Astrid, Sofie, Nicole… bedankt voor jullie grote inzet bij het testen van alle proefpersonen!

Alzheimer Nederland en **ISAO** wil ik graag hartelijk danken voor de financiele ondersteuning, die o.a. internationaal congresbezoek mogelijk heeft gemaakt.

Maria Eugenia López, thank you for bringing your Spanish temperament to cold Amsterdam, I do hope you have turned into a 'MEG-believer' by now…

Emi Saliasi, bedankt voor je hulp en alle grappige verhalen!

Kat Mott, the work you did while you were here was truly quite impressive, and without your early experiments our PLoS paper would not be the same. Thanks!

Guido, ik heb erg genoten van onze fantasieen over netwerk-visualizatie software. Dat we dan geregeld uitkwamen bij computerspellen die je met je hersens kunt besturen of machines die gedachten lezen en/of beinvloeden mocht de pret niet drukken! Ons 'Thoughtweaver' project – door jou gerealiseerd- was leerzaam op allerlei onvoorziene manieren.

De afdeling ICT van het VU medisch centrum wil ik graag hartelijk danken voor alle geboden ondersteuning bij mijn overstap van Windows naar OS X!

Rianne van Strien van Optima Grafische Communicatie bedankt voor het maken van de prachtige layout van dit boekje, en voor het doorvoeren van de vele correcties (en de correcties op de correcties…)!

Mijn nieuwe collega's van de **afdeling neurologie van het VUmc!** Ik had verwacht dat ik flink zou moeten overschakelen na het doen van dit geweldige project, maar ik voel me nu al thuis; we gaan er wat moois van maken!

Brad Mehldau, Oscar Peterson, Franz Liszt, Johan Sebastiaan Bach, de Beatles, Jimi Hendrix, Esperanza Spalding, Donny Hathaway, Stevie Wonder en bovenal Prince: bedankt voor jullie muzikale ondersteuning bij het schrijven van dit proefschrift.

Bouw, bedankt voor het lachen om al mijn slechte grappen sinds 22-11-2002!

Zoë Zwaantje…ik had al zo'n voorgevoel dat 2012 een enerverend jaar zou gaan worden, maar jij deed er nog een paar schepjes bovenop!

Pap & Mam, zonder jullie...

VU UNIVERSITY ALZHEIMER CENTER DISSERTATIONS

1. L. Gootjes: Hemispheric connectivity and laterality of language processing (14-9-2004)
2. R. Goekoop: Pharmacological fMRI: a clinical exploration (16-01-2005)
3. K. van Dijk: Peripheral electrical nerve stimulation in Alzheimer's Disease (6-9-2005)
4. N.S.M. Schoonenboom: Cerebrospinal fluid markers for the early and differential diagnosis of Alzheimer's disease (10-11-2006)
5. E.S.C. Korf: Medial Temporal Lobe atrophy on MRI: vascular risk factors and predictive value in dementia (29-11-2006)
6. B. van Harten: Aspects of subcortical vascular ischemic disease (22-12-2006).
7. B. F. Jones: Cingular cortex networks (23-03-2007)
8. L. van de Pol: Hippocampal atrophy from aging to dementia: a clinical perspective (11-05-2007)
9. Y.A.L. Pijnenburg: Frontotemporal dementia: towards an early diagnosis (5-7-2007)
10. A. J. Bastos Leite: Pathological ageing of the Brain (16-11-2007)
11. E.C.W. van Straaten: MRI correlates of vascualr cerebral lesions and cognitive impairment (11-1-2008)
12. R.L.C. Vogels: Cognitive impairment in heart failure (11-4-2008)
13. J. Damoiseaux: The brain at rest (20-5-2008)
14. G.B. Karas: MRI patterns of cerebral atrophy in dementia (19-6-2008)
15. F.H. Bouwman: Biomarkers in dementia: longitudinal aspects and combination with MRI (20-6-2008)
16. A.A. Gouw: Cerebral small vessel disease on MRI (20-03-2009)
17. H. van der Roest: Care needs in dementia and interactive digital information provisioning (12-10-2009)
18. C. Mulder: Biomarkers in Alzheimer's disease (11-11-2009)
19. W. Henneman. Advances in hippocampal atrophy measurement in dementia: beyond diagnostics (27-11-2009)
20. S.S. Staekenborg: Risk factors and clinical findings in relation to vascular changes on brain MRI (23-12-2009)
21. N. Tolboom: Imaging Alzheimer's disease pathology in vivo: towards an early diagnosis (12-02-2010)
22. E. Altena: Mapping insomnia: brain structure, function and sleep intervention (17-03-10).
23. N.A. Verwey: Biochemical markers in dementia: from mice to men (15-04-2010)
24. M.I. Kester: Biomarkers for Alzheimer's pathology; monitoring, predicting and understanding the disease (14-01-2011)
25. J.D. Sluimer: Visualizing the shrinking brain (28-04-11).
26. S.D Mulder: amyloid associated proteins in Alzheimer's disease (07-10-11)
27. S.A.M. Sikkes: measuring IADL in dementia (14-10-11)
28. A. Schuitemaker: Inflamation in Alzheimer's Disease: in vivo quatification (27-01-12)
29. K. Joling: Depression and anxiety in family caregivers of persons with dementia (2-4-12)
30. W. De Haan: In a network state of mind (02-11-12)

LIST OF PUBLICATIONS

van Straaten EC, **de Haan W**, de Waal H, Scheltens P, van der Flier WM, Barkhof F, Koene T, Stam CJ. Disturbed oscillatory brain dynamics in subcortical ischemic vascular dementia. BMC Neurosci. 2012 Jul 24;13(1):85.

de Haan W, Mott K, van Straaten ECW, Scheltens P, Stam CJ. Activity dependent degeneration explains hub vulnerability in Alzheimer's disease. PLoS Comput Biol 8(8): e1002582. doi:10.1371/journal.pcbi.1002582

de Haan W, van der Flier WM, Wang H, Van Mieghem PF, Scheltens P, Stam C. Disruption of functional brain networks in Alzheimer's disease: what can we learn from graph spectral analysis of resting-state MEG? Brain Connect. 2012 , 2(2): 45-55

de Haan W, van der Flier WM, Koene T, Smits LL, Scheltens P, Stam CJ. Disrupted modular brain dynamics reflect cognitive dysfunction in Alzheimer's disease. Neuroimage. 2012 Feb 15;59(4):3085-93.

C Li, H Wang, **W de Haan**, C J Stam and P Van Mieghem. The correlation of metrics in complex networks with applications in functional brain networks J. Stat. Mech. (2011) P11018

de Waal H, Stam CJ, **de Haan W**, van Straaten EC, Scheltens P, van der Flier WM. Young Alzheimer patients show distinct regional changes of oscillatory brain dynamics. Neurobiol Aging. 2012 May;33(5):1008.e25-31. Epub 2011 Nov 26.

Pievani M, **de Haan W**, Wu T, Seeley WW, Frisoni GB. Functional network disruption in the degenerative dementias. Lancet Neurol. 2011 Sep;10(9):829-43. Epub 2011 Jul 21. Review.

de Haan W, Pijnenburg YA, Strijers RL, van der Made Y, van der Flier WM, Scheltens P, Stam CJ. Functional neural network analysis in frontotemporal dementia and Alzheimer's disease using EEG and graph theory. BMC Neurosci. 2009 Aug 21;10:101.

Stam CJ, **de Haan W**, Daffertshofer A, Jones BF, Manshanden I, van Cappellen van Walsum AM, Montez T, Verbunt JP, de Munck JC, van Dijk BW, Berendse HW, Scheltens P. Graph theoretical analysis of magnetoencephalographic functional connectivity in Alzheimer's disease. Brain. 2009 Jan;132(Pt 1):213-24.

de Haan W, Stam CJ, Jones BF, Zuiderwijk IM, van Dijk BW, Scheltens P. Resting-state oscillatory brain dynamics in Alzheimer disease. J Clin Neurophysiol. 2008 Aug;25(4):187-93.

HERSENWEB

Wat moderne netwerktheorie ons leert over de werking van de hersenen
Kees Stam, Linda Douw en Willem de Haan
September 2010, Uitgeverij Bert Bakker, Amsterdam, Nederland. (Dutch).
ISBN 987 90 351 3533 8

ABOUT THE AUTHOR

Willem de Haan was born in Nijmegen on the 31st of December, 1975.

Elementary and High school years were spent in Nijmegen, Zwolle, Drachten, and Meppel. In 1993, he received his Gymnasium bèta diploma, and was not sure what to do next. A vocational test made during the final year of school indicated that Willem should pursue a career either in the agricultural or in the medical sector. He decided to consider these options while studying jazz piano at Hofstra University (Long Island, New York).

In 1994, Willem started his medical study at the University of Amsterdam (UvA), and after obtaining his Masters degree he took time off to continue jazz piano at the Conservatory of Amsterdam. He obtained his medical degree in 2003 after completing his internships, including a research internship in pediatric gastroenterology (Florence, Italy) and a clinical internship in tropical medicine (Kaoma, Zambia).

Since then Willem has gained clinical experience as a physician in neurology (Flevoziekenhuis and Slotervaartziekenhuis) and psychiatry (Mentrum). In 2008, he started his PhD research at the Alzheimer Center of the VU University. Clinical work during this period consisted of cognitive patient screening at the Alzheimer center, duty calls at the neurology clinic/emergency department, and participating as co-investigator in various clinical trials. Since 2012 he is resident neurology at the VU University Medical Center.

Contact information:
Willem de Haan
Department of Neurology
VU University Medical Center
P.O. Box 7057
1007 MB Amsterdam
w.dehaan@vumc.nl

network: a group or system of interconnected elements
networks are everywhere around us and inside us
they are much more than the sum of their parts,
and create new levels of meaning:

cognition emerges from our interconnected neurons

a face emerges from the words on the front cover
a new perspective on Alzheimer emerges from the words inside

please visit www.e-pubs.nl/?epub=willemdehaan
for a full colour PDF or eReader version of this thesis